Fatty Acyl-Specific Macrolipidomics and Microlipidomics for Nutritional Research

by

Juan J. Aristizábal Henao

A thesis

presented to the University of Waterloo

in fulfilment of the

thesis requirement for the degree of

Doctor of Philosophy

in

Kinesiology

Waterloo, Ontario, Canada, 2019

© Juan J. Aristizábal Henao 2019

Examining Committee Membership

The following served on the Examining Committee for this thesis. The decision of the Examining Committee is by majority vote.

External Examiner   Dr. Harold M. Aukema
                              Professor, Department of Human Nutritional Sciences
                              University of Manitoba

Supervisor   Dr. Ken D. Stark
                              Professor, Department of Kinesiology
                              University of Waterloo

Internal Members   Dr. Robin E. Duncan
                              Associate Professor, Department of Kinesiology
                              University of Waterloo

                              Dr. A. Russell Tupling, Department of Kinesiology
                              Professor
                              University of Waterloo

Internal-External Member   Dr. Scott Hopkins
                              Associate Professor, Department of Chemistry
                              University of Waterloo

Author's Declaration

This thesis consists of material all of which I authored or co-authored: see Statement of Contributions included in the thesus. This is a true copy of the thesis, including any required final revisions, as accepted by my examiners.

I understand that my thesis may be made electronically available to the public.

Statement of Contributions

Chapter 5: *A Cross-Platform and Cross-Acquisition Method Comparison for the Macrolipidomic Analysis of Human Whole Blood* was authored by J.J. Aristizabal Henao, N.S. Meitei, D. Chalil, R.W. Smith and K.D. Stark. JJAH, RWS and KDS designed the studies and JJAH completed all analyses. NSM and DC identified lipid features using automated software.

Chapter 6: *Microlipidomic Analysis of Lysophosphatidic Acid Regioisomeric Species in Mouse Plasma* was authored by J.J. Aristizabal Henao, M.F. Fernandes, R.E. Duncan and K.D. Stark. JJAH and KDS designed the studies and JJAH completed all analyses. MFF and RED provided mouse plasma and chemical standards. This is published as *Development of a rapid ultra-high performance liquid chromatography/tandem mass spectrometry method for the analysis of sn-1 and sn-2 lysophosphatidic acid regioisomers in mouse plasma, Lipids* (2019) 54: 479-486.

Chapter 7: *Macrolipidomic Analysis of Sunflower Oil and Mouse Striatum* was authored by J.J. Aristizabal Henao, C.T. Chen, J.R. Hibbeln JR and K.D. Stark. JJAH and KDS designed the studies and JJAH completed all analyses. CTC and JRH provided samples and financial support for the mouse striatum analyses.

Chapter 8: *Quantitative Lipidomics of Novel Whole Blood Biomarkers for the Dietary Intake of Omega-3 Polyunsaturated Fatty Acids* was authored by J.J. Aristizabal Henao, A.P. Biltoft-Jensen AP and K.D. Stark. JJAH and KDS designed the studies and JJAH completed all analyses. APBJ provided whole blood samples and dietary intake assessment data.

Chapter 9: *Identification of Omega-3 Fatty Acid Biomarkers in a Rat Model of Acute and Chronic Docosahexaenoic Acid Feeding* was authored by J.J. Aristizabal Henao, D. Chalil and K.D. Stark. JJAH and KDS designed the studies and JJAH completed all analyses. DC managed the rat study and assisted with sample collection.

Abstract

The field of lipidomics can further our understanding of the biochemical processes of human health and disease. Generally, lipidomics methods utilize high-performance liquid chromatography (HPLC) for lipid separation, followed by detection using tandem mass spectrometry (MS/MS). The joint use of HPLC and MS/MS has increased dramatically over the past few years, and novel technologies continue to increase the versatility and practical usability of various lipidomics methods. However, a lack of harmonized language, nomenclature and standardized analytical strategies can result in lipid misannotations, improper analyte identifications, and incorrect quantitative results. In this thesis, the importance of adopting appropriate analytical strategies to answer research hypothesis(es) will be highlighted. Specifically, this entails a comparison between analytical platforms and four HPLC-MS/MS data acquisition strategies for untargeted/global lipidomic profiling of highly-abundant lipids including phospholipids, triacylglycerols and cholesteryl esters in human whole blood. In addition, the advantages of targeted analytical approaches for the measurement of specific lipid classes will be examined through the development of a tailored method for the determination of regioisomers of lysophosphatidic acid in plasma (mouse), the acyl species of triacylglycerols in cooking oil (sunflower), and the acyl species of phospholipids in brain tissue (mouse). Finally, comprehensive profiling of various lipid classes in whole blood using a novel retention time-based negative/positive ion mode switching method will be used to screen for potential blood biomarkers of omega-3 polyunsaturated fatty acid intake. This will include samples from a cross-sectional dietary assessment study in humans, and an acute/chronic docosahexaenoic acid supplementation study in rats. The methods presented in this thesis have the potential to be expanded for use in agriculture, nutrition, research and clinical settings.

Acknowledgements

Firstly, I'd like to thank my Ph.D. advisor, Dr. Ken Stark. Ken, thank you for your support and friendship over the past 9 years. I was only 19 years old when I started working for you as a second-year student volunteer. I have grown up under your supervision and wouldn't be the person I am today without your guidance. You've been tough when you've had to be (and also sometimes when you didn't) but I know this is just you challenging me to be the best possible analyst, writer and speaker that I can be. I am proud of all of the projects and collaborations that we have worked on together and am happy to have shared countless cups of coffee and slices of pizza with you. I would also like to thank my committee members Dr. Robin Duncan and Dr. Russ Tupling for their friendship, advice and encouragement since before I started graduate school, as well as my Internal Examiner Dr. Scott Hopkins and External Examiner Dr. Harold Aukema for providing their expertise.

Thank you also to everyone past and present from the Stark Lab and the Physiology floor. There are too many people to list here, but I'd like to specifically thank my friends Dr. Kristin Marks, Dr. Ryan Bradley and Dr. Maria Fernanda Fernandes, Daniel Chalil for his help with the animal study, and Dr. Adam Metherel for being like an older brother to me. I'm also grateful to Dr. Richard Smith from the University of Waterloo Mass Spectrometry Facility for his invaluable expertise, Jing Ouyang, Emma Dare, Marg Burnett, Cheryl Kieswetter, Jenny Crowley, Jeff Rice, and Craig MacDonald, for their administrative and technical help, and Denise Hay for helping me ensure that all of my degree requirements were completed on time. I'd also like to acknowledge Dr. Sanjib Meitei from PREMIER Biosoft for software support, Dr. Chuck Chen from the National Institutes of Health and Dr. Anja Biltoft-Jensen from the Technical University of Denmark for allowing us to complete lipidomic analyses using their

Table of Contents

List of Figures

List of Tables

List of Abbreviations

ALA   Alpha-linolenic acid

ARA   Arachidonic acid

BEH   Ethylene bridged hybrid

CE   Collision energy

CSH   Charged surface hybrid

DDA   Data-dependent acquisition

ddH$_2$O   Double-distilled ultra-pure water

DHA   Docosahexaenoic acid

DIA   Data-independent acquisition

dma   Dimethyl acetal

EPA   Eicosapentaenoic acid

ESI   Electrospray ionization

FAID   Full-acyl identification

FAME   Fatty acid methyl ester

HD   High-definition

HILIC   Hydrophilic interaction liquid chromatography

HPLC   High performance liquid chromatography

HRAM   High-resolution/accurate mass

HSS-T3   High-strength silica

HUFA   Highly unsaturated fatty acid

LA   Linoleic acid

LC   Liquid chromatography

LPA	Lysophosphatidic acid
LPC	Lysophosphatidylcholine
LPE	Lysophosphatidylethanolamine
m/z	Mass-to-charge ratio
MALDI	Matrix-assisted/laser-desorption ionization
MRM	Multiple reaction monitoring
MS	Mass spectrometry
MS/MS	Tandem mass spectrometry
MUFA	Monounsaturated fatty acid
N6/N3	Ratio of omega-6-to-omega-3 fatty acids
PA	Phosphatidic acid
PC	Phosphatidylcholine
PCA	Principal Component Analysis
PE	Phosphatidylethanolamine
PEEK	Polyetheretherketone
PG	Phosphatidylglycerol
PI	Phosphatidylinositol
PS	Phosphatidylserine
PUFA	Polyunsaturated fatty acid
QE	Q-Exactive
QE DDA	Q-Exactive data-dependent acquisition
QToF	Quadrupole-Time-of-Flight
QToF DDA	Quadrupole-Time-of-Flight data-dependent acquisition

QToF HD-DDA	Quadrupole-Time-of-Flight high-definition data-dependent acquisition
QToF HD-DIA	Quadrupole-Time-of-Flight high-definition data-independent acquisition
RT	Retention time
SD	Standard deviation
SFA	Saturated fatty acid
SFO	Sunflower oil
SM	Sphingomyelin
SRM	Selected reaction monitoring
TAG	Triacylglycerol
ToF	Time-of-flight
ToF-MRM	Time-of-flight/multiple reaction monitoring
TDW+	Total Western Diet with docosahexaenoic acid
TWD-	Total Western Diet without docosahexaenoic acid
UHPLC	Ultra-high performance liquid chromatography
UHPLC-MS/MS	Ultra-high performance liquid chromatography/tandem mass spectrometry
XIC	Extracted ion chromatogram

CHAPTER 1

General Introduction

Lipids are involved in cellular structure and compartmentalization, energy storage, and signaling pathways [1]. Traditionally, fatty acid compositional data has been invaluable in our understanding of metabolism, as well as in characterizing how perturbations in lipid pathways are related to the onset and progression of various diseases [2-6]. However, the emergence of novel lipidomic measurements have enabled the elucidation of complex lipid structures in their naturally occurring states. The ability to monitor specific lipid molecules has the potential to provide more molecular information that could be of physiological relevance, rather than examining changes in gross fatty acid levels. The rapid growth of the field of lipidomics has been possible through the advent of high-resolution mass spectrometry, which has been essential in our ability to confidently measure individual lipid species and characterize biochemical processes [7-9]. Since the introduction of the term "lipidomics" in the mid-2000's, the evolution of the field has also been accompanied by the emergence of new challenges pertaining to the standardization of common language and nomenclature, analytical methods, and data reporting. Various international initiatives have been established in order to address these issues and set guidelines for quality assurance and quality control [10-16]. However, there are large gaps in the literature that still remain.

Many of the challenges associated with lipidomic measurements stem from the exceptional diversity of the thousands of different molecules that can be classified as lipids within a cell, as well as their dynamic concentrations, which can span over several orders of magnitude [17, 18]. In many cases, lipids that are found in high abundance can be profiled using untargeted and generic methods that can be considered "macrolipidomics". Conversely, lipids

that are part of the very-low abundance regime often require targeted and specialized methods for accurate and reliable identification and quantitation that can be considered "microlipidomics". Thus, methods that are tailored for the analysis of a specific lipid class may not be suitable when measuring other lipid classes. Intra- and inter-laboratory comparisons using standard reference materials have identified a lack of consensus in lipidomic approaches and methods, and have emphasized the high variance that is associated with various lipidomic measurements [14, 16, 19].

Several mass spectrometry platforms have previously been used for lipidomic analyses, but hybrid instruments including the quadrupole-orbitrap [20], quadrupole-time-of-flight [21], and triple-quadrupole mass spectrometers [22] are the most popular. Additionally, innovative data-dependent (DDA)/data-independent acquisition (DIA) and ion mobility methods have increased the versatility of lipidomic analyses. However, the advantages and pitfalls of these analytical strategies are still poorly understood. This thesis presents a systematic examination of analytical lipidomics methods. This includes a comparison between mass spectrometry platforms (quadrupole-orbitrap vs. quadrupole-time-of-flight), data acquisition modes (DDA vs. DIA) and a brief examination of ion mobility-mass spectrometry coupled to DDA. We found that the quadrupole-time-of-flight mass spectrometer was able to generate more data than the quadrupole-orbitrap mass spectrometer due to faster sampling frequencies. Additionally, higher-quality data was consistently generated from the DDA methods as compared with DIA, and the use of ion mobility resulted in significant losses in sensitivity but did not provide any advantages in terms of data quality or reducing the frequency of false positive identifications. DDA-based methods were utilized in all subsequent macrolipidomic profiling studies in this thesis, but future

technological developments may allow DIA and ion mobility-based methods to be used to make meaningful contributions in untargeted lipidomics.

Sample preparation and sample introduction approaches can greatly influence analytical results. This can include sample extraction protocols, sample introduction techniques such as direct infusion versus chromatography-based methods, and ionization settings. The impact of different mass spectrometry-based workflows will be examined through the development of a targeted microlipidomic method for lysophosphatidic acid (LPA) regioisomers in plasma (mouse), a semi-targeted macrolipidomic method for cooking oils (sunflower oil), and a semi-targeted macrolipidomic method for brain tissue (mouse striatum). Through the development of the targeted LPA profiling method, we demonstrated that measuring species from this lipid subclass requires a specialized lipid extraction protocol, and that chromatographic resolution of regioisomeric LPA species can be achieved using conventional-flow UHPLC. From the cooking oil and brain tissue experiments, we emphasized that semi-targeted methods can be optimized when the general lipid profile of a sample is known prior to analysis. This information can be used to generate high-quality data in a discovery-based approach. We then integrated features from both semi-targeted workflows to develop a retention time-based ionization polarity-switching method to improve the characterization of fatty acyl-containing complex lipids in the blood macrolipidome in a single analytical run. This method was applied for the identification of novel blood biomarkers of omega-3 polyunsaturated fatty acid intake in 120 human whole blood samples from a dietary assessment project of the Danish National Food Institute. This is the largest human study assessing lipidomic biomarkers of omega-3 polyunsaturated fatty acid intake, and the only study to be completed in a population-based observational study. To confirm some of the observations from the human study, a rodent study (rat) was completed to examine

blood lipidomic responses after controlled acute and chronic dietary interventions with

docosahexaenoic acid. The rodent study allowed us to identify potential acyl species of lipids as

biomarkers of acute and chronic omega-3 polyunsaturated fatty acid intake.

CHAPTER 2

Scientific Background

2.1 Lipidomics

"Lipidomics", is a rapidly growing discipline that has been fueled by technological developments in the separation sciences, specifically mass spectrometry (MS) and high-performance liquid chromatography (HPLC) [23, 24]. Although the principles of MS have been adapted for the analysis of lipid molecules for several decades, the emergence of electrospray ionization (ESI)-mediated soft ionization applications in the early 1990's propelled the expansion of the field by providing dramatic improvements in the versatility of MS-based lipid analyses. More recently, novel technologies have increased the sensitivity, resolution, mass accuracy and overall robustness of modern instruments and applications, allowing us to appreciate the vast structural diversity of lipid species and further our understanding of human disease.

Over the past few years, these analytical advancements have coincided with an increased interest in the physiological roles of lipids in health and disease. As such, the ability to identify and quantify species of lipids within their lipid classes can provide metabolic insight into the roles of lipids in cellular structure and cell signaling, along with energy-storage. Sophisticated methods have been developed to characterize and elucidate the structure of discrete lipid species at the molecular level in disease states [25, 26], genetic knock-out models [27, 28], agriculture [29, 30], and food science and nutrition [31, 32]. New subdisciplines such as neurolipidomics and functional lipidomics have emerged [33, 34] that aim to answer more focused research hypotheses through targeted methodological approaches. While "targeted" methods often refers to the process of screening a sample for defined compounds by *m/z* ratios or diagnostic

fragments, "targeting" can include tailored extraction techniques [35-37], complementary multi-dimensional separations [38, 39], and innovative ion separation and detection instruments [40, 41]. Still, the core of lipidomics as an -*omics* field remains at the study and characterization of all of the molecular moieties that can be defined as lipids in their naturally-occurring state.

To date, there exists a virtually unlimited number of MS-based applications employing different methodological approaches to answer specific research questions. The MS approach used can impact the data produced and has been defined in the literature as "levels of information" [31, 42]; this is discussed in detail below in Section 2.2. Analytical strategies used for lipidomics can generally be categorized as untargeted and targeted. In untargeted or discovery-based analyses, there may not be a specific *a priori* hypothesis, but rather an interest in capturing a global snapshot of the lipidome at a specific point in time. In this case, automated software packages can be used to identify and select compounds that are statistically different between experimental conditions. Untargeted lipidomic profiling generally utilizes exhaustive lipid extraction techniques and ESI coupled to full-scan MS and either data-dependent or data-independent MS/MS on a variety of platforms [36]. Conversely, targeted analyses are hypothesis-driven and typically aim to profile a specific set of well-characterized analytes in the samples of interest [43, 44]. This generally entails tailored extraction techniques, the use of appropriate internal standards, and more elaborate MS or MS/MS methods such as selected ion monitoring, multiple reaction monitoring and neutral-loss scanning, which can only be done using a few types of hybrid MS platforms.

Untargeted and targeted MS approaches influence the analytical workflow, from sample preparation choices, sample introduction and ionization techniques, analytical platforms and acquisition modes. Sample introduction can vary, but introduction by direct infusion or after

6

liquid chromatographic separation are the two main approaches, although the use of matrix-assisted/laser-desorption ionization in increasing. These techniques are described in detail in Sections 2.3, 2.4 and 2.5, respectively. Finally, the manner in which a mass spectrometer acquires data can influence the results and how they can be interpreted. The most popular acquisition modes in lipidomics are single/multiple reaction monitoring, data-dependent or data-independent acquisition, which are described in detail in Section 2.6.

2.2 Levels of Lipidomic Information

New challenges have also emerged with the evolution of the field, particularly relating to the standardization of language that can be used to easily describe, categorize and convey lipidomic information, as well as contrasting and translating published data [19, 45]. The term "lipidomics" is often used to describe the analysis and characterization of transient lipids that are natively found in low abundance and have highly bioactive and/or signaling properties [46-48]. In theory, "lipidomics" should refer to the comprehensive analysis of cellular lipidomes, which includes these low abundant lipids but also highly-abundant lipid species that play structural and/or energy-storing roles [19, 49, 50]. Recently, we introduced the terms "microlipidomics" to define the examination of lipids of low abundance and "macrolipidomics" to define the examination lipids of high abundance within a sample to quickly infer the analytical approach and define the experimental strategy [31].

Another challenge with the language of lipidomics involves the ability to convey the level of molecular information known about a specific lipid. A shorthand notation system to describe lipids that encompasses different fatty acyl-chain lengths, degrees of unsaturation, regioisomeric configurations and carbon-carbon double-bond locations has been defined [51]. At

7

the most basic level, full-scan accurate mass data may be used to deduce the sum composition of a lipid molecule, which includes the lipid class followed by the total number of carbon atoms: number of carbon-carbon double bonds across all fatty acyl chains. For example, a lipid with an m/z ratio of 802.5604 has elemental composition $C_{43}H_{81}NO_{10}P$ and corresponds to the formate adduct ([M+formate]$^-$) of PC 34:2 following ESI in the negative ion mode. This indicates that this specie is a phosphatidylcholine with fatty acyls that cumulatively have 34 carbon atoms and 2 carbon-carbon double bonds. This has been defined previously as the "brutto" level of information [52, 53]. In addition to "brutto", we have defined "medio", "genio" and "infinio" levels of information [31, 42] to refer to increasing molecular information known about of specific fatty acyl-containing complex lipids (Figure 1). At the medio level, MS/MS spectra can be used to discriminate between isomeric species and recognize the fatty acyl chains. Medio requires MS/MS level diagnostic ions that correspond to specific acyl chains. For example, if 16:0 (m/z 255.2330) and/or 18:2 (m/z 279.2330) are observed in the MS/MS spectra, the molecule previously defined as PC 34:2 at the brutto level could be defined as PC 16:0_18:2. The underscore denotes that the sn-1- and sn-2-regioisomeric configurations of the two acyl chains are not known. If these sn-1- and sn-2-regioisomeric configurations are known, this is indicated using a forward slash as PC 16:0/18:2, with sn-1 position first and the sn-2 position second. We have termed this regioisomeric level of information as the genio level. Genio information can be determined following the chromatographic separation of regioisomeric pairs, and the specific sn-glycerol fatty acyl configurations can be deduced by examining relative fragment ion intensities in MS/MS spectra [31, 54-56]. Finally, the infinio level of information relates to the most detailed characterization of a discrete lipid molecule by adding stereoisomeric configuration and carbon-carbon double bond positionality, for example PC 16:0/18:2 (9Z,12Z).

This type of information can be determined using more targeted approaches and novel fragmentation techniques such as ozone-induced dissociation [57], ion mobility [58, 59], and derivatization-dependent methods such as the Paternò–Büchi reaction [60]. Innovative methods are emerging [61, 62], which may allow for the simultaneous elucidation of structures from all lipid classes at the infinio level.

2.3 Direct-Infusion Mass Spectrometry (Shotgun Lipidomics)

Shotgun lipidomics refers to the analysis of complex samples by direct infusion of lipid extracts into the ionization source of a mass spectrometer, without prior chromatographic separation [7]. This technique relies on the intrinsic ability of lipid molecules belonging to different lipid classes to differentially ionize in the positive or negative ion modes. Specifically, this endogenous electric potential can be utilized to resolve individual lipid classes in the ion source, and individual molecular species can then be further discriminated by high-resolution mass spectrometry. One of the most appealing features of shotgun lipidomics is that it allows for the simultaneous acquisition of spectra from all lipid species at a constant concentration of the sample solution. This particular capability enables a limitless number of experiments to be performed using a constant analyte/solvent ratio, including numerous scanning and fragmentation techniques, collision energies, ionization voltages, etc., which makes this an ideal initial strategy for the development and optimization of methods for novel compounds. Additionally, the ability to acquire spectra and analyze lipid samples in just a few minutes makes shotgun lipidomics an optimal candidate for high-throughput applications [63].

One of the most prevalent challenges within shotgun lipidomics arises from the concurrent ionization of lipids from all lipid classes, which is the characterizing feature of this

technique. Notably, the presence of highly-ionizable lipids such as phosphatidylcholines (PC) and sphingomyelins (SM) can result in ionization suppression of species with lower electric potentials, causing significant decreases in sensitivity [64-66]. PC and SM are known to be present in high amounts in many biological samples as they are important components of cellular membranes [67, 68]. The quaternary nitrogen feature that these zwitterionic species possess allows them to generate intense cations as protonated molecular species by neutralizing the negative charge of the phosphate group (i.e., $[M+H]^+$) and/or alkali-metal adducts (i.e., $[M+Li]^+$, $[M+Na]^+$, $[M+K]^+$) following positive ESI. As such, PC and SM can exert strong inhibitory effects on molecules that are not easily ionized, including phosphatidylinositols (PI) and phosphatidylserines (PS), resulting in low ion intensities that could fall below the limits of detection. Furthermore, the deconvolution of isotopic contributions and the resolution of isomeric species using a direct-infusion approach can be a daunting and laborious task, especially in discovery-based experiments, and may require specialized MS instrumentation and software. Multi-dimensional MS-based strategies [69, 70], ion mobility technologies [71-74] and powerful software solutions [74-79] have emerged over the past few years in an attempt to make shotgun lipidomics more automated and increase its practical usability.

2.4 Lipidomics Methods with Front-End Liquid Chromatography Separations

As with mass spectrometry, the development of novel technologies for liquid chromatography (LC) has been crucial in our ability to characterize and quantitate cellular lipidomes for two particular reasons. Firstly, analyte separation by HPLC prior to sample introduction into the ionization source of a mass spectrometer circumvents many of the challenges that are typically encountered with direct-infusion approaches. The unmatched

robustness and versatility of chromatography have been shown to be critical in the resolution of acyl-isomers, regioisomers and stereoisomers using a variety of commercially-available columns and solvent systems [80, 81]. Secondly, the introduction of ultra-high performance liquid chromatography (UHPLC) and nano-flow LC methods have made it possible to achieve unprecedented levels of sensitivity, with some reporting limits of detection at the attomole-zeptomole level (i.e., 10^{-18} to 10^{-21} mole) [82-84]. As such, microlipidomic studies for the targeted characterization of lipids that are natively found in very low abundance remains a feat that only LC-based methods can accomplish.

Most HPLC- and UHPLC-based lipidomic methods utilize reversed-phase C18 columns and aqueous mobile phases, which results in analyte partitioning based on the degree of non-polarity of particular lipid classes [85]. This is dictated by the hydrophobic nature of different lipid species, considering the number of fatty acyl constituents (i.e., monoacylglycerols vs. diacylglycerols vs. triacylglycerols), fatty acyl chain lengths and degrees of unsaturation, and phospholipid head group composition. In some cases, specific reversed-phase methods have also been shown to have the ability to resolve lipid species by *sn*-glycerol regioisomeric configurations [31, 54, 86]. A representative full-scan total ion chromatogram from a reversed-phase UHPLC-MS run is shown in Figure 2, indicating the approximate retention times for the major lipid classes in human whole blood. More specialized methods also exist, and use tailored configurations of columns with different C18 chemistries and bond phases that change the selectivity of the analysis. Some examples of this will be shown in Chapter 6. The second most-popular type of modern LC-based methods for lipidomics involves the use of hydrophilic interaction liquid chromatography (HILIC), which enables the separation of lipids based on their hydrophilic properties, i.e., by lipid class rather than by number and type of fatty acyl chains

[87]. HILIC is a variant of normal-phase LC, but utilizes a semi-aqueous mobile phase system similar to what is used in reversed-phase LC. Consequently, as compared with normal-phase LC, HILIC run times are significantly shorter, there is less back-pressure which allows for higher mobile phase flow rates, and the avoidance of organic solvents such as chloroform and hexane allow HILIC use with most UHPLC systems. HILIC is traditionally used for the separation of highly polar metabolites such as sugars, peptides and nucleic acids [88-91], providing modest increases in sensitivity relative to what is typically seen using reversed-phase LC [92]. Although reversed-phase methods appear to provide the highest separation efficiency as compared with HILIC due to the higher hydrophobic content of the lipidome [93], it is often argued that there is still value in the use of HILIC in lipidomics for the separation of lipids based on their hydrophilic properties (i.e., by lipid class). By column elution over narrow timeframes, all of the species that belong to the same lipid class experience similar degrees of matrix- and ionization-suppression effects, allowing for the use of single internal standards per lipid class for peak area normalization and quantitation [94]. While HILIC may provide some advantages in specialized subdisciplines such as phospholipidomics [95], the resolution of organic lipids such as triacylglycerols and cholesteryl esters can be particularly challenging due to poor retentivity and early coelution near the void volume [96]. Furthermore, the need for dedicated software capable of performing isotope-overlap correction algorithms [97, 98] and the difficulty in deconvoluting isomeric species can limit the amount of lipidomic information that can be derived from HILIC-based methods [93].

Finally, the use of two-dimensional LC has increased in lipidomics, where orthogonal chromatographic techniques can be integrated by using two complimentary columns of different chemistries to separate the analytes of interest based on multiple physical and chemical

properties [99]. In this sense, both reversed-phase and HILIC columns can be connected in tandem, in parallel, or used offline to obtain two dimensions of separation, one which works on the hydrophilic (HILIC) and one on the hydrophobic (reversed-phase) properties of different lipids. While comprehensive two-dimensional LC can be used to generate remarkable amounts of data from cellular lipidomes, the need for costly state-of-the-art instrumentation have limited the widespread adoption of this technique by the lipidomics community thus far. Other specialized two-dimensional LC methods have also been reported and utilize a wide range of combinations of column technologies including normal-phase [100], reversed-phase [101], silver-ion [102], ion exchange [103], size-exclusion [104], HILIC [105] and chiral columns [106].

2.5 Matrix-Assisted/Laser-Desorption Ionization (MALDI) and Lipidomics

MALDI is a soft ionization technique that has been widely used in the proteomics field since the 1980s for the analysis of peptides and proteins that are difficult or impossible to ionize using conventional ionization techniques such as ESI [107, 108]. The versatility of MALDI has been more recently applied in lipidomics, enabling high throughput lipid analyses with little sample preparation [109-111], and the ability to visualize the spatial distribution of specific lipid species in biological tissues by imaging [112, 113]. One of the features that differentiate MALDI from other ionization techniques is the ability to use dry or solid samples. The sample is first mixed and cocrystallized with a ultra-violet (UV) absorbing matrix that enables the desorption and ionization of the analytes of interest upon irradiation with a UV laser [114, 115]. Following ionization, analyte ions in the gas phase are accelerated through an electric field and are separated based on their mass-to-charge ratios (i.e., *m/z*) typically using Time-of-Flight (ToF)

technology [116, 117]. Full-scan MS spectra can be acquired from dried target spots on a

MALDI plate following a laser blast, similar to what is obtained from shotgun lipidomic

analyses. Due to this, some of the limitations that were discussed regarding direct-infusion ESI in

Section 2.3 are also frequently observed in MALDI-based analyses, namely the ionization

suppression effects of highly-ionizable species and the extensive convolution and overlap of

isomeric species [118, 119]. Furthermore, the resolving power and mass accuracy of many

MALDI-ToF instruments is relatively poor compared to some of the best mass spectrometers

that are currently available [120, 121]. Nevertheless, its exceptional speed, unmatched potential

for automation, and high quantitative abilities have made MALDI an invaluable tool in lipidomic

discovery and screening applications [111, 122-124]. The ability to analyze solids through

MALDI has also enabled MALDI-based mass spectrometry imaging, which enables the

localization of specific lipids within a thin tissue section [125].

2.6 Collecting Lipidomic Data: Common Targeted and Untargeted MS Acquisition Modes

There are many mass spectrometry-based approaches that can be used to obtain lipidomic

data, encompassing various acquisition modes and ion fragmentation strategies. Most modern

mass spectrometers have MS/MS capabilities. This can offer various advantages depending on

the technology and vendor platform, but the decision of the type of mass spectrometer to be used

should be based primarily on the desired research outcome (i.e., accurate quantitation or

structural elucidation).

In targeted analyses, triple-quadrupole mass spectrometers are widely regarded as the

gold-standard instrument for quantitation [126]. These instruments typically acquire data using

selected-reaction monitoring (SRM) or multiple-reaction monitoring (MRM) methods, which

offer the highest sensitivity. In SRM and MRM, the first quadrupole serves as a mass filter for the *m/z* ratio of the precursor ion, collision-induced dissociation then takes place in the collision cell (second quadrupole), and the *m/z* ratio(s) or neutral losses of defined fragment structures are monitored by the third quadrupole. While most mass spectrometry vendors have developed their own triple quadrupole technologies, these instruments provide nominal mass data (integer precision) and are not capable of high resolution/accurate mass (HRAM) analyses. This can severely reduce the certainty with which unknown compounds are characterized, and limits the usability of this type of instrument in discovery-based analyses.

Orbitrap and Time-of-Flight (ToF) mass spectrometers offer HRAM capabilities, with resolving power greater than 10,000 and up to 500,000 on some of the newest platforms, as well as sub-ppm mass accuracy [127]. Orbitrap mass analyzers generate HRAM data by trapping ions and acquiring multiple measurements of their harmonic oscillation frequencies across rotational, axial and radial axes around a central spindle. Mathematical transformations are then applied to these data to generate *m/z* values [128]. In ToF instruments, *m/z* ratios are generated based on the amount of time that ions spend in the gas phase after they are accelerated towards the detector using discrete amounts of kinetic energy. Separation then takes place based on the molecular weight (i.e., *m*) and charge state (i.e., *z*), of different ions, where low molecular weight and multiply-charged species travel faster. ToF instruments have unmatched scanning speeds, but orbitraps generally have much higher resolving power. HRAM facilitates proper annotation of lipid species as the large number of molecules with isobaric nominal masses in complex lipid samples can be discriminated by differences in their accurate masses. Untargeted analyses can be completed using these instruments by integrating full-scan HRAM data with MS/MS. This results in the confident determination of the elemental make-up and medio-level (or higher)

composition of fatty acyl-containing complex lipids, while circumventing some of the challenges

associated with the resolution of isomers that were discussed in Section 2.2. With HRAM, there

are several ways in which MS/MS spectra can be obtained, depending on the platform, software,

and acquisition modes that are available. In addition to the targeted SRM and MRM techniques,

these instruments can acquire data using untargeted approaches. Generally, these can be

categorized as data-dependent (DDA) or data-independent acquisition (DIA) methods.

In DDA, top-n experiments can be defined where n is an integer that relates to the

number of MS/MS ions that are sequentially filtered by the quadrupole and fragmented in the

collision cell, starting with the most intense ion in the full-scan spectrum (i.e., the base peak)

followed by the ion with the second highest intensity, then the third, etc. Inclusion/exclusion lists

and dynamic exclusion settings are also widely implemented to enable the system to acquire

MS/MS spectra for as many analytes as possible while limiting the unwanted selection of intense

background ions. DDA is a powerful technique that can help in the characterization of

macrolipidomes due to its bias towards highly-abundant ion species. With microlipidomics,

untargeted DDA profiling can be particularly challenging when the precursor ions are not in the

top n most intense ions of an MS survey scan at a given point in time, as they will not be filtered

and fragmented to generate MS/MS data. While n can be set as any integer ≥ 1 (and typically

≤ 30), DDA-based methods that utilize HPLC or UHPLC are limited with regards to the number

of MS/MS scans that can be obtained in between full-scan MS survey scans. This is due to short

compound elution times and narrow peak widths. Additionally, as the n is set at higher values,

the frequency of MS survey scans decreases (i.e., individual scans are further apart in the

chromatogram), which can cause aliasing of the MS survey trace, resulting in inaccurate

quantitation.

Recently, DIA has been introduced by several MS vendors due to its ability to fragment all of the ions within a survey scan, including those of low intensity, without pre-selection or discrimination by a quadrupole mass filter [129-132]. This is achieved by allowing all of the ions within an MS survey scan to enter the collision cell to generate fragment ions for every precursor ion that is present. Alternating low-energy (i.e., MS survey) and high-energy (i.e., MS/MS) ion traces can then be processed and deconvoluted using time-matching algorithms, allowing product ions to be linked to their parent species based on their chromatographic retention times. In principle, DIA-based methods are an excellent solution for the untargeted analysis of low-abundant lipid species. In practice, however, the exceptional diversity of many biological samples renders the complete chromatographic resolution of structurally-similar lipids virtually impossible, resulting in considerable co-elution and the inability to match precursor and fragment ions by retention time with confidence. Newer technologies that incorporate ion mobility separations have been developed, notably the Sciex Lipidyzer Platform and Waters Travelling-Wave Ion Mobility feature which can be incorporated into SRM, MRM, DIA and DDA-based methods [133]. These technologies exploit the size, shape, charge and/or mass of compounds to provide an additional dimension of separation, which has the potential to increase the number of discrete lipid species that can be identified [71, 134-137].

A. Brutto: PC 34:2

B. Medio: PC 16:0_18:2

C. Genio: PC 16:0/18:2

D. Infinio: PC 16:0/18:2(9Z,12Z)
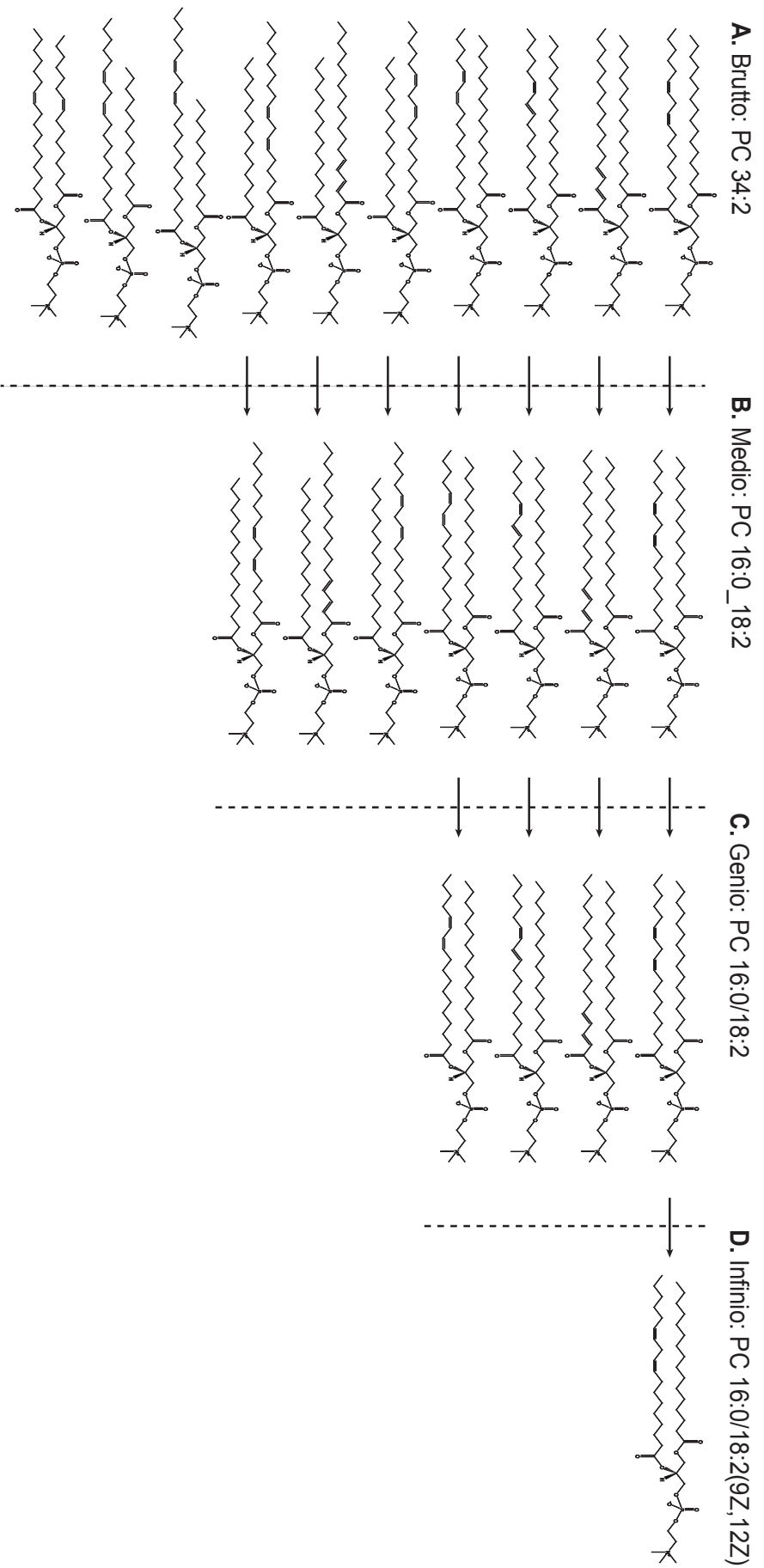
Figure 1. Terminology to denote different levels of hierarchal information common to lipidomic identifications. Palmitoyl-linolenoyl phosphatidylcholine is shown at various levels of information: **A.** Brutto species, where isomeric species containing various fatty acyl constituents cannot be discriminated. **B.** Medio species, where fatty acid constituents are defined but not their *sn*-glycerol regiospecificity. **C.** Genio species, where the regiospecific information is defined. **D.** Infinio species, where the carbon-carbon double bonds of fatty acyl constituents of defined regioisomers are characterized. PC, phosphatidylcholine.

18
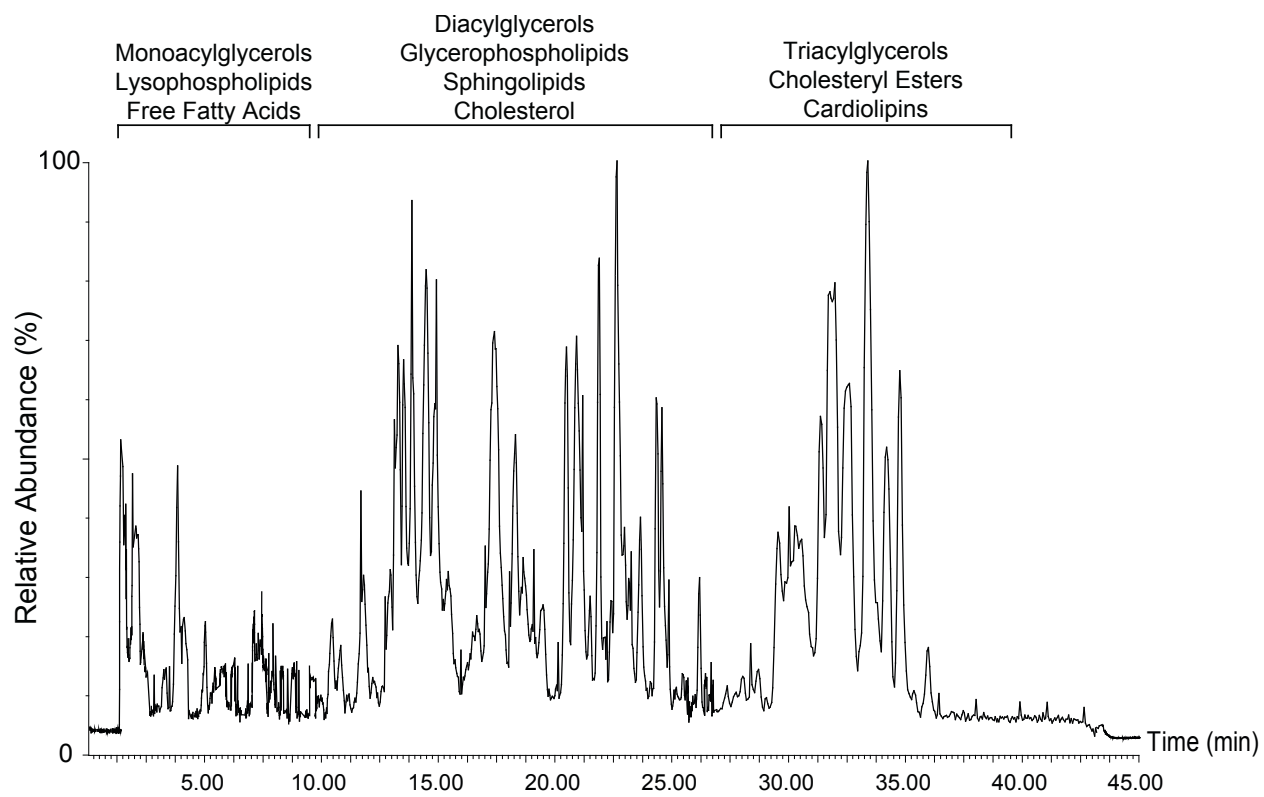
Figure 2. Total ion chromatogram from a UHPLC-MS/MS run of a human whole blood lipid extract sample. The approximate elution times of the major lipid classes in blood are shown.

CHAPTER 3

General Methods and Materials

3.1 Chemicals and Materials

All solvents, including chloroform, methanol, isopropanol, n-butanol, acetonitrile and

hexane (HPLC grade or higher) were purchased from Thermo-Fisher Scientific (Napean, ON,

Canada). Citric acid, disodium phosphate, ammonium formate, formic acid, and 14% BF_3 in

methanol were purchased from Sigma-Aldrich (Oakville, ON, Canada). All lipid standards used

for peak area normalization were purchased from Avanti Polar Lipids (Alabaster, AL, USA).

3.2 Instrumentation

UHPLC-MS/MS was completed using two analytical platforms. A Dionex UltiMate 3000

UHPLC system (Dionex Corporation, Bannockburn, IL, USA) coupled to a Thermo Q-Exactive

Quadrupole-Orbitrap mass spectrometer (QE; Thermo-Fisher Scientific, Waltham, MA, USA)

and a Waters Acquity UPLC system coupled to a Waters Synapt G2Si Quadrupole-Time-of-

Flight mass spectrometer (QToF; Waters Corporation, Milford, MA, USA). The column used

was a Waters Acquity UPLC Charged Surface Hybrid (CSH) 1.7 μm x 2.1 mm x 150 mm, unless

stated otherwise.

3.3 Lipid Extraction

In general, lipids were extracted from samples (whole blood, sunflower oil, brain tissue)

using a modified Folch-based protocol [138]. Briefly, samples were mixed with 3 mL of 2:1

chloroform/methanol (v/v) which contained the internal standard(s). This was followed by

vigorous vortexing for 1 min, the addition of 500 μL of 0.2 M NaH_2PO_4 buffer, inversion, and

centrifugation at 1734 *rcf* at room temperature for 5 min. The organic layer was carefully

extracted and saved, and 2 mL of chloroform were added to the remaining aqueous phases. The

samples were vortexed and centrifuged, and the organic layer was again carefully extracted and

combined with the first set of extracts. Samples were dried under N_2 gas and stored in

chloroform at 4 ºC until analysis. Prior to analysis by UHPLC-MS/MS, the samples were

evaporated again, and lipids were solubilized in 100 μL of the reconstitution solvent (65:35:5

acetonitrile/isopropanol/water (v/v/v) +0.1% formic acid).

3.4 Untargeted Macrolipidomics of Biological Samples by UHPLC-MS/MS

UHPLC was performed using a multi-step reversed-phase gradient described previously

[31, 36]. The mobile phase consisted of (A) 60:40 acetonitrile/water (v/v) +10 mM ammonium

formate +0.1% formic acid, and (B) 90:10 isopropanol/acetonitrile (v/v) +10 mM ammonium

formate +0.1% formic acid. The multi-step gradient used was as follows: solvent B was 32%

from 0-1.5min, followed by a linear increase to 45% B from 1.5-4 min, 50% B from 4-8 min,

55% B from 8-18 min, 60% B from 18-20 min, 70% B from 20-35 min, 95% B from 35-40 min,

95% B from 40-45 min, a decrease to 32% B at 45.1 min and a hold at 32% B until the 48 min

mark. The flow was 250 μL/min, column compartment temperature was 45 ºC, autosampler

temperature was 4 ºC, and the injection volume was 5 μL. The QE and QToF mass spectrometers

were operated in positive and/or negative ESI modes, detailed methods for the various

experiments in this thesis are presented in the appropriate Chapters.

3.5 Fatty Acid Analysis by Gas Chromatography-Flame Ionization Detection

Fatty acid analyses were completed by gas chromatography of fatty acid methyl esters (FAME) [139]. Lipid extracts (obtained as described in Section 3.3) were dried fully under a gentle stream of N_2 gas, followed by the addition of 1.0 mL of 14% BF_3 in methanol and 300 μL of hexane. The samples were capped, vortexed for 1min, and placed in a heating block at 95 ºC for 1hr to generate FAME. Samples were then cooled to room temperature, and 1 mL of double-distilled ultra-pure water (ddH$_2$O) and 1 mL of hexane were added, followed by vigorous vortexing for 1min and centrifugation at 1734 *rcf* for 5 min. The hexane layer, which contained the FAME, was collected and evaporated under N_2 gas. The FAME were then resuspended in 65 μL of heptane and were stored in vials until analysis. The FAME were analyzed by gas chromatography-flame ionization detection using a Varian 3900 gas chromatograph equipped with a DB-FFAP 15 m x 0.1 mm x 0.1 μm film thickness nitroterephthalic acid-modified polyethylene glycol capillary column (J&W Scientific from Agilent Technologies, Mississauga, ON, Canada). Hydrogen was used as the carrier gas at a flow rate of 0.5 mL/min with a split ratio of 100:1. The inlet was heated to 250 ºC and the flame ionization detector was heated to 300 ºC with an air flow rate of 100 mL/min, hydrogen flow rate of 30 mL/min, and nitrogen make-up gas flow rate of 25 mL/min. The detector sampling frequency was set at 50 Hz. The initial oven temperature was 150 ºC with a hold for 0.25 min, followed by a 35 ºC/min ramp to 200 ºC, at 8 ºC ramp to 245 ºC and a hold at 245 ºC for 15 min. Peaks were identified by comparison of retention times to an external standard mix (GLC-462, Nu-Chek Prep, Elysian, MN, USA).

3.6 Data Handling, Automated Lipid Identifications and Statistical Analyses

Peak areas from QE-based analyses were integrated using the Thermo Xcalibur QualBrowser software (version 2.1; Thermo-Fisher Scientific, Waltham, MA, USA), while peak areas from QToF-based analyses were integrated using MassLynx software (version 4.1; Waters Corporation, Milford, MA, USA). Peak areas were normalized by comparison to the area under the curve for the internal standard(s). Automated lipid identifications were made with SimLipid software (version 6.02; PREMIER Biosoft, Palo Alto, CA, USA) using 0.1 Da and 10 ppm precursor and product mass tolerances, respectively. Progenesis QI software (version 2.3; Nonlinear Dynamics, Waters Corporation, Milford, MA, USA) was also used for automated compound identifications using 25 ppm and 5 ppm precursor and product mass tolerances, respectively, with the ChemSpider [140] and LipidBlast [141] databases. One-way ANOVAs and bi-variate Pearson correlations were completed using SPSS for Windows software (release 11.5.1; SPSS Inc. Chicago, IL, USA), Principal Component Analysis (PCA) was completed using Progenesis QI software.

CHAPTER 4

Rationale

Technological advancements in mass spectrometry have enabled the development of sophisticated methods for targeted and untargeted lipidomic profiling, as well as the development of extensive spectral libraries for the identification of tens of thousands of lipid molecules. This has allowed us to better understand and characterize physiological mechanisms that influence human disease. However, the expansion of the field has also resulted in the emergence of several new challenges pertaining to the spectra that is obtained from mass spectrometry-based analyses, as well as the manner in which data are handled and interpreted. In this thesis, special attention will be drawn to particular challenges related to the targeted and untargeted analyses of various sample types. Instrument selection and settings, data acquisition methods, collection preparation and introduction of different types of samples into the mass spectrometer, and interpretation approaches for determining nutritional biomarkers will be examined. Critical differences between various methodological workflows and how they are appropriate to the research question and sample will be highlighted.

In the first study, the impact of two different HRAM analytical platforms and four untargeted data acquisition modes on the lipidomic profile of human whole blood will be contrasted to assess the feasibility of macrolipidomic profiling for biomarker screening. Human whole blood was chosen as it contains a wide spectrum and mix of lipid classes. This will include an evaluation of a novel DIA method and the utility of ion mobility separation using traveling-wave technology, but also an assessment of the abilities of automated software for data processing. In the second study, the ability to perform targeted microlipidomic analyses on an HRAM instrument to support mechanistic research will be examined. Specifically, levels of

lysophosphatidic acid, an endogenously-synthesized lipid signaling molecule that is relatively polar will be determined in mouse plasma. In the third study, macrolipidomic approaches to profile plant oils and mouse brain samples will be developed. These sample types are different in lipid content with plant oils being largely nonpolar lipids such as triacylglycerols, and brain tissue consisting mainly of polar lipids such as glycerophospholipids. Lipidomic profiling of plant oils has potential applications in the food industry for verification of authenticity of types of oils [142]. It is also well known that lipid composition of the brain impacts function and is implicated in neurodegeneration [143, 144], therefore, lipidomic profiling has tremendous potential for understanding brain lipid metabolism. Finally, these methods will be applied to discover novel blood biomarkers for the dietary intake of omega-3 polyunsaturated fatty acids. This will include an examination of human whole blood samples and dietary intake data from a Danish cohort, and blood samples from rats under tight dietary control with and without docosahexaenoic acid (DHA) for different lengths of time. Specific objectives and hypotheses will be presented at the beginning of each project Chapter.

CHAPTER 5

A Cross-Platform and Cross-Acquisition Method Comparison for the Macrolipidomic

Analysis of Human Whole Blood

5.1 Objectives

The ability to identify lipids using automated computer solutions is critical for the future

of untargeted macrolipidomic profiling. Commercially-available software packages can match

experimental data to extensive spectral libraries [75, 133, 141, 145, 146]. However, different

instruments and settings within an instrument employing different separation and detection

technologies that influence the ions generated in MS and MS/MS spectra, which differentially

impacts the number and quality of lipid identifications by automated software [147]. Although

there are some reports of cross-platform and inter-laboratory comparisons for lipidomic and

metabolomic profiling [19, 148-152], a systematic examination of the advantages of ion mobility

in untargeted lipidomic profiling by UHPLC-MS/MS on different analytical platforms for fatty

acyl-containing complex lipids has not been completed.

The purpose of this study was to examine the total number and quality of positive lipid

identifications in human whole blood samples across different HRAM MS platforms and

acquisition modes using automated identification software. Specifically, a Quadrupole/Orbitrap

mass spectrometer (QE) and a Quadrupole/Time-of-Flight mass spectrometer (QToF) were used.

Data dependent acquisition (DDA) was possible on both instruments, the QToF instrument is

also capable of ion mobility separations (annotated as HD for "high-definition") as well as data-

independent acquisition (DIA). Preliminary experiments on the QToF revealed that HD

separation was critical for DIA mode. Therefore, QE data-dependent acquisition (QE DDA),

QToF data-dependent acquisition (QToF DDA), QToF high-definition data-dependent

acquisition (QToF HD-DDA) and QToF high-definition data-independent acquisition (QToF HD-DIA) were examined. Whole blood was selected as the reference sample due to its comprehensive complex lipid profile and the potential in biomarker discovery through dried blood spot screening and analysis.

5.2 Hypotheses

1. Based on the faster scanning capabilities of the QToF instrument, more MS/MS spectra will be acquired, resulting in a higher number of lipid identifications as compared with the QE.

2. The use of ion mobility in the QToF HD-DDA method will result in the identification of a higher number of lipid species as compared with the QToF DDA method.

3. The unbiased QToF HD-DIA method will generate the highest number of lipid identifications using automated software as compared with the QE DDA, QToF DDA and QToF HD-DDA and methods.

5.3 Methods and Materials

In order to minimize the potential effects of other variables, protocols for sample collection, lipid extraction and chromatographic separation by UHPLC were kept identical. Based on the technological differences between the QE and QToF mass spectrometers, some initial differences were expected, including linear dynamic ranges, limits of detection/quantitation, and detector saturation thresholds. Due to this, some preliminary experiments were completed in order to assimilate MS and MS/MS spectra between the two platforms, which included optimizing sample dilution factors and ESI voltages.

5.3.1 Sample Collection and Lipid Extraction

This study received ethics clearance from the University of Waterloo Office of Research Ethics. Venous blood was obtained by a phlebotomist from the antecubital vein of the volunteer study participant (26-year-old healthy male) into ethylenediaminetetraacetic acid-lined vacutainers. The samples were inverted gently on a rocker for 10min and aliquots (500 µL) were saved in cryovials at -80 ºC until lipid extraction. Lipids were prepared from 16 technical replicate samples (20 µL aliquots of whole blood each) as explained in Section 3.3, with 500 pmol of the internal standard (diheptadecanoyl phosphatidylcholine; PC 17:0/17:0) added to each sample. Four samples each were allocated for four different acquisition analysis modes described below.

5.3.2 UHPLC-MS/MS Conditions and Data Handling

Technical replicate whole blood lipid extract samples were analyzed using identical UHPLC conditions on the Waters Acquity UPLC and Dionex UHPLC systems, using the multi-step mobile phase gradient described in Section 3.4 and the Waters Acquity UPLC Charged Surface Hybrid (CSH) 1.7 µm x 2.1 mm x 150 mm column, equipped with a VanGuard CSH 1.7 µm pre-column (Waters Corporation, Milford, MA, USA).

Tandem mass spectrometry was completed using four data acquisition strategies in order to examine the effect that different analytical platforms and data acquisition modes may have on the quality of MS/MS spectra. The four conditions were: (1) QE DDA for top-5 ions with a ± 1.0 Da isolation window and used a normalized collision energy of 17.5 units; (2) QToF DDA for top-5 ions with a ± 1.0 Da isolation window, scan frequency of 0.1 s and transfer cell collision energy ramps of 20 V to 30 V at low mass (*m/z* 50) and 30 V to 50 V at high mass (*m/z*

1000) ; (3) QToF HD-DDA for top-5 ions using the same isolation window and collision energy settings as in QToF DDA ; and (4) QToF HD-DIA with scan frequency 0.2 s, transfer cell collision energy ramp of 20 V to 50 V. For the QE experiment, the mass spectrometer (Thermo Q-Exactive) was operated in positive ESI mode, spray voltage 2.5 kV, 35,000 resolution in MS and 17,500 resolution in MS/MS, scan range m/z 70 to 1000, sheath gas flow rate 35 and capillary temperature 300 ºC. All spectra were lock mass-corrected using di-isooctyl phthalate (m/z 391.28429) which was present in the mobile phase. For the 3 QToF experiments, the mass spectrometer (Water Synapt G2Si) was operated in positive ESI mode, spray voltage 2.5 kV, high-resolution mode (continuum; approximately 55,000 resolution in HD, 42,000 resolution in non-HD), scan range m/z 50 to 1000, scan time 0.2 s/scan, cone voltage 40 V, cone gas flow 100 L/hr, desolvation gas flow 600 L/hr, nebulizer gas flow 7.0b ar, source temperature 140 ºC, desolvation temperature 400 ºC. All spectra were lock mass-corrected using a dedicated ESI spray that infused a 0.2 µg/mL solution of leucine enkephalin (m/z 556.2771) in 1:1 acetonitrile/water (v/v) +0.1% formic acid.

Automated lipid identifications were made using SimLipid software for each of the four data acquisition strategies, using the search parameters described in Section 3.6. Consensus identifications within each of the four data acquisition strategies were determined using custom rule-based algorithms (if/then conditional statements) in Microsoft Excel (version 16.14; Microsoft Corporation, Redmond, WA, USA). Repeated analyte hits were collapsed into a single identification by data-sorting based on lipid confirmation names and fragmentation scores, then removing redundant features to generate harmonized lists of compounds. The quality of lipid identifications was assessed by determining the number of observed fatty acyl fragments within MS/MS spectra for all lipids. If only some fragments were observed (e.g., only 1 acyl fragment

for diacylglycerophospholipids), the other acyl chain(s) were deduced mathematically by mass

subtraction using the *m/z* ratio of the precursor ion. If all fragments were observed (e.g., 2 acyl

fragments for diacylglycerophospholipids), these species were labelled as Full-Acyl

Identifications (FAID). Analyte abundances were determined by adding the absolute intensities

of all fragment ions within individual MS/MS scans. Relative-quantitative abundances were

generated by normalizing all analyte summed ion values by the summed ion value of the internal

standard (PC 17:0/17:0). The quantitative abilities of the four methods were assessed by

converting normalized analyte abundances into Log2-transformed values.

5.4 Results

5.4.1 Number and Quality of Lipid Identifications and the Effect of HD on MS/MS Spectra

There were 678 identifications made with the QE DDA method, including 240

glycerophospholipids, 5 cholesteryl esters, and 433 triacylglycerols (TAG) (Table 1). There were

substantially more lipid identifications made with the QToF HD-DDA (1,695) and QToF DDA

(1,258) methods, but only815 lipids that were identified using the QToF HD-DIA method. Of

these, there were only 344 species that were identified in consensus across all four methods.

Using the QToF HD-DDA method, a larger number of triacylglycerols were identified (906) as

compared with the QToF DDA method (474), as well as a higher number of

phosphatidylethanolamines (250 in QToF HD-DDA vs. 108 in QToF DDA) and a lower number

of phosphatidylcholines (500 in QToF HD-DDA vs. 646 in QToF DDA). Upon closer

examination, it was apparent that the intensity of precursor ions (for example *m/z* 876.8024 for

TAG 16:0_18:1_18:1 in Figure 3) was much higher in MS/MS spectra from the QToF HD-DDA

method (Figure 3C) as compared with spectra from the QToF DDA method (Figure 3B)

suggesting less fragmentation. Similarly, glycerophospholipid MS/MS spectra from the QToF HD-DDA method showed much higher intensities of precursor ions as compared with spectra from the QToF DDA method (spectra not shown).

The QToF DDA method produced the highest number of total lipid identifications with FAID with 432; there were only 238 lipids with FAID from the QE DDA 280 from QToF HD-DDA, and 201 from QToF HD-DIA method (Figure 4). The QToF DDA method had the highest number of total phospholipids (77) and triacylglycerols (355) with FAID as compared with the other methods. The three DDA-based methods had the highest level of agreement as similar proportions of lipids with FAID were identified (approximately 20% of total identifications were phospholipids, 80% were triacylglycerols). However, the QToF HD-DIA method was particularly ineffective at making phospholipid FAID confirmations (only 3% of total identifications). Furthermore, 77 consensus species were found with FAID between QE DDA, QToF DDA and QToF HD-DDA, but this number dropped to 49 when the QToF HD-DIA method was included (Table 2). This included 46 triacylglycerols, only 2 lysophosphatidylcholines and 1 phosphatidylethanolamine.

5.4.2 Differences in DDA Spectra between MS Platforms & Method Quantitative Potentials

The fragmentation behaviour of all lipids was similar between the QE DDA and QToF DDA methods. Ions in the low mass range (i.e., < m/z 200) were moderately more intense in the QToF DDA spectrum (Figure 3B) as compared with QE DDA (Figure 3A), and the intensity of precursor ions was moderately lower in QToF DDA spectra (approximately 1% of the base peak ion) as compared with QE DDA (approximately 5% of the base peak ion). Although the quality

of MS/MS spectra between these two methods was similar, the QToF DDA method produced 77,404 individual MS/MS scans while the QE DDA method only produced 54,754.

Log2-transformed normalized abundances of the 49 consensus FAID species were similar between the three DDA methods (QToF HD-DDA, QToF DDA, QE DDA), but they were not in agreement with data from QToF HD-DIA method (Figure 5). Inter-sample variability was measured at < 5% for all four methods by comparison of normalized peak areas.

5.5 Discussion

There are many variables that can affect the behaviour and detection of lipids from biological samples in UHPLC-MS/MS-based analyses, including various sample preparations, the utilization and type of chromatographic separations, ion creation, separation, fragmentation and detection techniques, and compound identification software solutions. Within our four different mass spectrometry-based strategies, there were comparisons between platforms (QE vs. QToF), MS/MS acquisition modes (DDA vs. DIA) and analyte ion separations in the gas phase with or without ion mobility (DDA vs. HD-DDA).

Only minor differences were visible between QToF DDA and QE DDA spectra which was somewhat surprising. However, the higher number of total identifications with FAID by QToF DDA versus QE DDA may be explained by the much faster sampling frequency of the QToF. The increased identifications appear to be a result of the acquisition of over 22,000 additional MS/MS scans with the QToF, which is in agreement with the first hypothesis.

The QToF HD-DDA method resulted in the highest number of raw identifications, but the QToF DDA method generated the highest quality data, as determined from the high number of lipid confirmations with FAID. The lower number of species with FAID in the QToF HD-

DDA method was associated with lower intensity of product ions in MS/MS scans. Interestingly, the ion mobility (QToF HD-DDA) appeared to have a dampening effect on the amount of energy that was actually applied in MS/MS mode as compared with the non-HD method (QToF DDA), despite having set the collision energy ramps in both methods at the same voltages. This was suggested by the higher intensity of precursor ions in MS/MS spectra from the QToF HD-DDA method (Figure 3C and 3B for QToF HD-DDA and QToF DDA, respectively). This behaviour may be due to the utilization of He and N_2 gases in HD-mode, which are necessary for ion mobility separations [153]. When a specific collision energy voltage is set in a gas-filled region, some portion of this energy is lost due to non-fragment-inducing collisions with the collision partner (in this case Argon), resulting in less energetic collisions of analytes in the transfer cell (i.e., less fragmentation of precursor ions). Additionally, some N_2 from the ion mobility cell can leak into the collision cell, producing in an Ar/N_2 mixture that would result in the deposition of less internal energy in precursor ions through the collision-induced dissociation process [154, 155]. This phenomenon also appears to be dependent on molecule type, structure, charge, size and mass [155], which may explain the inconsistencies that were observed in the number of lipid identifications of different lipid classes that were made between both methods (i.e., higher triacylglycerols & phosphatidylethanolamines, lower phosphatidylcholines in QToF HD-DDA as compared with QToF DDA). These ion "cooling" effects have not yet been fully characterized, and a correction factor that can be used to provide the same amount of kinetic energy to all precursor ions in the collision cell in HD and non-HD methods does not exist for this platform. In regard to the second hypothesis, it appears that ion mobility may increase the number of identifications, but additional experiments examining increased collision energies appear to be

required to determine if meaningful MS/MS spectra can be generated to confirm the identifications at the FAID level.

The QToF HD-DIA method resulted in a remarkably low number of identifications relative to the QToF HD-DDA and QToF DDA methods. Based on the unbiased ion fragmentation approach that is utilized by the QToF HD-DIA approach, it was hypothesized that this method would result in the highest total number of lipid identifications as compared with the three DDA-based methods. These contrary observations may be explained by the fact that the DIA method relies on retention time-matching of precursor (low-energy scanning) and product ions (high-energy scanning) in order to associate ion transitions. In this case, the high degree of complexity and diversity of lipids in whole blood resulted in significant chromatographic co-elution. This appears to have limited the abilities of the peak picking/spectral deconvolution algorithms in identifying lipids. The DIA approach was especially limited in identifying phospholipid species. In the positive ion mode, phospholipids generate fatty acyl product ions of very low intensity, which in a DIA-based approach, may be difficult to discern from signal contributions of other co-eluting species or background chemical noise. With the fundamental difference in the DIA approach, it should not have been a surprise that the DIA approach had the lowest quantitative agreement of product ion sums.

Most lipid identification databases contain MS/MS spectra that have been generated using computer models to simulate fragmentation patterns and quickly build *in silico* libraries [78, 141, 156-158]. These artificial spectra typically rely on ideal conditions where the fragmentation behaviour of specific lipid classes is conserved, considering factors such as the common losses of head groups (i.e., *m/z* 184.0733 ion corresponding to the choline group of all phosphatidylcholines in the positive ion mode), predictable fatty acyl chain length fragments or

neutral losses, etc. Through this, similarity scores can be generated to provide an idea of the confidence of the identification. However, as shown in this Chapter and elsewhere [156, 159], the intensity of lipid fragments can vary considerably between MS platforms and acquisition modes. This can result in a decreased ability to match experimental spectra to lipid libraries, lowering the number of positive lipid identifications and an increasing the likelihood of lipid misannotations. Other factors are known to influence the number of false-positives (i.e., incorrect identifications) and false-negatives (i.e., missing annotations) including unintentional in-source fragments [160] and sample preparation-related artifacts [161]. From this project, it is clear that further work is needed in order to characterize the ion cooling effects that were observed here in HD mode, and the DIA method requires technological advances that allows matching of product ions to their respective precursor ions.

Table 1. Number of lipid identifications from whole blood samples using four mass spectrometry acquisition strategies

Main Class	Lipid Sub-Class	Acquisition Mode			
		QE DDA	QToF DDA	QToF HD-DDA	QToF HD-DIA
Glycerophosphocholines	Diacylglycerophosphocholines	104	400	268	69
Glycerophosphocholines	1-alkyl,2-acylglycerophosphocholines	42	114	77	38
Glycerophosphocholines	Monoacylglycerophosphocholines	14	21	17	14
Glycerophosphocholines	1-(1Z-alkenyl),2-acylglycerophosphocholines	7	67	44	7
Glycerophosphocholines	Dialkylglycerophosphocholines	4	22	16	5
Glycerophosphocholines	1-acyl,2-(1Z-alkenyl)-glycerophosphocholines	1	7	4	0
Glycerophosphocholines	1-acyl,2-alkylglycerophosphocholines	0	7	2	1
Glycerophosphocholines	1Z-alkenylglycerophosphocholines	0	3	2	1
Glycerophosphocholines	Monoalkylglycerophosphocholines	0	2	2	2
Oxidized Glycerophospholipids	Oxidized glycerophosphocholines	0	3	0	0
Glycerophosphoethanolamines	Diacylglycerophosphoethanolamines	34	95	164	16
Glycerophosphoethanolamines	1-(1Z-alkenyl),2-acylglycerophosphoethanolamines	10	8	35	6
Glycerophosphoethanolamines	Monoacylglycerophosphoethanolamines	6	0	9	0
Glycerophosphoethanolamines	1-alkyl,2-acylglycerophosphoethanolamines	1	0	35	1
Glycerophosphoethanolamines	Dialkylglycerophosphoethanolamines	0	0	2	0
Glycerophosphoethanolamines	1-acyl,2-alkylglycerophosphoethanolamines	0	0	1	1
Oxidized Glycerophospholipids	Oxidized glycerophosphoethanolamines	5	5	4	4
Glycerophosphoserines	Diacylglycerophosphoserines	12	25	25	7
Glycerophosphoinositols	Diacylglycerophosphoinositols	0	0	7	0
Glycerophosphoglycerols	Dialkylglycerophosphoglycerols	0	0	3	1
Glycerophosphoglycerols	Diacylglycerophosphoglycerols	0	0	0	1
Glycerophosphates	Diacylglycerophosphates	0	0	67	4
Glycerophosphates	Monoacylglycerophosphates	0	0	1	0
Sterols	Steryl esters	5	5	4	6
Triradylglycerols	Triacylglycerols	433	474	906	631
	Total	**678**	**1258**	**1695**	**815**

QE, Q-Exactive mass spectrometer; QToF, Quadrupole-Time-of-Flight mass spectrometer; HD, high-definition; DDA, data-dependent acquisition; DIA, data-independent acquisition.

A. QE DDA MS/MS Spectrum
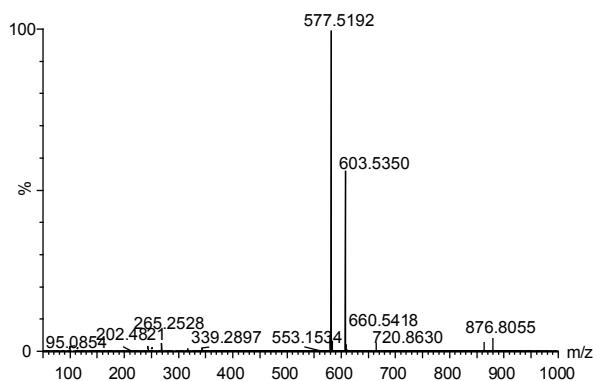
B. QToF DDA MS/MS Spectrum
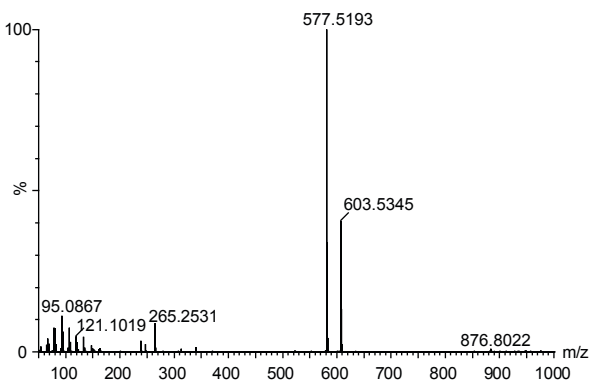
C. QToF HD-DDA MS/MS Spectrum
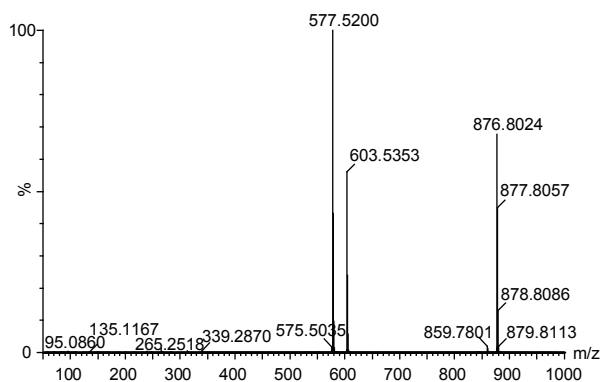
D. QToF HD-DIA MS/MS Spectrum
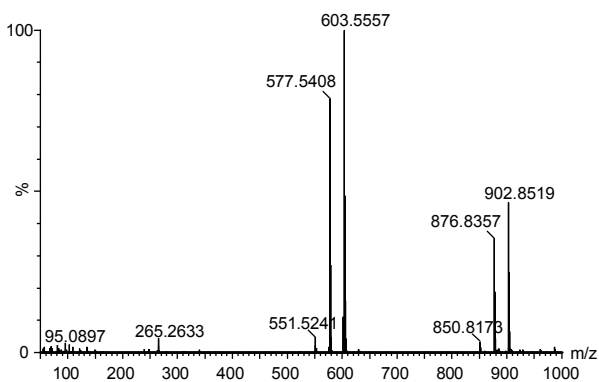
Figure 3. MS/MS Spectra for TAG 16:0_18:1_18:1 (m/z 876.8015 as [M+NH$_4$]$^+$) acquired using **A.** the QE DDA method, **B.** the QToF DDA method, **C.** QToF HD-DDA method, and **D.** QToF HD-DIA method. QE, Q-Exactive mass spectrometer; QToF, Quadrupole-Time-of-Flight mass spectrometer; HD, high-definition; DDA, data-dependent acquisition; DIA, data-independent acquisition; MS/MS tandem mass spectrometry; TAG, triacylglycerol.
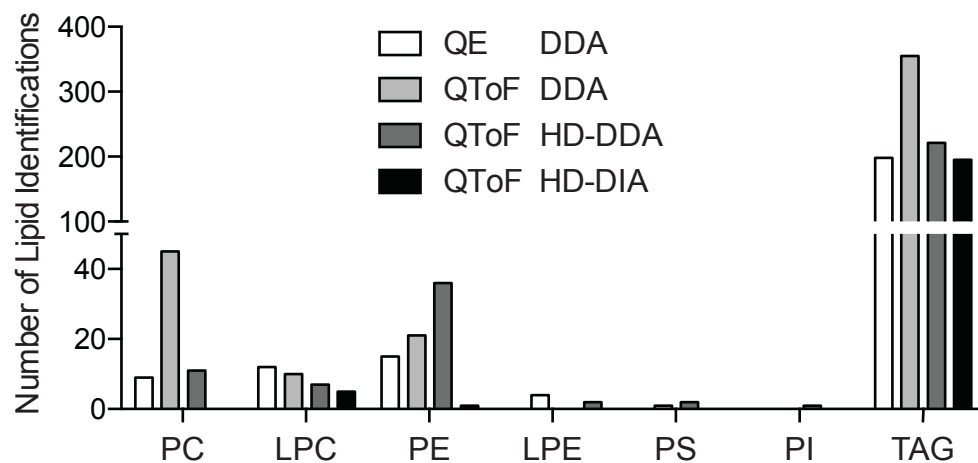
Figure 4. Number of lipid identifications with full-acyl identifications. PC, phosphatidylcholine; LPC lysophosphatidylcholine; PE, phosphatidylethanolamine; LPE, lysophosphatidylethanolamine; PS, phosphatidylserine; PI, phosphatidylinositol; TAG, triacylglycerol; QE, Q-Exactive mass spectrometer; QToF, Quadrupole-Time-of-Flight mass spectrometer; HD, high-definition; DDA, data-dependent acquisition; DIA, data-independent acquisition.

Table 2. Lipid species with full-acyl identifications that were found in consensus

Main Class	Lipid Sub-Class	Lipid Identification
Glycerophosphocholines	Monoacylglycerophosphocholines	PC 0:0_17:0
Glycerophosphocholines	Monoacylglycerophosphocholines	PC 0:0_18:1
Glycerophosphoethanolamines	Diacylglycerophosphoethanolamines	PE 16:0_18:2
Triradylglycerols	Triacylglycerols	TAG 12:0_18:1_18:1
Triradylglycerols	Triacylglycerols	TAG 12:0_18:1_18:2
Triradylglycerols	Triacylglycerols	TAG 14:0_16:0_18:2
Triradylglycerols	Triacylglycerols	TAG 14:0_16:1_18:1
Triradylglycerols	Triacylglycerols	TAG 14:0_16:1_18:2
Triradylglycerols	Triacylglycerols	TAG 14:0_18:1_18:3
Triradylglycerols	Triacylglycerols	TAG 14:0_18:2_18:2
Triradylglycerols	Triacylglycerols	TAG 15:0_18:1_18:1
Triradylglycerols	Triacylglycerols	TAG 15:0_18:1_18:2
Triradylglycerols	Triacylglycerols	TAG 15:0_18:2_18:2
Triradylglycerols	Triacylglycerols	TAG 16:0_16:0_18:1
Triradylglycerols	Triacylglycerols	TAG 16:0_16:1_16:1
Triradylglycerols	Triacylglycerols	TAG 16:0_17:0_18:1
Triradylglycerols	Triacylglycerols	TAG 16:0_17:1_18:0
Triradylglycerols	Triacylglycerols	TAG 16:0_17:1_18:1
Triradylglycerols	Triacylglycerols	TAG 16:0_17:1_18:2
Triradylglycerols	Triacylglycerols	TAG 16:0_18:0_18:1
Triradylglycerols	Triacylglycerols	TAG 16:0_18:1_18:2
Triradylglycerols	Triacylglycerols	TAG 16:0_18:1_22:0
Triradylglycerols	Triacylglycerols	TAG 16:0_18:1_22:5
Triradylglycerols	Triacylglycerols	TAG 16:0_18:1_22:6
Triradylglycerols	Triacylglycerols	TAG 16:0_18:2_18:2
Triradylglycerols	Triacylglycerols	TAG 16:0_18:2_18:3
Triradylglycerols	Triacylglycerols	TAG 16:1_17:0_18:1
Triradylglycerols	Triacylglycerols	TAG 16:1_17:1_18:1
Triradylglycerols	Triacylglycerols	TAG 16:1_18:1_18:1
Triradylglycerols	Triacylglycerols	TAG 16:1_18:1_18:3
Triradylglycerols	Triacylglycerols	TAG 16:1_18:1_19:1
Triradylglycerols	Triacylglycerols	TAG 16:1_18:2_18:2
Triradylglycerols	Triacylglycerols	TAG 17:0_17:0_17:1
Triradylglycerols	Triacylglycerols	TAG 17:0_17:1_19:1
Triradylglycerols	Triacylglycerols	TAG 17:0_18:1_18:1
Triradylglycerols	Triacylglycerols	TAG 17:0_18:1_18:2
Triradylglycerols	Triacylglycerols	TAG 17:1_18:0_18:1
Triradylglycerols	Triacylglycerols	TAG 17:1_18:1_18:1
Triradylglycerols	Triacylglycerols	TAG 17:1_18:1_18:2
Triradylglycerols	Triacylglycerols	TAG 17:1_18:1_19:1
Triradylglycerols	Triacylglycerols	TAG 18:0_18:1_18:2
Triradylglycerols	Triacylglycerols	TAG 18:0_18:1_20:0
Triradylglycerols	Triacylglycerols	TAG 18:1_18:1_18:1
Triradylglycerols	Triacylglycerols	TAG 18:1_18:1_18:2
Triradylglycerols	Triacylglycerols	TAG 18:1_18:1_20:0
Triradylglycerols	Triacylglycerols	TAG 18:1_18:1_20:4
Triradylglycerols	Triacylglycerols	TAG 18:1_18:1_20:5
Triradylglycerols	Triacylglycerols	TAG 18:1_19:0_19:0
Triradylglycerols	Triacylglycerols	TAG 18:2_18:2_18:3

PC, phosphatidylcholine; PE, phosphatidylethanolamine; TAG, triacylglycerol.
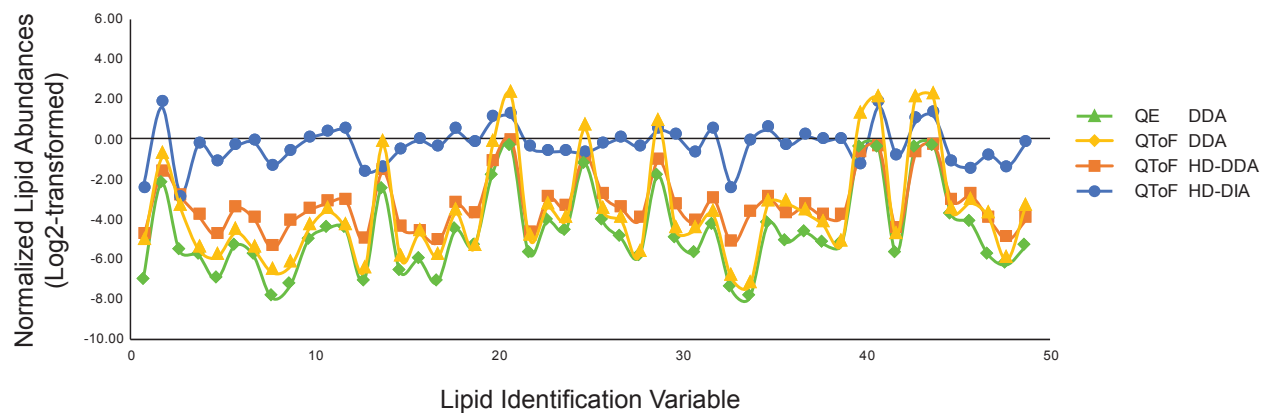
Figure 5. Log2-transformed normalized abundances of the 49 consensus lipid species with full acyl identifications between the four mass spectrometry acquisition strategies. Lipid Identification Variable: species can be found in Table 2. QE, Q-Exactive mass spectrometer; QToF, Quadrupole-Time-of-Flight mass spectrometer; HD, high-definition; DDA, data-dependent acquisition DIA, data-independent acquisition.

CHAPTER 6

Microlipidomic Analysis of Lysophosphatidic Acid Regioisomeric Species in Mouse Plasma

6.1 Objectives

Lysophosphatidic acids (LPA) are highly-polar lipids that can act as potent signaling molecules, and which have been implicated in many pathophysiological processes including glucose intolerance, cancer, cardiovascular disease, arthritis, and asthma [162-164]. LPA are the simplest form of all glycerophospholipids. They are comprised of a single fatty acyl moiety esterified to the *sn*-1 or *sn*-2 position of glycerol-3-phosphate and can range in molecular weight from approximately 215 Da (for LPA 2:0) to 522 Da (for LPA 24:0). These bioactive lipids are highly polar in nature, and as such, they are relatively immiscible in organic solvents. This presents a major analytical challenge as compared with other phospholipids which are easily solubilized in solvents like chloroform and methanol, rendering global liquid-liquid extraction techniques inadequate for LPA analysis [161]. Furthermore, LPA are typically found in the very-low abundance regime, with LPA 18:2 being the specie of highest abundance in plasma (concentration < 1.0 μmol/L) [161]. Therefore, LPA measurements necessitate the implementation of targeted analytical methods for accurate quantitation.

Several extraction protocols have been compared [161, 165], and regioisomeric discrimination of LPA species (i.e., specifying *sn*-1-acyl or *sn*-2-acyl localization on the glycerol backbone) has been demonstrated using untargeted nano-flow liquid chromatography-tandem mass spectrometry [86]. Like other lysophospholipids, LPA species appear to have a regioisomer distribution ratio of *sn*-1-acyl:*sn*-2-acyl of approximately 9:1, which is due to a higher molecular stability when the fatty acyl chain is located at the *sn*-1 position at physiological pH and temperature [166-168]. In this study, a butanol-based extraction was modified by reducing the

volume of solvents used. We also sought to determine regioisomeric species of LPA in plasma using conventional-flow UHPLC-MS/MS with standard instrumentation. This was achieved by evaluating the chromatographic resolution of LPA 16:0 using various commercially-available reversed-phase C18 UHPLC columns with different chemistries. Generally, C18 columns consist of alkyl chains (18 carbons) covalently linked to a silicon base to form a stationary phase. C18 columns can vary based on modifications to the size and porosity of the particles, the addition of functional groups, and bridged or cross-linked residues on the silica matrix. Three of the columns examined (Supelco Ascentis Express, Waters BEH, Waters CSH) were purchased for lipidomic analyses of various samples in our laboratory [31, 36, 169, 170], and have also been used by others [171-173]. The fourth column has been used for polar compound separations (Waters HSS-T3) [174, 175]. Additionally, we optimized collision energy voltages to maximize the abundance of a glycerol-phosphate rearrangement product ion to enable high sensitivity with Time-of-Flight/Multiple Reaction Monitoring technology (ToF-MRM). Finally, the method presented here was used to quantitate regioisomeric LPA species in mouse plasma.

6.2 Hypotheses

1. The use of a UHPLC column compatible with polar analytes (Waters HSS-T3) will result in the best chromatographic separation of LPA species as compared with other reversed-phase C18 UHPLC columns.

2. A modified butanol-based extraction protocol will result in satisfactory LPA yields similar to what has been reported for the original protocol.

6.3 Methods, Materials and Study Design

6.3.1 Sample Collection and Standards

The collection of blood samples from mice received ethics clearance from the University

of Waterloo Office of Research Ethics. Male C57BL/6 mice (18 weeks old, n = 4) were used in

this study. The mice were housed in groups of 5 per cage, they were fed a Teklad standard rodent

diet (Envigo Mississauga, ON, Canada) and had *ad libitum* access to food. The mice were

sacrificed by cervical dislocation and whole blood was collected via cardiac puncture into

ethylenediaminetetraacetic acid-lined vacutainers. Blood samples were centrifuged at 1734 *rcf* at

4 ºC for 15 min, and the plasma fraction was collected, aliquoted (100 µL) and stored at -80 ºC

until lipid extraction. LPA 16:0 and LPA 17:0 lipid standards containing a mix of both *sn*-1 and

sn-2 regioisomers in a ratio of approximately 9:1 *sn*-1-acyl:*sn*-2-acyl were purchased from

Avanti Polar Lipids (Alabaster, AL, USA).

6.3.2 Instrument Settings

UHPLC-MS/MS was completed using the Waters Acquity UPLC System and Waters

Synapt G2S*i* QToF mass spectrometer. Chromatography was evaluated using four commercially-

available reversed phase UHPLC columns (details in Section 6.3.3). The mobile phase consisted

of (A) 60:40 methanol/water (v/v) +5 mM ammonium formate +1% formic acid and (B) 100%

methanol +5 mM ammonium formate +1% formic acid. The multi-step gradient used was as

follows: solvent B was 10% from 0-1min at 350 µL/min, followed by a linear increase to 100%

B from 1-3 min at 400 µL/min, 100% B from 3-8 min at 400 µL/min, a decrease to 10% B at

8.1 min at 350 µL/min and a hold at 10% B until the 10 min mark. The column compartment was

40 ºC, autosampler temperature was 4 ºC, and the injection volume was 10 µL.

The mass spectrometer was operated in negative electrospray ionization mode, spray voltage -2.0 kV, sensitivity mode (centroid), scan time 0.2 s/scan, scan range *m/z* 60 to 600, cone voltage 40 V, cone gas flow 100 L/hr, desolvation gas flow 600 L/hr, nebulizer gas flow 7.0 bar, source temperature 140 ºC, desolvation temperature 400 ºC. Spectra were lock mass-corrected using leucine enkephalin (*m/z* 554.2615). Fragmentation in the transfer cell using several collision energy ramps was optimized in a series of trial and error experiments described in Section 6.3.4.

6.3.3 Column Evaluation

An LPA 16:0 stock solution was prepared at a concentration of 50 pmol/μL in 3:1 methanol/isopropanol (v/v) and columns were evaluated using the same mobile phase gradient. The columns were a Waters Acquity UPLC Ethylene Bridged Hybrid (BEH), 1.7 μm x 2.1 mm x 50 mm; a Waters Acquity UPLC Charged Surface Hybrid (CSH), 1.7 μm x 2.1 mm x 150 mm; a Waters Acquity UPLC High-Strength Silica (HSS-T3), 1.8 μm x 2.1 mm x 100 mm; and a Supelco Ascentis Express, 2.7 μm x 2.1 mm x 150 mm. The application of this method for the analysis of mouse plasma was completed using the Waters Acquity UPLC High-Strength Silica (HSS-T3), 1.8 μm x 2.1 mm x 100 mm equipped with a VanGuard HSS-T3 1.8 μm pre-column (Milford, MA, USA). The resolution of extracted peak profiles were assessed using the following formula: Resolution = (difference in peak apex retention times)/(average peak widths at baseline), and satisfactory separations were considered with Resolution values $\geq$ 1 [176].

6.3.4 Time-of-Flight Multiple Reaction Monitoring Optimization

For the optimization of ToF-MRM settings, several combinations of collision energy ramps were examined in order to maximize the abundance of product ions in MS/MS using the LPA 16:0 stock solution. The specific voltages that were tested can be found in Table 3. The analyte transitions that were monitored included the deprotonated molecular ion for LPA 16:0 (as precursor and product), the acyl fragment from this molecule as a carboxylate anion (R-COO$^-$ product), and the dehydrated cyclic glycerol-3-phosphate ion with m/z 152.9954 (product).

6.3.5 Assessment of Extraction Efficiency and Linearity

Lipids were extracted using a modified n-butanol-based protocol described earlier [161], using half of the volumes of all solvents while keeping the same ratios. The extraction solvents were 1.5:4:2 buffer/butanol/water-saturated butanol (v/v/v); the buffer was 30 mM citric acid and 40 mM disodium phosphate at pH = 4.0, and the water-saturated butanol was 9:1 butanol/water (v/v). The efficiency of this modified protocol was assessed using a spike and recovery approach using LPA 16:0 in methanol at a concentration of 0.02 nmol/µL. Aliquots (25 µL) delivering 0.5 nmol of LPA 16:0 (sum of both sn-1 and sn-2 regioisomers) were pipetted into nine 10 mL test tubes, and samples were dried fully under N$_2$ gas. Three aliquots were prepared for analysis by reconstituting into 100 µL of the reconstitution solvent (Spike), which was 3:1 methanol/isopropanol (v/v), with 0.5 nmol of the internal standard (LPA 17:0). Another three aliquots went through the extraction protocol (Spike-Extract) and the matrix effect was examined in the remaining three aliquots (Spike+Plasma-Extract) by resuspending in 50 µL of mouse plasma prior to extraction. Extraction of the Spike-Extract and Spike+Plasma-Extract samples began with the addition of 750 µL of the buffer followed by vigorous vortexing. The n-butanol

45

(2.0 mL) was added to the samples followed by vigorous vortexing. Water-saturated n-butanol (1 mL) was then added. Samples were then vortexed, centrifuged at 2000 *rcf* for 15min, and the resulting top organic layer, which contained the lipids, was collected. The lipid extracts were then dried fully under N_2 gas, resuspended in the reconstitution solvent and stored at 4 ºC until analysis.

A series of standard dilutions were prepared using LPA 17:0 in the presence of 50 µL plasma in order to assess linearity between 125 µmol/L (1250 pmol on column) down to 0.00064 µmol/L (0.0064 pmol on column), with a total of 9 points on the curve. Lipids were extracted using the modified butanol-based protocol described above, and the samples were reconstituted in 100 µL of 3:1 methanol/isopropanol (v/v) to achieve the desired internal standard concentrations. The samples were then analyzed by UHPLC-MS/MS using the Waters Acquity UPLC High-Strength Silica (HSS-T3) column, and a 20 V to 30 V collision energy ramp. Details for these latter choices are provided in Section 6.4.

6.3.6 Application of Method Using Mouse Plasma

Lipids were extracted from plasma samples using n-butanol containing 20 pmol LPA 17:0 as the internal standard in each sample. Lipid extracts were then analyzed by the UHPLC-MS/MS with conditions described above, following the inclusion of precursor-product ion transitions in ToF-MRM for 6 LPA species that have been previously measured in plasma [161, 177, 178].

For the evaluation of collision energy ramps in ToF-MRM, data are presented as raw peak areas from extracted ion chromatograms. For the spike and recovery and the quantitative mouse plasma experiments, raw peak areas were normalized using the area under the curve for the LPA 17:0 internal standard, and concentrations were adjusted to the volume of plasma used. Regioisomer identifications of resolved chromatographic peaks were confirmed using the known ratio of *sn*-1-acyl:*sn*-2-acyl of the LPA 16:0 standard, where the *sn*-2 isomer eluted earlier in the chromatogram than the *sn*-1 isomer. Comparisons of LPA 16:0 abundances in the spike and recovery experiments were assessed by one-way ANOVA with Tukey post-hoc test (significance was inferred at $p < 0.05$). Differences in regioisomer distributions in mouse plasma were assessed using two-tailed Student's *t*-tests (significance was inferred at $p < 0.05$). Values are presented as mean ± standard deviation of technical replicates (n=3) and biological replicates (n=4) for the spike and recovery experiment and the quantitative mouse plasma experiments, respectively.

6.4 Results

6.4.1 Development of the Chromatographic Method

We examined the ability of four commercially-available reversed-phase columns to resolve LPA 16:0 *sn*-1 and *sn*-2 regioisomers using a methanol/water-based mobile phase. Both the BEH and CSH columns performed poorly, and resulted in broad, tailing peaks that eluted over the course of 5 min and 2.5 min, respectively (Figure 6A and B). There was a modest improvement in peak shape with the use of the Ascentis Express column (Figure 6C) despite having a larger particle size (2.7 μm) as compared with the BEH and CSH columns (both

1.7 μm), but the extracted ion peak profiles from the Ascentis Express column were approximately 1 min wide and regioisomers were still unresolved. Finally, the use of the HSS-T3 column resulted in the best peak shapes, with peak widths < 20 s (Figure 6D) and a base peak ion intensity that was over 10-fold higher (7.74×10^5) than that of the extracted ion chromatogram from the Ascentis Express run (5.97×10^4). Resolution values of all regioisomeric peak pairs were calculated to be greater than 1.0, suggesting adequate separations.

6.4.2 Optimization of the Time-of-Flight/Multiple-Reaction Monitoring (ToF-MRM) Method

Direct infusion-MS/MS of the LPA 16:0 stock standard solution revealed a characteristic LPA spectrum with a base peak ion at *m/z* 152.9954, corresponding to the dehydrated cyclic anion of glycerol-3-phosphate (Figure 7). Less intense fragment ions corresponding to the carboxylate anion form of the fatty acyl moiety (as R-COO⁻), and three other glycerol-3-phosphate or phosphate head group-related ions were also observed. In preliminary ToF-MRM experiments, we observed that the inclusion of the *m/z* 152.9954 ion in the list of product transitions was critical in achieving the highest sensitivity. The exclusion of this ion resulted in a nearly 100-fold decrease in the intensity of the base peak ion in ToF-MRM extracted ion chromatograms. To optimize the sensitivity of this method, several combinations of collision energy ramp voltages were examined to maximize the intensity of the *m/z* 152.9954 ion (Table 3). We determined that a ramp of 20 V to 30 V resulted in the highest product ion intensity, as it appears to balance providing enough kinetic energy to maximize the fragmentation of precursor ions without causing significant ion scattering. This collision energy ramp was used to assess the efficiency of the modified butanol-based extraction procedure. Precursor and product ion ToF-MRM transitions were generated theoretically for LPA 17:0 (internal standard), 18:0, 18:1, 18:2,

20:4 and 22:6 by examining the fragmentation behaviour of LPA 16:0 (Figure 7), this information can be found in Table 4.

6.4.3 Assessment of Extraction Efficiency, Linearity, and Quantitative Profiling of Mouse Plasma LPA Species

LPA 16:0 recoveries of approximately 91% (0.45 nmol recovered from the 0.5 nmol that were spiked) were observed following lipid extraction (i.e., Spike-Extract samples; Figure 8). Furthermore, losses of approximately 31% were observed in the Spike+Plasma-Extract samples (0.34 nmol recovered from 0.5 nmol spiked). The present method was evaluated using a series of standard dilutions in order to determine linear dynamic ranges and limits of detection (Figure 9). A linear response was observed between 0.0032 pmol and 50 pmol of the LPA 17:0 standard on column, and a plateau in the response was observed at higher concentrations up to 1250 pmol on column. The limits of detection were estimated at 0.00064 pmol on column (signal:noise ratio = 3:1).

Finally, the UHPLC-MS/MS method developed was used to quantitatively profile highly-abundant species of LPA in mouse plasma by including ToF-MRM precursor-product ion transitions for 6 common LPA species previously measured in plasma [161, 177, 178]. All of the measured LPA species elute in under 1.0min of each other, starting with LPA 22:6 at approximately 3.4 min and finishing with LPA 18:0 at approximately 3.9 min. We observed that LPA *sn*-1-18:2 was the most highly-abundant molecule from this family (0.56 ± 0.13 μmol/L; Figure 10), which is in agreement with previous literature [161, 177, 178]. From highest to lowest, the concentrations of the species identified here were as follows: 18:2 > 22:6 > 20:4 > 16:0 > 18:0 > 18:1. Additionally, it appears that the *sn*-1-acyl isomers are more abundant than

their *sn*-2-acyl counterparts for 16:0, 18:0, 18:2, 20:4 and 22:6 species, but no significant differences were observed in the abundances of *sn*-1- and *sn*-2-18:1 species ($p = 0.79$).

6.5 Discussion

Although the analysis of most lipids is possible using untargeted macrolipidomic workflows, profiling LPA species in plasma requires careful sampling, specialized extraction protocols, and highly-sensitive detection techniques. In this study, we have optimized a method for the measurement of six regioisomeric LPA pairs through 1) assessing the chromatographic peak resolution of an LPA 16:0 regioisomer standard mix with four reversed-phase C18 UHPLC columns, 2) evaluating the extraction efficiency of a modified butanol-based extraction method, and 3) optimizing ToF-MRM technology for sensitive analyte detection.

Regioisomeric discrimination of LPA species has been shown previously using untargeted nano-flow LC-MS [86]. Although this technique promises better sensitivity than conventional-flow applications [179], it appears to be less robust in terms of sample capacity and retention time precision [180], and remains largely unadopted by the lipidomics community. Additionally, long run times (approximately 50 min) do not make these methods amenable for high-throughput and screening applications. In this Chapter, we examined four reversed-phase C18 UHPLC columns in their ability to resolve regioisomeric pairs of LPA using conventional instrumentation. We found that the BEH and CSH columns performed poorly, and while there was a modest improvement in peak shapes through the use of the Ascentis Express column, the use of the HSS-T3 column resulted in the best peak shapes and the resolution of regioisomeric LPA pairs. These observations may be due to the larger surface area of the of the HSS-T3 particles (230 m^2/g) as compared with the others (185 m^2/g for BEH and CSH, and 225 m^2/g for

Ascentis Express), which enables faster interactions of the analytes with the stationary phase, resulting in better retentivity [181, 182]. Additionally, the T3-endcapping and lower ligand density of this column has been shown to perform well with low molecular weight, polar analytes [174, 175]. Based on these findings, the HSS-T3 column was used in subsequent analyses.

Previously, butanol-based protocols have been criticized for being time-consuming relative to other liquid-liquid extraction procedures [165]. Here, halving of all solvent volumes resulted in a reduced environmental impact of the extraction and reduced evaporation times during sample processing, which improved throughput. With this modified extraction protocol, only small lipid losses were observed as determined from the spike and recovery experiments, and the losses were similar to previous findings [177, 183, 184]. Additionally, matrix-related ion suppression effects were also in agreement with what has been reported in the literature [165, 184, 185]. There are other extraction protocols that have been evaluated in their ability to extract highly-polar lipids, including some that use methyl-*tert*-butyl ether [165] and modified Folch [36, 138] and Bligh-Dyer methods [186-188]. Many of these techniques utilize strong acids, such as concentrated HCl, to shift the equilibrium of the polar analytes and increase their partitioning into the organic phase. However, it has been noted in several studies [177, 183-185, 189] that the use of strong acids can result in the non-enzymatic/spontaneous hydrolysis of the phospholipid head groups of other lysophospholipids, especially lysophosphatidylcholine, which introduces extraction-produced LPA artefacts into the sample. Although only 2% of total lysophosphatidylcholine has been observed to undergo acid-mediated hydrolysis into LPA in plasma [185], the large proportion of lysophosphatidylcholine that is present in plasma relative to LPA could artefactually increase LPA levels by several fold.

Finally, we applied this method for the quantitation of *sn*-1/*sn*-2 regioisomeric pairs of

LPA with 16:0, 18:0, 18:1, 18:2, 20:4 and 22:6 fatty acyl chains, and found that the

concentrations of these species were similar to those reported earlier [161, 190-192].

Interestingly, it appears that the *sn*-1-acyl isomers are more abundant than the *sn*-2-acyl isomers

for 16:0, 18:0, 18:2, 20:4 and 22:6 species which was in agreement with the literature [166-168],

but no significant differences were observed in the abundances of *sn*-1- and *sn*-2-18:1 species

($p = 0.8$). This suggests that there may be an underlying physiological mechanism responsible for

regulating the levels of specific LPA regioisomers in plasma, which can act as preferred

substrates to different LPA-receptors [193, 194].

In addition to plasma, serum is often collected in research and clinical settings as part of

routine laboratory procedures. It has been previously reported that LPA concentrations in serum

are approximately 10-fold higher than in plasma [195, 196]. We confirmed this phenomenon in

an *ad hoc* analysis (total LPA were 8.45 µmol/L in serum from a similar rodent model). LPA are

generated through the onset of the clotting process by platelet activation and phospholipase-D-

mediated hydrolysis of lysophosphatidylcholines and other lysophospholipids. Although LPA

levels are higher in serum than in plasma, these concentrations are still within the linear dynamic

range of the present method. However, the use of serum for LPA measurements should be

avoided due to potential for high variability that is related to sample collection. Therefore, blood

samples should be collected in the presence of anticoagulants such as ethylenediaminetetraacetic

acid or lithium-heparin.

Although several papers exist in which regioisomeric species of phospholipids and

lysophospholipids have been resolved by reversed-phase UHPLC [183, 197, 198], to our

knowledge this is the first method that has been developed specifically for the targeted analysis

of LPA regioisomeric species using conventional flow UHPLC-MS/MS. Additionally, the short run times (10 min) and the ability to monitor several precursor/product ion transitions using ToF-MRM with high sensitivity and selectivity allows for fast profiling of plasma LPA species. Novel solid phase extraction cartridges are also available [199], which have shown excellent selectivity and high extraction efficiencies and can be coupled to the present UHPLC-MS/MS workflow for high-throughput analyses. Further work remains in evaluating the behaviour and regioisomeric distributions of LPA species in plasma that contain other fatty acids besides the ones that were identified here, as well as adapting this method for the analysis of other biological samples.

Table 3. Collision energy (CE) ramps and the resulting peak areas from extracted ion chromatograms (arbitrary units) for LPA 16:0.

Initial CE (V)	Final CE (V)	Area Under the Curve (AU)
10	10	0.71
10	20	2.86
10	30	3.98
10	40	3.12
10	50	2.64
20	20	5.50
20	**30**	**5.82***
20	40	3.54
20	50	2.54
30	30	4.01
30	40	1.60
30	50	0.98
40	40	0.46
40	50	0.14
50	50	0.02

* The highest peak area from ToF-MRM extracted ion chromatograms was obtained by using a collision energy ramp of 20 V to 30 V. LPA, lysophosphatidic acid; CE, collision energy; AU, arbitrary units.

A. Waters BEH Column Extracted Ion Chromatogram

2.59 X 10³

B. Waters CSH Column Extracted Ion Chromatogram

4.10 X 10³

C. Supelco Ascentis Express Column Extracted Ion Chromatogram

5.97 X 10⁴

D. Waters HSS-T3 Column Extracted Ion Chromatogram

7.74 X 10⁵
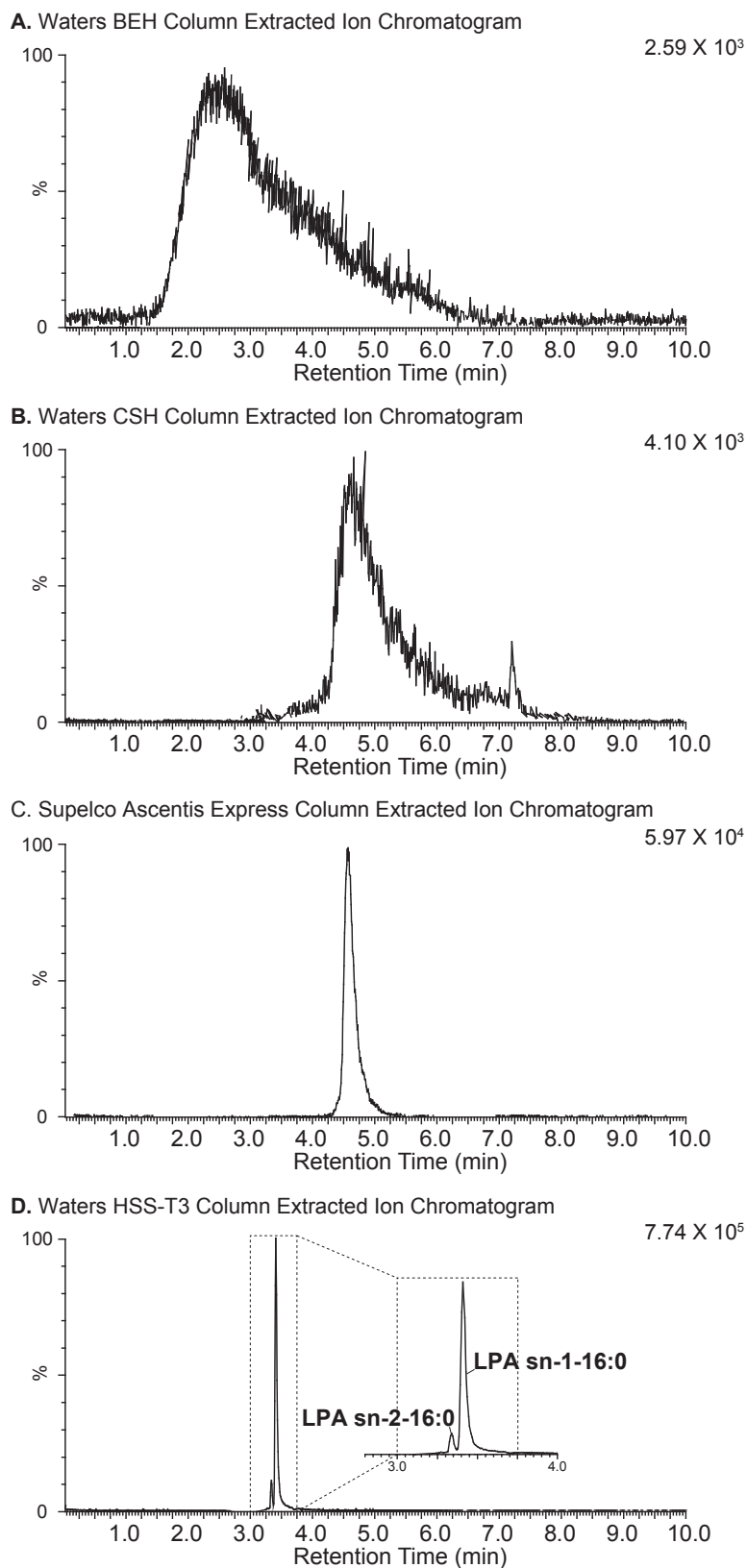
Figure 6. Extracted ion chromatograms for LPA 16:0 (*m/z* 409.2361 ± 0.02 Da) using various reversed-phase columns including **A.** Waters ethylene-bridged hybrid (BEH); **B.** Waters charged surface hybrid (CSH); **C.** Supelco Ascentis Express; and **D.** Waters high-strength silica-T3 (HSS-T3). Peak intensities shown are in ion counts.
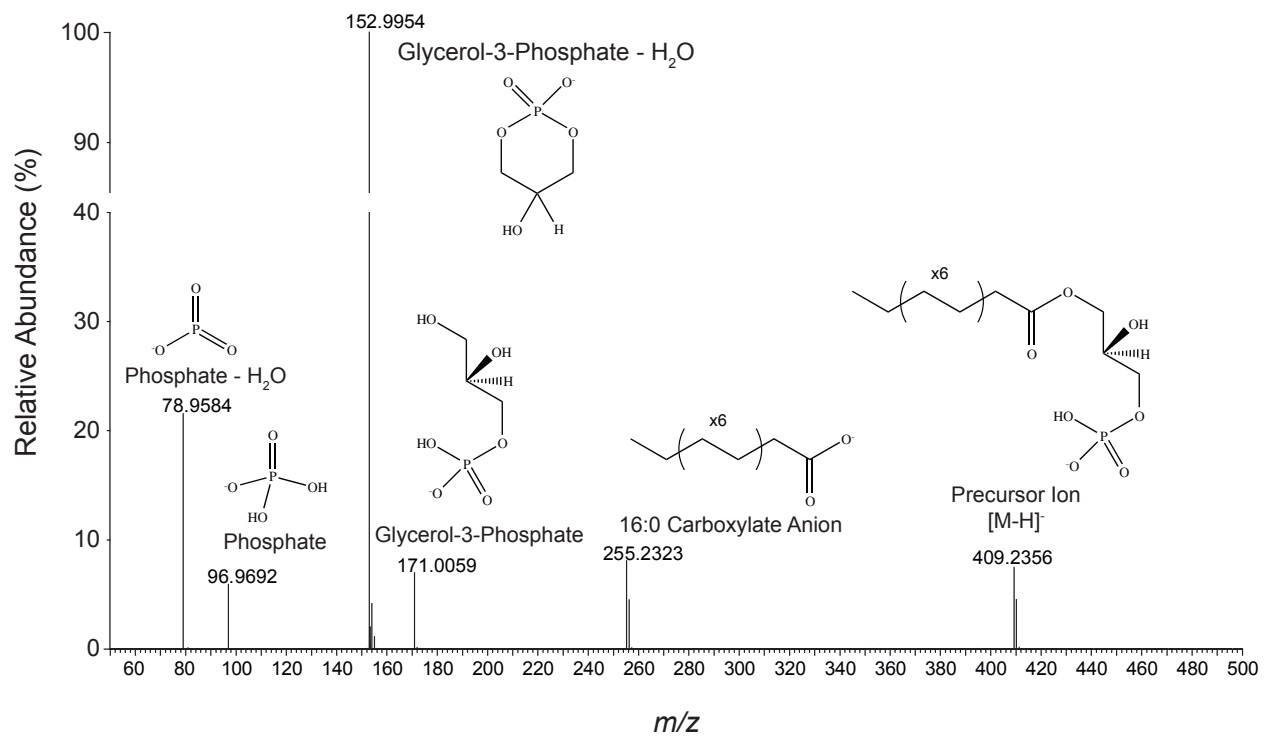
Figure 7. MS/MS spectrum for LPA 16:0 and structures for the major product ions.

Table 4. Precursor and product ion ToF-MRM transitions and collision energy (CE) voltages used for plasma LPA profiling

Species	CE Ramp (V)	Precursor Ion	Carboxylate Anions*
LPA 16:0	20 → 30	409.2361	255.2330
LPA 17:0	20 → 30	423.2517	269.2486
LPA 18:0	20 → 30	437.2674	283.2643
LPA 18:1	20 → 30	435.2517	281.2486
LPA 18:2	20 → 30	433.2361	279.2330
LPA 20:4	20 → 30	457.2361	303.2330
LPA 22:6	20 → 30	481.2361	327.2330

*Product ion ToF-MRM transitions for all LPA species included the precursor ion of each molecule in the product ion spectra, as well as several product ions common to all LPA species, including the glycerol-3-phosphate ion (*m/z* 171.0064), the dehydrated cyclic ion of glycerol-3-phosphate (*m/z* 152.9958), phosphate (*m/z* 96.9696) and dehydrated phosphate ion (*m/z* 78.9591). ToF-MRM, time-of-flight/multiple reaction monitoring; LPA, lysophosphatidic acid; CE, collision energy.
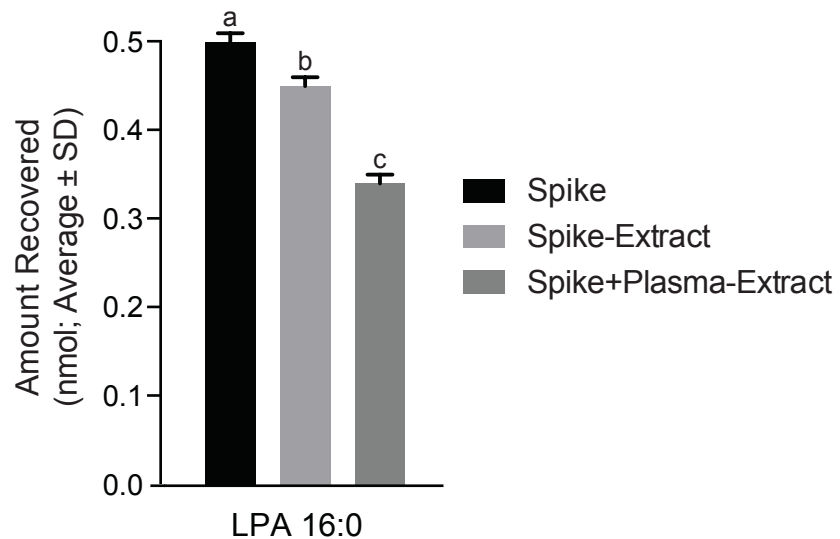
Figure 8. Recoveries of LPA 16:0 following extraction without plasma (Spike-Extract) and with plasma (Spike+Plasma-Extract). The values shown are based on analyses of technical replicates (n=3 per condition, mean ± standard deviation). Different letters indicate statistically-significant differences inferred at $p < 0.05$ following a one-way analysis of variance (ANOVA). LPA, lysophosphatidic acid; SD, standard deviation.
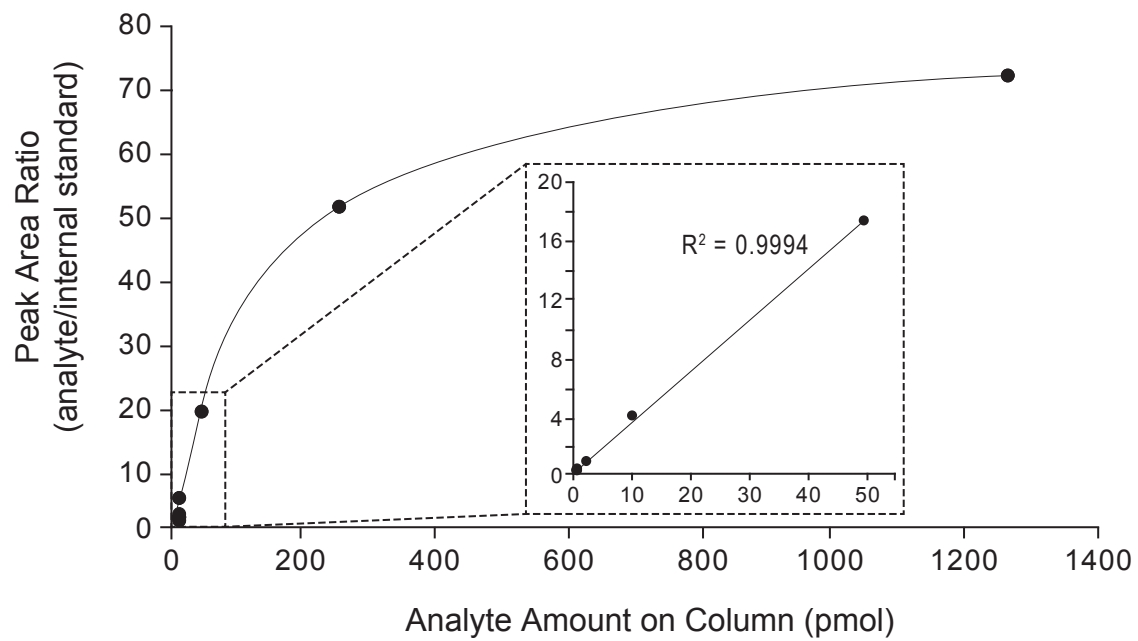
Figure 9. Serial dilutions of LPA 17:0. Linearity appears to be maintained between 0.0032 pmol and 50 pmol on column.
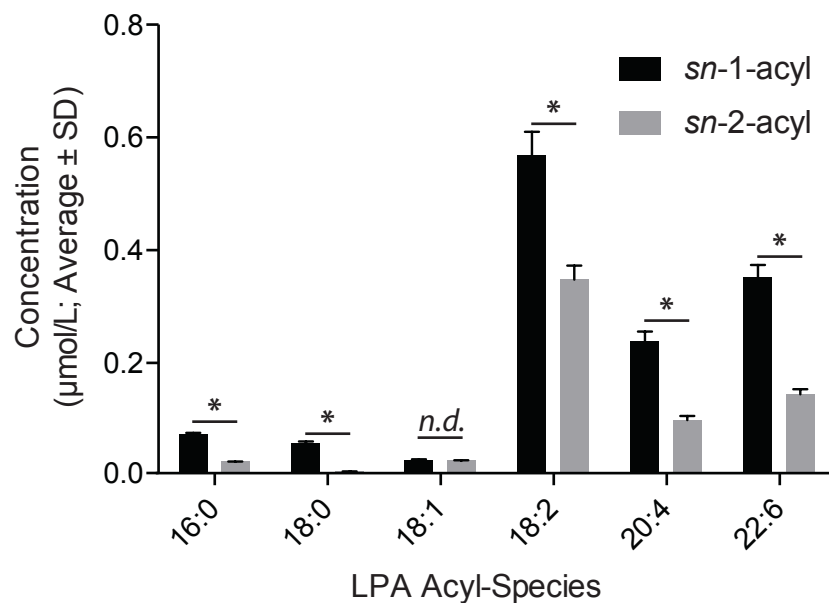
Figure 10. Regioisomers of common LPA species in mouse plasma. Values reported are based on analyses of biological replicates (n = 4, mean ± standard deviation). Statistical significance was inferred at $p < 0.05$ following Student's t-tests. LPA, lysophosphatidic acid; SD, standard deviation.

CHAPTER 7

Macrolipidomic Analysis of Sunflower Oil and Mouse Striatum

7.1 Objectives

UHPLC-MS/MS-based methods have been shown to be remarkably versatile, but untargeted macrolipidomic methods are often overestimated in their abilities to accurately profile lipids from multiple lipid classes simultaneously. Generally, the lack of knowledge regarding the complex lipid composition of new samples can lead to the generation of artefacts through sample preparation and analysis, resulting in improper annotations of lipid species [37, 160, 200]. Semi-targeted workflows where the general lipid profile is known can still be used for the discovery of novel compounds. In this sense, generic analytical protocols can be tuned for the accurate detection of lipids from known lipid classes that share similar physical and chemical properties, increasing the adaptability of these methods. This will be illustrated in this Chapter through the development and application of two semi-targeted macrolipidomic profiling methods, one for the analysis of sunflower oil, and the other for the analysis of mouse striatum.

7.1.1 Sunflower Oil Analysis

Triacylglycerol (TAG) analysis has not been a major priority of lipidomic characterizations [19, 201], as they are considered, perhaps inappropriately, as relatively inert storage lipids. Given that most dietary fat is in the form of TAG [42], and there has been an increased appreciation of the importance of adipocyte function [202], methods to better characterize TAG species are needed. Sunflower oil is 95% TAG by weight and is one of the most highly consumed vegetable oils worldwide [203]. Traditionally, the fatty acid composition of sunflower oil is mainly linoleic acid (18:2n-6), with considerable amounts of oleic (18:1n-9),

palmitic (16:0) and stearic (18:0) acids [204]. While fatty acid composition data is informative in characterizing novel seed oils, the ability to quantitate and elucidate the fatty acyl chains of complex lipids in their native state has the potential to provide even further insights into their nutritional value, palatability, stability and impact on livestock and human health [205, 206].

The large number of distinct TAG species that may be present in oils and biological samples such as plasma and adipose tissue can encompass various fatty acyls with differing carbon chain lengths, degrees of unsaturation, regioisomeric configurations as well as double bond locations and geometries. Thus, TAG profiling can present a significant analytical challenge as compared with less complex lipid classes. Many of these species are structurally and chemically-similar, and may not be fully resolved using shotgun approaches or conventional liquid chromatography techniques [207, 208]. As a result, serial and parallel column couplings, multi-dimensional UHPLC configurations, and supercritical fluid chromatography applications have been adapted to improve TAG analyses in the past few years [38, 205, 209-213]. Increased chromatographic separation enables the discrimination of species of lipids from a brutto level of information to more detailed fatty acyl species at the medio (acyl-isomers) or even genio (regioisomers) level. In this study, we developed a UHPLC-MS/MS method that utilizes a dual UHPLC column serial coupling setup and data-dependent tandem mass spectrometry in the positive ion mode to profile the macrolipidome of sunflower oil.

7.1.2 Mouse Striatum Analysis

The second part of this Chapter focuses on the analysis of phospholipids in mouse striatum samples. Brain lipidomic approaches are of considerable interest to explore associations between perturbed lipid homeostasis and lipid signaling with the onset and progression of

various neurodegenerative diseases such as Alzheimer's Disease [214-216]. The striatum was chosen as this brain region is known to be important in various aspects of cognition and behaviour [217, 218]. Approximately 1/3 of the dry weight of the human brain is made up by phospholipids [219-222], with high proportions of phosphatidylcholines (PC) and phosphatidylethanolamines (PE) and intermediate amounts of phosphatidylserines (PS) and phosphatidylinositols (PI). Other than free cholesterol, non-polar lipids such as triacylglycerols, diacylglycerols and cholesteryl esters constitute less than 1% of the brain lipidome [219]. Additionally, this tissue is particularly rich in long-chain polyunsaturated fatty acids, such as arachidonic acid (ARA) and docosahexaenoic acid (DHA), which account for approximately 25-30% of total fatty acids [223, 224]. As such, brain lipidomics presents a very different analytical challenge as compared with TAG-rich sunflower oil.

Although brain lipids can be detected using untargeted lipidomics techniques with positive ESI, the characterization of phospholipids can be completed more effectively and reliably in the negative ion mode for two main reasons: 1) the fragment ions that are diagnostic for the fatty acyl chains of phospholipids are much more intense in the negative ion mode as compared with fragment ions in the positive ion mode, which results in a lower frequency of false positive identifications (this was discussed in Chapter 5); and 2) the ion suppression effects that phosphatidylcholine species impart upon other co-eluting lipids (described in Chapter 2) are significantly reduced. This method utilizes reversed-phase UHPLC and data-dependent MS/MS in the negative ion mode to profile phospholipids in mouse striatum.

7.2 Hypotheses

1. The use of a two-column coupling setup in the analysis of sunflower oil will enable the resolution of isomeric TAG species and the identification of the most abundant lipids in sunflower oil.

2. The analysis of mouse striatum samples using negative ESI-MS/MS will enable the detection and quantitation of highly-abundant lipid species across the major phospholipid classes (PC, PE, PI, PS).

7.3 Methods, Materials and Study Design

7.3.1 Sample Collection and Lipid Extraction

7.3.1.1 *Sunflower Oil*

Sunflower oil (Compliments, Sobeys Inc.) was purchased from a local grocery store in Waterloo, ON, Canada in November of 2018. Lipid extracts were obtained in triplicate using the Folch-based protocol described in Section 3.3. Briefly, 3 mL of 2:1 chloroform/methanol (v/v) were added to 20 µL oil aliquots, delivering 30 µmol of triheptadecanoin (TAG 17:0/17:0/17:0) as the internal standard. Samples were vortexed, and 500 µL of 0.2M NaH_2PO_4 buffer were added. Samples were inverted, centrifuged at 1734 *rcf* for 5min, and the organic layer was carefully extracted and saved. The samples were then diluted by aliquoting 2 µL of the lipid extract and adding 2500 µL of the reconstitution solvent (65:35:5 acetonitrile/isopropanol/water (v/v/v) +0.1% formic acid). Samples were then vortexed briefly and stored at 4 ºC until analysis.

7.3.1.2 Mouse Striatum Samples

Mouse tissue samples were provided from a study conducted by the Laboratory of Membrane Biophysics and Biochemistry (Section of Nutritional Neuroscience) of the National Institute on Alcohol Abuse and Alcoholism, National Institutes of Health. The samples were part of a larger study examining the interaction between polyunsaturated fatty acids and ethanol consumption that received ethics clearance from the National Institutes of Health and the sample analyses were ethically approved by the University of Waterloo Office of Research Ethics. Male C57BL/6 mice (20 weeks old, n = 3) were used in this study. The mice were housed individually and had *ad libitum* access to food. The diets were custom-made with 35% energy from fat, 19% energy from protein and 44% energy from carbohydrate (Dyets Inc., Bethlehem, PA, USA). The mice were sacrificed by cervical dislocation following anesthetization with isofluorane, and striatum samples were harvested, flash frozen in liquid nitrogen, and stored at -80 ºC. The samples were shipped to the University of Waterloo, ON, Canada, on dry ice, and were kept at -80 ºC until sample preparation. Lipid extracts were obtained by homogenizing the samples in 3 mL of 2:1 chloroform/methanol (v/v) which delivered known amounts of various deuterium-labelled internal standards for the major lipid classes (Splash Lipidomix, Avanti Polar Lipids, Alabaster, AL, USA). This was followed by the addition of a sodium-phosphate buffer as described in Section 3.3. Lipid extracts were dried under N_2 gas and reconstituted in 100 μL of the reconstitution solvent. Samples were then vortexed briefly and stored at 4 ºC until analysis.

7.3.2 Gas Chromatography-Flame Ionization Detection

Due to the anticipated challenge in characterizing TAG using lipidomics, the fatty acid composition of sunflower oil was quantitatively determined by gas chromatography-flame

ionization detection. Lipid extracts were obtained from 20 μL aliquots of the sunflower oil as

technical triplicates as explained in Section 3.3, using 3 mL of 2:1 chloroform/methanol (v/v)

that contained 500 μg of triheptadecanoin as the internal standard (NuChek-Prep, Elysian, MN,

USA). The extracts were derivatized with 14% BF_3 in methanol to generate fatty acid methyl

esters as explained in Section 3.5 prior to analysis.

7.3.3 UHPLC-MS/MS Instrument Settings

Untargeted macrolipidomic analyses of sunflower oil and mouse brain samples were

completed using the Waters Acquity UPLC System and Waters Synapt G2S*i* QToF mass

spectrometer. Initially, a subset of samples were analyzed in pilot work using the UHPLC-

MS/MS method described in Chapter 5, which used conventional UHPLC with a Waters Acquity

UPLC CSH C18 column, 1.7 μm x 2.1 mm I.D. x 150 mm equipped with a VanGuard CSH

1.7 μm pre-column (Milford, MA, USA), positive ESI-MS and top-5 DDA. Two semi-targeted

workflows were then developed in order to increase the quality of the data. The specific

experiments used different UHPLC and MS/MS data acquisition settings, which are described in

detail below.

7.3.3.1 *Sunflower Oil Lipidomics*

UHPLC was completed using a dual column coupling setup with two reversed-phase C18

columns connected in series. The first column was an Ascentis Express C18 column, 2.0 μm x

2.1 mm I.D. x 150 mm equipped with an Ascentis Express 2.0 μm Guard (Sigma-Aldrich, St.

louis, MO, USA). The second column was a Waters Acquity UPLC BEH C18 column, 1.7 μm x

2.1 mm I.D. x 100 mm equipped with a VanGuard BEH 1.7 μm pre-column (Milford, MA,

USA). Both columns were connected using a 5 cm piece of polyetheretherketone (PEEK) tubing (Figure 11). The first column (Supelco Ascentis Express) was chosen as it has the same length (150 mm) and internal diameter (2.1 mm) as the Waters Acquity CSH column which is used in all other untargeted macrolipidomic profiling methods in this thesis, but has a larger particle size (2.0 μm as compared with 1.7 μm in the Waters CSH column), which enables faster solvent flow rates at lower instrument pressures. The second column (Waters Acquity BEH 100 mm) was chosen as the column compartment of the Waters Acquity UPLC system was too small to fit two 150 mm columns, and a 100 mm Supelco column was unavailable at the time of these experiments. Although both columns have a C18-particle base structure, the chemistry of the BEH column (porous bridged ethyl-siloxane/silica C18 hybrid, 130 Å pore size) is different than that of the Supelco column (fused-core C18, 90 Å pore size). However, the main objective of adopting this serial column coupling setup was to increase the surface area of the stationary phase, rather than using columns with different C18 chemistries. The joining of these two columns in series also had implications on the mobile phase gradient protocol, as solvent flow rates had to be reduced to 150 μL/min to account for the increased instrument pressures. The mobile phase gradient ramps were kept similar to that of the protocol described in Section 3.4, with (A) 60:40 acetonitrile/water (v/v) +10 mM ammonium formate +0.1% formic acid, and (B) 90:10 isopropanol/acetonitrile (v/v) +10m M ammonium formate +0.1% formic acid. The multi-step gradient used was as follows: solvent B was 32% from 0-1min, followed by a linear increase to 55% B from 1-12min, 70% B from 12-24min, 80% B from 24-35min, 95% B from 35-50min, 95% B from 50-60min, a decrease to 32% B at 60.1min and a hold at 32% B until the 65min mark. The column compartment temperature was 50 ºC, autosampler temperature was 4 ºC, and the injection volume was 5 μL.

The mass spectrometer was operated in positive ESI mode, spray voltage 1.0 kV, enhanced resolution mode (continuum, approximately 60,000 resolution), scan range *m/z* 100 to 1200, scan time 0.2 s/scan, cone voltage 40 V, cone gas flow 100 L/hr, desolvation gas flow 600 L/hr, nebulizer gas flow 7.0 bar, source temperature 140 ºC, desolvation temperature 400 ºC. Spectra were lock mass-corrected using leucine enkephalin (*m/z* 554.2615). Tandem mass spectrometry was performed under DDA conditions for top-5 ions with a ± 1.0 Da isolation window, scan frequency 0.1 s/scan, transfer cell collision energy ramp of 30 V to 50 V at low mass (*m/z* 100) and 40 V to 60 V at high mass (*m/z* 1200).

7.3.3.2 *Mouse Striatum Lipidomics*

UHPLC was completed using the binary multi-step gradient described in Section 3.4 with the Waters Acquity UPLC Charged Surface Hybrid (CSH), 1.7 μm x 2.1 mm x 150 mm column equipped with a VanGuard CSH 1.7 μm pre-column. The two-column setup that was used for the analysis of sunflower oil was not used in the analysis of striatum tissue samples, as we have shown that a single column (Waters CSH 150 mm) is sufficient to achieve chromatographic resolution of isomeric phospholipids [31]. The mass spectrometer was operated in negative ESI mode, spray voltage -2.5 kV, resolution mode (continuum; approximately 30,000 resolution), scan range *m/z* 100 to 1200, scan time 0.2 s/scan, cone voltage 40 V, cone gas flow 100 L/hr, desolvation gas flow 600 L/hr, nebulizer gas flow 7.0 bar, source temperature 140 ºC, desolvation temperature 400 ºC. Spectra were lock mass-corrected using leucine enkephalin (*m/z* 554.2615). Tandem mass spectrometry was performed under DDA conditions for top-5 ions with a ± 1.0 Da isolation window, scan frequency 0.1 s/scan, transfer cell collision energy ramp of 30 V to 45 V at low mass (*m/z* 100) and 35 V to 60 V at high mass (*m/z* 1200).

7.3.4 Data Normalization and Statistical Analyses

Peak areas under the curve were integrated using Progenesis QI. In the sunflower oil

experiments, the chromatographic resolution of extracted peak profiles was assessed using the

following formula: Resolution = (difference in peak apex retention times)/(average peak widths

at baseline), and satisfactory separations were considered if the resolution coefficients were

≥ 1.0. Lipid abundances were normalized using the internal standard belonging to the same lipid

class as the analyte of interest (i.e., all TAG species in oil were normalized using the TAG

internal standard, PC lipid species in mouse striatum were normalized using the PC internal

standard). Concentration data are presented as mean ± standard deviation of all analytes in μmol

lipid/mL for the sunflower oil samples, and as nmol lipid/mg tissue for the mouse striatum

samples. Peak alignment, integration and compound identifications were made using Progenesis

QI.

7.4 Results

<u>7.4.1 Sunflower Oil Macrolipidomics</u>

There was significant isomeric coelution of TAG species in sunflower oil when using

conventional (i.e., single-column) UHPLC. This was determined based on the presence of

diagnostic fragment ions from multiple TAG precursor species in MS/MS spectra (Figure 12,

showing the extracted ion chromatogram for TAG 54:3, m/z 902.8171 as $[M+NH_4]^+$ in A, and

MS/MS spectrum in B). Specifically, the ion highlighted in blue represents the DAG fragment of

TAG 18:1/18:1/18:1, and the ions highlighted in red represent DAG fragments of TAG

18:0_18:1_18:2 following neutral losses of fatty acyl chains and ammonium as $[R-COOH +NH_3]$

(m/z 601.5190, 603.5348 and 605.5488 represent neutral losses of 18:0, 18:1 and 18:2,

respectively). There was a significant improvement in chromatography and the resolution of isomeric TAG species with the use of the dual-column setup (Figure 12C, resolution coefficient = 1.02), which enabled the deconvolution of MS/MS spectra and the characterization of fragment ions from the two different precursor ions (Figures 12D and 12E for TAG 18:1/18:1/18:1 and TAG 18:0_18:1_18:2, respectively). However, upon further examination of MS/MS spectra, we still observed coelution of other TAG species, even with the dual-column setup (Figure 13). Despite the persistent coelution of some isomeric species in sunflower oil, we identified (at the medio or genio level) and quantitated 20 highly-abundant TAG, and specified isomeric contributions of multiple species if they were unresolved (Figure 14). We found that trilinolein (TAG 18:2/18:2/18:2) was the TAG molecule of highest abundance in sunflower oil, accounting for approximately 2.4% of the weight of this oil. There were considerable amounts of 18:2- and/or 18:1-containing TAG in sunflower oil, as these fatty acids were present in all 20 of the species that were profiled. These observations are consistent with the fatty acid composition of sunflower oil (Table 5), as linoleic acid and oleic acid constitute approximately 49% and 38% by weight of total fatty acids, respectively. From the 20 TAG species of highest abundance in sunflower oil, it appears that there was only one instance in which coelution of multiple TAG acyl-isomers occurred (TAG 18:0_18:1_22:0, denoted with an asterisk in Figure 14, coeluted with TAG 16:0_18:1_24:0). The other 19 species were isomerically pure (at the medio-level), after manual confirmation of diagnostic fragments from single TAG precursor ions in MS/MS scans.

Using negative ESI-MS/MS, we were able to obtain fragment spectra that contained

diagnostic ions for fatty acyl chains that were of much higher intensity relative to what is

typically seen in the positive ion mode (an example of a negative ion MS/MS spectrum of PC

16:0/22:6 can be found in Figure 15A, and positive ion MS/MS spectrum in B). Specifically,

fatty acyl carboxylate anions are typically in the range of approximately 10% to 30% of the base

peak ion in MS/MS (m/z 255 and 327 ions correspond to 16:0 and 22:6, respectively).

Interestingly, the relative intensity of these ions can be used to determine regio-specific

information, where the fatty acyl ion of highest intensity indicates its localization to the *sn*-2

position of the glycerol backbone [31, 54]. In contrast, positive-ion MS/MS gives rise to

fragments of very low intensity that can be difficult to discern from baseline noise (Figure 15B).

Similar to the interpretation of TAG MS/MS spectra, phospholipid acyl information in the

positive ion mode is determined based on the presence of lysophospholipid fragments that result

from the neutral losses of fatty acids as [R-COOH]. These weak fragment ions are generally

< 1% of the base peak ion (Figure 15B), where m/z 496 and 550 are 16:0- and 22:6-

lysophosphatidylcholine (LPC) fragments corresponding to the neutral losses of 22:6 and 16:0,

respectively, and the base peak ion (m/z 184) corresponds to the phosphocholine head group.

Using the negative-ion method, we profiled phospholipid species from the major

phospholipid classes in striatum and generated genio-level information for 20 highly-abundant

lipids by manually examining MS/MS spectra (Figure 16 A). We found high proportions of

phosphatidylcholines and phosphatidylethanolamines, with PC 16:0/18:1 (1.72 ± 0.26 nmol/mg)

and PE 18:0/22:6 (2.35 ± 0.21 nmol/mg), being the PC and PE species of highest abundance,

respectively. Phosphatidylinositols and phosphatidylserines were also found in considerable

amounts, with PI 18:0/20:4 (1.44 ± 0.03 nmol/mg) and PS 18:0/22:6 (3.44 ± 0.84 nmol/mg) being the species of highest abundance in these respective lipid classes. In addition, we were able to quantitate phospholipids of lower abundance containing fatty acyl groups of high interest for nutritional studies (Figure 16 B). This included three EPA-containing species (PC 16:0/20:5, 0.04 ± 0.01 nmol/mg; PC 16:1/20:5, 0.014 ± 0.01 nmol/mg; PI 18:0/20:5, 0.04 ± 0.01 nmol/mg), a PS specie with two DHA fatty acyl chains (PS 22:6/22:6, 0.07 ± 0.02 nmol/mg), and two omega-6 PUFA-containing species (PE 16:0/20:4, 0.22 ± 0.02 nmol/mg and PS 22:4/22:6, 0.12 ± 0.03 nmol/mg).

7.5 Discussion

Although untargeted mass spectrometry-based methods can be used to easily generate lipid spectra, there are several considerations that should be taken in order to accurately identify and measure lipid structures. Cellular lipidomes can be vastly diverse, and the concentrations of individual lipid species are known to range over several orders of magnitude [16]. These characteristics can present significant analytical challenges, but semi-targeted methods can be created from untargeted or generic lipidomic profiling methods in order to increase the quality of the data for specific lipid classes. This was illustrated in this Chapter through the development and tuning of two semi-targeted methods, one for the analysis of TAG in sunflower oil, and the other for the analysis of phospholipids in mouse brain samples.

The analysis of TAG in complex lipid samples is notoriously difficult due to the large number of isobaric and isomeric structures (both acyl-isomers and regioisomers) that may be present. While high-resolution/accurate-mass applications can be used to resolve isobaric lipids, chromatography is still the best approach for the separation of TAG isomers. Presently, we

showed that conventional reversed-phase UHPLC can separate TAG species based on their brutto-level composition (i.e., number of carbon atoms and carbon-carbon double bonds across all three fatty acyl chains), but not at the level of identifying acyl-isomers (medio-level). Using a two-column serial coupling setup, we demonstrated that TAG structures can be further resolved based on the distribution of carbon-carbon double bonds on fatty acyl chains. For example, TAG 18:1_18:1_22:1 has three monounsaturated fatty acids, and can be resolved from its acyl-isomer TAG 18:1_18:2_22:0 since this lipid has one saturated (22:0), one monounsaturated (18:1), and one polyunsaturated (18:2) fatty acid. However, other TAG species with the same distribution of classes of fatty acids (e.g., a different TAG that also contains three monounsaturated fatty acids such as TAG 18:1_20:1_20:1) may not be resolved. Nevertheless, this two-column method enabled the characterization of 20 of the most abundant TAG in sunflower oil, which cumulatively account for approximately 15% of the weight of sunflower oil. These results were in general agreement with the fatty acid composition data we generated by gas chromatography, and with analyses using supercritical CO_2 ultra-performance convergence chromatography-tandem mass spectrometry [205].

Overall, the two-column coupling approach allowed the successful identification of highly abundant lipids in sunflower oil at the acyl species or medio-level, in agreement with the first hypothesis of this Chapter. Beyond the medio-level data that was presented here for TAG in this type of oil, determining regioisomeric distributions is challenging due to the presence of three fatty acyl chains, as compared with just two acyl chains in phospholipids. There are some reports examining the effects of various ionization techniques on TAG fragmentation behaviour (e.g., atmospheric-pressure chemical ionization, atmospheric pressure photoionization, ESI) [38, 225], as well as mathematical models for determining regiospecificity [226], but these

applications often require more targeted methods and can be impractical in discovery-based approaches. Furthermore, recent developments in silver-ion UHPLC have been shown to enable the resolution of TAG regioisomers [227, 228].

For the mouse striatum analyses, we were able to successfully characterize the most abundant lipids, as well as lower abundance lipids containing EPA and DHA. The PC class of lipids was the most abundant, followed by PE-P, PE, PS and PI. We were unable to confirm these results as we appear to have been the first to characterize mouse striatum at the lipidomic level, however, these results generally resembled the lipidomic profiles of other brain regions [229, 230]. As such, we can accept our second hypothesis that a negative mode MS/MS can be used to identify and quantitate the macrolipidome of mouse striatum. Most phospholipids exhibit zwitterionic properties, which enables their detection in both positive and negative polarities. Although high sensitivities may be achieved in the positive ion mode for phospholipid species with high electric potentials, there are three major advantages for analyzing phospholipid-rich samples in the negative ion mode. Firstly, the strong ion-suppression effects that phosphatidylcholines and sphingomyelins impart upon less ionizable phospholipids are ameliorated (this was discussed in Chapter 2). Secondly, there is generally less chemical noise and background interference from ESI contaminants in the negative ion mode as compared with the positive ion mode [231]. Finally, and perhaps most importantly, the fragmentation of phospholipids in the negative ion mode gives rise to intense fatty acyl carboxylate anions that can be easily recognized and annotated. This information can significantly increase the confidence of lipid identifications, reducing the frequency of analyte misannotations and false-positive features. Furthermore, regioisomeric distributions can be deduced from the relative intensities of fatty acyl fragments in MS/MS scans.

In this Chapter, we have demonstrated that there are various advantages associated with positive and negative ESI depending on the lipid class of interest, as well as the importance of chromatography in the resolution of isomeric lipids. These data illustrate that while there is a virtually-unlimited number of mass spectrometry-based methods that can be adapted for lipid analysis, knowing the general lipid profile of a sample can help in tailoring the analytical method to increase the confidence in the results, as well as answering the research question appropriately. Combining some of the features from the methods presented in this Chapter has the potential to create robust and comprehensive methods that have the ability to simultaneously measure polar and non-polar lipids in complex matrices. This will be illustrated in Chapter 8 through the application of a retention time-based polarity-switching UHPLC-MS/MS method for the analysis of human whole blood samples.
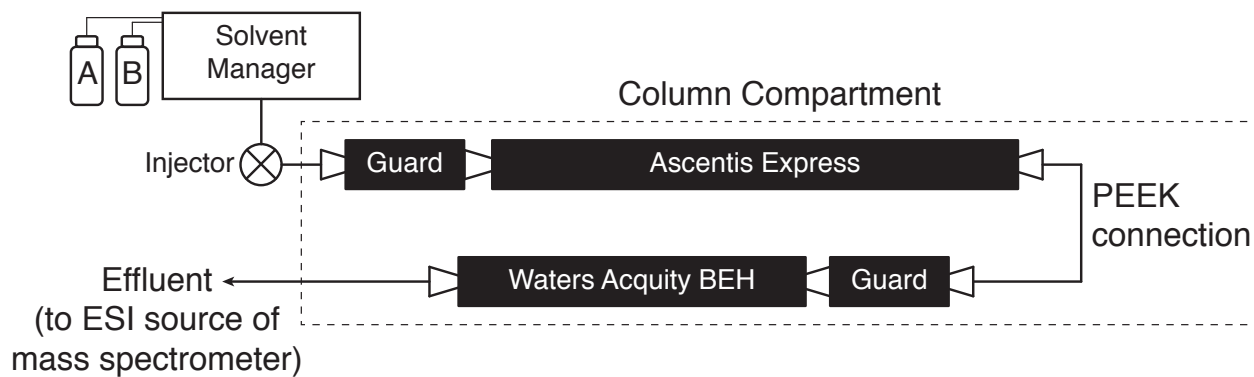
Figure 11. Illustration of the dual UHPLC column serial coupling setup. Column specifications: Ascentis Express C18 2.0 μm x 2.1 mm I.D. x 150 mm; Ascentis Express 2.0 μm guard; Acquity UPLC BEH C18 1.7 μm x 2.1 mm I.D. x 100 mm; VanGuard BEH 2.0 μm pre-column; columns are connected using a 5 cm piece of polyetheretherketone (PEEK) tubing. UHPLC, ultra-high performance liquid chromatography; ESI, electrospray ionization; BEH, ethylene bridged hybrid; PEEK, polyetheretherketone.

A. Single-Column UHPLC: XIC

100
%
0
30   32   Time

*

TAG 54:3

B. MS/MS Spectrum of TAG 54:3

100
%
0
601 602 603 604 605 606 607 608 m/z

DAG 18:1_18:2
601.5190

DAG 18:0_18:2
602.5224

DAG 18:1_18:1
603.5348

604.5381

DAG 18:0_18:1
605.5488

606.5553

607.5566

C. Dual-Column UHPLC: XIC

100
%
0
48   50   Time

TAG 18:1/18:1/18:1

TAG 18:0_18:1_18:2

R = 1.02

#
$

D. MS/MS Spectrum of TAG 18:1/18:1/18:1

100
%
0
603 604 605 606 607 608 m/z

DAG 18:1_18:1
603.5364

604.5392

605.5426

606.5461

E. MS/MS Spectrum of TAG 18:0_18:1_18:2

100
%
0
601 602 603 604 605 606 607 608 m/z

DAG 18:1_18:2
601.5187

602.5231

DAG 18:0_18:2
603.5341

604.5376

DAG 18:0_18:1
605.5483

606.5530

607.5569

Fragments from TAG 18:1/18:1/18:1

Fragments from TAG 18:0_18:1_18:2

Figure 12. A. Extracted ion chromatogram for TAG 54:3 (m/z 902.8171 as [M+NH$_4$]$^+$) using conventional UHPLC (i.e., single column), * denotes an isotopic contribution from TAG 54:4; **B.** MS/MS spectrum of TAG 54:3, highlighting fragment ions of TAG 18:1/18:1/18:1 (blue) and TAG 18:0_18:1_18:2 (red); **C.** Extracted ion chromatogram for TAG 54:3 (m/z 902.8171 as [M+NH$_4$]$^+$) using a dual-column serial coupling setup, # and $ denote isotopic contributions from TAG 18:1_18:1_18:2 and TAG 18:0_18:2_18:2, respectively, (m/z 900.8015 ± 0.02 Da as [M+NH$_4$]$^+$ for all); **D.** MS/MS spectrum of TAG 18:1/18:1/18:1; **E.** MS/MS spectrum of TAG 18:0_18:1_18:2. TAG, triacylglycerol; UHPLC, ultra-high performance liquid chromatography; XIC, extracted ion chromatogram.

77

A. Extracted Ion Chromatogram for TAG 58:3
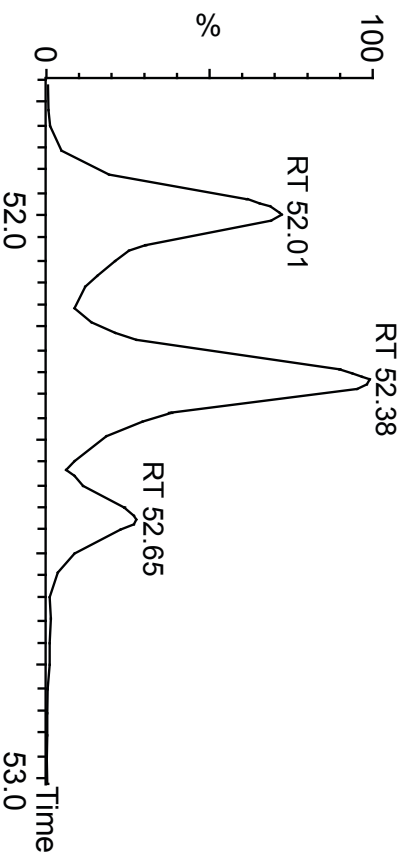
B. MS/MS at RT 52.01
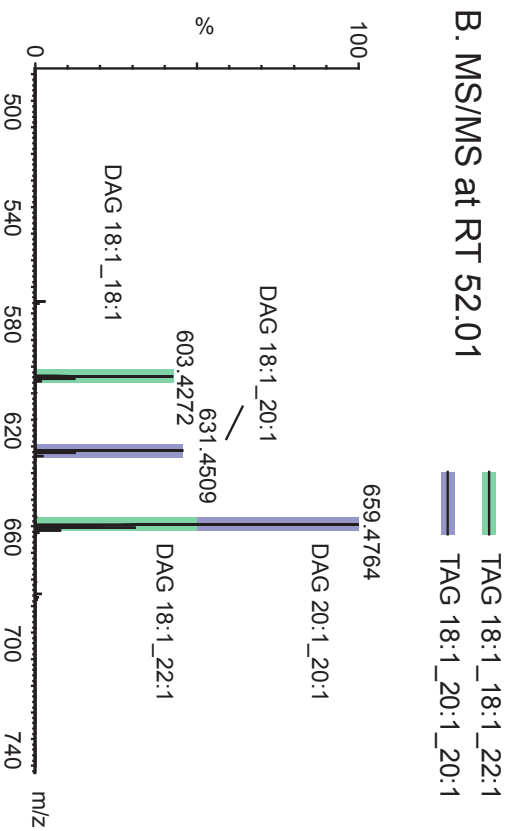
C. MS/MS at RT 52.38min
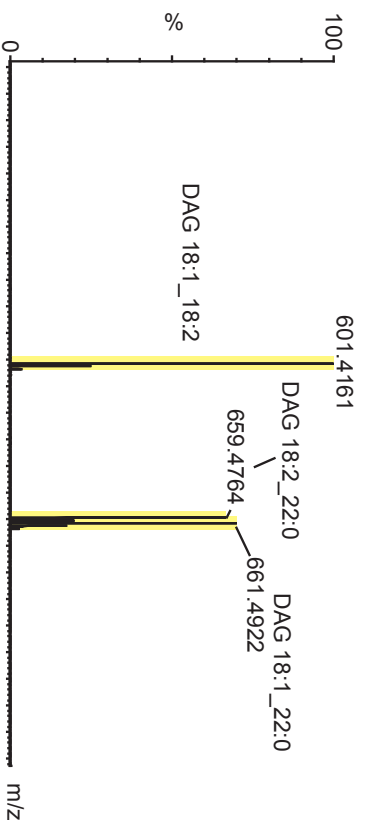
D. MS/MS at RT 52.65
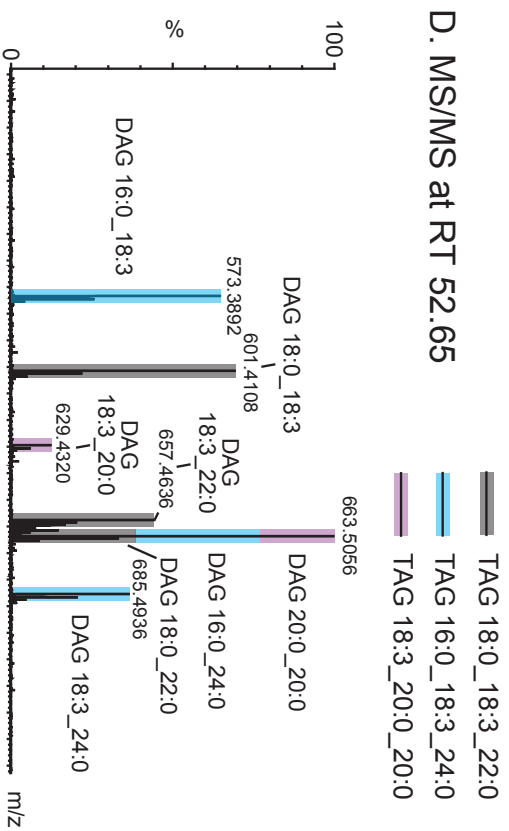
Figure 13. **A.** Extracted ion chromatogram for TAG 58:3(*m/z* 958.8797 as [M+NH₄]⁺), showing MS/MS spectra for this precursor ion at **B.** RT 52.01min , **C.** RT 52.38min, and **D.** 52.65min. Fragment ions are highlighted for the various combinations of precursor TAG species that were detected. RT, retention time; DAG, diacylglycerol; TAG, triacylglycerol

78
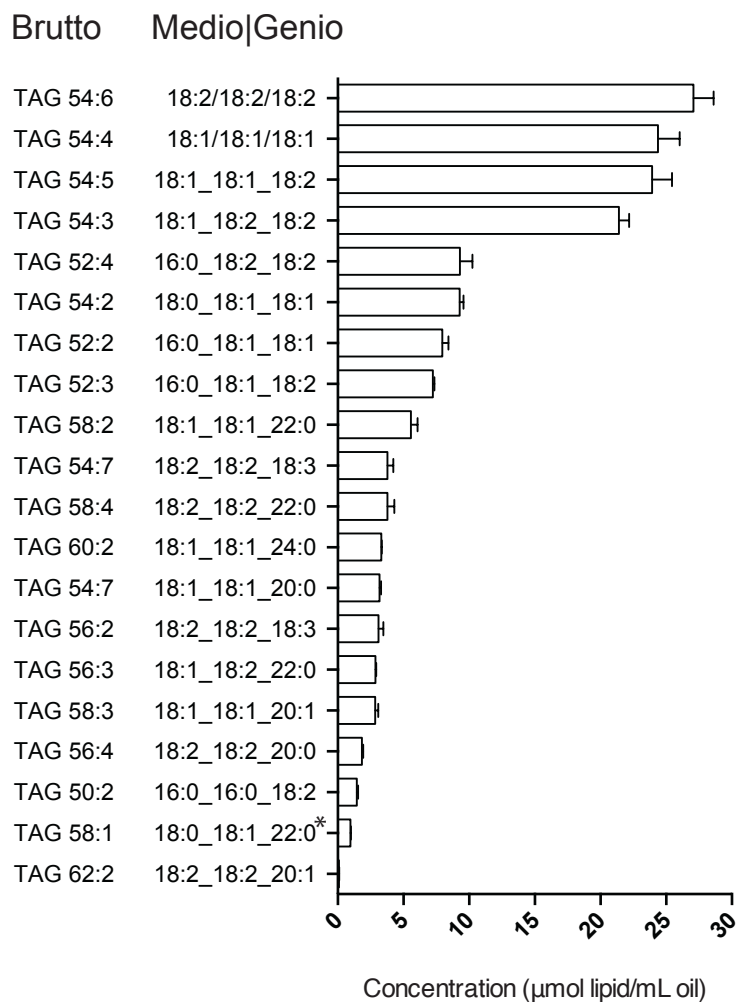
Figure 14. Concentrations of twenty of the major lipid species in sunflower oil. The values shown are based on analyses of technical replicates (n = 3, mean ± standard deviation). The molecule with the asterisk (*) was confirmed to be a contribution of two coeluting isomeric species (TAG 18:0_18:1_22:0 and TAG 16:0_18:1_24:0). TAG, triacylglycerol. All other species were confirmed to be isomerically-pure at the medio-level.

Table 5. Fatty acid composition of sunflower oil.

Fatty Acid	Weight percent of total fatty acids
10:0	0.01 ± 0.01
12:0	0.01 ± 0.01
14:0	0.06 ± 0.01
16:0	5.55 ± 0.04
18:0	3.57 ± 0.01
20:0	0.25 ± 0.01
22:0	0.69 ± 0.02
23:0	0.04 ± 0.01
24:0	0.22 ± 0.02
Total saturates	**10.37 ± 0.02**
12:1	0.01 ± 0.01
14:1	0.01 ± 0.01
16:1	0.09 ± 0.01
18:1n-7	0.72 ± 0.01
18:1n-9	38.44 ± 0.04
20:1n-9	0.17 ± 0.01
22:1n-9	0.01 ± 0.01
24:1n-9	0.01 ± 0.01
Total monounsaturates	**39.43 ± 0.02**
18:2n-6	48.60 ± 0.20
18:3n-6	0.01 ± 0.01
20:2n-6	0.01 ± 0.01
20:3n-6	0.01 ± 0.01
20:4n-6	0.01 ± 0.01
22:2n-6	0.01 ± 0.01
22:4n-6	0.01 ± 0.01
22:5n-6	0.01 ± 0.01
Total omega-6 polyunsaturates	**48.60 ± 0.20**
18:3n-3	0.28 ± 0.01
20:3n-3	0.01 ± 0.01
20:5n-3	0.01 ± 0.01
22:5n-3	0.01 ± 0.01
22:6n-3	0.01 ± 0.01
Total omega-3 polyunsaturates	**0.28 ± 0.01**
Total fatty acids (*mg/mL*)	**955 ± 8**

Values are mean ± standard deviation of technical triplicate samples.

A. Negative Ion-MS/MS
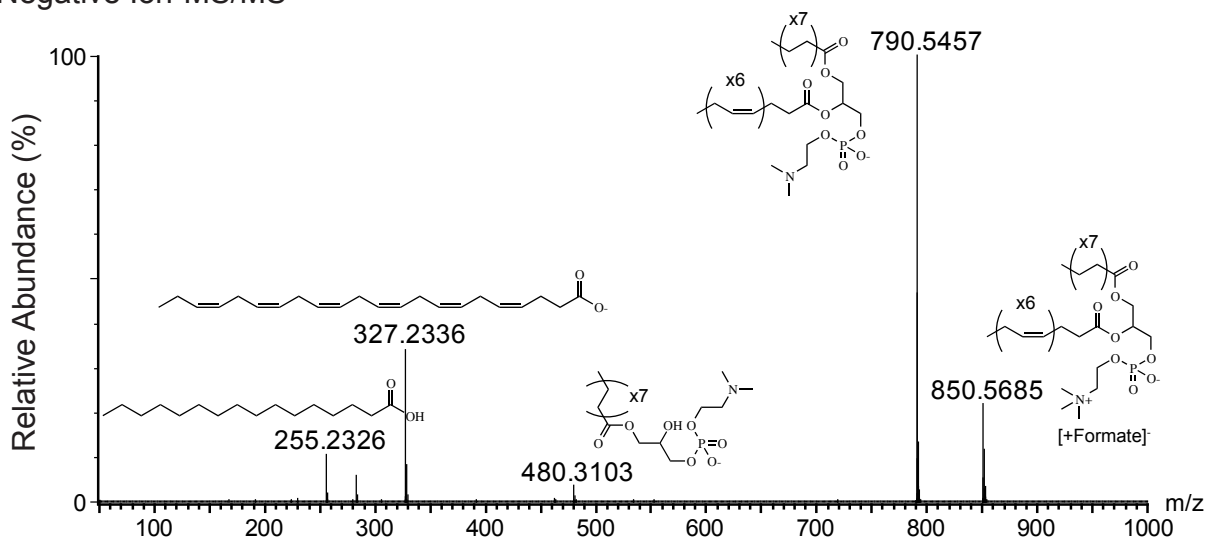
B. Positive Ion-MS/MS
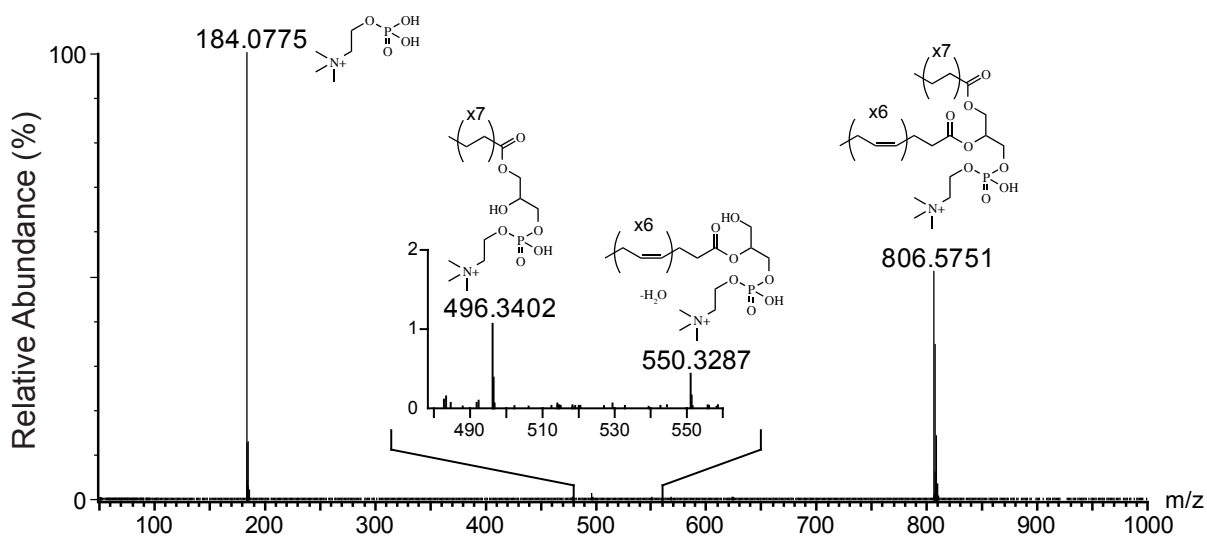
Figure 15. MS/MS spectra for PC 16:0/22:6 in **A.** the negative ion mode (precursor ion = *m/z* 850.5604 as [M+formate]⁻), and **B.** the positive ion mode (precursor ion = *m/z* 806.5694 as [M+H]⁺), highlighting the structures of the major product ions in both polarities.

A. Species of high abundance

Brutto	Medio|Genio
PC 34:1	16:0/18:1
PC 32:0	16:0/16:0
PC 38:6	16:0/22:6
PC 36:1	18:0/18:1
PC 40:6	18:0/22:6
PC 36:4	16:0/20:4
PC 38:4	18:0/20:4
PE P-40:6	P-18:0/22:6
PE P-36:2	P-18:1/18:1
PE P-36:1	P-18:0/18:1
PE P-34:1	P-16:0/18:1
PE P-38:4	P-18:0/20:4
PE 40:6	18:0/22:6
PE 38:4	18:0/20:4
PE 38:6	16:0/22:6
PE 36:1	18:0/18:1
PE 36:2	18:1/18:1
PS 40:6	18:0/22:6
PI 38:4	18:0/20:4
PI 36:4	16:0/20:4

Concentration (nmol lipid/mg tissue)

B. HUFA-species of low abundance

Brutto	Medio|Genio
PC 36:5	16:0/20:5
PC 36:6	16:1/20:5
PE 36:4	16:0/20:4
PS 44:10	22:4/22:6
PS 44:12	22:6/22:6
PI 38:5	18:0/20:5

Concentration (nmol lipid/mg tissue)
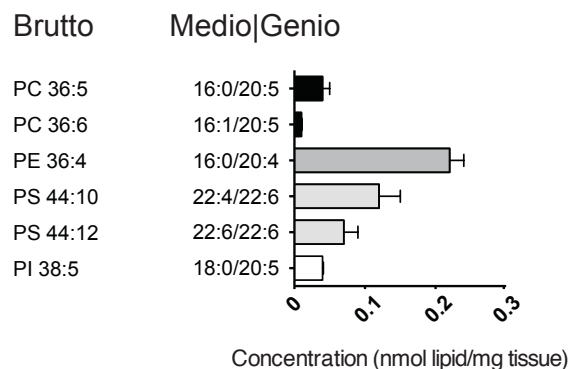
Figure 16. Concentrations of **A.** twenty of the major lipid species in mouse striatum, and **B.** low-abundant species containing HUFA (highly unsaturated fatty acids). The values shown are based on analyses of technical replicates (n = 3, mean ± standard deviation). PC, phosphatidylcholine; PE, phosphatidylethanolamine; PS, phosphatidylserine; PI, phosphatidylinositol.

CHAPTER 8

Quantitative Lipidomics of Novel Whole Blood Biomarkers for the Dietary Intake of Omega-3 Polyunsaturated Fatty Acids

8.1 Objectives

The relationship between diet and blood levels of omega-3 polyunsaturated fatty acids (omega-3 PUFA) has been examined [232-234]. Most of this research has been focused on gross levels of fatty acids in total lipids or lipid fractions of plasma/serum and erythrocytes, which has led to the development of blood biomarkers for stratifying disease risk [235], and estimating dietary intakes of EPA and DHA [236, 237]. These observations were developed from fatty acid compositional data which uses gas chromatography-based analyses that rely on removing fatty acyl chains from complex lipids and derivatizing to fatty acid methyl esters [238]. This limits the ability to characterize complex lipid structures, and specific structural information of lipids that could be of physiological relevance is lost. UHPLC-MS/MS-based analyses have the potential to characterize complex lipids as they exist in their natural states. This "lipidomic" characterization can be considered a metabolic phenotype resulting from genetic and environmental influences. The lipidome therefore has considerable potential to be able to provide information about dietary habits and lipid metabolism.

Blood is a difficult matrix to analyze as it contains a mixture of polar and non-polar lipids. As demonstrated previously (in Chapter 7), the characterization of polar and non-polar lipids improves with semi-targeted analytical approaches. A previous solution has been to complete repeated iterations of analytical runs of the same sample to achieve comprehensive characterizations of the plasma lipidome [201]. This increases the analytical burden and decreases throughput, which is particularly problematic in blood-based screening exercises.

Based on the differences in ionization polarities that are exhibited by the various lipid classes [7], and the fact that polar lipids tend to elute first with standard C18 reverse-phase LC we developed a retention time-based ESI polarity-switching method to capture both polar (ionized in the negative ion mode) and non-polar lipids (ionized in the positive ion mode).

This novel method was then used to complete lipidomic analyses on blood samples collected to evaluate dietary assessment methods of the Danish National Survey of Dietary Habits and Physical Activity. Validating food surveys is typically done using fatty acid analyses [239-243]. Lipidomics has seldom been used to examine the relationship between dietary omega-3 PUFA intake and the levels of fatty acyl-containing complex lipids in human whole blood. Most lipidomic studies have focused on the examination of isolated blood fractions of humans or rodents using interventions with fish, fish oil or DHA supplementation [244-250]. Previous pilot work from our laboratory [251] has indicated that levels of PC 16:0_20:5 and PE P-16:0_20:5 in whole blood are positively correlated with intakes of EPA, while PC 16:0_22:6 and PE P-16:0_22:6 are positively correlated with intakes of DHA. However, these relationships remain to be confirmed using larger sample sizes and with precise assessments of dietary omega-3 PUFA intakes. In regard to dietary ALA, most of the lipidomic studies have focused on the downstream oxidative metabolites of this essential fatty acid along with other oxylipins [252-254]. Despite the fact that there can be relatively high amounts of ALA in PC and PE relative to other complex lipid [251], there are no reports on the role of ALA in the macrolipidome of whole blood.

The purpose of this study is to identify complex lipids in human whole blood that are correlated with dietary intakes of ALA, eicosapentaenoic acid (EPA) and docosahexaenoic acid (DHA). To do this, quantitative lipidomic analyses will be completed on whole blood samples collected by the Technical University of Denmark as part of their National Dietary Survey. The

estimated dietary intakes of omega-3 PUFA including ALA, EPA and DHA will be correlated with the lipidomic data in order to identify acyl-specific lipids that could serve as novel blood biomarkers for dietary habits around omega-3 PUFA consumption.

8.2 Hypotheses

1. A retention time-based polarity switching method will characterize both polar (PC, PE, PI, PS, FFA) and non-polar (TAG, CE) lipids in whole blood within a single UHPLC MS/MS analytical run.

2. The concentrations of ALA-containing PC and PE species will be positively correlated with the dietary intake of ALA.

3. The concentrations of PC 16:0_20:5 and PE P-16:0_20:5 will be positively correlated with the dietary intake of EPA.

4. The concentrations of PC 16:0_22:6 and PE P-16:0_22:6 will be positively correlated with the dietary intake of DHA.

8.3 Methods, Materials and Study Design

8.3.1 Sample Collection and Lipid Extraction

Human blood samples (n = 120) were collected as part of the National Surveys of Diet and Physical Activity by the Danish National Food Institute, which received ethics clearance from the Danish National Committee of Health Research Ethics. Sample analyses were ethically approved by the University of Waterloo Office of Research Ethics. Dietary intakes for all participants were assessed using 7-day food records for macronutrients, fatty acid classes, and some individual fatty acids through the Danish Food Composition Database

(https://frida.fooddata.dk) [255, 256]. Whole blood samples were shipped to the University of Waterloo, ON, Canada, in dry ice, and were kept at -80 ºC until sample preparation. Lipid extracts were obtained from 20 μL aliquots of whole blood as described in Section 3.3, using 3 mL of 2:1 chloroform/methanol (v/v) which delivered known amounts of various deuterium-labelled internal standards for the major lipid classes (Splash Lipidomix, Avanti Polar Lipids, Alabaster, AL, USA). Lipid extracts were dried under N_2 gas and reconstituted in 100 μL of the reconstitution solvent (65:35:5 acetonitrile/isopropanol/water (v/v/v) +0.1% formic acid). Samples were then vortexed briefly and stored in vials at 4 ºC until analysis by UHPLC-MS/MS.

8.3.2 Instrument Settings

UHPLC was completed using the binary multi-step gradient described in Section 3.4 with the Waters Acquity UPLC Charged Surface Hybrid (CSH), 1.7 μm x 2.1 mm x 150 mm column equipped with a VanGuard CSH 1.7 μm pre-column. A retention time-based polarity-switching MS/MS method was developed by first identifying a thirty-second region in the chromatogram between the elution times of phospholipids/sphingolipids and triacylglycerols/cholesteryl esters when no other lipids could be identified (Figure 17). This was done by manually evaluating all MS/MS spectra in the positive and negative ion modes between 27 and 27.5 min of the LC gradient for the presence of diagnostic ions for phospholipid head groups (e.g., *m/z* 184 for phosphatidylcholines and sphingolipids), fatty acyl chains (acylium ions in the positive ion mode, carboxylate anions in the negative ion mode), as well as any precursor ions with *m/z* ratios > 400 that could yield recognizable MS/MS patterns. Upon confirmation that no lipids were being eluting in that region of the chromatogram, the sequence and instrument were set up so that the mass spectrometer was operated in the negative ion mode from 0 – 27 min, followed

86

by a 0.5 μL dummy injection of the eluent, a dwell time of approximately 20 s between ionization polarities, and then positive ESI until the 45 min mark. This allowed for the simultaneous characterization of polar lipids (free fatty acids, lysophospholipids, phospholipids, sphingolipids) and non-polar lipids (triacylglycerols and cholesteryl esters) which can be better characterized in the negative- and positive-ion modes, respectively, using a single sample injection and within the same analytical run. The spray voltages were -2.25 kV and +2.25 kV for the negative and positive-ion modes, respectively. In both ion modes, the mass spectrometer was operated in high-resolution mode (continuum; approximately 42,000 resolution), scan range *m/z* 100 to 1200, scan time 0.2 s/scan, cone voltage 40 V, cone gas flow 100 L/hr, desolvation gas flow 600 L/hr, nebulizer gas flow 7.0 bar, source temperature 140 ºC, desolvation temperature 400 ºC. Spectra were lock mass-corrected using leucine enkephalin (*m/z* 554.2615 for [M-H]⁻ and *m/z* 556.2771 for [M+H]⁺). Tandem mass spectrometry was performed under DDA conditions for top-5 ions with a ± 1.0 Da isolation window, scan frequency 0.1 s/scan. Collision energies in the transfer cell were ramped from 30 V to 45 V at low mass (*m/z* 100) and 35 V to 60 V at high mass (*m/z* 1200) for negative-ESI, and from 30 V to 50 V at low mass (*m/z* 100) and 40 V to 60 V at high mass (*m/z* 1200) for positive ESI.

8.3.3 Gas Chromatography-Flame Ionization Detection

Lipid extracts were obtained from 20 μL aliquots of whole blood as explained in Section 3.3, using 3 mL of 2:1 chloroform/methanol (v/v) with 10 μg of docosatrienoate methyl ester as the internal standard (NuChek-Prep, Elysian, MN, USA). The fatty acid composition of lipid extracts was determined by gas chromatography-flame ionization detection following

derivatization with 14% BF_3 in methanol to generate fatty acid methyl esters as explained in Section 3.5.

<u>8.3.4 Data Normalization and Statistical Analyses</u>

Lipid identifications were made using SimLipid software, which provides a list of lipid features in the sample(s) of interest by automatically comparing experimental and reference fragment spectra, but it is unable to perform peak picking/peak area integration. To determine peak areas of manually-confirmed analytes, Progenesis QI was used. Lipid abundances were normalized using the internal standard belonging to the same lipid class as the analyte of interest (i.e., all PC lipid species were normalized using the PC internal standard). Concentration data are presented as mean ± standard deviation of all analytes in nmol lipid/mL blood. Two-tailed bivariate correlations were performed between dietary intake data and lipid concentrations to generate Pearson r-values as a measure of the strength of the associations, and Fisher's exact z-test [257] was used for comparisons of correlations between complex lipids, fatty acid concentrations and intake levels. Statistical significance was inferred at $p < 0.05$.

8.4 Results

The polarity-switching method enabled the detection and characterization of free fatty acids, lysophospholipids, phosphatidylcholines, phosphatidylethanolamines, phosphatidylserines, phosphatidylinositols and sphingolipids in the negative ion mode, as well as triacylglycerols and cholesteryl esters in the positive ion mode (Figure 17). Monoacylglycerols, diacylglycerols, and free cholesterol were not characterized as their detection requires positive ion mode, but they elute in the first half of the chromatographic run with the polar lipids. Similarly, cardiolipins

were not identified as they require negative ion mode and they eluted in the second half of the chromatographic run with the nonpolar lipids. In total, there were 710 positive lipid identifications that were made with FAID (Table 6). Of these, 54 lipids contained 18:3, 61 contained 20:5, and 54 contained 22:6. The majority of these PUFA-containing lipids were distributed across the major phospholipids (72%, 79%, and 89% of total 18:3, 20:5 and 22:6 identifications were phospholipids, respectively), where most of the 18:3-lipids were found as PC, and most of the 20:5- and 22:6-lipids as PS. A detailed list of all of the species that were identified with FAID can be found in Appendix A. Quantitative data was generated for 140 lipids of high abundance, including two 18:3-species, twenty-four 20:5-species, and thirty-one 22:6-species (Table 7). The 18:3-, 20:5- and 22:6-containing phospholipid species with the highest abundance were PC 18:0_18:3 (33.07 ± 7.33 nmol/mL), PC 16:0_20:5 (60.81 ± 15.68 nmol/mL) and PC 16:0_22:6 (81.90 ± 17.80 nmol/mL), respectively.

Dietary intakes of ALA, EPA, DHA and total omega-3 PUFA were 1.73 ± 1.04, 0.10 ± 0.10, 0.16 ± 0.17, and 2.16 ± 1.14 g/d, respectively (participant characteristics and dietary intakes can be found in Table 8). Fatty acid compositional analyses indicated relative weight percent of EPA+DHA in total fatty acids in whole blood was 4.41 ± 1.13 % (Table 9). By correlating quantitative lipidomic data for all 140 lipids versus dietary intakes of omega-3 PUFA, several associations were found to reach statistical significance. We plotted the three complex lipids that had the strongest Pearson correlation r-values with individual fatty acid intakes (Figure 18; ALA intakes A – C; EPA intakes E – G; and DHA intakes I – K), and sums of fatty acids (Figure 19; EPA+DHA intakes A – C; and Total Omega-3 PUFA intakes E – G). Interestingly, the three lipids that were the most strongly correlated with ALA intakes were all TAG species that did not contain ALA. This included TAG 16:0_18:1_22:5 ($r = 0.245$,

$p = 0.007$), TAG 16:0_18:1_22:6 ($r = 0.228$, $p = 0.012$) and TAG 18:0_18:1_18:2 ($r = 0.209$,

$p = 0.022$). PC 18:0_18:3 and CE 18:3, which both contained 18:3 were not correlated

significantly with ALA intakes ($r = 0.090$ and -0.024, respectively and $p > 0.05$ for both).

Further inspection of the scatterplots between the intake of ALA and the concentrations of the

three blood TAG species indicated that a single participant with an estimated ALA intake of

11.3g/d was influencing the correlations. After removing this outlier from the sample set, two

different TAG (TAG 18:1_20:5_22:6 and TAG 16:1_18:2_22:6) and a CE (CE 20:4) were found

to have statistically-significant associations to ALA intakes (Figure 20 A – C; $p \leq 0.001$ for all).

The lipids that were the most-strongly correlated with EPA, DHA and EPA+DHA intakes

were all DHA-containing phosphatidylethanolamine plasmalogens. For EPA intakes, the top-

three correlated lipids were PE P-16:0_22:6, PE P-18:1_22:6 and PE P 18:0_22:6 ($r = 0.465$,

0.445 and 0.410, respectively; $p < 0.001$ for all). From our hypothesis, PE P-16:0_20:5

($r = 0.379$; $p < 0.001$) was correlated, but PC 16:0_20:5 was not correlated ($r < 0.15$, $p > 0.05$)

with EPA intake. For DHA intakes, the top-three correlated lipids were PE P-16:0_22:6, PE P-

18:1_22:6 and PE P-20:0_22:6 ($r = 0.425$, 0.399 and 0.383, respectively; $p < 0.001$ for all). This

included PE P-16:0_22:6 but not PC 16:0_22:6 from our hypothesis, although PC 16:0_22:6 was

still correlated with DHA intake ($r = 0.302$; $p < 0.01$). For EPA+DHA intakes, the top-three

correlated lipids were PE P-16:0_22:6, PE P-18:1_22:6 and PE P-18:0_22:6 ($r = 0.445$, 0.420

and 0.389, respectively; $p < 0.001$ for all). The removal of the outlier with the highest ALA

intake did not change the lipid species that had the strongest associations to EPA (Figure 20 E –

G), DHA (Figure 20 I – K) and EPA+DHA intakes (Figure 21 A – C).

The correlations between lipidomic markers and total omega-3 PUFA intakes resembled

the correlations with ALA intakes. TAG 16:0_18:1_22:6 ($r = 0.232$, $p < 0.05$) that was correlated

with ALA intake was again a top-three correlated lipid, with TAG 18:1_20:5_22:6 ($r = 0.253$, $p < 0.05$) and TAG 18:0_18:1_22:6 ($r = 0.239$, $p < 0.05$) also being within the top-three lipids correlated with total omega-3 PUFA intake. Removal of the participant with unusually high ALA intake again changed the intake-blood lipid correlations. Interestingly, TAG 18:1_20:5_22:6 remained in the top 3 with an increased strength ($r = 0.369$, $p < 0.001$), with PE P-16:0_22:6 ($r = 0.289$, $p = 0.001$), and PE P-16:0_20:5 ($r = 0.273$, $p = 0.003$) replacing the other TAG species in the top-three lipids correlated with total omega-3 PUFA intake (Figure 21 A – C).

Dietary intakes of ALA, EPA, and DHA, (Figure 18 D, H, and L) and EPA+DHA and total omega-3 PUFA (Figure 19 D and H) were correlated against their corresponding levels in whole blood as fatty acids. DHA intake and DHA as a fatty acid in blood tended to have the strongest correlation which was relatively similar to DHA intake correlations to the DHA-containing lipidomic measurements. Correlations between ALA and EPA intake and blood fatty acid levels appeared slightly weaker, but not statistically different than the correlations with lipidomic measurements ($p > 0.05$ by Fisher's exact z-test). Interestingly, the lipidomic approach highlighted that ALA and EPA may correlate more strongly with lipid species that do not contain ALA and EPA, respectively. Ad hoc comparisons to all fatty acids revealed that ALA intake correlated significantly only with 18:0 ($r = 0.182$, $p = 0.047$) and 18:1n-9 ($r = 0.206$, $p = 0.024$). EPA intake correlated with several blood fatty acids, with DHA being the strongest ($r = 0.407$, $p < 0.001$).

8.5 Discussion

<u>8.5.1 Method Application and Assessment</u>

In this study, we utilized a UHPLC-MS/MS method with retention time-based ESI polarity switching to achieve the optimal ionization of the major polar and non-polar lipids in whole blood within a single analytical run. Similar approaches have been adapted previously for the analysis of targeted drugs and metabolites in pharmacological studies [258-261], but not in discovery-based lipidomics. The inherent problems of acquiring data in only positive or negative polarities (discussed in Chapter 7) have also been addressed with newer technologies that enable fast polarity switching with alternating positive and negative scans [22, 130, 262-264]. However, this capability is technologically-demanding, and only a few analytical platforms have polarity-switching dwell times that are fast enough (a few milliseconds) to make them amenable for HPLC- and UHPLC-based protocols [99, 265]. Special attention should also be given in top-n DDA-based applications since MS-survey scans would be acquired less frequently, and true chromatographic peak profiles may not be captured. On the mass spectrometer that was used for the experiments in this Chapter (Waters Synapt G2S*i* QToF), the total dwell time for switching between positive and negative ion modes is approximately 20 s, making fast polarity-switching unfeasible on our platform.

There were lipids from a few lipid classes that were not detected since they eluted at times when the mass spectrometer was being operated in an ESI polarity that was not optimal for these classes. Specifically, monoacylglycerols, diacylglycerols and free cholesterol eluted within the first 27 min of the LC gradient when spectra are being acquired in the negative ion mode, but species from these lipid classes are more easily ionized in the positive ion mode [266-268]. Similarly, cardiolipins are eluted at approximately the same time as triacylglycerols and

cholesteryl esters when the mass spectrometer is being operated in the positive ion mode (27-45 min), but these species can be better characterized in the negative ion mode [170, 269]. Therefore, the present method has limitations in characterizing the full lipidome, but it is well suited for examining differences in the acyl species of complex blood lipids in response to different intakes of fatty acids. While free cholesterol is an important biomarker for health and disease [270], it does not contain a fatty acyl moiety and cannot be used to directly differentiate intakes of different fatty acids. Monoacylglycerols, diacylglycerols and cardiolipins do contain fatty acids, but their abundance in human whole blood is relatively low and they contain < 10% of total fatty acids in blood [251]. Measuring the low-abundant species of these lipid classes is important [271], but targeted methods may be better suited for their characterization. For assessing omega-3 PUFA intake, monoacylglycerols and diacylglycerols are metabolically linked to TAG, which are more abundant [234] and have low EPA and DHA content [271]. Cardiolipin acyl composition is tightly regulated and more resistant to differences in dietary intake [272] and the complexity of the cardiolipin molecule is better suited using targeted analyses [170].

Only a small proportion of the lipid features that were identified using SimLipid software (710 features) were fully characterized using Progenesis QI (140 total identifications, 57 were confirmed to contain 18:3, 20:5 or 22:6). Although SimLipid is an automated solution designed for the identification of lipid features without necessitating user confirmation, at the time of this thesis this software package is incapable of determining compound peak areas which would be used to determine analyte concentrations. As a measure of abundance, it provides absolute product ion intensity sums (as a surrogate measure of peak height) but does not consider chromatographic peak widths. Conversely, Progenesis QI does have peak picking and peak area

integration tools in addition to an assisted compound identification algorithm. This latter workflow is time-consuming as it requires user confirmation of every lipid identification, and while the resulting list of analytes may not be exhaustive, these high-quality identifications are quantitated. As discussed in Chapter 5, the process of searching for all possible fatty acyl fragments within a given MS/MS scan to classify a lipid feature as FAID within SimLipid can significantly increase the confidence in the results by lowering the number of false positive identifications. However, background ions or noise in MS/MS spectra can be misidentified as fatty acyl fragments. This is evident from some of the identifications that are reported in Appendix A, which includes a large number of lipids with odd-chain fatty acids which are relatively uncommon in human blood [273]. Although some of these identified lipids could be real, it is highly unlikely that multiple odd chain fatty acids would be arranged together on the same molecule. For example, TAG 15:1_19:0_19:1 was reported as a lipid feature with FAID, but upon manual examination of MS/MS spectra, all of the diagnostic fragments that were used to confirm this lipid were background ions. Conversely to SimLipid's lipid identification workflow, Progenesis QI relies on a user-assisted approach, whereby possible identifications with a high level of agreement are presented based on precursor ion mass error and fragmentation pattern matches. The software then allows the user to pick the most likely candidate. Due to the conservative nature of this workflow which requires human input in order to annotate lipid species, the list of 140 identified compounds is not exhaustive. Overall, by adopting a retention time-based polarity-switching algorithm to our upfront UHPLC protocol, we were able to acquire high-quality spectra for the major lipids in human whole blood, including phospholipids, triacylglycerols and cholesteryl esters which is in agreement with the first hypothesis.

8.5.2 Lipidomic Blood biomarkers of Omega-3 PUFA Intake

We identified several lipid molecules that could serve as potential biomarkers of intake for ALA, EPA, DHA, EPA+DHA and total omega-3 PUFA. Although the correlations between the concentrations of three different TAG species and ALA as well as total omega-3 PUFA intakes reached statistical significance, they were relatively weak. Regarding the second hypothesis, there were only two 18:3-containing lipids (PC 18:0_18:3 and CE 18:3) that were identified and quantitated, but neither of these were significantly correlated with ALA intakes. More targeted analyses may enable the detection and characterization of a higher number of 18:3-containing complex lipids, which could be stronger predictors of ALA and total omega-3 PUFA intake. However, it appears that predicting ALA intakes from blood biomarkers is difficult and may require other statistical approaches such a multiple linear regression [274].

We found that 22:6-containing phosphatidylethanolamine plasmalogens (PE P-16:0_22:6, PE P-18:0_22:6, PE P-18:0_22:6 and PE P-20:0_22:6) were better predictors of EPA, DHA and EPA+DHA intakes as compared with 20:5-containing lipids. From the lipids that were hypothesized to be strongly correlated with EPA intakes, only PE P-16:0_20:5 reached statistical significance. However, both PC 16:0_22:6 and PE P-16:0_22:6 which were hypothesized to be correlated with DHA intakes reached statistical significance. These observations could be due to differences in the rates of turnover of PE lipids and 22:6-containing lipids as compared with others [236, 251, 275, 276], and suggests that these species could be used as indicators of chronic or habitual intake of EPA+DHA.

Several studies have examined the relationship between dietary omega-3 PUFA and the adaptations that take place in blood [277]. This has led to the identification of various PUFA-containing species such as PC 38:6, PC 38:8 and PC 40:6 which are associated with omega-3

PUFA intake [244-246, 250]. One of the limitations of many of these studies is that lipidomic data are presented at the brutto level. While assumptions can be made regarding the specific fatty acyl composition of discrete lipid species from brutto-level data, the large number of isomeric species that may be present in a biological sample limit our ability to make definite conclusions about the metabolism of specific lipid molecules. Some studies have reported medio-level information for species that are responsive to omega-3 PUFA supplementation, including PC 18:0_20:5, PC 16:0_22:6, PE 16:0_22:6 and PS 18:0_22:6 [247, 248], all of which were found to be significantly correlated with EPA or DHA intake in this Chapter. Interestingly, only one recent study on the post-prandial response in plasma to omega-3 PUFA intake has reported an enrichment of specific EPA- or DHA-containing ether-linked phospholipid species [249]. Although the digestion, absorption and gross metabolism of ether-linked lipids is still poorly understood, several studies have observed relatively higher proportions of both omega-3 and omega-6 PUFA in these lipids as compared with di-acyl phospholipids of the same subclass [278-281].

One of the limitations of the present work is that the population that was studied has relatively higher consumption and blood levels of omega-3 PUFA than most of the world [238, 282], which could limit the translatability of these findings and necessitates confirmation in populations with lower/more infrequent intakes. In addition, a 7-day food record was used to assess omega-3 PUFA intakes which only represents dietary intakes of the 7 days prior to sample collections, which may not necessarily reflect usual long-term intakes [283]. Contrasting lipidomic blood biomarkers of intake with other common methods of dietary assessment such as food frequency questionnaires and 24h dietary recalls should be examined.

The inability to determine the specific locations of carbon-carbon double bonds within fatty acyl chains using the current methodology could also limit the interpretation of these results. While this may not be an issue for 20:5 (EPA)- and 22:6 (DHA)-containing lipids which have all methylene-interrupted *cis*-double bonds, 18:3 can be either ALA (18:3n-3) or gamma-linolenic acid (18:3n-6), both of which are present in human blood [284]. Infinio level characterization of the acyl species in blood should be pursued through complex double bond-locating methods [57-60], which could then be used to assess the ability of simplified methods to discriminate these acyl species for example by retention time. Nevertheless, to our knowledge this is the largest lipidomic examination of complex blood lipids as potential biomarkers of omega-3 PUFA intake and the only lipidomic assessment in a national observational survey study that has been completed. Moreover, studies using controlled intakes of omega-3 PUFA under different conditions (acute/sporadic and chronic/frequent intake) are needed to confirm these observations and increase our understanding of changes in lipidomic biomarkers in response to diet.
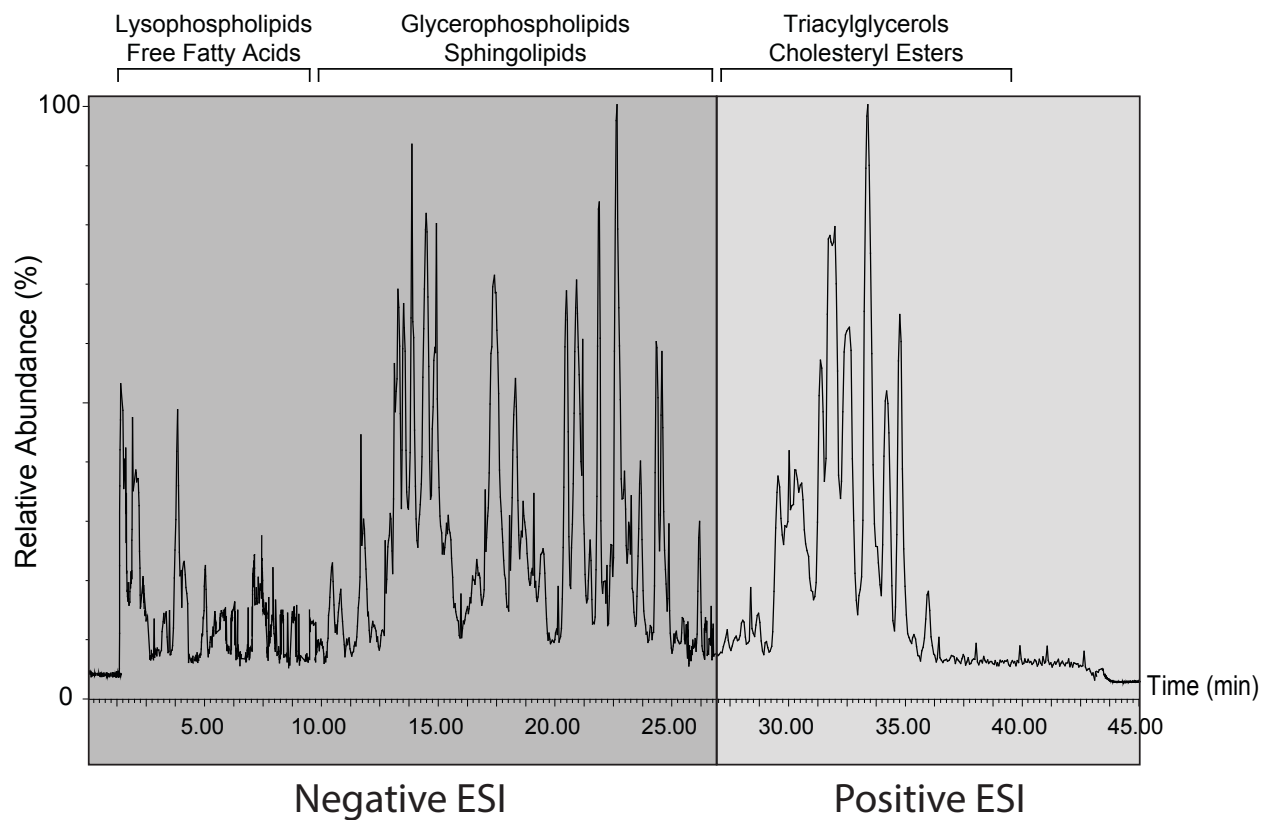
Figure 17. Total ion chromatogram and approximate elution times of the major lipid classes in whole blood, highlighting the ionization polarity used to acquire spectra. ESI, electrospray ionization.

Table 6. Distribution of lipid species with full acyl identifications (FAID) in whole blood

Main Class	Lipid Sub-Class	Number of Species with FAID			
		18:3-Lipids	20:5-Lipids	22:6-Lipids	Total Lipids
Phosphosphingolipids	Ceramide phosphocholines (sphingomyelins)	0	0	0	12
Phosphosphingolipids	Ceramide phosphoethanolamines	0	0	0	1
Glycerophosphates	Diacylglycerophosphates	0	0	0	10
Glycerophosphocholines	Diacylglycerophosphocholines	15	12	11	172
Glycerophosphoethanolamines	Diacylglycerophosphoethanolamines	11	11	11	127
Glycerophosphoglycerols	Diacylglycerophosphoglycerols	1	2	4	28
Glycerophosphoinositols	Diacylglycerophosphoinositols	3	3	4	41
Glycerophosphoserines	Diacylglycerophosphoserines	8	18	16	137
Glycerophosphocholines	Monoacylglycerophosphocholines	1	1	1	14
Glycerophosphoethanolamines	Monoacylglycerophosphoethanolamines	0	1	1	9
Glycerophosphoinositols	Monoacylglycerophosphoinositols	0	0	0	2
Glycerophosphoserines	Monoacylglycerophosphoserines	0	0	0	2
Ceramides	N-acylsphingosines (ceramides)	0	0	0	1
Oxidized glycerophospholipids	Oxidized glycerophosphocholines	0	0	0	1
Fatty Acyls	Fatty Acids & Conjugates	1	1	1	8
Sterols	Steryl Esters	1	1	1	6
Triradylglycerols	Triacylglycerols	13	11	4	139
	Total	**54**	**61**	**54**	**710**

Table 7. Concentrations of lipid species in the macrolipidome of whole blood samples from the Danish National Surveys of Diet and Physical Activity

Lipid Sub-Class	Brutto-Species	Medio-Species	m/z	Concentration (nmol/mL)
N-acylsphingosines (ceramides)	CER d42:1	CER d18:1_24:0	694.6351	1.86 ± 0.41
N-acylsphingosines (ceramides)	CER d42:2	CER d18:1_24:1	692.6194	4.34 ± 0.97
Monoacylglycerophosphocholines	LPC 14:0	LPC 14:0	512.2988	1.20 ± 0.40
Monoacylglycerophosphocholines	LPC 16:0	LPC 16:0	540.3303	47.27 ± 10.36
Monoacylglycerophosphocholines	LPC 18:0	LPC 18:0	568.3617	51.52 ± 11.07
Monoacylglycerophosphocholines	LPC 18:1	LPC 18:1	566.3460	13.30 ± 3.99
Monoacylglycerophosphocholines	LPC 18:2	LPC 18:2	564.3303	18.46 ± 6.65
Monoacylglycerophosphocholines	LPC 20:5	LPC 20:5	586.3145	1.76 ± 0.73
Monoacylglycerophosphocholines	LPC 22:6	LPC 22:6	612.3302	1.16 ± 0.52
Monoalkylglycerophosphocholines	LPC O-16:0	LPC O-16:0	526.3505	0.93 ± 0.19
Monoalkylglycerophosphocholines	LPC O-18:1	LPC O-18:1	552.3664	0.77 ± 0.17
Monoacylglycerophosphoethanolamines	LPE 16:0	LPE 16:0	452.2778	0.75 ± 0.24
Monoacylglycerophosphoethanolamines	LPE 18:0	LPE 18:0	480.3091	2.88 ± 0.79
Monoacylglycerophosphoethanolamines	LPE 20:0	LPE 20:0	554.3459	0.83 ± 0.22
Monoacylglycerophosphoethanolamines	LPE 20:5	LPE 20:5	498.2619	0.13 ± 0.08
Monoacylglycerophosphoethanolamines	LPE 22:6	LPE 22:6	524.2776	0.44 ± 0.12
Diacylglycerophosphocholines	PC 32:2	PC 14:0_18:2	774.5280	6.22 ± 2.50
Diacylglycerophosphocholines	PC 34:4	PC 14:0_20:4	798.5274	1.51 ± 0.75
Diacylglycerophosphocholines	PC 34:5	PC 14:0_20:5	796.5127	0.39 ± 0.47
Diacylglycerophosphocholines	PC 36:6	PC 14:0_22:6	822.5280	1.63 ± 0.80
Diacylglycerophosphocholines	PC 32:0	PC 16:0_16:0	778.5595	43.28 ± 6.73
Diacylglycerophosphocholines	PC 34:1	PC 16:0_18:1	804.5756	226.18 ± 36.29
Diacylglycerophosphocholines	PC 34:2	PC 16:0_18:2	802.5600	282.79 ± 35.33
Diacylglycerophosphocholines	PC 36:4	PC 16:0_20:4	826.5598	94.83 ± 22.57
Oxidized Glycerophosphocholines	PC 36:4(OH)	PC 16:0_20:4(OH)	842.5527	0.80 ± 0.60
Diacylglycerophosphocholines	PC 36:5	PC 16:0_20:5	824.5440	60.81 ± 15.68
Diacylglycerophosphocholines	PC 38:5	PC 16:0_22:5	852.5753	18.69 ± 3.41
Diacylglycerophosphocholines	PC 38:6	PC 16:0_22:6	850.5597	81.90 ± 17.80
Diacylglycerophosphocholines	PC 34:3	PC 16:1_18:2	800.5437	20.55 ± 6.32
Diacylglycerophosphocholines	PC 36:6	PC 16:1_20:5	822.5280	0.28 ± 0.37
Diacylglycerophosphocholines	PC 38:7	PC 16:1_22:6	848.5439	2.39 ± 1.17
Diacylglycerophosphocholines	PC 36:1	PC 18:0_18:1	832.6068	80.31 ± 12.19
Diacylglycerophosphocholines	PC 36:3	PC 18:0_18:3	828.5754	33.07 ± 7.33
Diacylglycerophosphocholines	PC 38:4	PC 18:0_20:4	854.5910	63.00 ± 11.29
Diacylglycerophosphocholines	PC 38:5	PC 18:0_20:5	852.5752	12.25 ± 4.43
Diacylglycerophosphocholines	PC 40:5	PC 18:0_22:5	880.6062	3.64 ± 1.00
Diacylglycerophosphocholines	PC 40:6	PC 18:0_22:6	878.5909	21.61 ± 6.56
Diacylglycerophosphocholines	PC 36:2	PC 18:1_18:1	830.5912	218.61 ± 29.33
Diacylglycerophosphocholines	PC 38:6	PC 18:1_20:5	850.5582	0.16 ± 0.08
Diacylglycerophosphocholines	PC 40:7	PC 18:1_22:6	876.5746	2.91 ± 0.85
Diacylglycerophosphocholines	PC 38:7	PC 18:2_20:5	848.5432	1.05 ± 0.56
Diacylglycerophosphocholines	PC 40:8	PC 18:2_22:6	874.5593	1.16 ± 0.38
Alkylacylglycerophosphocholines	PC O-38:4	PC O-18:0_20:4	840.6106	8.13 ± 1.70
Alkylacylglycerophosphocholines	PC O-40:5	PC O-18:0_22:5	866.6256	1.33 ± 0.32
Alkenylacylglycerophosphocholines	PC P-34:2	PC P-16:0_18:2	786.5625	10.12 ± 2.12

Alkenylacylglycerophosphocholines	PC P-36:5	PC P-16:0_20:5	808.5495	5.67 ± 1.25
Diacylglycerophosphoethanolamines	PE 36:6	PE 14:0_22:6	734.4754	0.07 ± 0.07
Diacylglycerophosphoethanolamines	PE 32:1	PE 16:0_16:1	776.5436	10.02 ± 4.59
Diacylglycerophosphoethanolamines	PE 34:1	PE 16:0_18:1	716.5229	69.45 ± 13.28
Diacylglycerophosphoethanolamines	PE 36:4	PE 16:0_20:4	738.5072	29.89 ± 5.43
Diacylglycerophosphoethanolamines	PE 36:5	PE 16:0_20:5	736.4914	5.18 ± 2.50
Diacylglycerophosphoethanolamines	PE 38:6	PE 16:0_22:6	762.5071	15.27 ± 3.83
Diacylglycerophosphoethanolamines	PE 38:7	PE 16:1_22:6	760.4916	0.10 ± 0.08
Diacylglycerophosphoethanolamines	PE 37:5	PE 17:1_20:4	796.5126	3.59 ± 0.82
Diacylglycerophosphoethanolamines	PE 36:1	PE 18:0_18:1	744.5560	35.70 ± 6.42
Diacylglycerophosphoethanolamines	PE 38:4	PE 18:0_20:4	766.5383	46.91 ± 7.88
Diacylglycerophosphoethanolamines	PE 40:6	PE 18:0_22:6	790.5393	9.09 ± 1.63
Diacylglycerophosphoethanolamines	PE 36:2	PE 18:1_18:1	788.5417	3.35 ± 0.92
Diacylglycerophosphoethanolamines	PE 38:5	PE 18:1_20:4	764.5227	40.41 ± 6.85
Diacylglycerophosphoethanolamines	PE 38:6	PE 18:1_20:5	762.5071	2.28 ± 0.73
Diacylglycerophosphoethanolamines	PE 40:7	PE 18:1_22:6	788.5227	6.03 ± 1.48
Diacylglycerophosphoethanolamines	PE 38:7	PE 18:2_20:5	760.4911	0.47 ± 0.24
Diacylglycerophosphoethanolamines	PE 40:8	PE 18:2_22:6	786.5071	1.96 ± 0.70
Diacylglycerophosphoethanolamines	PE 39:3	PE 19:0_20:3	828.5754	62.01 ± 15.64
Diacylglycerophosphoethanolamines	PE 39:4	PE 19:0_20:4	826.5598	88.78 ± 20.99
Diacylglycerophosphoethanolamines	PE 40:9	PE 20:4_20:5	784.4916	0.06 ± 0.07
Diacylglycerophosphoethanolamines	PE 42:10	PE 20:4_22:6	810.5074	0.74 ± 0.29
Alkenylacylglycerophosphoethanolamines	PE P-36:4	PE P-16:0_20:4	722.5123	45.46 ± 8.95
Alkenylacylglycerophosphoethanolamines	PE P-36:5	PE P-16:0_20:5	720.4966	3.90 ± 2.22
Alkenylacylglycerophosphoethanolamines	PE P-38:5	PE P-16:0_22:5	748.5275	54.84 ± 9.46
Alkenylacylglycerophosphoethanolamines	PE P-38:6	PE P-16:0_22:6	746.5122	13.57 ± 3.25
Alkenylacylglycerophosphoethanolamines	PE P-38:4	PE P-18:0_20:4	750.5436	110.47 ± 19.49
Alkenylacylglycerophosphoethanolamines	PE P-38:5	PE P-18:0_20:5	748.5277	10.94 ± 4.14
Alkenylacylglycerophosphoethanolamines	PE P-40:4	PE P-18:0_22:4	778.5742	40.59 ± 8.86
Alkenylacylglycerophosphoethanolamines	PE P-40:5	PE P-18:0_22:5	776.5581	36.87 ± 5.89
Alkenylacylglycerophosphoethanolamines	PE P-40:6	PE P-18:0_22:6	774.5434	32.83 ± 7.43
Alkenylacylglycerophosphoethanolamines	PE P-38:6	PE P-18:1_20:5	746.5123	5.14 ± 2.06
Alkenylacylglycerophosphoethanolamines	PE P-40:7	PE P-18:1_22:6	772.5276	9.35 ± 2.51
Alkenylacylglycerophosphoethanolamines	PE P-42:6	PE P-20:0_22:6	802.5739	0.80 ± 0.20
Ceramide phosphoethanolamines	PE-Cer d35:1	PE-Cer d14:1_21:0	719.5340	2.84 ± 0.52
Ceramide phosphoethanolamines	PE-Cer d35:2	PE-Cer d14:2_21:0	717.5180	0.26 ± 0.09
Ceramide phosphoethanolamines	PE-Cer d37:2	PE-Cer d14:2_23:0	745.5494	2.31 ± 0.31
Ceramide phosphoethanolamines	PE-Cer d33:1	PE-Cer d15:1_18:0	691.5024	0.14 ± 0.07
Diacylglycerophosphoinositols	PI 36:5	PI 16:0_20:5	855.5022	0.20 ± 0.24
Diacylglycerophosphoinositols	PI 38:6	PI 16:0_22:6	881.5176	0.97 ± 0.50
Diacylglycerophosphoinositols	PI 38:4	PI 18:0_20:4	885.5492	42.74 ± 9.28
Diacylglycerophosphoinositols	PI 38:5	PI 18:0_20:5	883.5330	0.43 ± 0.29
Diacylglycerophosphoinositols	PI 40:6	PI 18:0_22:6	909.5491	16.72 ± 7.28
Diacylglycerophosphoserines	PS 36:5	PS 16:0_20:5	780.4823	0.05 ± 0.07
Diacylglycerophosphoserines	PS 38:6	PS 16:0_22:6	806.4970	1.44 ± 0.60
Diacylglycerophosphoserines	PS 38:4	PS 18:0_20:4	810.5297	85.01 ± 12.96
Diacylglycerophosphoserines	PS 38:5	PS 18:0_20:5	808.5160	4.88 ± 1.36
Diacylglycerophosphoserines	PS 40:6	PS 18:0_22:6	834.5288	39.19 ± 9.36
Diacylglycerophosphoserines	PS 40:7	PS 18:1_22:6	832.5154	0.40 ± 0.17

Diacylglycerophosphoserines	PS 42:10	PS 20:4_22:6	854.4969	5.36 ± 2.40
Alkenylacylglycerophosphoserines	PS P-36:1	PS P-18:0_18:1	818.5532	1.74 ± 1.09
Sphingomyelins	SM d34:1	SM d18:0_16:1	747.5651	270.86 ± 38.11
Sphingomyelins	SM d34:1(OH)	SM d18:0_16:1(OH)	761.5434	0.75 ± 0.33
Sphingomyelins	SM d42:1	SM d18:0_24:1	859.6905	174.57 ± 25.77
Sphingomyelins	SM d36:1	SM d18:1_18:0	775.5958	46.50 ± 9.75
Sphingomyelins	SM d40:1	SM d18:1_22:0	831.6592	113.39 ± 20.12
Sphingomyelins	SM d41:2	SM d18:1_23:1	797.6535	48.60 ± 7.09
Sphingomyelins	SM d42:2	SM d18:1_24:1	857.6751	341.34 ± 46.65
Sphingomyelins	SM d44:2	SM d18:1_26:1	885.7059	18.05 ± 4.20
Steryl Esters	CE 18:1	CE 18:1	668.6347	320.43 ± 58.92
Steryl Esters	CE 18:2	CE 18:2	666.6192	1306.22 ± 188.87
Steryl Esters	CE 18:3	CE 18:3	664.6035	194.12 ± 77.23
Steryl Esters	CE 20:4	CE 20:4	690.6193	778.34 ± 172.31
Steryl Esters	CE 20:5	CE 20:5	688.6036	437.84 ± 224.80
Steryl Esters	CE 22:6	CE 22:6	714.6191	222.70 ± 116.61
Triacylglycerols	TAG 46:2	TAG 12:0_18:1_16:1	792.7079	1.42 ± 2.26
Triacylglycerols	TAG 46:0	TAG 14:0_16:0_16:0	796.7395	0.66 ± 0.78
Triacylglycerols	TAG 48:1	TAG 14:0_16:0_18:1	822.7553	6.39 ± 6.77
Triacylglycerols	TAG 50:1	TAG 16:0_16:0_18:1	850.7867	12.20 ± 8.91
Triacylglycerols	TAG 50:2	TAG 16:0_16:1_18:1	848.7710	23.01 ± 14.44
Triacylglycerols	TAG 51:1	TAG 16:0_17:0_18:1	864.8019	2.32 ± 2.35
Triacylglycerols	TAG 51:2	TAG 16:0_17:1_18:1	862.7866	3.09 ± 2.55
Triacylglycerols	TAG 52:2	TAG 16:0_18:1_18:1	876.8030	48.38 ± 18.80
Triacylglycerols	TAG 52:3	TAG 16:0_18:1_18:2	874.7872	47.64 ± 16.94
Triacylglycerols	TAG 56:6	TAG 16:0_18:1_22:5	924.8014	10.16 ± 4.38
Triacylglycerols	TAG 56:7	TAG 16:0_18:1_22:6	922.7854	6.54 ± 2.96
Triacylglycerols	TAG 52:4	TAG 16:0_18:2_18:2	872.7706	38.83 ± 17.83
Triacylglycerols	TAG 54:7	TAG 16:0_18:2_20:5	894.7546	2.04 ± 1.48
Triacylglycerols	TAG 60:12	TAG 16:0_22:6_22:6	968.7670	0.28 ± 0.24
Triacylglycerols	TAG 56:9	TAG 16:1_18:2_22:6	918.7548	0.65 ± 0.46
Triacylglycerols	TAG 53:2	TAG 17:0_18:1_18:1	890.8178	3.62 ± 2.32
Triacylglycerols	TAG 53:3	TAG 17:0_18:1_18:2	888.8022	2.69 ± 1.46
Triacylglycerols	TAG 54:2	TAG 18:0_18:1_18:1	904.8334	14.32 ± 7.94
Triacylglycerols	TAG 54:3	TAG 18:0_18:1_18:2	902.8176	22.26 ± 7.92
Triacylglycerols	TAG 58:7	TAG 18:0_18:1_22:6	950.8181	0.25 ± 0.14
Triacylglycerols	TAG 54:4	TAG 18:1_18:1_18:2	900.8016	20.90 ± 7.98
Triacylglycerols	TAG 58:8	TAG 18:1_18:1_22:6	948.8020	2.04 ± 1.01
Triacylglycerols	TAG 58:3	TAG 18:1_18:2_22:0	958.8797	0.61 ± 0.68
Triacylglycerols	TAG 58:9	TAG 18:1_18:2_22:6	946.7856	2.36 ± 1.36
Triacylglycerols	TAG 60:11	TAG 18:1_20:4_22:6	970.7859	0.38 ± 0.28
Triacylglycerols	TAG 60:12	TAG 18:1_20:5_22:6	968.7698	0.05 ± 0.05
Triacylglycerols	TAG 62:13	TAG 18:1_22:6_22:6	994.7874	0.15 ± 0.16
Triacylglycerols	TAG 58:10	TAG 18:2_18:2_22:6	944.7706	0.68 ± 0.48

Concentration values are reported as mean ± standard deviation (n = 120). CER, ceramide; LPC, lysophosphatidylcholine; LPE, lysophosphatidylethanolamine; PC, phosphatidylcholine; PE, phosphatidylethanolamine; PE-Cer, Ceramide phosphoethanolamine; PI, phosphatidylinositol; PS, phosphatidylserine; SM, sphingomyelin; CE, cholesteryl ester; TAG, triacylglycerol.

Table 8. Participant characteristics and dietary intakes

Characteristic	N = 120 (52 M, 68 F)
Age (*years*)	39.1 ± 12.0
Body mass index	24.2 ± 3.2
Dietary intake	
Total energy (*kJ*)	9449 ± 2456
Protein (*g/d*)	83 ± 24
Carbohydrate (g/d)	238 ± 70
Fat (g/d)	90 ± 27
Saturated fat	33.57 ± 11.49
12:0	1.30 ± 0.75
14:0	3.25 ± 1.40
16:0	17.97 ± 5.91
18:0	7.55 ± 2.82
Monounsaturated fat	31.18 ± 10.57
16:1n-7	1.52 ± 0.66
18:1n-9	29.66 ± 10.10
Polyunsaturated fat	13.49 ± 4.64
Omega-6 fatty acids	11.15 ± 3.85
18:2n-6	11.09 ± 3.84
20:4n-6	0.12 ± 0.07
Omega-3 fatty acids	2.06 ± 1.14
18:3n-3	1.73 ± 1.04
20:5n-3	0.10 ± 0.11
22:5n-3	0.04 ± 0.04
22:6n-3	0.16 ± 0.17

Values are mean ± SD, n = 120.

Table 9. Fatty acid composition of whole blood

Fatty Acid	Weight percent of total fatty acids
10:0	0.08 ± 0.04
12:0	0.03 ± 0.02
14:0	0.60 ± 0.19
16:0	21.03 ± 1.26
17:0	0.32 ± 0.05
18:0	11.95 ± 1.24
20:0	0.38 ± 0.06
22:0	0.98 ± 0.13
23:0	0.24 ± 0.05
24:0	1.81 ± 0.24
Total saturates	**39.86 ± 1.90**
12:1	0.01 ± 0.01
14:1	0.03 ± 0.02
16:1	1.02 ± 0.41
18:1n-7	1.56 ± 0.16
18:1n-9	16.19 ± 1.60
20:1n-9	0.23 ± 0.04
22:1n-9	0.24 ± 0.08
24:1n-9	2.30 ± 0.34
Total monounsaturates	**21.93 ± 1.72**
18:2n-6	19.01 ± 2.31
18:3n-6	0.20 ± 0.10
20:2n-6	0.22 ± 0.04
20:3n-6	1.47 ± 0.31
20:4n-6	9.29 ± 1.13
22:2n-6	0.07 ± 0.01
22:4n-6	1.06 ± 0.24
22:5n-6	0.19 ± 0.06
Total omega-6 polyunsaturates	**31.51 ± 2.30**
18:3n-3	0.41 ± 0.14
20:3n-3	0.03 ± 0.01
20:5n-3	0.97 ± 0.46
22:5n-3	1.27 ± 0.22
22:6n-3	3.44 ± 0.77
Total omega-3 polyunsaturates	**6.11 ± 1.24**
20:3n-9	0.10 ± 0.04
Total polyunsaturates	**37.72 ± 2.34**
Total HUFA	**17.82 ± 1.71**
EPA+DHA	**4.41 ± 1.13**
Omega-6/omega-3 ratio	**5.37 ± 1.18**
%n-3 HUFA in total HUFA	**31.92 ± 5.61**
Total Concentration *(μg/100μL)*	**213 ± 29**

HUFA, highly-unsaturated fatty acid; EPA, eicosapentaenoic acid;
DHA, docosahexaenoic acid. Values are mean ± SD, n = 120.
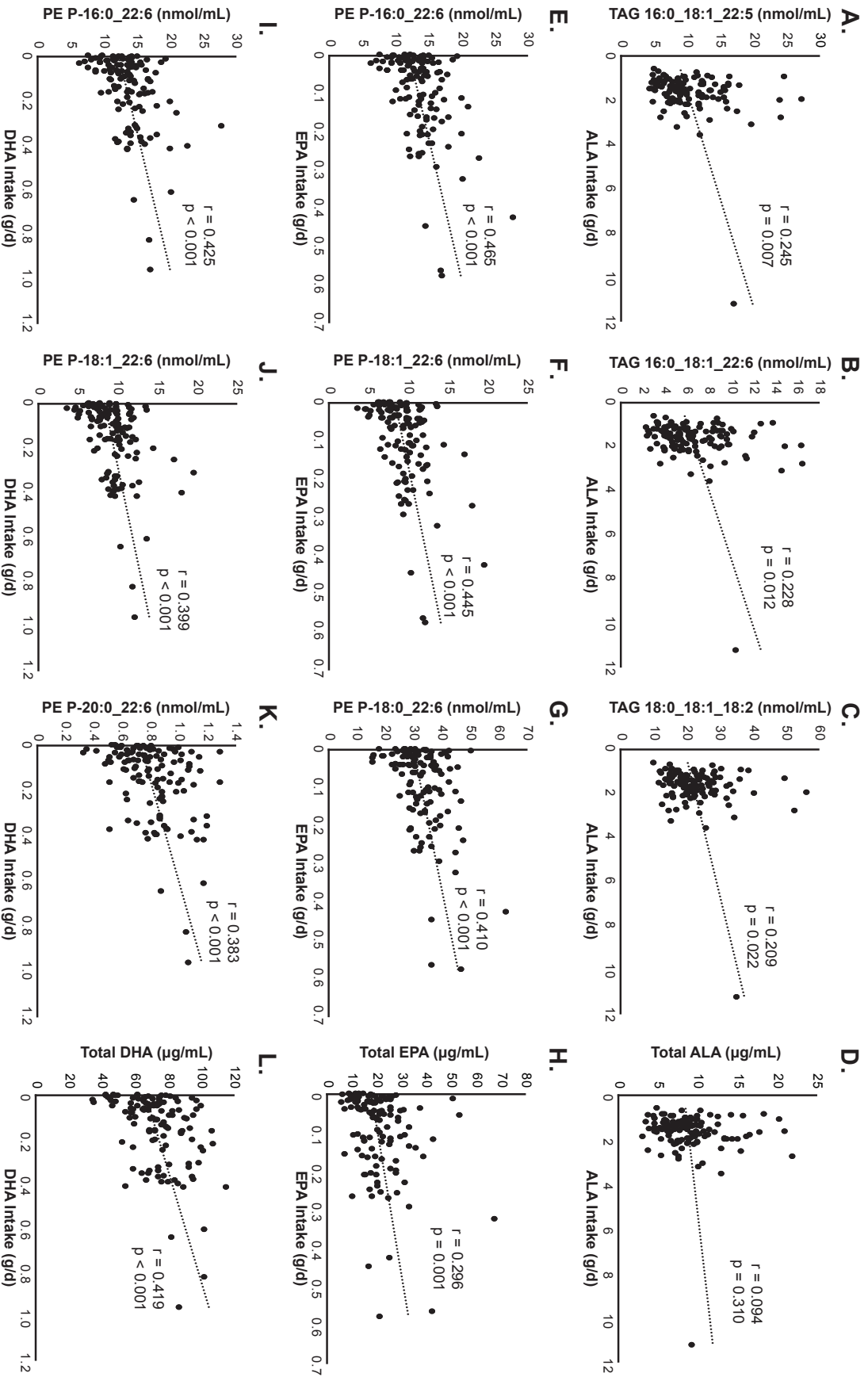
Figure 18. The top-3 complex lipids with the strongest Pearson correlation *r*-values for ALA (**A – C**), EPA (**E – G**) and DHA (**I – K**), as well as fatty acid concentrations in whole blood (ALA in **D**, EPA in **H**, DHA in **L**). Statistical significance was inferred at *p* < 0.05. ALA, alpha-linolenic acid; EPA, eicosapentaenoic acid; DHA, docosahexaenoic acid; TAG, triacylglycerol; PE, phosphatidylethanolamine.

105
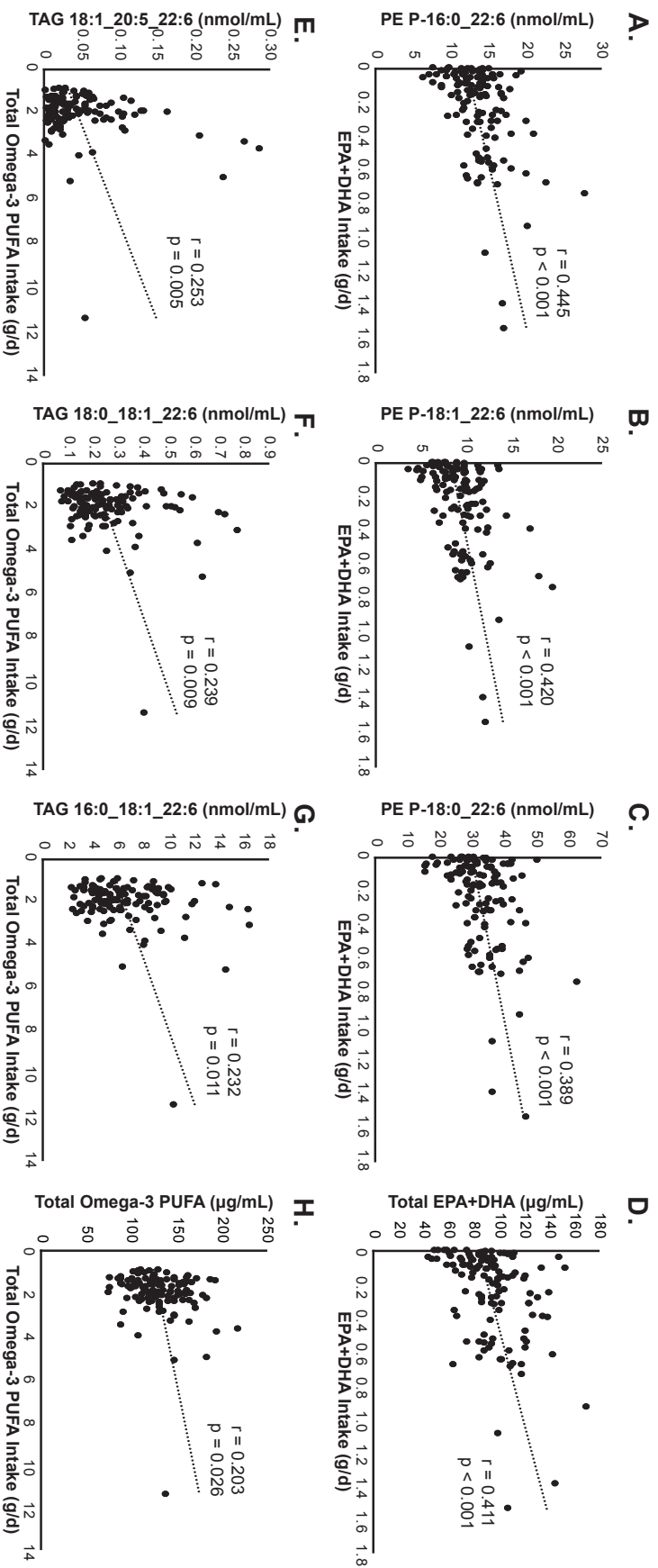
Figure 19. The top-3 complex lipids with the strongest Pearson correlation *r*-values for EPA+DHA (**A** – **C**) and total omega-3 PUFA (**E** – **G**), as well as fatty acid concentrations in whole blood (EPA+DHA in **D**, total omega-3 PUFA in **H**). Statistical significance was inferred at *p* < 0.05. EPA+DHA, sum of eicosapentaenoic acid and docosahexaenoic acid; PUFA, polyunsaturated fatty acid; PE, phosphatidylethanolamine; TAG, triacylglycerol.
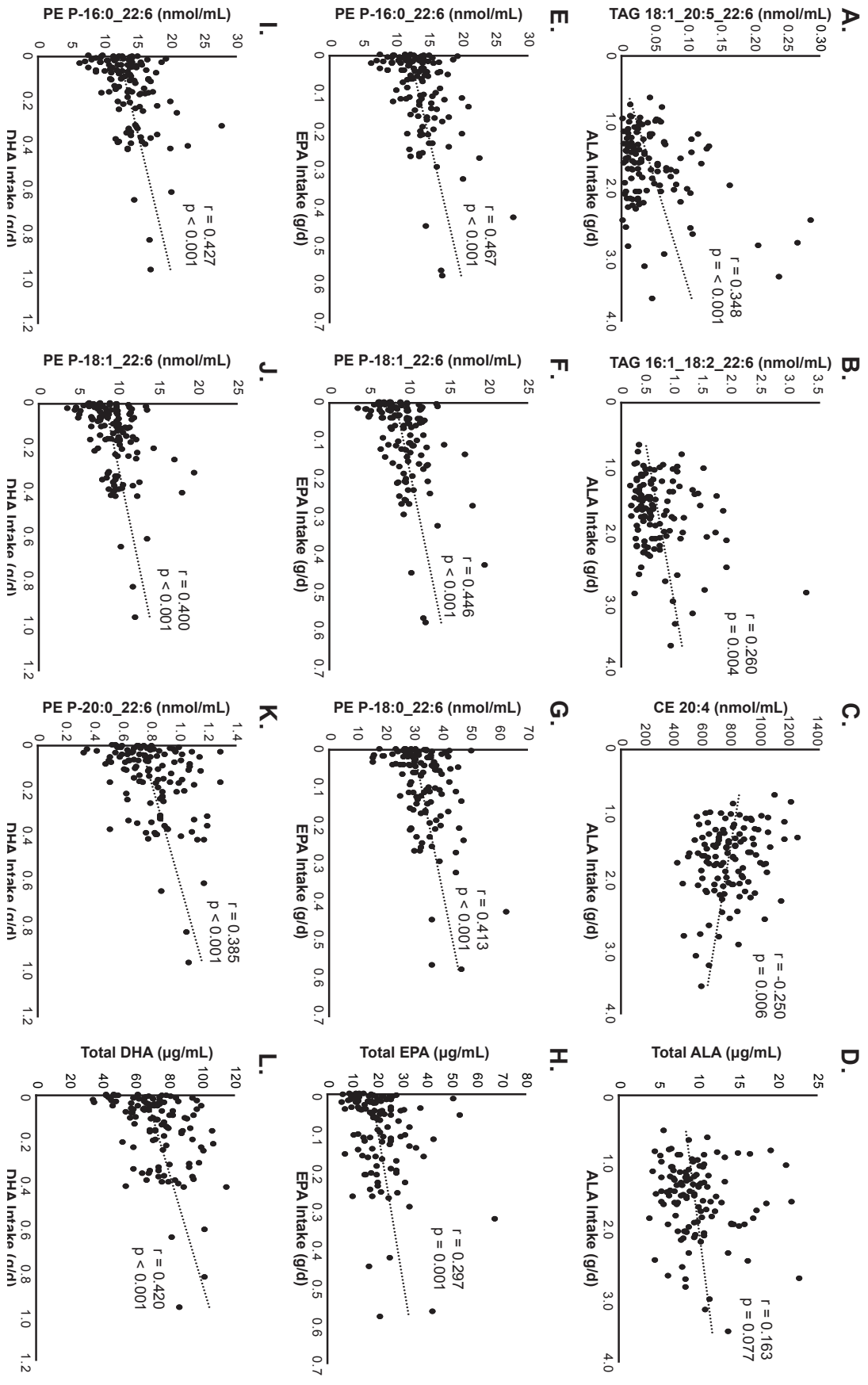
Figure 20. Excluding an outlier, the top-3 complex lipids with the strongest Pearson correlation *r*-values for ALA (**A – C**), EPA (**E – G**) and DHA (**I – K**), as well as fatty acid concentrations in whole blood (ALA in **D**, EPA in **H**, DHA in **L**). Statistical significance was inferred at *p* < 0.05. ALA, alpha-linolenic acid; EPA, eicosapentaenoic acid; DHA, docosahexaenoic acid; TAG, triacylglycerol; PE, phosphatidylethanolamine.

107
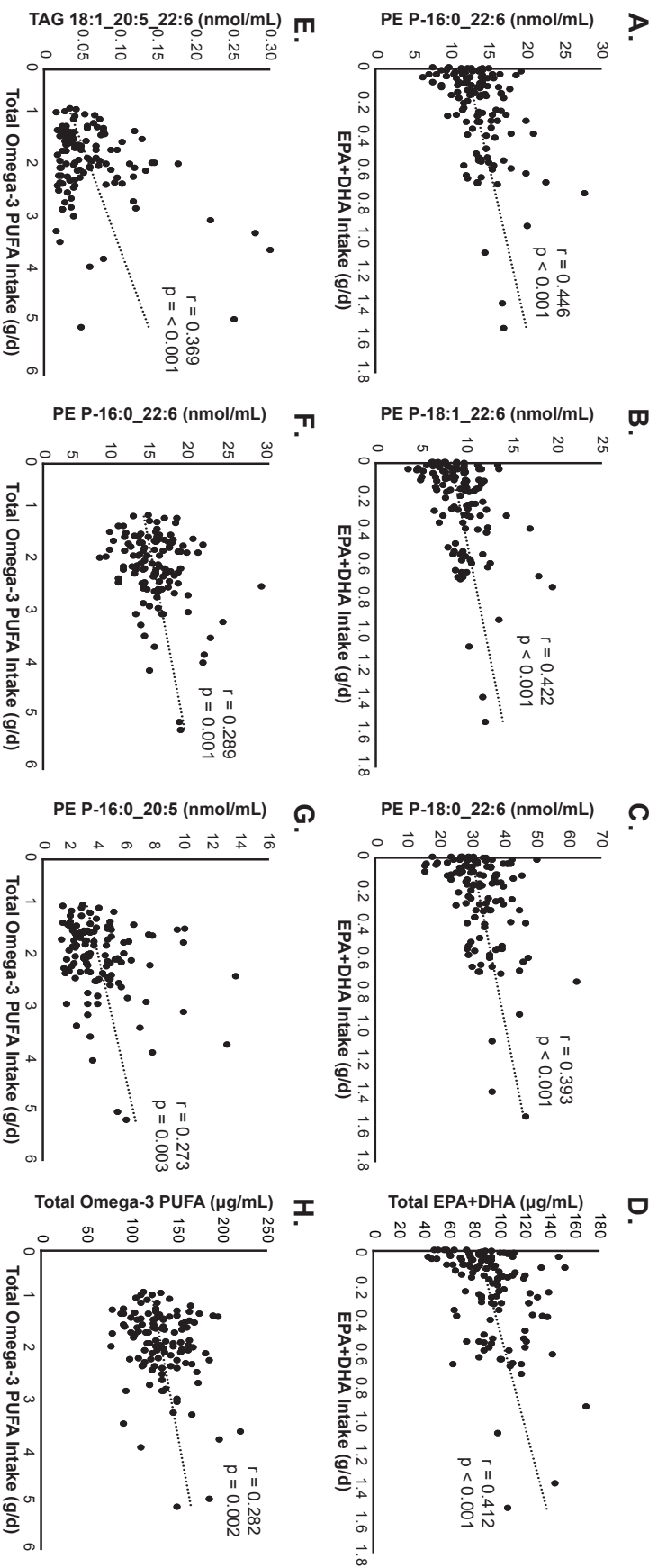
Figure 21. Excluding an outlier, the top-3 complex lipids with the strongest Pearson correlation *r*-values for EPA+DHA (**A** – **C**) and total omega-3 PUFA (**E** – **G**), as well as fatty acid concentrations in whole blood (EPA+DHA in **D**, total omega-3 PUFA in **H**). Statistical significance was inferred at *p* < 0.05. EPA+DHA, sum of eicosapentaenoic acid and docosahexaenoic acid; PUFA, polyunsaturated fatty acid; PE, phosphatidylethanolamine; TAG, triacylglycerol.

108

CHAPTER 9

Identification of Omega-3 Fatty Acid Biomarkers in a Rat Model of Acute and Chronic Docosahexaenoic Acid Feeding

9.1 Objectives

Although many studies have reported positive associations between the dietary intake of omega-3 PUFA and various health benefits [237, 285-290], contradictory results are not uncommon in the literature. Reasons for these discrepancies have been discussed [42, 237], including a lack of attention to baseline dietary intake of EPA and DHA, as well as poor measures of compliance/adherence to fish oil interventions. Blood fatty acid biomarkers can be used as surrogate measures of other blood pools and dietary fatty acid intake [275, 291]. Earlier in this thesis, it was demonstrated that applying a lipidomic approach can identify hundreds of fatty acyl-containing complex lipids, which could provide insights on metabolism and be used to monitor adherence to omega-3 PUFA supplementation trials. Lipid species such as LPC 22:6 and PE 18:1_22:6 are elevated acutely in humans after ingestion of fish oil [249], but it is not known if these species remain elevated in blood with continued intake and if they could be used to monitor omega-3 PUFA intake up to a few days. In Chapter 8, PE P-16:0_22:6 was associated with DHA intakes with humans and there is evidence that PE lipids with 22:6 turnover more slowly [276]. Additionally, in previous collaborative work in rodents fed DHA we identified PS 18:0_22:6 as a potential marker of intake over 8 weeks [292].

Previous studies using fatty acid compositional analyses indicate that there are lipid pools in blood that respond to omega-3 PUFA intakes at different rates [236, 275, 276]. Specifically, a lack of increase in the percentage of DHA in erythrocytes has been used to detect non-adherence in a long-term intervention study [236]. EPA appears to be incorporated into plasma and

erythrocytes rapidly with intake, while DHA incorporates into plasma much more rapidly than erythrocytes [275]. It is possible that there are lipid species containing DHA that incorporate DHA rapidly and then serve as a source of DHA for other lipid species with slower incorporation rates.

We are not aware of lipidomic studies examining changes in acyl species of high abundant lipids (medio-level macrolipidome characterization) after acute and chronic interventions with n-3 PUFA. Given the strong associations between DHA intake and DHA-containing lipids, we chose a DHA source without EPA (DHASCO, DSM Nutritional, Baltimore, MD, USA) as oil to add to a diet that had a fat profile similar to that of humans (TWD; total western diet). In this study, we examined changes in the blood lipidome of Sprague-Dawley rats after consuming a control diet without (TWD-) and after acute (5 days) and chronic (9 weeks) DHA feeding (TWD+).

9.2 Hypotheses

1. The concentrations of LPC 22:6 and PE 18:1_22:6 will be higher in the acute (5-day TWD+) group as compared with the chronic (9-week TWD+) and control group (9-week TWD-) groups.

2. The concentrations of PE P-16:0_22:6 and PS 18:0_22:6 will be higher in the chronic DHA group (9-week TWD+) as compared with the acute (5-day TWD+) and control (9-week TWD-) groups.

9.3 Methods and Materials

9.3.1 Sample Collection and Lipid Extraction

The study received ethics clearance from the University of Waterloo Office of Research Ethics. Six male and six female Sprague-Dawley Rats were bred at the University of Waterloo Central Animal Facility from dams that were fed a Teklad 22/5 Rodent Diet (Envigo Mississauga, ON, Canada). Male and female rats were used to account for potential sex differences in macrolipidomic responses to DHA feeding. After weaning, 4 pups (2M, 2F) were placed on a TD.110424 Total Western Diet with DHA (TWD+) providing 1.13mg DHA/g diet (0.36% of total energy) and 8 pups (4M, 4F) were placed on a Total Western Diet without DHA (TWD-) providing 0.01mg DHA/g diet (<0.01% of total energy). Dietary details are provided in Table 10. The four TWD+ (chronic DHA group) and four TWD- rats (control group) were sacrificed at 9 weeks of age by exsanguination following anesthesia using isofluorane after an overnight fast. The remaining 4 TWD- rats were placed on a TWD+ diet for five days (acute DHA group), at which point they were sacrificed (study design in Figure 22). Whole blood was collected via cardiac puncture into ethylenediaminetetraacetic acid-lined vacutainers, and aliquots were saved at -80 ºC.

Lipid extracts were obtained from whole blood samples as explained in Section 3.3. Briefly, samples were aliquoted (20 µL of blood), and 3 mL of 2:1 chloroform:methanol (v/v) were added, delivering known amounts of various deuterium-labelled internal standards for the major lipid classes (Splash Lipidomix, Avanti Polar Lipids, Alabaster, AL, USA). Lipid extracts were dried under N_2 gas and reconstituted in 100 µL of the reconstitution solvent (65:35:5 acetonitrile/isopropanol/water (v/v/v) +0.1% formic acid). Samples were then vortexed briefly and stored at 4 ºC until analysis.

9.3.2 Instrument Settings

UHPLC was completed using the binary multi-step gradient described in Section 3.4 with the Waters Acquity UPLC Charged Surface Hybrid (CSH), 1.7 μm x 2.1 mm x 150 mm column equipped with a VanGuard CSH 1.7 μm pre-column. Mass spectrometry was completed using the polarity-switching method described in Chapter 8, where from 0min to 27min, the mass spectrometer was operated in negative ESI mode, and from 27min to 47min, it was operated in positive ESI mode. Spray voltages, DDA MS/MS settings and all other parameters were similar to those described in Section 8.3.2.

9.3.3 Data Normalization and Statistical Analyses

Lipids were identified and peak areas were integrated using Progenesis QI. Lipid abundances were normalized using the internal standard belonging to the same lipid class as the analyte of interest (i.e., all PC lipid species were normalized using the PC internal standard). Principal component analysis was completed using Progenesis QI. Concentration data are presented as mean ± standard deviation of all analytes in pmol/mL blood. The lipid concentrations between the three groups were examined by one-way ANOVA followed by Tukey post-hoc testing, statistical significance was inferred at $p < 0.05$.

9.4 Results

Each experimental group formed distinct clusters by principal component analysis (PCA), with the controls (9-week TWD-) being particularly isolated (Figure 23). This latter isolation was driven primarily by various 20:4-, 22:4- and 22:5-containing PC and PE species such as PC 16:0_20:4, PC 16:0_22:5 and PE P-18:0_22:4 that were significantly higher in the

control group as compared with the acute (5-day TWD+) and chronic (9-week TWD+) groups (Table 11; $p < 0.05$ for all). Additionally, there were several 20:5- and 22:6-containing PC, PE, PI and PS species such as PC 16:0_20:5, PE P-18:0_22:6, PI 18:0_20:5 and PS 18:0_22:6 that were significantly higher in the chronic group as compared with the other two groups ($p < 0.05$ for all). Although there is less isolation of the acute group which indicates a higher degree of similarity with the other groups, there were two lipid species (PC 16:0_20:4 and TAG 16:0_22:6_22:6) in the acute group that fell between levels observed in the control group, and chronic group ($p < 0.05$ for both).

When examining relative changes in lipid abundances, a common –*omic* approach, LPC 20:5 and PE 16:0_20:5 were flagged as having an "infinity" maximum fold change between the control and chronic groups. However, this is due to the extremely low concentrations of these lipids in the control group (both were < 0.01 nmol/mL). Therefore, we added the control concentrations data to the fold change data as a reference (Figure 24). The absolute changes in LPC 20:5 (+0.31 nmol/mL, $p < 0.01$) and PE 16:0_20:5 (+1.52 nmol/mL, $p < 0.01$) in the chronic group as compared with control were small but significant. Similarly, other species of low abundance such as PI 18:0_20:5 have high maximum fold changes, with small changes in absolute concentrations (fold change for PI 18:0_20:5 was 11.95, absolute change was +1.30 nmol/mL in the chronic group as compared with control; $p < 0.001$). Other species such as PC 16:0_20:4, PE 18:1_20:4, PE P-18:0_22:6 and PE P-18:1_22:6 had relatively small maximum fold changes between the three groups (1.40, 1.72, 1.63 and 2.39), but these differences were statistically significant in the ANOVA analysis due to the large absolute changes in the concentrations of these highly-abundant lipids (-48.54, -282.27, +176.38 and

+131.95 nmol/mL in the chronic group vs. control for PC 16:0_20:4, PE 18:1_20:4, PE P-18:0_22:6 and PE P-18:1_22:6, respectively; $p < 0.01$ for all).

We identified six lipids that were similar between the acute and chronic groups, but were statistically different than the control group (Table 11). This included four lipids that were elevated in the acute and chronic groups (LPC 18:2, LPC 22:6, PC 18:1_22:6 and PS 16:0_22:6), and two lipids that decreased as compared with the controls (PC 16:0_22:5 and PE P-18:0_22:4; $p < 0.05$ for all). Additionally, we identified 13 lipids that were significantly higher in the chronic group, but were not different between the acute and control groups (Table 12). The majority of these lipids were phosphatidylethanolamines with 20:5 (PE 16:0_20:5), 22:6 (PE 18:1_22:6, PE 18:2_22:6, PE P-18:0_22:6, PE P-18:1_22:6 and PE P-20:0_22:6) which were higher in the chronic group as compared with the other groups ($p < 0.05$ for all), or omega-6 PUFA such as docosatetraenoic acid (PE P-16:0_22:4) and docosapentaenoic acid (PE O-18:1_22:5) which were lower in the chronic group ($p < 0.05$ for both). Other lipids followed similar trends, including LPC 20:5, PC 16:0_20:5 and PS 18:0_22:6, which were all higher in the chronic group ($p < 0.05$ for all). Next, we identified lipids that were significantly different between the chronic and control groups, but the levels of these species in the acute group were in between the other groups (Table 13). PC 18:0_18:2, PE 18:0_22:6 and PI 16:0_22:6 were higher in the chronic group than in the control ($p < 0.05$) but the levels in the acute group were not different from either group. PE 16:0_20:4, PE 18:0_20:4, PE 18:1_20:4 and PS 18:0_20:4 were lower in the chronic group as compared with the control, but the levels in the acute group were not significantly different from the other two. Interestingly, the levels of PC 16:0_20:4 and TAG 18:1_22:6_22:6 were significantly different between all three groups. PC 16:0_20:4 was highest in the control, followed by the acute, and then chronic DHA feeding ($p < 0.05$ for all). TAG

114

18:1_22:6_22:6 was highest with chronic feeding, followed by acute feeding, and then the control group ($p \leq 0.01$ for all). Lastly, there were 16 species that were measured that did not differ between experimental groups (Table 14). Surprisingly, this included various omega-3 and omega-6-containing lipids such as PC 16:0_22:6, PC 18:0_20:4 and PE P-18:0_22:5 ($p > 0.08$ for all).

9.5 Discussion

Fatty acyl-containing complex lipid species can be used as biomarkers for DHA consumption. We hypothesized that we would be able to find individual lipid species that would serve as biomarkers of acute and chronic intake. Our results indicate that identifying blood biomarkers that are specific to acute intake is problematic. In general, we identified six lipid species that increased in both acute and chronic DHA intervention. This included LPC 22:6 that we hypothesized would be specific for acute DHA intake. The acute biomarker that we proposed was PE 18:1_22:6, which increased only with chronic DHA intake. Therefore, we must reject our first hypothesis. For biomarkers of chronic DHA consumption, we identified 13 lipid species with increased concentrations with chronic DHA feeding while the acute DHA concentrations remained similar to controls. This included the PS 18:0_22:6 which we hypothesized, but not the PE P-16:0_22:6. PE P-16:0_22:6 levels were similar across all groups, but other phosphatidylethanolamine plasmalogens (PE P-18:0_22:6 and PE P-18:1_22:6) did increase specifically with chronic feeding. Our second hypothesis was therefore only partially correct.

LPC 22:6, PC 16:0_20:4, PC 16:0_22:5 and PS 18:0_22:6 have been associated with omega-3 PUFA intake in the few studies that have examined the fatty acyl-specific complex lipids in blood with dietary intervention [247, 248, 292]. Our findings also reflect previous

115

observations on the competition of omega-3 and omega-6 PUFA for incorporation into phospholipids, with the concentrations of ten 20:4-, 22:4-, or 22:5-containing species being significantly reduced in the 9-week DHA supplementation group as compared with the control group [247, 248]. As indirect biomarkers of omega-3 PUFA intake, additional research with different diets are needed to evaluate their predictive value in human populations. Additionally, we observed significant increases in EPA-containing species despite this being a DHA-only feeding trial. These observations have also been reported previously [247, 292, 293], and have recently been attributed to a slowed rate of turnover resulting in an accumulation of EPA with DHA feeding [294], rather than peroxisomal retroconversion of DHA back to EPA [295]. Nevertheless, this study is the first to apply an unbiased discovery-based macrolipidomic approach for the identification of complex lipids as blood biomarkers of acute and chronic DHA intake.

For acute intake biomarkers, we found nine lipids with concentrations after acute supplementation that fell between control and chronic intake. Most of these acute levels were significantly similar to both control with the exception of PC 16:0_20:4 and TAG 18:1_22:6_22:6. As an indirect marker of DHA intake, the ability to use PC 16:0_20:4 in human populations remains questionable. TAG 18:1_22:6_22:6 appears to be unique, but routine quantitation for biomarker use may be a challenge. It is of relatively low abundance, and as a triacylglycerol, blood levels are subject to considerable variation based on lipoprotein metabolism which has been documented for fatty acid-based biomarkers [296]. Rather than individual biomarkers of acute intake, it is possible that combining multiple measurements (e.g., ratios or sums) of various lipid species could result in the identification of a valid strategy for assessing acute DHA intake. For example, examining the relationship between the levels of LPC

22:6 and PS 18:0_22:6 could allow the investigator to determine if a participant has consumed DHA recently and regularly (if LPC 22:6 and PS 18:0_22:6 are both high), regularly but not recently (if LPC 22:6 is low but PS 18:0_22:6 is high) or recently but not regularly (if LPC 22:6 is high but PS 18:0_22:6 is low).

For chronic biomarkers, concentrations of DHA in phosphatidylserine has been previously proposed to be a good marker of DHA intake [292]. The use of DHA in PS as a fatty acid biomarker has been limited, as isolation of the PS fraction prior to fatty acid analysis is tedious and difficult to adapt to large clinical studies that require cost-efficient high throughput screening [297]. The finding that PE P-16:0_22:6 did not change with chronic DHA feeding while PE P-18:0_22:6 and PE P-18:1_22:6 did was not expected. DHA is known to accumulate in phosphatidylethanolamine plasmalogens [298] particularly in brain tissue [299] through fatty acyl remodeling by plasmalogen-specific PLA_2 [300]. In blood plasmalogens, the content of 16:0 and 18:0 tend to be similar while 18:1 is about half when determined as dimethyl acetyls with gas chromatography [301]. In rat brain, 18:1n-9 tends to be the dominant fatty acid followed closely by levels of 16:0 while levels of 18:0 are much lower [302]. While phosphatidylethanolamine plasmalogen remodeling is known to occur, the mechanisms through which this occur are not well elucidated [303]. 1-Alkenylglycerophosphoethanolamine O-acyltransferase activity and specificity for the incorporation of certain acyl-CoA have been documented [304] but the specificity of different lysophosphatidylethanolamine plasmalogens does not appear to have been examined. Our results appear to be the first to document a lack of change in PE P-16:0_22:6 with DHA feeding and follow up studies of examining phosphatidylethanolamine plasmalogen metabolism with lipidomic analyses could be particularly informative.

The observations of the present study are limited to DHA-only feeding. In free-living humans, DHA is typically consumed with dietary EPA, therefore studies using acute and chronic fish oil supplementation should be pursued to identify blood biomarkers of omega-3 PUFA. However, feeding DHA only did simplify our research approach and provided some insight on the interplay between EPA and DHA metabolism, such that studies using EPA-only feeding should also be considered. Within this rodent model, the relationship between lipidomic profiles in blood against those of organs and tissues can be examined to further our understanding of fatty acyl-specific lipid metabolism. In the future, in both rodent and human studies, it will be important to examine sex differences in the lipidomic profiles as sex differences in lipoprotein and fatty acid metabolism are well documented [305-308].

Table 10. Nutrient and fatty acid composition of the DHA-deficient (TWD-) and DHA-supplemented (TWD+) Total Western Diets.

Diet	TWD-	TWD+
Energy Density (*kcal/g*)	4.4	4.4
Macronutrients (*g/100g*)		
Protein (*% weight*)	16.8	16.8
Carbohydrate (*% weight*)	54.6	54.6
Fat (*% weight*)	16.7	16.7
Saturated fatty acids	32.80 ± 0.13	32.15 ± 0.10
16:0	18.79 ± 0.04	18.27 ± 0.07
18:0	8.44 ± 0.07	8.04 ± 0.03
Monounsaturated fatty acids	40.55 ± 0.10	40.53 ± 0.11
16:1	1.16 ± 0.01	1.18 ± 0.01
18:1n-7	1.22 ± 0.17	1.23 ± 0.11
18:1n-9	37.55 ± 0.20	37.50 ± 0.04
Omega-6 fatty Acids	20.85 ± 0.09	19.64 ± 0.02
18:2n-6	20.53 ± 0.09	19.34 ± 0.02
20:4n-6	0.07 ± 0.01	0.07 ± 0.01
Omega-3 fatty Acids	1.78 ± 0.01	2.82 ± 0.01
18:3n-3	1.70 ± 0.01	1.61 ± 0.01
20:3n-3	0.02 ± 0.01	0.02 ± 0.01
20:5n-3	0.02 ± 0.01	0.02 ± 0.01
22:5n-3	0.03 ± 0.01	0.04 ± 0.01
22:6n-3	0.01 ± 0.01	1.13 ± 0.01

Fatty acid composition data are presented as mean ± standard deviation of technical triplicates as % weight of fatty acids in total fatty acids. Samples were analyzed by gas chromatography-flame ionization detection as described in Section 3.5. TWD+, Total Western Diet with DHA; TWD-, Total Western Diet without DHA.
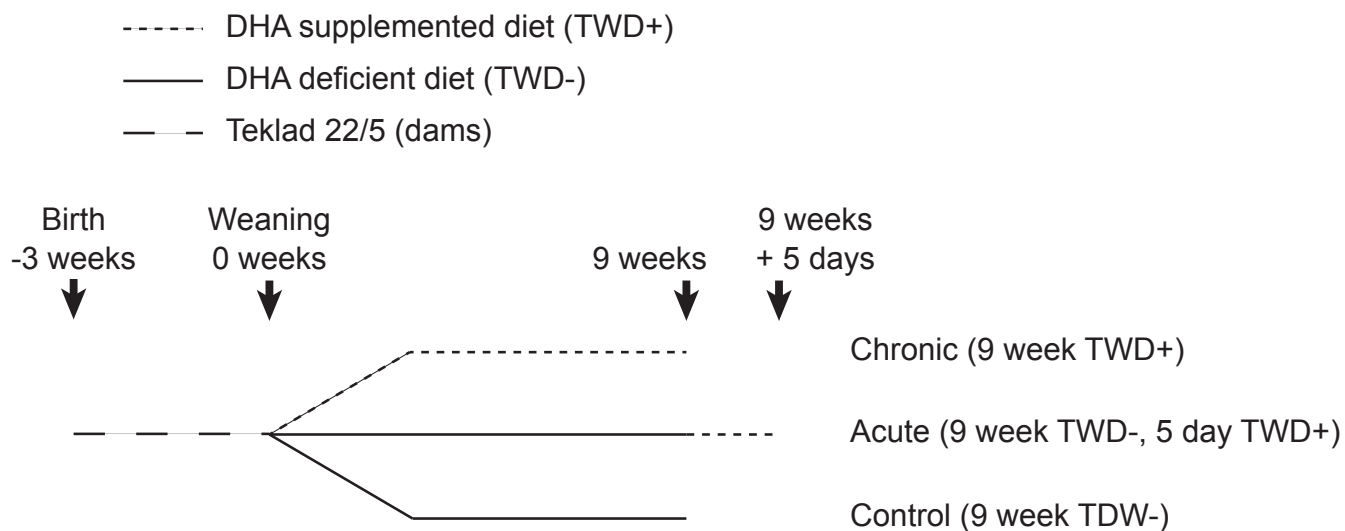
Figure 22. Experiment design. The nutrient and fatty acid composition of the DHA supplemented (TWD+) and DHA deficient (TWD-) Total Western Diets can be found in Table 10. DHA, docosahexaenoic acid; n = 4 (2 males, 2 females) per diet group.
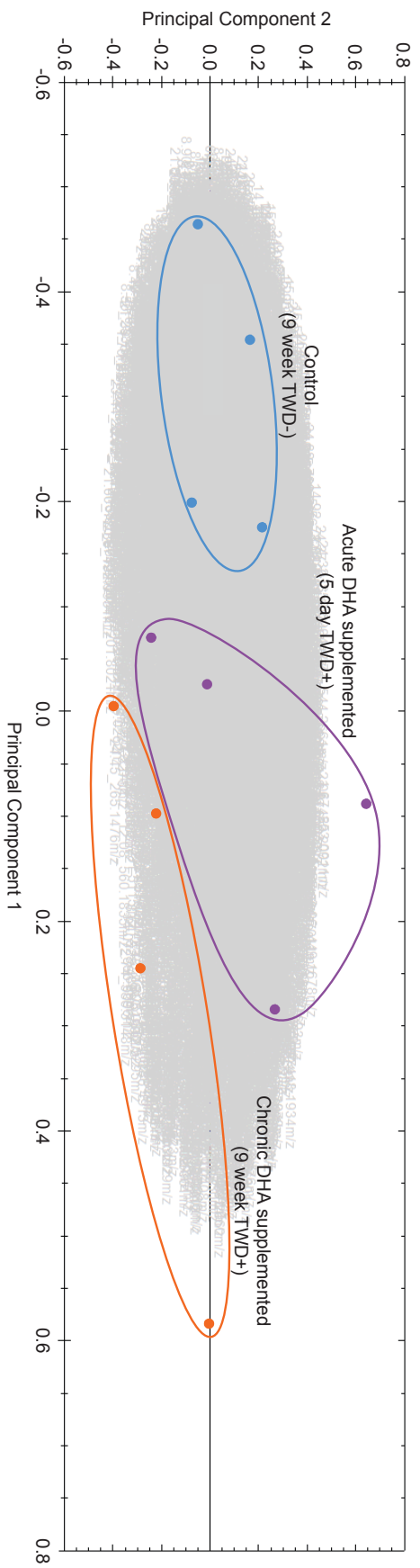
Figure 23. Principal Component Analysis (PCA) of whole blood samples in the control (9-week TWD-, in blue), acute DHA supplemented (5-day TWD+, in purple), and chronic DHA supplemented (9-week TWD+, in orange). Principal Component 1 accounts for 21.32% of the variance, while Principal Component 2 accounts for 12.32% of the variance.

Table 11. Markers of DHA intake

Lipid	*m/z*	Control	5-day DHA+	9-week DHA+
		nmol/mL		
LPC 18:2	564.3291	23.54 ± 3.86[a]	36.35 ± 4.45[b]	42.45 ± 7.69[b]
LPC 22:6	612.3289	4.90 ± 1.70[a]	15.86 ± 3.18[b]	17.73 ± 2.86[b]
PC 16:0_22:5	852.5743	34.92 ± 2.74[a]	23.26 ± 5.02[b]	19.34 ± 2.54[b]
PC 18:1_22:6	876.5730	0.20 ± 0.14[a]	0.53 ± 0.07[b]	0.60 ± 0.15[b]
PE P-18:0_22:4	778.5737	425.45 ± 48.56[a]	396.96 ± 28.21[b]	273.71 ± 32.76[b]
PS 16:0_22:6	806.4963	1.41 ± 0.56[a]	6.05 ± 2.32[b]	7.44 ± 1.73[b]

Concentration data are presented as mean ± standard deviation of biological replicates (n = 4 per group). Letter superscripts represent statistically-significant differences between diet groups following one-way ANOVA with Tukey post-hoc test; significance was inferred at $p < 0.05$. LPC, lysophosphatidylcholine; PC, phosphatidylcholine; PE, phosphatidylethanolamine; PS, phosphatidylserine.

Table 12. Markers of chronic DHA intake

Lipid	*m/z*	Control	5-day DHA+	9-week DHA+
		nmol/mL		
LPC 20:5	586.3148	< 0.01 ± 0.01[a]	< 0.01 ± 0.01[a]	0.31 ± 0.18[b]
PC 16:0_20:5	824.5425	1.71 ± 0.75[a]	7.15 ± 2.70[a]	13.41 ± 4.46[b]
PE 16:0_20:5	736.4913	< 0.01 ± 0.01[a]	0.04 ± 0.04[a]	1.52 ± 0.41[b]
PE 18:1_22:6	788.5218	20.86 ± 5.82[a]	30.37 ± 4.08[a]	62.02 ± 16.12[b]
PE 18:2_22:6	832.5113	42.15 ± 3.32[a]	44.77 ± 1.55[a]	101.55 ± 21.87[b]
PE O-18:1_22:5	776.5579	109.90 ± 9.68[a]	92.03 ± 8.83[a]	44.67 ± 8.82[b]
PE P-16:0_22:4	750.5427	426.61 ± 58.75[a]	361.07 ± 32.09[a]	198.66 ± 36.99[b]
PE P-18:0_22:6	774.5430	282.20 ± 22.91[a]	279.50 ± 13.28[a]	455.88 ± 61.18[b]
PE P-18:1_22:6	772.5271	94.98 ± 17.76[a]	105.14 ± 3.63[a]	226.93 ± 46.12[b]
PE P-20:0_22:6	802.5716	2.75 ± 1.08[a]	4.27 ± 0.88[a]	9.56 ± 3.95[b]
PI 16:0_18:2	833.5162	11.27 ± 2.27[a]	11.56 ± 0.32[a]	15.66 ± 2.25[b]
PI 18:0_20:5	883.5306	0.12 ± 0.03[a]	0.29 ± 0.14[a]	1.42 ± 0.48[b]
PS 18:0_22:6	834.5277	9.49 ± 1.22[a]	9.47 ± 1.61[a]	21.54 ± 4.92[b]

Concentration data are presented as mean ± standard deviation of biological replicates (n = 4 per group). Letter superscripts represent statistically-significant differences between diet groups following one-way ANOVA with Tukey post-hoc test; significance was inferred at $p < 0.05$. LPC, lysophosphatidylcholine; PC, phosphatidylcholine; PE, phosphatidylethanolamine; PI, phosphatidylinositol; PS, phosphatidylserine.

Table 13. Markers of the transition to chronic DHA intake

Lipid	*m/z*	Control	5-day DHA+	9-week DHA+
		nmol/mL		
PC 16:0_20:4	826.5601	171.33 ± 8.76[a]	145.47 ± 9.49[b]	122.79 ± 9.84[c]
PC 18:0_18:2	830.5910	142.04 ± 9.05[a]	168.32 ± 24.85[ab]	191.20 ± 26.18[b]
PE 16:0_20:4	738.5067	100.13 ± 8.71[a]	84.67 ± 10.51[ab]	81.87 ± 8.15[b]
PE 18:0_20:4	766.5382	225.36 ± 42.36[a]	196.94 ± 24.75[ab]	165.77 ± 10.51[b]
PE 18:0_22:6	790.5373	3.73 ± 1.22[a]	6.66 ± 2.86[ab]	8.64 ± 1.14[b]
PE 18:1_20:4	764.5245	675.43 ± 57.94[a]	519.34 ± 100.84[ab]	393.15 ± 90.45[b]
PI 16:0_22:6	881.5164	1.15 ± 0.68[a]	1.96 ± 0.93[ab]	3.41 ± 1.20[b]
PS 18:0_20:4	810.5290	147.29 ± 21.81[a]	114.80 ± 10.92[ab]	85.97 ± 17.59[b]
TAG 18:1_22:6_22:6	994.7866	1.82 ± 0.41[a]	9.56 ± 3.43[b]	22.14 ± 3.56[c]

Concentration data are presented as mean ± standard deviation of biological replicates (n = 4 per group). Letter superscripts represent statistically-significant differences between diet groups following one-way ANOVA with Tukey post-hoc test; significance was inferred at $p < 0.05$. PC, phosphatidylcholine; PE, phosphatidylethanolamine; PI, phosphatidylinositol; PS, phosphatidylserine; TAG, triacylglycerol.

Table 14. Lipids unaffected by DHA supplementation

Lipid	*m/z*	Control	5-day DHA+	9-week DHA+
		nmol/mL		
PC 16:0_18:2	802.5600	156.91 ± 18.16	159.52 ± 23.97	168.12 ± 34.93
PC 16:0_22:6	850.5595	25.82 ± 4.33	28.25 ± 4.99	30.75 ± 2.48
PC 18:0_20:4	854.5915	159.86 ± 34.42	137.22 ± 41.07	122.10 ± 42.24
PC 18:0_22:6	878.5905	18.15 ± 6.14	22.38 ± 9.10	28.52 ± 15.37
PC 18:1_18:2	828.5737	7.67 ± 1.50	7.70 ± 0.89	8.59 ± 1.88
PE 18:0_18:1	744.5536	50.02 ± 8.69	42.99 ± 6.15	44.69 ± 9.27
PE 18:0_18:2	742.5380	48.33 ± 10.51	47.10 ± 11.62	56.15 ± 14.89
PE P-16:0_22:6	746.5117	200.77 ± 24.51	143.76 ± 57.05	158.18 ± 54.59
PE P-18:0_22:5	776.5586	65.83 ± 16.70	56.24 ± 7.84	62.57 ± 13.36
PE P-18:1_20:4	748.5276	418.70 ± 79.25	356.61 ± 61.04	326.24 ± 86.95
PI 18:1_20:4	883.5325	12.25 ± 1.25	12.72 ± 0.91	12.86 ± 0.45
PS 16:0_20:4	782.4962	78.18 ± 24.12	64.82 ± 28.80	72.70 ± 20.14
PS 18:1_20:4	808.5121	115.70 ± 25.25	103.92 ± 32.59	109.44 ± 34.81
TAG 16:0_18:2_20:5	894.7537	123.38 ± 19.11	82.90 ± 32.26	98.87 ± 11.34
TAG 18:0_18:1_22:6	950.8166	11.35 ± 3.95	15.39 ± 4.93	16.73 ± 8.12
TAG 18:2_18:2_20:4	920.7687	127.73 ± 11.15	78.57 ± 49.46	79.98 ± 21.72

Concentration data are presented as mean ± standard deviation of biological replicates (n = 4 per group). PC, phosphatidylcholine; PE, phosphatidylethanolamine; PI, phosphatidylinositol; PS, phosphatidylserine; TAG, triacylglycerol.
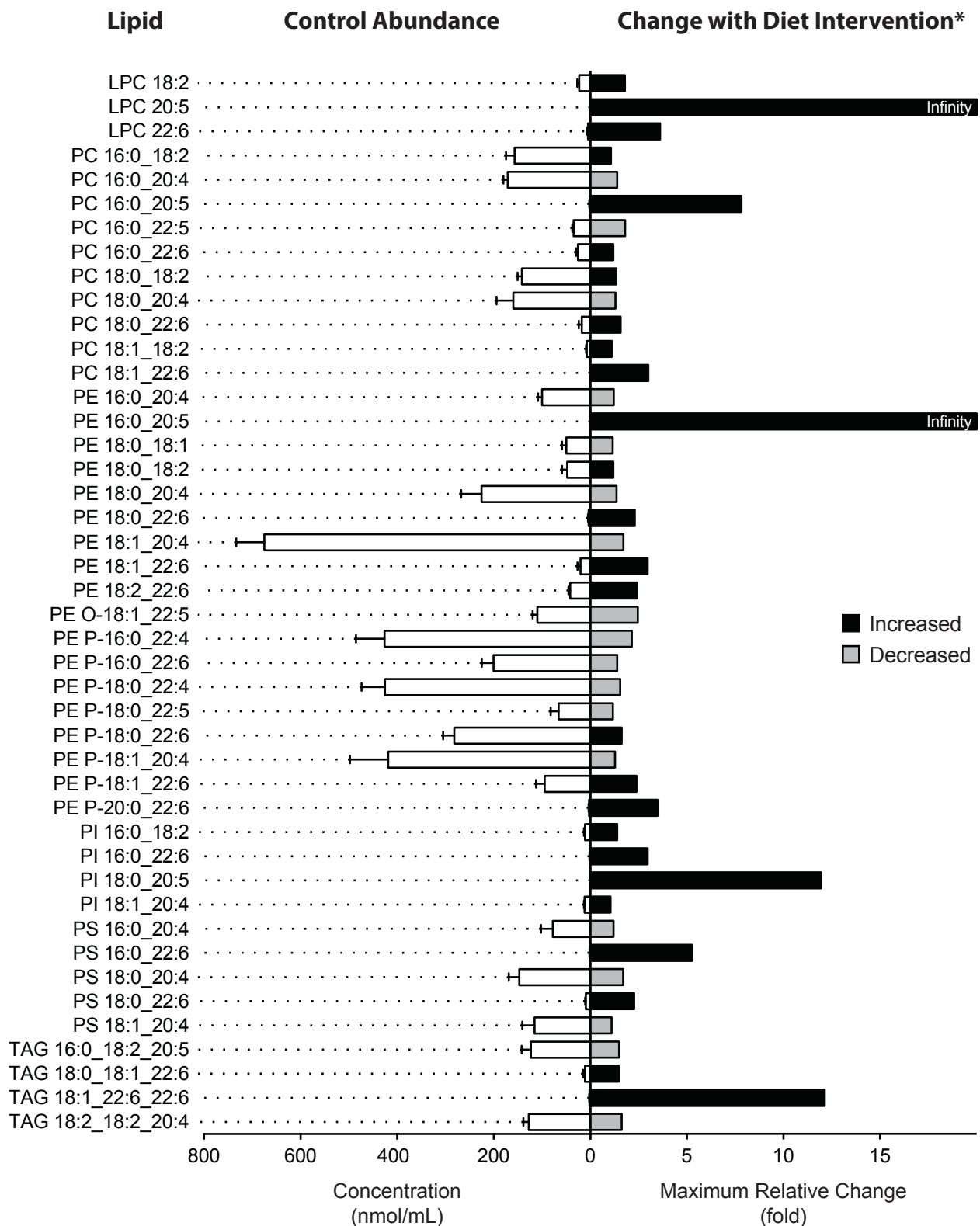
Figure 24. Baseline concentrations and maximum fold-changes in response to diet intervention in the complex lipids of whole blood. Concentration data are presented as mean ± standard deviation of biological replicates (n = 4). *The largest fold change of either diet from baseline is shown. LPC, lysophosphatidylcholine; PC, phosphatidylcholine; PE, phosphatidylethanolamine; PI, phosphatidylinositol; PS, phosphatidylserine; TAG, triacylglycerol.

CHAPTER 10

Summary and General Discussion

The purpose of this thesis was to develop microlipidomic and macrolipidomic methods that could be adopted for use in nutritional research. This included five primary objectives: (1) a cross-platform and cross-acquisition mode comparison of untargeted workflows for the macrolipidomic analysis of whole blood, (2) the development of a targeted method for the analysis of LPA regioisomers in plasma, (3) the development of semi-targeted methods for the analysis of TAG in cooking oil and phospholipids brain tissue, (4) the application of a retention time-based polarity switching method for the identification of blood biomarkers of omega-3 PUFA intake in an observational study in humans, and (5) the identification of complex lipids as biomarkers of acute and chronic DHA intake in rodents.

In the first objective, we compared two mass spectrometers (QToF vs. QE), explored the advantages of ion mobility coupled to DDA (HD-DDA vs. DDA) and evaluated two data acquisition strategies (HD-DDA vs. HD-DIA). We observed that the QToF-DDA method resulted in a higher number of lipid identifications with FAID as compared with the QE-DDA method, but both platforms performed comparably in terms of sensitivity and quantitative potential. Additionally, there were no advantages for using ion mobility, and the HD-DIA method resulted in the lowest number of lipid identifications due to the inability to deconvolute coeluting lipid species. Logistically, the QE instrument is more user-friendly, but it is a shared instrument in the University of Waterloo Mass Spectrometry Facility with limited access. The QToF instrument was purchased through NSERC and CFI infrastructure grants by Dr. Stark and the Department of Kinesiology and the agreement to place the QToF in the Mass Spectrometry Facility included priority access. Given the similarities between QToF-DDA and QE-DDA, we

125

completed all subsequent experiments in this thesis on this the QToF instrument and used the DDA method for any discovery-based experiments.

Although lipid data for highly-abundant species can be generated easily using untargeted mass spectrometry, the analysis of lipids that are natively found in very low abundance is generally limited to triple-quadrupole mass spectrometers which have been shown to be remarkably sensitive instruments [309]. Therefore, the second objective of this thesis was to evaluate our ability to measure LPA species in plasma which are known to be part of the very-low abundance regime, using the QToF instrument with ToF-MRM technology. After optimizing our extraction protocol and UHPLC-MS/MS settings, we obtained plasma LPA profiles which were consistent with those published in the literature [161]. It is important to reiterate that while triple-quadrupole mass spectrometers are sensitive, they are not capable of HRAM measurements, which are becoming the new standard in mass spectrometry [310].

Our third objective was to develop semi-targeted lipidomics methods for the analysis of TAG in sunflower oil and phospholipids in mouse striatum. We demonstrated that preexisting information on the general lipid classes of a sample can be used to tune generic mass spectrometry methods prior to sample analysis in discovery-based studies to significantly increase the quality of the results. Specifically, we applied a two-column UHPLC-MS/MS setup and positive ESI-DDA-MS/MS for TAG analysis of sunflower oil, and conventional reversed-phase UHPLC with negative ESI-DDA-MS/MS for phospholipid analysis in mouse striatum. We characterized the 20 lipids of highest abundance in both sample types and it was clear that numerous other lipids could be identified and quantitated.

Through the improvements that were observed in data quality by adopting semi-targeted approaches, we then re-evaluated our whole blood QToF DDA method from Chapter 5, and

developed a retention time-based ESI polarity-switching method that was used to characterize both polar (FFA, PC, PE, PI, PS in negative ESI) and non-polar lipids (TAG and CE in positive ESI) within a single UHPLC-MS/MS analytical run. Therefore, the fourth objective of this thesis was to apply this method for the analysis of whole blood samples from an observational study by the Danish National Food Institute. This observational study had fatty acid dietary intake estimates, therefore we were able to correlate lipidomic data to known intakes of omega-3 PUFA to identify blood biomarkers of omega-3 PUFA intake. Through this, we identified several lipids that were associated with omega-3 PUFA intake, but these results also highlighted that ALA and EPA may correlate more strongly with complex lipids that do not contain ALA and EPA, respectively.

In the last objective of this thesis, we examined the intake-blood biomarker response in a more controlled research protocol. Given the finding that DHA-containing lipids, tended to dominate as biomarkers of omega-3 PUFA intake in general, we examined the relationship between DHA feeding and the blood levels of complex lipids in whole blood using an acute/chronic model in rodents with a rodent diet designed to resemble the fat consumption of humans. We identified several complex lipids that were indicative of DHA intake in general (elevated with both acute and chronic feeding), and lipids that were elevated only with chronic intake, but no lipids were found to reflect only acute intake.

Across these objectives, numerous lipids were identified, largely based on the type of sample and the type of analytical approach. In the first objective, the instrument platforms, and the ion mobility and acquisition modes were compared by the number of lipid compounds identified within each lipid class by accurate mass (MS level) and with confirmation of the fatty acyl fragments by MS/MS, which we defined as FAID (Full Acyl Identification). A detailed

comparison of the exact lipid molecules was not completed as the number of compounds identified by accurate mass ranged from 678 to 1695. In general, the pattern of lipid classes identified reflected what is known and published about the lipid composition of blood. When specific acyl lipids were identified in the subsequent objectives, a pattern of a high content of 16:0, 18:0, 18:1 and 18:2 was apparent which has been documented and reflects both endogenous fatty acid synthesis and the abundance of these fatty acids in the food supply [42]. The mouse striatum analyses also confirmed known tissue and lipid class specificity for certain fatty acyls [311] as the abundance of 20:4- and 22:6-containing lipids was high. For the omega-3 PUFA blood biomarkers, there were some biomarkers that were identified in both the human and rodent studies despite the DHA only intake in the rodents. In human blood, PE P-16:0_22:6, PE P-18:0_22:6, PE P-20:0_22:6 had the strongest correlation with DHA intakes, although there were a total of 50/140 correlations between blood lipids and DHA intake that were significant. In the rat study, 28 lipids increased with DHA intake, with 13 of these lipids requiring chronic DHA intake. These chronic markers included P-18:0_22:6 and PE P-20:0_22:6 that were observed in the human study but not PE P-16:0_22:6. From this thesis, it is not clear if this is due to differences between species, or a mixed intake of EPA+DHA versus DHA only intakes, but it is clear that tightly controlled dietary interventions in rodent models are informative for nutritional biomarker research in humans.

Limitations specific to each of these studies were discussed in their respective Chapters. However, one challenge that carried over across all of these studies was the difficulty in comparing our lipidomic data to the existing literature. This was largely driven by a lack of consensus in the field with regards to standardized language [31] and methodological approaches [99, 312]. This has been identified in the lipidomic field by a recent interlaboratory comparison

exercise for lipidomics using the Standard Reference Material (SRM)-1950 "Metabolites in Human Plasma" sample [19]. Specifically, 31 international laboratories participated in this exercise, and provided submissions of quantitative lipidomic data for species in this reference plasma sample. Though 1527 individual lipids were reported across all laboratories, only 339 were identified by consensus of 5 or more laboratories. Furthermore, there were inconsistencies in lipid annotations (e.g., reporting brutto vs. medio-level information), and importantly, methods for quantitation. As such, the data was reported at the brutto level only, and reference data on acyl-specific species of highly-abundant lipids is still not available at the time of this thesis.

One of the underpinning reasons for the lack of harmonization in the field is the difficulty in lipidomic quantitation [313-315]. There is no clear community-wide consensus on the best approach for determining lipid concentrations, which stems from fundamental differences for the word "quantitation" including absolute-, semi-, and relative-quantitation. These differences are translated from methodological strategies in the selection of internal standards, and can have profound effects on the validity of the quantitative results. For absolute quantitation, the use of stable isotope-labeled versions of the analyte(s) of interest (i.e., deuterated or ^{13}C-labeled) is ideal, as these allow for correcting analyte losses during lipid extraction and matrix- and/or ionization-suppression effects in ESI [85, 315, 316]. However, these standards may not always be commercially-available, and in discovery-based lipidomics it is unfeasible to have stable-isotope standards for every analyte that is measured. Thus, exogenous lipids that are chemically- and structurally-similar to the lipids of interest may be used instead [315, 317, 318]. This often includes the use of odd-chain fatty acid-containing complex lipids, which are generally less costly than stable-isotope standards. With this approach, it is critical to screen the sample of

interest for the analyte that is anticipated for use as an exogenous standard. Furthermore, the effects of lipid class chemistry, and fatty acyl carbon chain length and degree of unsaturation on ionization efficiency must be considered [317, 318]. The use of multiple internal standards for all types and classes of lipids is recommended as this can improve quantitation, especially in untargeted lipidomic studies. Nevertheless, the implementation of semi- and relative-quantitative approaches is still valuable for monitoring lipid species between experimental conditions (i.e., disease state vs. healthy; wild-type vs. knock-out), rather than determining absolute concentrations.

The lipidomic field will benefit from increased quantitation. This will allow researchers to evaluate their methods by comparing their results of quality control samples to reference values, such as the SRM 1950 plasma sample [15]. In addition, the emergence of several international initiatives have emphasized the importance of adopting common language such as the short-hand system for annotating lipid features, and the implementation of minimum reporting guidelines by journals that cover common types of workflows [12, 51, 315, 319, 320]. Characterizing the lipids that are present in various types of blood and tissue samples, from different populations and/or animal species with different dietary intakes, will allow for the creation of reference lipid profiles that can be used to build future inclusion lists. These lists of compounds can be generated manually with the help of repeated MS/MS iterations in top-n DDA approaches, and should be made available in shared repositories for public access.

In conclusion, through the development and application of microlipidomic and macrolipidomic methods, we have highlighted the importance of appropriate sample handling, lipid extraction, and analysis using mass spectrometry in order to generate high quality data. In addition, the work presented in this thesis expands on the current state of knowledge of the field

of lipidomics in health and nutrition. We identified significant limitations of current DIA and ion mobility methods, which should be addressed in future platforms in order to enable the use of these technologies in untargeted macrolipidomics. With the LPA experiments, we have demonstrated that HRAM instruments and not just triple quadrupole mass spectrometers can be used in targeted analyses with high sensitivity to quantitate and provide genio-level information for lipid species in the microlipidome. The sunflower and mouse striatum studies highlighted the importance of semi-targeted approaches in the characterization of lipids in samples with different matrices. As lipidomic initiatives move towards standardization in the field, it will be important to allow analysts flexibility in tailoring their analytical workflows to their specific research questions and sample types. While comparing different methods will be confusing, emphasis on reporting quantitative results will be a better path towards standardization as methods will also continue to evolve with the technology of mass spectrometers. The blood omega-3 PUFA biomarker experiments in humans and rats indicate that the adoption of lipidomic approaches will have significant implications in all aspects of nutritional research. The ability to characterize fatty acyl species of lipids will greatly enhance our ability to study and understand lipid metabolism under various physiological and environmental challenges including diet. In this thesis, we identified potential selective incorporation of 22:6 into 18:0- and 18:1-containing lysophosphatidylethanolamine plasmalogens. Detailed mechanistic studies using metabolic tracers can easily be adapted to the mass spectrometry workflows described herein. We also identified that lipidomic blood biomarkers can provide insight on dietary patterns and habits of the consumption of omega-3 PUFA in addition to estimates of daily intake. The use of lipidomic blood biomarkers in clinical populations has the potential to revolutionize the ability of

nutritional epidemiology to uncover and characterize the relationship between diet and disease in human populations.

References

1. Lizardo, D.Y., et al., *Noncanonical Roles of Lipids in Different Cellular Fates.* Biochemistry, 2018. **57**(1): p. 22-29.

2. Seneviratne, A.K., et al., *The Mitochondrial Transacylase, Tafazzin, Regulates for AML Stemness by Modulating Intracellular Levels of Phospholipids.* Cell Stem Cell, 2019. **24**(4): p. 621-636 e16.

3. Wong, M.W., et al., *Dysregulation of lipids in Alzheimer's disease and their role as potential biomarkers.* Alzheimers Dement, 2017. **13**(7): p. 810-827.

4. Yang, L., et al., *LPA Receptor 4 deficiency attenuates experimental atherosclerosis.* J Lipid Res, 2019.

5. Fang, Z., S. Pyne, and N.J. Pyne, *Ceramide and sphingosine 1-phosphate in adipose dysfunction.* Prog Lipid Res, 2019. **74**: p. 145-159.

6. Moravcevic, K., et al., *Kinase associated-1 domains drive MARK/PAR1 kinases to membrane targets by binding acidic phospholipids.* Cell, 2010. **143**(6): p. 966-77.

7. Han, X. and R.W. Gross, *Global analyses of cellular lipidomes directly from crude extracts of biological samples by ESI mass spectrometry: a bridge to lipidomics.* J Lipid Res, 2003. **44**(6): p. 1071-9.

8. Wang, M., et al., *Novel advances in shotgun lipidomics for biology and medicine.* Prog Lipid Res, 2016. **61**: p. 83-108.

9. Hyotylainen, T. and M. Oresic, *Systems biology strategies to study lipidomes in health and disease.* Prog Lipid Res, 2014. **55**: p. 43-60.

10. Hoffmann, N., et al., *mzTab-M: A Data Standard for Sharing Quantitative Results in Mass Spectrometry Metabolomics.* Anal Chem, 2019. **91**(5): p. 3302-3310.

11. DeFelice, B.C., et al., *Mass Spectral Feature List Optimizer (MS-FLO): A Tool To Minimize False Positive Peak Reports in Untargeted Liquid Chromatography-Mass Spectroscopy (LC-MS) Data Processing.* Anal Chem, 2017. **89**(6): p. 3250-3255.

12. Fahy, E., et al., *Update of the LIPID MAPS comprehensive classification system for lipids.* J Lipid Res, 2009. **50 Suppl**: p. S9-14.

13. Gabelica, V., et al., *Recommendations for reporting ion mobility Mass Spectrometry measurements.* Mass Spectrom Rev, 2019.

14. Bowden, J.A., et al., *NIST lipidomics workflow questionnaire: an assessment of community-wide methodologies and perspectives.* Metabolomics, 2018. **14**(5): p. 53.

15. Ulmer, C.Z., et al., *LipidQC: Method Validation Tool for Visual Comparison to SRM 1950 Using NIST Interlaboratory Comparison Exercise Lipid Consensus Mean Estimate Values.* Anal Chem, 2017. **89**(24): p. 13069-13073.

16. Burla, B., et al., *MS-based lipidomics of human blood plasma: a community-initiated position paper to develop accepted guidelines.* J Lipid Res, 2018. **59**(10): p. 2001-2017.

17. Chocholouskova, M., et al., *Reversed phase UHPLC/ESI-MS determination of oxylipins in human plasma: a case study of female breast cancer.* Anal Bioanal Chem, 2019. **411**(6): p. 1239-1251.

18. Serna, J., et al., *Quantitative lipidomic analysis of plasma and plasma lipoproteins using MALDI-TOF mass spectrometry.* Chem Phys Lipids, 2015. **189**: p. 7-18.

19. Bowden, J.A., et al., *Harmonizing lipidomics: NIST interlaboratory comparison exercise for lipidomics using SRM 1950-Metabolites in Frozen Human Plasma.* J Lipid Res, 2017. **58**(12): p. 2275-2288.

20. Narvaez-Rivas, M. and Q. Zhang, *Comprehensive untargeted lipidomic analysis using core-shell C30 particle column and high field orbitrap mass spectrometer.* J Chromatogr A, 2016. **1440**: p. 123-134.

21. Forest, A., et al., *Comprehensive and Reproducible Untargeted Lipidomic Workflow Using LC-QTOF Validated for Human Plasma Analysis.* J Proteome Res, 2018. **17**(11): p. 3657-3670.

22. Takeda, H., et al., *Widely-targeted quantitative lipidomics method by supercritical fluid chromatography triple quadrupole mass spectrometry.* J Lipid Res, 2018. **59**(7): p. 1283-1293.

23. Giles, C., et al., *Contemporary lipidomic analytics: opportunities and pitfalls.* Prog Lipid Res, 2018. **71**: p. 86-100.

24. Wolf, C. and P.J. Quinn, *Lipidomics: practical aspects and applications.* Prog Lipid Res, 2008. **47**(1): p. 15-36.

25. Watson, A.D., *Thematic review series: systems biology approaches to metabolic and cardiovascular disorders. Lipidomics: a global approach to lipid analysis in biological systems.* J Lipid Res, 2006. **47**(10): p. 2101-11.

26. Afshinnia, F., et al., *Lipidomics and Biomarker Discovery in Kidney Disease.* Semin Nephrol, 2018. **38**(2): p. 127-141.

27. Moon, S.H., et al., *Cardiac Myocyte-specific Knock-out of Calcium-independent Phospholipase A2gamma (iPLA2gamma) Decreases Oxidized Fatty Acids during Ischemia/Reperfusion and Reduces Infarct Size.* J Biol Chem, 2016. **291**(37): p. 19687-700.

28. Bradley, R.M., et al., *Lpaatdelta/Agpat4 deficiency impairs maximal force contractility in soleus and alters fibre type in extensor digitorum longus muscle.* Biochim Biophys Acta Mol Cell Biol Lipids, 2018. **1863**(7): p. 700-711.

29. Xie, Y., et al., *Profiling and quantification of lipids in cold-pressed rapeseed oils based on direct infusion electrospray ionization tandem mass spectrometry.* Food Chem, 2019. **285**: p. 194-203.

30. Liu, Z., S. Rochfort, and B. Cocks, *Milk lipidomics: What we know and what we don't.* Prog Lipid Res, 2018. **71**: p. 70-85.

31. Aristizabal Henao, J.J., et al., *Categorizing and qualifying nutritional lipidomic data: defining brutto, medio, genio, and infinio lipid species within macrolipidomics and microlipidomics.* Curr Opin Clin Nutr Metab Care, 2018. **21**(5): p. 352-359.

32. Liu, Y., et al., *Dietary oils modify lipid molecules and nutritional value of fillet in Nile tilapia: A deep lipidomics analysis.* Food Chem, 2019. **277**: p. 515-523.

33. Bennett, S.A., et al., *Using neurolipidomics to identify phospholipid mediators of synaptic (dys)function in Alzheimer's Disease.* Front Physiol, 2013. **4**: p. 168.

34. Masoodi, M. and D.A. Volmer, *Comprehensive quantitative determination of PUFA-related bioactive lipids for functional lipidomics using high-resolution mass spectrometry.* Methods Mol Biol, 2014. **1198**: p. 221-32.

35. Carter, J.E.A. and P.M. Sluss, *Estradiol Solubility in Aqueous Systems: Effect of Ionic Concentrations, pH, and Organic Solvents.* Journal of Hormones, 2013. **2013**: p. 4.

36. Aristizabal Henao, J.J., et al., *Tailored Extraction Procedure Is Required To Ensure Recovery of the Main Lipid Classes in Whole Blood When Profiling the Lipidome of Dried Blood Spots.* Anal Chem, 2016. **88**(19): p. 9391-9396.

37. Baker, D.L., et al., *Quantitative analysis of lysophosphatidic acid in human blood fractions.* Ann N Y Acad Sci, 2000. **905**: p. 267-9.

38. Byrdwell, W.C., *Comprehensive Dual Liquid Chromatography with Quadruple Mass Spectrometry (LC1MS2 x LC1MS2 = LC2MS4) for Analysis of Parinari Curatellifolia and Other Seed Oil Triacylglycerols.* Anal Chem, 2017. **89**(19): p. 10537-10546.

39. Baglai, A., et al., *Comprehensive lipidomic analysis of human plasma using multidimensional liquid- and gas-phase separations: Two-dimensional liquid chromatography-mass spectrometry vs. liquid chromatography-trapped-ion-mobility-mass spectrometry.* J Chromatogr A, 2017. **1530**: p. 90-103.

40. Garikapati, V., et al., *High-resolution atmospheric-pressure MALDI mass spectrometry imaging workflow for lipidomic analysis of late fetal mouse lungs.* Sci Rep, 2019. **9**(1): p. 3192.

41. Bodzon-Kulakowska, A., et al., *Brain lipidomic changes after morphine, cocaine and amphetamine administration - DESI - MS imaging study.* Biochim Biophys Acta Mol Cell Biol Lipids, 2017. **1862**(7): p. 686-691.

42. Stark, K.D., *Applications of Innovative Lipidomic Methods for Blood Lipid Biomarkers.* J Oleo Sci, 2019. **68**(6): p. 503-510.

43. Wang, Y., et al., *Comprehensive ultra-performance liquid chromatographic separation and mass spectrometric analysis of eicosanoid metabolites in human samples.* J Chromatogr A, 2014. **1359**: p. 60-9.

44. Zhang, Q., et al., *A Novel Strategy for Targeted Lipidomics Based on LC-Tandem-MS Parameters Prediction, Quantification, and Multiple Statistical Data Mining: Evaluation of Lysophosphatidylcholines as Potential Cancer Biomarkers.* Anal Chem, 2019.

45.   Koelmel, J.P., et al., *Common cases of improper lipid annotation using high-resolution tandem mass spectrometry data and corresponding limitations in biological interpretation.* Biochim Biophys Acta Mol Cell Biol Lipids, 2017. **1862**(8): p. 766-770.

46.   Hennebelle, M., et al., *Brain oxylipin concentrations following hypercapnia / ischemia: effects of brain dissection and dissection time.* J Lipid Res, 2018.

47.   Devassy, J.G., et al., *Distinct effects of dietary flax compared to fish oil, soy protein compared to casein, and sex on the renal oxylipin profile in models of polycystic kidney disease.* Prostaglandins Leukot Essent Fatty Acids, 2017. **123**: p. 1-13.

48.   Yuan, Z.X., et al., *Lipidomic profiling of targeted oxylipins with ultra-performance liquid chromatography-tandem mass spectrometry.* Anal Bioanal Chem, 2018. **410**(23): p. 6009-6029.

49.   Zacek, P., et al., *Dietary saturated fatty acid type impacts obesity-induced metabolic dysfunction and plasma lipidomic signatures in mice.* J Nutr Biochem, 2019. **64**: p. 32-44.

50.   Vale, G., et al., *Three Phase Liquid Extraction (3PLE): A Simple, and Fast Method for Lipidomic Workflows.* J Lipid Res, 2019.

51.   Liebisch, G., et al., *Shorthand notation for lipid structures derived from mass spectrometry.* J Lipid Res, 2013. **54**(6): p. 1523-30.

52.   Campbell, J.L. and T. Baba, *Near-complete structural characterization of phosphatidylcholines using electron impact excitation of ions from organics.* Anal Chem, 2015. **87**(11): p. 5837-45.

53.   Sundaram, S., et al., *Lipidomic Impacts of an Obesogenic Diet Upon Lewis Lung Carcinoma in Mice.* Front Oncol, 2018. **8**: p. 134.

54.   Zacek, P., et al., *Quantitation of isobaric phosphatidylcholine species in human plasma using a hybrid quadrupole linear ion-trap mass spectrometer.* J Lipid Res, 2016. **57**(12): p. 2225-2234.

55.   Nakanishi, H., et al., *Separation and quantification of sn-1 and sn-2 fatty acid positional isomers in phosphatidylcholine by RPLC-ESIMS/MS.* J Biochem, 2010. **147**(2): p. 245-56.

56.   Hou, W., et al., *Lyso-form fragment ions facilitate the determination of stereospecificity of diacyl glycerophospholipids.* Rapid Commun Mass Spectrom, 2011. **25**(1): p. 205-17.

57.   Kozlowski, R.L., et al., *Combining liquid chromatography with ozone-induced dissociation for the separation and identification of phosphatidylcholine double bond isomers.* Anal Bioanal Chem, 2015. **407**(17): p. 5053-64.

58.   Baba, T., et al., *Distinguishing Cis and Trans Isomers in Intact Complex Lipids Using Electron Impact Excitation of Ions from Organics Mass Spectrometry.* Anal Chem, 2017. **89**(14): p. 7307-7315.

59.   Bowman, A.P., R.R. Abzalimov, and A.A. Shvartsburg, *Broad Separation of Isomeric Lipids by High-Resolution Differential Ion Mobility Spectrometry with Tandem Mass Spectrometry.* J Am Soc Mass Spectrom, 2017. **28**(8): p. 1552-1561.

60.   Ma, X. and Y. Xia, *Pinpointing double bonds in lipids by Paterno-Buchi reactions and mass spectrometry.* Angew Chem Int Ed Engl, 2014. **53**(10): p. 2592-6.

61.   Cao, W., et al., *Locating Carbon-Carbon Double Bonds in Unsaturated Phospholipids by Epoxidation Reaction and Tandem Mass Spectrometry.* Anal Chem, 2018. **90**(17): p. 10286-10292.

62.   Feng, Y., et al., *Identification of Double Bond Position Isomers in Unsaturated Lipids by m-CPBA Epoxidation and Mass Spectrometry Fragmentation.* Anal Chem, 2019. **91**(3): p. 1791-1795.

63.   Gross, R.W., *The evolution of lipidomics through space and time.* Biochim Biophys Acta Mol Cell Biol Lipids, 2017. **1862**(8): p. 731-739.

64.   Khoury, S., et al., *A study of inter-species ion suppression in electrospray ionization-mass spectrometry of some phospholipid classes.* Anal Bioanal Chem, 2016. **408**(5): p. 1453-65.

65.   Harayama, T., et al., *Establishment of LC-MS methods for the analysis of palmitoylated surfactant proteins.* J Lipid Res, 2015. **56**(7): p. 1370-9.

66.   Ismaiel, O.A., et al., *Investigation of endogenous blood plasma phospholipids, cholesterol and glycerides that contribute to matrix effects in bioanalysis by liquid chromatography/mass spectrometry.* J Chromatogr B Analyt Technol Biomed Life Sci, 2010. **878**(31): p. 3303-16.

67.   Lykidis, A. and S. Jackowski, *Regulation of mammalian cell membrane biosynthesis.* Prog Nucleic Acid Res Mol Biol, 2001. **65**: p. 361-93.

68.   Slotte, J.P., *Biological functions of sphingomyelins.* Prog Lipid Res, 2013. **52**(4): p. 424-37.

69.   Yang, K., et al., *Automated lipid identification and quantification by multidimensional mass spectrometry-based shotgun lipidomics.* Anal Chem, 2009. **81**(11): p. 4356-68.

70.   Han, X., K. Yang, and R.W. Gross, *Multi-dimensional mass spectrometry-based shotgun lipidomics and novel strategies for lipidomic analyses.* Mass Spectrom Rev, 2012. **31**(1): p. 134-78.

71.   Keating, J.E. and G.L. Glish, *Dual Emitter Nano-Electrospray Ionization Coupled to Differential Ion Mobility Spectrometry-Mass Spectrometry for Shotgun Lipidomics.* Anal Chem, 2018. **90**(15): p. 9117-9124.

72.   Leng, J., et al., *Direct infusion electrospray ionization-ion mobility-mass spectrometry for comparative profiling of fatty acids based on stable isotope labeling.* Anal Chim Acta, 2015. **887**: p. 148-154.

73.   Lintonen, T.P., et al., *Differential mobility spectrometry-driven shotgun lipidomics.* Anal Chem, 2014. **86**(19): p. 9662-9.

74.   Ejsing, C.S., et al., *Automated identification and quantification of glycerophospholipid molecular species by multiple precursor ion scanning.* Anal Chem, 2006. **78**(17): p. 6202-14.

75. Kochen, M.A., et al., *Greazy: Open-Source Software for Automated Phospholipid Tandem Mass Spectrometry Identification.* Anal Chem, 2016. **88**(11): p. 5733-41.

76. Taguchi, R., M. Nishijima, and T. Shimizu, *Basic analytical systems for lipidomics by mass spectrometry in Japan.* Methods Enzymol, 2007. **432**: p. 185-211.

77. Song, H., et al., *Algorithm for processing raw mass spectrometric data to identify and quantitate complex lipid molecular species in mixtures by data-dependent scanning and fragment ion database searching.* J Am Soc Mass Spectrom, 2007. **18**(10): p. 1848-58.

78. Koelmel, J.P., et al., *LipidMatch: an automated workflow for rule-based lipid identification using untargeted high-resolution tandem mass spectrometry data.* BMC Bioinformatics, 2017. **18**(1): p. 331.

79. Ulmer, C.Z., et al., *LipidPioneer : A Comprehensive User-Generated Exact Mass Template for Lipidomics.* J Am Soc Mass Spectrom, 2017. **28**(3): p. 562-565.

80. Kuksis, A. and Y. Itabashi, *Regio- and stereospecific analysis of glycerolipids.* Methods, 2005. **36**(2): p. 172-85.

81. Wozny, K., et al., *A method for the quantitative determination of glycerophospholipid regioisomers by UPLC-ESI-MS/MS.* Anal Bioanal Chem, 2019. **411**(4): p. 915-924.

82. Harada, M., et al., *Biaryl axially chiral derivatizing agent for simultaneous separation and sensitive detection of proteinogenic amino acid enantiomers using liquid chromatography-tandem mass spectrometry.* J Chromatogr A, 2019.

83. Daikoku, S., et al., *Fluorescence-monitored zero dead-volume nanoLC-microESI-QIT-TOF MS for analysis of fluorescently tagged glycosphingolipids.* Analyst, 2011. **136**(5): p. 1046-50.

84. Kuzyk, M.A., et al., *Development of MRM-based assays for the absolute quantitation of plasma proteins.* Methods Mol Biol, 2013. **1023**: p. 53-82.

85. Ovcacikova, M., et al., *Retention behavior of lipids in reversed-phase ultrahigh-performance liquid chromatography-electrospray ionization mass spectrometry.* J Chromatogr A, 2016. **1450**: p. 76-85.

86. Lee, J.Y., H.K. Min, and M.H. Moon, *Simultaneous profiling of lysophospholipids and phospholipids from human plasma by nanoflow liquid chromatography-tandem mass spectrometry.* Anal Bioanal Chem, 2011. **400**(9): p. 2953-61.

87. Zhu, C., et al., *An efficient hydrophilic interaction liquid chromatography separation of 7 phospholipid classes based on a diol column.* J Chromatogr A, 2012. **1220**: p. 26-34.

88. Yoshida, T., *Peptide separation by Hydrophilic-Interaction Chromatography: a review.* J Biochem Biophys Methods, 2004. **60**(3): p. 265-80.

89. Langrock, T., P. Czihal, and R. Hoffmann, *Amino acid analysis by hydrophilic interaction chromatography coupled on-line to electrospray ionization mass spectrometry.* Amino Acids, 2006. **30**(3): p. 291-7.

90. Antonio, C., et al., *Hydrophilic interaction chromatography/electrospray mass spectrometry analysis of carbohydrate-related metabolites from Arabidopsis thaliana leaf tissue.* Rapid Commun Mass Spectrom, 2008. **22**(9): p. 1399-407.

91.   Alpert, A.J., *Hydrophilic-interaction chromatography for the separation of peptides, nucleic acids and other polar compounds.* J Chromatogr, 1990. **499**: p. 177-96.

92.   Jian, W., et al., *Analysis of polar metabolites by hydrophilic interaction chromatography--MS/MS.* Bioanalysis, 2011. **3**(8): p. 899-912.

93.   Sandra, K. and P. Sandra, *Lipidomics from an analytical perspective.* Curr Opin Chem Biol, 2013. **17**(5): p. 847-53.

94.   Cifkova, E., et al., *Nontargeted quantitation of lipid classes using hydrophilic interaction liquid chromatography-electrospray ionization mass spectrometry with single internal standard and response factor approach.* Anal Chem, 2012. **84**(22): p. 10064-70.

95.   Losito, I., et al., *Phospholipidomics of human blood microparticles.* Anal Chem, 2013. **85**(13): p. 6405-13.

96.   Lisa, M., E. Cifkova, and M. Holcapek, *Lipidomic profiling of biological tissues using off-line two-dimensional high-performance liquid chromatography-mass spectrometry.* J Chromatogr A, 2011. **1218**(31): p. 5146-56.

97.   Liebisch, G., et al., *High-throughput quantification of phosphatidylcholine and sphingomyelin by electrospray ionization tandem mass spectrometry coupled with isotope correction algorithm.* Biochim Biophys Acta, 2004. **1686**(1-2): p. 108-17.

98.   Scherer, M., et al., *A rapid and quantitative LC-MS/MS method to profile sphingolipids.* J Lipid Res, 2010. **51**(7): p. 2001-11.

99.   Cajka, T. and O. Fiehn, *Comprehensive analysis of lipids in biological systems by liquid chromatography-mass spectrometry.* Trends Analyt Chem, 2014. **61**: p. 192-206.

100.   Yang, L., et al., *Lipidomic analysis of plasma in patients with lacunar infarction using normal-phase/reversed-phase two-dimensional liquid chromatography-quadrupole time-of-flight mass spectrometry.* Anal Bioanal Chem, 2017. **409**(12): p. 3211-3222.

101.   Shen, Y., et al., *Online 2D-LC-MS/MS assay to quantify therapeutic protein in human serum in the presence of pre-existing antidrug antibodies.* Anal Chem, 2015. **87**(16): p. 8555-63.

102.   Yang, Q., et al., *On-line two dimensional liquid chromatography/mass spectrometry for the analysis of triacylglycerides in peanut oil and mouse tissue.* J Chromatogr B Analyt Technol Biomed Life Sci, 2012. **895-896**: p. 48-55.

103.   Bang, D.Y. and M.H. Moon, *On-line two-dimensional capillary strong anion exchange/reversed phase liquid chromatography-tandem mass spectrometry for comprehensive lipid analysis.* J Chromatogr A, 2013. **1310**: p. 82-90.

104.   Scoparo, C.T., et al., *Analysis of Camellia sinensis green and black teas via ultra high performance liquid chromatography assisted by liquid-liquid partition and two-dimensional liquid chromatography (size exclusion x reversed phase).* J Chromatogr A, 2012. **1222**: p. 29-37.

105.   Berkecz, R., et al., *Comprehensive phospholipid and sphingomyelin profiling of different brain regions in mouse model of anxiety disorder using online two-dimensional (HILIC/RP)-LC/MS method.* J Pharm Biomed Anal, 2018. **149**: p. 308-317.

106.   Ishii, C., et al., *Development of an online two-dimensional high-performance liquid chromatographic system in combination with tandem mass spectrometric detection for enantiomeric analysis of free amino acids in human physiological fluid.* J Chromatogr A, 2018. **1570**: p. 91-98.

107.   Karas, M., D. Bachmann, and F. Hillenkamp, *Influence of the wavelength in high-irradiance ultraviolet laser desorption mass spectrometry of organic molecules.* Analytical Chemistry, 1985. **57**(14): p. 2935-2939.

108.   Tanaka, K., et al., *Protein and polymer analyses up to m/z 100 000 by laser ionization time-of-flight mass spectrometry.* Rapid Communications in Mass Spectrometry, 1988. **2**(8): p. 151-153.

109.   Cheng, H., et al., *Selective desorption/ionization of sulfatides by MALDI-MS facilitated using 9-aminoacridine as matrix.* J Lipid Res, 2010. **51**(6): p. 1599-609.

110.   Schiller, J., et al., *Lipid analysis by matrix-assisted laser desorption and ionization mass spectrometry: A methodological approach.* Anal Biochem, 1999. **267**(1): p. 46-56.

111.   Blanksby, S.J. and T.W. Mitchell, *Advances in mass spectrometry for lipidomics.* Annu Rev Anal Chem (Palo Alto Calif), 2010. **3**: p. 433-65.

112.   Shi, Y., et al., *Mass Spectrometric Imaging Reveals Temporal and Spatial Dynamics of Bioactive Lipids in Arteries Undergoing Restenosis.* J Proteome Res, 2019.

113.   van Smaalen, T.C., et al., *Rapid Identification of Ischemic Injury in Renal Tissue by Mass-Spectrometry Imaging.* Anal Chem, 2019.

114.   Fuchs, B. and J. Schiller, *Application of MALDI-TOF mass spectrometry in lipidomics.* European Journal of Lipid Science and Technology, 2009. **111**(1): p. 83-98.

115.   Schiller, J., et al., *Matrix-assisted laser desorption and ionization time-of-flight (MALDI-TOF) mass spectrometry in lipid and phospholipid research.* Prog Lipid Res, 2004. **43**(5): p. 449-88.

116.   Fuchs, B., R. Suss, and J. Schiller, *An update of MALDI-TOF mass spectrometry in lipid research.* Prog Lipid Res, 2010. **49**(4): p. 450-75.

117.   *MALDI MS: A Practical Guide to Instrumentation, Methods and Applications*, F.H.J. Peter-Katalinic, Editor. 2013, Wiley-Blackwell. p. 480.

118.   McCombie, G. and R. Knochenmuss, *Small-molecule MALDI using the matrix suppression effect to reduce or eliminate matrix background interferences.* Anal Chem, 2004. **76**(17): p. 4990-7.

119.   Petkovic, M., et al., *Detection of individual phospholipids in lipid mixtures by matrix-assisted laser desorption/ionization time-of-flight mass spectrometry: phosphatidylcholine prevents the detection of further species.* Anal Biochem, 2001. **289**(2): p. 202-16.

120.   Moreno-Gordaliza, E., et al., *MALDI-LTQ-Orbitrap mass spectrometry imaging for lipidomic analysis in kidney under cisplatin chemotherapy.* Talanta, 2017. **164**: p. 16-26.

121.   Chagovets, V., M. Lisa, and M. Holcapek, *Effects of fatty acyl chain length, double-bond number and matrix on phosphatidylcholine responses in matrix-assisted laser*

desorption/ionization on an Orbitrap mass spectrometer. Rapid Commun Mass Spectrom, 2015. **29**(24): p. 2374-84.

122.   Petkovic, M., et al., *The signal-to-noise ratio as the measure for the quantification of lysophospholipids by matrix-assisted laser desorption/ionisation time-of-flight mass spectrometry.* Analyst, 2001. **126**(7): p. 1042-50.

123.   Passos-Castilho, A.M., et al., *Plasma lipidomic fingerprinting to distinguish among hepatitis C-related hepatocellular carcinoma, liver cirrhosis, and chronic hepatitis C using MALDI-TOF mass spectrometry: a pilot study.* J Gastrointestin Liver Dis, 2015. **24**(1): p. 43-9.

124.   Stubiger, G., et al., *Analysis of human plasma lipids and soybean lecithin by means of high-performance thin-layer chromatography and matrix-assisted laser desorption/ionization mass spectrometry.* Rapid Commun Mass Spectrom, 2009. **23**(17): p. 2711-23.

125.   Ellis, S.R., et al., *Surface analysis of lipids by mass spectrometry: more than just imaging.* Prog Lipid Res, 2013. **52**(4): p. 329-53.

126.   Chen, S., et al., *Pseudotargeted metabolomics method and its application in serum biomarker discovery for hepatocellular carcinoma based on ultra high-performance liquid chromatography/triple quadrupole mass spectrometry.* Anal Chem, 2013. **85**(17): p. 8326-33.

127.   Lesur, A. and B. Domon, *Advances in high-resolution accurate mass spectrometry application to targeted proteomics.* Proteomics, 2015. **15**(5-6): p. 880-90.

128.   Hu, Q., et al., *The Orbitrap: a new mass spectrometer.* J Mass Spectrom, 2005. **40**(4): p. 430-43.

129.   Vorkas, P.A., *Expanding lipidome coverage using MS/MS-aided untargeted data-independent RP-UPLC-TOF-MS(E) acquisition.* Bioanalysis, 2018. **10**(5): p. 307-319.

130.   Gallart-Ayala, H., et al., *Versatile lipid profiling by liquid chromatography-high resolution mass spectrometry using all ion fragmentation and polarity switching. Preliminary application for serum samples phenotyping related to canine mammary cancer.* Anal Chim Acta, 2013. **796**: p. 75-83.

131.   Schlotterbeck, J., et al., *Comprehensive MS/MS profiling by UHPLC-ESI-QTOF-MS/MS using SWATH data-independent acquisition for the study of platelet lipidomes in coronary artery disease.* Anal Chim Acta, 2019. **1046**: p. 1-15.

132.   Lozano, A., C. Ferrer, and A.R. Fernandez-Alba, *Selectivity enhancement using sequential mass isolation window acquisition with hybrid quadrupole time-of-flight mass spectrometry for pesticide residues.* J Chromatogr A, 2019. **1591**: p. 99-109.

133.   Ubhi, B.K., *Direct Infusion-Tandem Mass Spectrometry (DI-MS/MS) Analysis of Complex Lipids in Human Plasma and Serum Using the Lipidyzer Platform.* Methods Mol Biol, 2018. **1730**: p. 227-236.

134.   Leaptrot, K.L., et al., *Ion mobility conformational lipid atlas for high confidence lipidomics.* Nat Commun, 2019. **10**(1): p. 985.

135. Baker, P.R., et al., *Three-dimensional enhanced lipidomics analysis combining UPLC, differential ion mobility spectrometry, and mass spectrometric separation strategies.* J Lipid Res, 2014. **55**(11): p. 2432-42.

136. Maccarone, A.T., et al., *Characterization of acyl chain position in unsaturated phosphatidylcholines using differential mobility-mass spectrometry.* J Lipid Res, 2014. **55**(8): p. 1668-77.

137. Blazenovic, I., et al., *Increasing Compound Identification Rates in Untargeted Lipidomics Research with Liquid Chromatography Drift Time-Ion Mobility Mass Spectrometry.* Anal Chem, 2018. **90**(18): p. 10758-10764.

138. Folch, J., M. Lees, and G.H. Sloane Stanley, *A simple method for the isolation and purification of total lipides from animal tissues.* J Biol Chem, 1957. **226**(1): p. 497-509.

139. Metherel, A.H., J.J. Aristizabal Henao, and K.D. Stark, *EPA and DHA levels in whole blood decrease more rapidly when stored at -20 degrees C as compared with room temperature, 4 and -75 degrees C.* Lipids, 2013. **48**(11): p. 1079-91.

140. Little, J.L., et al., *Identification of "known unknowns" utilizing accurate mass data and ChemSpider.* J Am Soc Mass Spectrom, 2012. **23**(1): p. 179-85.

141. Kind, T., et al., *LipidBlast in silico tandem mass spectrometry database for lipid identification.* Nat Methods, 2013. **10**(8): p. 755-8.

142. Di Girolamo, F., et al., *A Simple and Effective Mass Spectrometric Approach to Identify the Adulteration of the Mediterranean Diet Component Extra-Virgin Olive Oil with Corn Oil.* Int J Mol Sci, 2015. **16**(9): p. 20896-912.

143. Barber, C.N. and D.M. Raben, *Lipid Metabolism Crosstalk in the Brain: Glia and Neurons.* Front Cell Neurosci, 2019. **13**: p. 212.

144. Astarita, G., M. Stocchero, and G. Paglia, *Unbiased Lipidomics and Metabolomics of Human Brain Samples.* Methods Mol Biol, 2018. **1750**: p. 255-269.

145. Koelmel, J.P., et al., *Examining heat treatment for stabilization of the lipidome.* Bioanalysis, 2018. **10**(5): p. 291-305.

146. Seyer, A., et al., *Annotation of the human cerebrospinal fluid lipidome using high resolution mass spectrometry and a dedicated data processing workflow.* Metabolomics, 2016. **12**: p. 91.

147. Ammar, C., et al., *Multi-Reference Spectral Library Yields Almost Complete Coverage of Heterogeneous LC-MS/MS Data Sets.* J Proteome Res, 2019. **18**(4): p. 1553-1566.

148. Cajka, T., J.T. Smilowitz, and O. Fiehn, *Validating Quantitative Untargeted Lipidomics Across Nine Liquid Chromatography-High-Resolution Mass Spectrometry Platforms.* Anal Chem, 2017. **89**(22): p. 12360-12368.

149. Benton, H.P., et al., *Intra- and interlaboratory reproducibility of ultra performance liquid chromatography-time-of-flight mass spectrometry for urinary metabolic profiling.* Anal Chem, 2012. **84**(5): p. 2424-32.

150. Contrepois, K., et al., *Cross-Platform Comparison of Untargeted and Targeted Lipidomics Approaches on Aging Mouse Plasma.* Sci Rep, 2018. **8**(1): p. 17747.

151. Djekic, D., et al., *Replication of LC-MS untargeted lipidomics results in patients with calcific coronary disease: An interlaboratory reproducibility study.* Int J Cardiol, 2016. **222**: p. 1042-1048.

152. Glauser, G., et al., *Ultra-high pressure liquid chromatography-mass spectrometry for plant metabolomics: a systematic comparison of high-resolution quadrupole-time-of-flight and single stage Orbitrap mass spectrometers.* J Chromatogr A, 2013. **1292**: p. 151-9.

153. Morris, C.B., et al., *Evaluating Separation Selectivity and Collision Cross Section Measurement Reproducibility in Helium, Nitrogen, Argon, and Carbon Dioxide Drift Gases for Drift Tube Ion Mobility-Mass Spectrometry.* J Am Soc Mass Spectrom, 2019.

154. Schneider, B.B., D.J. Douglas, and D.D. Chen, *Ion fragmentation in an electrospray ionization mass spectrometer interface with different gases.* Rapid Commun Mass Spectrom, 2001. **15**(4): p. 249-57.

155. Florencio, M.H., D. Despeyroux, and K.R. Jennings, *Collision gas effects in the collision-induced decomposition of protonated and cationized molecules of carbohydrate antibiotics.* Organic Mass Spectrometry, 1994. **29**(9): p. 483-490.

156. Hutchins, P.D., J.D. Russell, and J.J. Coon, *Mapping Lipid Fragmentation for Tailored Mass Spectral Libraries.* J Am Soc Mass Spectrom, 2019. **30**(4): p. 659-668.

157. Hartler, J., et al., *Deciphering lipid structures based on platform-independent decision rules.* Nat Methods, 2017. **14**(12): p. 1171-1174.

158. Hutchins, P.D., J.D. Russell, and J.J. Coon, *LipiDex: An Integrated Software Package for High-Confidence Lipid Identification.* Cell Syst, 2018. **6**(5): p. 621-625 e5.

159. Hsu, F.F. and J. Turk, *Electrospray ionization with low-energy collisionally activated dissociation tandem mass spectrometry of glycerophospholipids: mechanisms of fragmentation and structural characterization.* J Chromatogr B Analyt Technol Biomed Life Sci, 2009. **877**(26): p. 2673-95.

160. Gathungu, R.M., et al., *Optimization of Electrospray Ionization Source Parameters for Lipidomics To Reduce Misannotation of In-Source Fragments as Precursor Ions.* Anal Chem, 2018. **90**(22): p. 13523-13532.

161. Baker, D.L., et al., *Direct quantitative analysis of lysophosphatidic acid molecular species by stable isotope dilution electrospray ionization liquid chromatography-mass spectrometry.* Anal Biochem, 2001. **292**(2): p. 287-95.

162. D'Souza, K., G.V. Paramel, and P.C. Kienesberger, *Lysophosphatidic Acid Signaling in Obesity and Insulin Resistance.* Nutrients, 2018. **10**(4).

163. Gotoh, M., et al., *Controlling cancer through the autotaxin-lysophosphatidic acid receptor axis.* Biochem Soc Trans, 2012. **40**(1): p. 31-6.

164. Ackerman, S.J., et al., *Polyunsaturated lysophosphatidic acid as a potential asthma biomarker.* Biomark Med, 2016. **10**(2): p. 123-35.

165. Triebl, A., et al., *Quantitation of phosphatidic acid and lysophosphatidic acid molecular species using hydrophilic interaction liquid chromatography coupled to electrospray ionization high resolution mass spectrometry.* J Chromatogr A, 2014. **1347**: p. 104-10.

166. Sugasini, D. and P.V. Subbaiah, *Rate of acyl migration in lysophosphatidylcholine (LPC) is dependent upon the nature of the acyl group. Greater stability of sn-2 docosahexaenoyl LPC compared to the more saturated LPC species.* PLoS One, 2017. **12**(11): p. e0187826.

167. Okudaira, M., et al., *Separation and quantification of 2-acyl-1-lysophospholipids and 1-acyl-2-lysophospholipids in biological samples by LC-MS/MS.* J Lipid Res, 2014. **55**(10): p. 2178-92.

168. D'Arrigo, P. and S. Servi, *Synthesis of lysophospholipids.* Molecules, 2010. **15**(3): p. 1354-77.

169. Bradley, R.M., et al., *Mice Deficient in lysophosphatidic acid acyltransferase delta (Lpaatdelta)/acylglycerophosphate acyltransferase 4 (Agpat4) Have Impaired Learning and Memory.* Mol Cell Biol, 2017. **37**(22).

170. Seneviratne, A.K., et al., *The Mitochondrial Transacylase, Tafazzin, Regulates for AML Stemness by Modulating Intracellular Levels of Phospholipids.* Cell Stem Cell, 2019. **24**(4): p. 621-636 e16.

171. Bird, S.S., et al., *Qualitative Characterization of the Rat Liver Mitochondrial Lipidome using LC-MS Profiling and High Energy Collisional Dissociation (HCD) All Ion Fragmentation.* Metabolomics, 2013. **9**(1 Suppl): p. 67-83.

172. Ulmer, C.Z., et al., *A Robust Lipidomics Workflow for Mammalian Cells, Plasma, and Tissue Using Liquid-Chromatography High-Resolution Tandem Mass Spectrometry.* Methods Mol Biol, 2017. **1609**: p. 91-106.

173. Damen, C.W., et al., *Enhanced lipid isomer separation in human plasma using reversed-phase UPLC with ion-mobility/high-resolution MS detection.* J Lipid Res, 2014. **55**(8): p. 1772-83.

174. Li, Y., et al., *A novel approach to the simultaneous extraction and non-targeted analysis of the small molecules metabolome and lipidome using 96-well solid phase extraction plates with column-switching technology.* J Chromatogr A, 2015. **1409**: p. 277-81.

175. Gros, M., S. Rodriguez-Mozaz, and D. Barcelo, *Rapid analysis of multiclass antibiotic residues and some of their metabolites in hospital, urban wastewater and river water by ultra-high-performance liquid chromatography coupled to quadrupole-linear ion trap tandem mass spectrometry.* J Chromatogr A, 2013. **1292**: p. 173-88.

176. *Chapter 1 General theory of chromatography*, in *Journal of Chromatography Library*, B.G. Belenkii and L.Z. Vilenchik, Editors. 1983, Elsevier. p. 1-67.

177. Onorato, J.M., et al., *Challenges in accurate quantitation of lysophosphatidic acids in human biofluids.* J Lipid Res, 2014. **55**(8): p. 1784-96.

178. Shan, L., et al., *Quantitative determination of lysophosphatidic acid by LC/ESI/MS/MS employing a reversed phase HPLC column.* J Chromatogr B Analyt Technol Biomed Life Sci, 2008. **864**(1-2): p. 22-8.

179. Danne-Rasche, N., C. Coman, and R. Ahrends, *Nano-LC/NSI MS Refines Lipidomics by Enhancing Lipid Coverage, Measurement Sensitivity, and Linear Dynamic Range.* Anal Chem, 2018. **90**(13): p. 8093-8101.

180. Percy, A.J., et al., *Comparison of standard- and nano-flow liquid chromatography platforms for MRM-based quantitation of putative plasma biomarker proteins.* Anal Bioanal Chem, 2012. **404**(4): p. 1089-101.

181. Wyndham, K.D., et al., *Characterization and evaluation of C18 HPLC stationary phases based on ethyl-bridged hybrid organic/inorganic particles.* Anal Chem, 2003. **75**(24): p. 6781-8.

182. Ali, I., et al., *Recent trends in ultra-fast HPLC: new generation superficially porous silica columns.* J Sep Sci, 2012. **35**(23): p. 3235-49.

183. Murph, M., et al., *Liquid chromatography mass spectrometry for quantifying plasma lysophospholipids: potential biomarkers for cancer diagnosis.* Methods Enzymol, 2007. **433**: p. 1-25.

184. Jesionowska, A., E. Cecerska, and B. Dolegowska, *Methods for quantifying lysophosphatidic acid in body fluids: a review.* Anal Biochem, 2014. **453**: p. 38-43.

185. Scherer, M., G. Schmitz, and G. Liebisch, *High-throughput analysis of sphingosine 1-phosphate, sphinganine 1-phosphate, and lysophosphatidic acid in plasma samples by liquid chromatography-tandem mass spectrometry.* Clin Chem, 2009. **55**(6): p. 1218-22.

186. Aaltonen, N., J.T. Laitinen, and M. Lehtonen, *Quantification of lysophosphatidic acids in rat brain tissue by liquid chromatography-electrospray tandem mass spectrometry.* J Chromatogr B Analyt Technol Biomed Life Sci, 2010. **878**(15-16): p. 1145-52.

187. Bligh, E.G. and W.J. Dyer, *A rapid method of total lipid extraction and purification.* Can J Biochem Physiol, 1959. **37**(8): p. 911-7.

188. Kraemer, M.P., et al., *Measurement of Lysophosphatidic Acid and Sphingosine-1-Phosphate by Liquid Chromatography-Coupled Electrospray Ionization Tandem Mass Spectrometry.* Methods Mol Biol, 2018. **1697**: p. 31-42.

189. Liebisch, G. and M. Scherer, *Quantification of bioactive sphingo- and glycerophospholipid species by electrospray ionization tandem mass spectrometry in blood.* J Chromatogr B Analyt Technol Biomed Life Sci, 2012. **883-884**: p. 141-6.

190. Yang, B., et al., *Elevated plasma levels of lysophosphatidic acid and aberrant expression of lysophosphatidic acid receptors in adenomyosis.* BMC Womens Health, 2017. **17**(1): p. 118.

191. Salous, A.K., et al., *Mechanism of rapid elimination of lysophosphatidic acid and related lipids from the circulation of mice.* J Lipid Res, 2013. **54**(10): p. 2775-84.

192. Morris, A.J., et al., *Blood relatives: dynamic regulation of bioactive lysophosphatidic acid and sphingosine-1-phosphate metabolism in the circulation.* Trends Cardiovasc Med, 2009. **19**(4): p. 135-40.

193. Yanagida, K., et al., *Identification and characterization of a novel lysophosphatidic acid receptor, p2y5/LPA6.* J Biol Chem, 2009. **284**(26): p. 17731-41.

194.   Hama, K. and J. Aoki, *LPA(3), a unique G protein-coupled receptor for lysophosphatidic acid.* Prog Lipid Res, 2010. **49**(4): p. 335-42.

195.   Aoki, J., et al., *Serum lysophosphatidic acid is produced through diverse phospholipase pathways.* J Biol Chem, 2002. **277**(50): p. 48737-44.

196.   Tigyi, G. and R. Miledi, *Lysophosphatidates bound to serum albumin activate membrane currents in Xenopus oocytes and neurite retraction in PC12 pheochromocytoma cells.* J Biol Chem, 1992. **267**(30): p. 21360-7.

197.   Aristizabal Henao, J.J., et al., *Categorizing and qualifying nutritional lipidomic data: defining brutto, medio, genio, and infinio lipid species within macrolipidomics and microlipidomics.* Curr Opin Clin Nutr Metab Care, 2018.

198.   Zhao, Y.Y., et al., *Ultra-performance liquid chromatography-mass spectrometry as a sensitive and powerful technology in lipidomic applications.* Chem Biol Interact, 2014. **220**: p. 181-92.

199.   Wang, J., et al., *Templated polymers enable selective capture and release of lysophosphatidic acid in human plasma via optimization of non-covalent binding to functional monomers.* Analyst, 2015. **140**(22): p. 7572-7.

200.   Chaffin, M.D., et al., *MetProc: Separating Measurement Artifacts from True Metabolites in an Untargeted Metabolomics Experiment.* J Proteome Res, 2019. **18**(3): p. 1446-1450.

201.   Quehenberger, O., et al., *Lipidomics reveals a remarkable diversity of lipids in human plasma.* J Lipid Res, 2010. **51**(11): p. 3299-305.

202.   Wang, Q.A., P.E. Scherer, and R.K. Gupta, *Improved methodologies for the study of adipose biology: insights gained and opportunities ahead.* J Lipid Res, 2014. **55**(4): p. 605-24.

203.   Gunstone, F.D., *Movements towards tailor-made fats.* Prog Lipid Res, 1998. **37**(5): p. 277-305.

204.   Skoric, D., et al., *Genetic possibilities for altering sunflower oil quality to obtain novel oils.* Can J Physiol Pharmacol, 2008. **86**(4): p. 215-21.

205.   Gao, B., et al., *Triacylglycerol compositions of sunflower, corn and soybean oils examined with supercritical CO2 ultra-performance convergence chromatography combined with quadrupole time-of-flight mass spectrometry.* Food Chem, 2017. **218**: p. 569-574.

206.   Warner, K., P. Orr, and M. Glynn, *Effect of fatty acid composition of oils on flavor and stability of fried foods.* Journal of the American Oil Chemists' Society, 1997. **74**(4): p. 347-356.

207.   Holcapek, M., et al., *Characterization of triacylglycerol and diacylglycerol composition of plant oils using high-performance liquid chromatography-atmospheric pressure chemical ionization mass spectrometry.* J Chromatogr A, 2003. **1010**(2): p. 195-215.

208.   Murphy, R.C., et al., *Detection of the abundance of diacylglycerol and triacylglycerol molecular species in cells using neutral loss mass spectrometry.* Anal Biochem, 2007. **366**(1): p. 59-70.

209. Pyke, J.S., et al., *A tandem liquid chromatography–mass spectrometry (LC–MS) method for profiling small molecules in complex samples.* Metabolomics, 2015. **11**(6): p. 1552-1562.

210. Wei, F., et al., *Quantitation of triacylglycerols in edible oils by off-line comprehensive two-dimensional liquid chromatography-atmospheric pressure chemical ionization mass spectrometry using a single column.* J Chromatogr A, 2015. **1404**: p. 60-71.

211. Navarro-Reig, M., et al., *Chemometric analysis of comprehensive LCxLC-MS data: Resolution of triacylglycerol structural isomers in corn oil.* Talanta, 2016. **160**: p. 624-635.

212. Herrero, M., et al., *Serial coupled columns reversed-phase separations in high-performance liquid chromatography. Tool for analysis of complex real samples.* J Chromatogr A, 2008. **1188**(2): p. 208-15.

213. Duval, J., et al., *Hyphenation of ultra high performance supercritical fluid chromatography with atmospheric pressure chemical ionisation high resolution mass spectrometry: Part 1. Study of the coupling parameters for the analysis of natural non-polar compounds.* J Chromatogr A, 2017. **1509**: p. 132-140.

214. Fraser, T., H. Tayler, and S. Love, *Fatty acid composition of frontal, temporal and parietal neocortex in the normal human brain and in Alzheimer's disease.* Neurochem Res, 2010. **35**(3): p. 503-13.

215. Hopperton, K.E., et al., *Fish oil feeding attenuates neuroinflammatory gene expression without concomitant changes in brain eicosanoids and docosanoids in a mouse model of Alzheimer's disease.* Brain Behav Immun, 2018. **69**: p. 74-90.

216. Grimm, M.O.W., D.M. Michaelson, and T. Hartmann, *Omega-3 fatty acids, lipids, and apoE lipidation in Alzheimer's disease: a rationale for multi-nutrient dementia prevention.* J Lipid Res, 2017. **58**(11): p. 2083-2101.

217. Balleine, B.W., M.R. Delgado, and O. Hikosaka, *The role of the dorsal striatum in reward and decision-making.* J Neurosci, 2007. **27**(31): p. 8161-5.

218. Kim, H., et al., *Role of striatum in updating values of chosen actions.* J Neurosci, 2009. **29**(47): p. 14701-12.

219. Chan, R.B., et al., *Comparative lipidomic analysis of mouse and human brain with Alzheimer disease.* J Biol Chem, 2012. **287**(4): p. 2678-88.

220. Veloso, A., et al., *Distribution of lipids in human brain.* Anal Bioanal Chem, 2011. **401**(1): p. 89-101.

221. Taha, A.Y., et al., *Altered fatty acid concentrations in prefrontal cortex of schizophrenic patients.* J Psychiatr Res, 2013. **47**(5): p. 636-43.

222. Favreliere, S., et al., *Chronic dietary n-3 polyunsaturated fatty acids deficiency affects the fatty acid composition of plasmenylethanolamine and phosphatidylethanolamine differently in rat frontal cortex, striatum, and cerebellum.* Lipids, 1998. **33**(4): p. 401-7.

223. Carrie, I., et al., *Specific phospholipid fatty acid composition of brain regions in mice. Effects of n-3 polyunsaturated fatty acid deficiency and phospholipid supplementation.* J Lipid Res, 2000. **41**(3): p. 465-72.

224. Cardoso, H.D., et al., *Differential vulnerability of substantia nigra and corpus striatum to oxidative insult induced by reduced dietary levels of essential fatty acids.* Front Hum Neurosci, 2012. **6**: p. 249.

225. Byrdwell, W.C. and W.E. Neff, *Dual parallel electrospray ionization and atmospheric pressure chemical ionization mass spectrometry (MS), MS/MS and MS/MS/MS for the analysis of triacylglycerols and triacylglycerol oxidation products.* Rapid Commun Mass Spectrom, 2002. **16**(4): p. 300-19.

226. Byrdwell, W.C., *The Simulacrum System as a Construct for Mass Spectrometry of Triacylglycerols and Others.* Lipids, 2016. **51**(2): p. 211-27.

227. Santoro, V., et al., *Characterization and Determination of Interesterification Markers (Triacylglycerol Regioisomers) in Confectionery Oils by Liquid Chromatography-Mass Spectrometry.* Foods, 2018. **7**(2).

228. Adlof, R., *Analysis of triacylglycerol and fatty acid isomers by low-temperature silver-ion high performance liquid chromatography with acetonitrile in hexane as solvent: limitations of the methodology.* J Chromatogr A, 2007. **1148**(2): p. 256-9.

229. Choi, J., et al., *Comprehensive analysis of phospholipids in the brain, heart, kidney, and liver: brain phospholipids are least enriched with polyunsaturated fatty acids.* Mol Cell Biochem, 2018. **442**(1-2): p. 187-201.

230. Almeida, R., et al., *Quantitative spatial analysis of the mouse brain lipidome by pressurized liquid extraction surface analysis.* Anal Chem, 2015. **87**(3): p. 1749-56.

231. Liigand, P., et al., *Think Negative: Finding the Best Electrospray Ionization/MS Mode for Your Analyte.* Anal Chem, 2017. **89**(11): p. 5665-5668.

232. Baker, E.J., et al., *Metabolism and functional effects of plant-derived omega-3 fatty acids in humans.* Prog Lipid Res, 2016. **64**: p. 30-56.

233. Gibson, R.A., *Musings about the role dietary fats after 40 years of fatty acid research.* Prostaglandins Leukot Essent Fatty Acids, 2018. **131**: p. 1-5.

234. Hodson, L., C.M. Skeaff, and B.A. Fielding, *Fatty acid composition of adipose tissue and blood in humans and its use as a biomarker of dietary intake.* Prog Lipid Res, 2008. **47**(5): p. 348-80.

235. Harris, W.S. and C. Von Schacky, *The Omega-3 Index: a new risk factor for death from coronary heart disease?* Prev Med, 2004. **39**(1): p. 212-20.

236. Patterson, A.C., et al., *The percentage of DHA in erythrocytes can detect non-adherence to advice to increase EPA and DHA intakes.* Br J Nutr, 2014. **111**(2): p. 270-8.

237. Patterson, A.C., et al., *Omega-3 polyunsaturated fatty acid blood biomarkers increase linearly in men and women after tightly controlled intakes of 0.25, 0.5, and 1 g/d of EPA + DHA.* Nutr Res, 2015. **35**(12): p. 1040-1051.

238.	Stark, K.D., et al., *Global survey of the omega-3 fatty acids, docosahexaenoic acid and eicosapentaenoic acid in the blood stream of healthy adults.* Prog Lipid Res, 2016. **63**: p. 132-52.

239.	Patterson, A.C., et al., *Biomarker and dietary validation of a Canadian food frequency questionnaire to measure eicosapentaenoic and docosahexaenoic acid intakes from whole food, functional food, and nutraceutical sources.* J Acad Nutr Diet, 2012. **112**(7): p. 1005-14.

240.	Andersen, L.F., et al., *Evaluation of a food frequency questionnaire with weighed records, fatty acids, and alpha-tocopherol in adipose tissue and serum.* Am J Epidemiol, 1999. **150**(1): p. 75-87.

241.	Baylin, A., et al., *Fasting whole blood as a biomarker of essential fatty acid intake in epidemiologic studies: comparison with adipose tissue and plasma.* Am J Epidemiol, 2005. **162**(4): p. 373-81.

242.	McNaughton, S.A., M.C. Hughes, and G.C. Marks, *Validation of a FFQ to estimate the intake of PUFA using plasma phospholipid fatty acids and weighed foods records.* Br J Nutr, 2007. **97**(3): p. 561-8.

243.	Bagel, J., J. Zapata, and E. Nelson, *A Prospective, Open-Label Study Evaluating Adjunctive Calcipotriene 0.005%/Betamethasone Dipropionate 0.064% Foam in Psoriasis Patients With Inadequate Response to Biologic Therapy.* J Drugs Dermatol, 2018. **17**(8): p. 845-850.

244.	Ottestad, I., et al., *Fish oil supplementation alters the plasma lipidomic profile and increases long-chain PUFAs of phospholipids and triglycerides in healthy subjects.* PLoS One, 2012. **7**(8): p. e42550.

245.	Pastor, O., et al., *A comprehensive evaluation of omega-3 fatty acid supplementation in cystic fibrosis patients using lipidomics.* J Nutr Biochem, 2019. **63**: p. 197-205.

246.	Lankinen, M., et al., *Fatty fish intake decreases lipids related to inflammation and insulin signaling--a lipidomics approach.* PLoS One, 2009. **4**(4): p. e5258.

247.	Uhl, O., et al., *Changes of molecular glycerophospholipid species in plasma and red blood cells during docosahexaenoic acid supplementation.* Lipids, 2013. **48**(11): p. 1103-13.

248.	Pacetti, D., et al., *High-performance liquid chromatography/electrospray ionization ion-trap tandem mass spectrometric analysis and quantification of phosphatidylcholine molecular species in the serum of cystic fibrosis subjects supplemented with docosahexaenoic acid.* Rapid Commun Mass Spectrom, 2004. **18**(20): p. 2395-400.

249.	Sung, H.H., et al., *Differential plasma postprandial lipidomic responses to krill oil and fish oil supplementations in women: A randomized crossover study.* Nutrition, 2019. **65**: p. 191-201.

250.	Stanley, E.G., et al., *Lipidomics Profiling of Human Adipose Tissue Identifies a Pattern of Lipids Associated with Fish Oil Supplementation.* J Proteome Res, 2017. **16**(9): p. 3168-3179.

251. Aristizabal Henao, J.J., *Development and Validation of a Human Blood Acyl-Specific Lipidomic Profiling Method for Clinical Applications*, in *Department of Kinesiology*. 2015, University of Waterloo: Waterloo, ON, Canada. p. 152.

252. Leng, S., T. Winter, and H.M. Aukema, *Dietary LA and sex effects on oxylipin profiles in rat kidney, liver, and serum differ from their effects on PUFAs.* J Lipid Res, 2017. **58**(8): p. 1702-1712.

253. Caligiuri, S.P., et al., *Dietary linoleic acid and alpha-linolenic acid differentially affect renal oxylipins and phospholipid fatty acids in diet-induced obese rats.* J Nutr, 2013. **143**(9): p. 1421-31.

254. Mendonca, A.M., et al., *Distinct effects of dietary ALA, EPA and DHA on rat adipose oxylipins vary by depot location and sex.* Prostaglandins Leukot Essent Fatty Acids, 2018. **129**: p. 13-24.

255. Knudsen, V.K., et al., *Identifying dietary patterns and associated health-related lifestyle factors in the adult Danish population.* Eur J Clin Nutr, 2014. **68**(6): p. 736-40.

256. Biltoft-Jensen, A., et al., *Validation of the Danish 7-day pre-coded food diary among adults: energy intake v. energy expenditure and recording length.* Br J Nutr, 2009. **102**(12): p. 1838-46.

257. Stark, K.D., *The percentage of n-3 highly unsaturated fatty acids in total HUFA as a biomarker for omega-3 fatty acid status in tissues.* Lipids, 2008. **43**(1): p. 45-53.

258. Apostolou, C., et al., *An improved and fully validated LC-MS/MS method for the simultaneous quantification of simvastatin and simvastatin acid in human plasma.* J Pharm Biomed Anal, 2008. **46**(4): p. 771-9.

259. Sreenivasulu, V., et al., *Simultaneous determination of carisoprodol and aspirin in human plasma using liquid chromatography-tandem mass spectrometry in polarity switch mode: application to a human pharmacokinetic study.* Biomed Chromatogr, 2013. **27**(2): p. 179-85.

260. Zhang, J.Y., D.M. Fast, and A.P. Breau, *Development and validation of a liquid chromatography-tandem mass spectrometric assay for Eplerenone and its hydrolyzed metabolite in human plasma.* J Chromatogr B Analyt Technol Biomed Life Sci, 2003. **787**(2): p. 333-44.

261. Saito, A., M. Hamano, and H. Kataoka, *Simultaneous analysis of multiple urinary biomarkers for the evaluation of oxidative stress by automated online in-tube solid-phase microextraction coupled with negative/positive ion-switching mode liquid chromatography-tandem mass spectrometry.* J Sep Sci, 2018. **41**(13): p. 2743-2749.

262. Breitkopf, S.B., et al., *A relative quantitative positive/negative ion switching method for untargeted lipidomics via high resolution LC-MS/MS from any biological source.* Metabolomics, 2017. **13**(3).

263. Schwaiger, M., et al., *Merging metabolomics and lipidomics into one analytical run.* Analyst, 2018. **144**(1): p. 220-229.

264. Yamada, T., et al., *Development of a lipid profiling system using reverse-phase liquid chromatography coupled to high-resolution mass spectrometry with rapid polarity*

switching and an automated lipid identification software. J Chromatogr A, 2013. **1292**: p. 211-8.

265. Holcapek, M., R. Jirasko, and M. Lisa, *Recent developments in liquid chromatography-mass spectrometry and related techniques.* J Chromatogr A, 2012. **1259**: p. 3-15.

266. Gao, F., et al., *Monoacylglycerol Analysis Using MS/MS(ALL) Quadruple Time of Flight Mass Spectrometry.* Metabolites, 2016. **6**(3).

267. Gardner, M.S., et al., *Simultaneous Quantification of Free Cholesterol, Cholesteryl Esters, and Triglycerides without Ester Hydrolysis by UHPLC Separation and In-Source Collision Induced Dissociation Coupled MS/MS.* J Am Soc Mass Spectrom, 2017. **28**(11): p. 2319-2329.

268. Mu, H., H. Sillen, and C.-E. Hiy, *Identification of diacylglycerols and triacylglycerols in a structured lipid sample by atmospheric pressure chemical ionization liquid chromatography/mass spectrometry.* Journal of the American Oil Chemists' Society, 2000. **77**(10): p. 1049-1060.

269. Zhou, Y., H. Peisker, and P. Dormann, *Molecular species composition of plant cardiolipin determined by liquid chromatography mass spectrometry.* J Lipid Res, 2016. **57**(7): p. 1308-21.

270. Berger, S., et al., *Dietary cholesterol and cardiovascular disease: a systematic review and meta-analysis.* Am J Clin Nutr, 2015. **102**(2): p. 276-94.

271. Polewski, M.A., et al., *Plasma diacylglycerol composition is a biomarker of metabolic syndrome onset in rhesus monkeys.* J Lipid Res, 2015. **56**(8): p. 1461-70.

272. Bradley, R.M., K.D. Stark, and R.E. Duncan, *Influence of tissue, diet, and enzymatic remodeling on cardiolipin fatty acyl profile.* Mol Nutr Food Res, 2016. **60**(8): p. 1804-18.

273. Jenkins, B., J.A. West, and A. Koulman, *A review of odd-chain fatty acid metabolism and the role of pentadecanoic Acid (c15:0) and heptadecanoic Acid (c17:0) in health and disease.* Molecules, 2015. **20**(2): p. 2425-44.

274. Stark, K.D., et al., *Translating plasma and whole blood fatty acid compositional data into the sum of eicosapentaenoic and docosahexaenoic acid in erythrocytes.* Prostaglandins Leukot Essent Fatty Acids, 2016. **104**: p. 1-10.

275. Metherel, A.H., et al., *Assessment of blood measures of n-3 polyunsaturated fatty acids with acute fish oil supplementation and washout in men and women.* Prostaglandins Leukot Essent Fatty Acids, 2009. **81**(1): p. 23-9.

276. Kuypers, F.A., et al., *The distribution of erythrocyte phospholipids in hereditary spherocytosis demonstrates a minimal role for erythrocyte spectrin on phospholipid diffusion and asymmetry.* Blood, 1993. **81**(4): p. 1051-7.

277. Janssen, C.I. and A.J. Kiliaan, *Long-chain polyunsaturated fatty acids (LCPUFA) from genesis to senescence: the influence of LCPUFA on neural development, aging, and neurodegeneration.* Prog Lipid Res, 2014. **53**: p. 1-17.

278. Gaposchkin, D.P. and R.A. Zoeller, *Plasmalogen status influences docosahexaenoic acid levels in a macrophage cell line. Insights using ether lipid-deficient variants.* J Lipid Res, 1999. **40**(3): p. 495-503.

279. Thomas, S.E., et al., *Incorporation of polyunsaturated fatty acids into plasmalogens, compared to other phospholipids of cultured glioma cells, is more dependent on chain length than on selectivity between (n - 3) and (n - 6) families.* Biochim Biophys Acta, 1990. **1044**(3): p. 349-56.

280. Ford, D.A. and R.W. Gross, *The discordant rates of sn-1 aliphatic chain and polar head group incorporation into plasmalogen molecular species demonstrate the fundamental importance of polar head group remodeling in plasmalogen metabolism in rabbit myocardium.* Biochemistry, 1994. **33**(5): p. 1216-22.

281. Wilkinson, T., et al., *Marked enrichment of the alkenylacyl subclass of plasma ethanolamine glycerophospholipid with eicosapentaenoic acid in human subjects consuming a fish oil concentrate.* Lipids, 1996. **31 Suppl**: p. S211-5.

282. Micha, R., et al., *Global, regional, and national consumption levels of dietary fats and oils in 1990 and 2010: a systematic analysis including 266 country-specific nutrition surveys.* BMJ, 2014. **348**: p. g2272.

283. Fratesi, J.A., et al., *Direct quantitation of omega-3 fatty acid intake of Canadian residents of a long-term care facility.* Appl Physiol Nutr Metab, 2009. **34**(1): p. 1-9.

284. Schantz, M.M., et al., *Interlaboratory analytical comparison of fatty acid concentrations in serum or plasma.* Clin Chim Acta, 2016. **462**: p. 148-152.

285. Preston Mason, R., *New Insights into Mechanisms of Action for Omega-3 Fatty Acids in Atherothrombotic Cardiovascular Disease.* Curr Atheroscler Rep, 2019. **21**(1): p. 2.

286. Bisgaard, H., et al., *Fish Oil-Derived Fatty Acids in Pregnancy and Wheeze and Asthma in Offspring.* N Engl J Med, 2016. **375**(26): p. 2530-9.

287. Albert, C.M., et al., *Blood levels of long-chain n-3 fatty acids and the risk of sudden death.* N Engl J Med, 2002. **346**(15): p. 1113-8.

288. Pinel, A., B. Morio-Liondore, and F. Capel, *n-3 Polyunsaturated fatty acids modulate metabolism of insulin-sensitive tissues: implication for the prevention of type 2 diabetes.* J Physiol Biochem, 2014. **70**(2): p. 647-58.

289. Janakiram, N.B. and C.V. Rao, *Role of lipoxins and resolvins as anti-inflammatory and proresolving mediators in colon cancer.* Curr Mol Med, 2009. **9**(5): p. 565-79.

290. Fasano, E., et al., *Long-chain n-3 PUFA against breast and prostate cancer: Which are the appropriate doses for intervention studies in animals and humans?* Crit Rev Food Sci Nutr, 2017. **57**(11): p. 2245-2262.

291. Fenton, J.I., et al., *Red blood cell PUFAs reflect the phospholipid PUFA composition of major organs.* Prostaglandins Leukot Essent Fatty Acids, 2016. **112**: p. 12-23.

292. Metherel, A.H., et al., *Two weeks of docosahexaenoic acid (DHA) supplementation increases synthesis-secretion kinetics of n-3 polyunsaturated fatty acids compared to 8 weeks of DHA supplementation.* J Nutr Biochem, 2018. **60**: p. 24-34.

293.   Metherel, A.H., et al., *Retroconversion is a minor contributor to increases in eicosapentaenoic acid following docosahexaenoic acid feeding as determined by compound specific isotope analysis in rat liver.* Nutr Metab (Lond), 2017. **14**: p. 75.

294.   Metherel, A.H., et al., *Compound-specific isotope analysis reveals no retroconversion of DHA to EPA but substantial conversion of EPA to DHA following supplementation: a randomized control trial.* Am J Clin Nutr, 2019.

295.   Brossard, N., et al., *Retroconversion and metabolism of [13C]22:6n-3 in humans and rats after intake of a single dose of [13C]22:6n-3-triacylglycerols.* Am J Clin Nutr, 1996. **64**(4): p. 577-86.

296.   Brenna, J.T., et al., *Best practices for the design, laboratory analysis, and reporting of trials involving fatty acids.* Am J Clin Nutr, 2018. **108**(2): p. 211-227.

297.   Stark, K., *Analytical implications of routine clinical testing for omega-3 fatty acid biomarkers.* Lipid Technology, 2008. **20**(8): p. 177-179.

298.   Braverman, N.E. and A.B. Moser, *Functions of plasmalogen lipids in health and disease.* Biochim Biophys Acta, 2012. **1822**(9): p. 1442-52.

299.   Farooqui, A.A. and L.A. Horrocks, *Plasmalogens, phospholipase A2, and docosahexaenoic acid turnover in brain tissue.* J Mol Neurosci, 2001. **16**(2-3): p. 263-72; discussion 279-84.

300.   Kitson, A.P., K.D. Stark, and R.E. Duncan, *Enzymes in brain phospholipid docosahexaenoic acid accretion: a PL-ethora of potential PL-ayers.* Prostaglandins Leukot Essent Fatty Acids, 2012. **87**(1): p. 1-10.

301.   Glick, N.R. and M.H. Fischer, *Low DHA and plasmalogens associated with a precise PUFA-rich diet devoid of DHA.* Clin Biochem, 2010. **43**(16-17): p. 1305-8.

302.   Andre, A., et al., *Effects of aging and dietary n-3 fatty acids on rat brain phospholipids: focus on plasmalogens.* Lipids, 2005. **40**(8): p. 799-806.

303.   Watschinger, K. and E.R. Werner, *Orphan enzymes in ether lipid metabolism.* Biochimie, 2013. **95**(1): p. 59-65.

304.   Arthur, G., L. Page, and P.C. Choy, *Acylation of 1-alkenylglycerophosphoethanolamine and 1-acylglycerophosphoethanolamine in guinea-pig heart microsomes.* Biochim Biophys Acta, 1987. **921**(2): p. 259-65.

305.   Stark, K.D. and B.J. Holub, *Differential eicosapentaenoic acid elevations and altered cardiovascular disease risk factor responses after supplementation with docosahexaenoic acid in postmenopausal women receiving and not receiving hormone replacement therapy.* Am J Clin Nutr, 2004. **79**(5): p. 765-73.

306.   Kitson, A.P., et al., *Tissue-specific sex differences in docosahexaenoic acid and Delta6-desaturase in rats fed a standard chow diet.* Appl Physiol Nutr Metab, 2012. **37**(6): p. 1200-11.

307.   Marks, K.A., A.P. Kitson, and K.D. Stark, *Hepatic and plasma sex differences in saturated and monounsaturated fatty acids are associated with differences in expression*

of elongase 6, but not stearoyl-CoA desaturase in Sprague-Dawley rats. Genes Nutr, 2013. **8**(3): p. 317-27.

308. Decsi, T. and K. Kennedy, *Sex-specific differences in essential fatty acid metabolism.* Am J Clin Nutr, 2011. **94**(6 Suppl): p. 1914S-1919S.

309. Hopfgartner, G., et al., *Triple quadrupole linear ion trap mass spectrometer for the analysis of small molecules and macromolecules.* J Mass Spectrom, 2004. **39**(8): p. 845-55.

310. Crutchfield, C.A. and W. Clarke, *Chapter 12 - High resolution accurate mass (HRAM) mass spectrometry*, in *Mass Spectrometry for the Clinical Laboratory*, H. Nair and W. Clarke, Editors. 2017, Academic Press: San Diego. p. 247-259.

311. Stark, K.D., S.Y. Lim, and N. Salem, Jr., *Artificial rearing with docosahexaenoic acid and n-6 docosapentaenoic acid alters rat tissue fatty acid composition.* J Lipid Res, 2007. **48**(11): p. 2471-7.

312. Holcapek, M., G. Liebisch, and K. Ekroos, *Lipidomic Analysis.* Anal Chem, 2018. **90**(7): p. 4249-4257.

313. Lam, S.M., H. Tian, and G. Shui, *Lipidomics, en route to accurate quantitation.* Biochim Biophys Acta Mol Cell Biol Lipids, 2017. **1862**(8): p. 752-761.

314. Wang, M., C. Wang, and X. Han, *Selection of internal standards for accurate quantification of complex lipid species in biological extracts by electrospray ionization mass spectrometry-What, how and why?* Mass Spectrom Rev, 2017. **36**(6): p. 693-714.

315. Liebisch, G., et al., *Reporting of lipidomics data should be standardized.* Biochim Biophys Acta Mol Cell Biol Lipids, 2017. **1862**(8): p. 747-751.

316. Kauhanen, D., et al., *Development and validation of a high-throughput LC-MS/MS assay for routine measurement of molecular ceramides.* Anal Bioanal Chem, 2016. **408**(13): p. 3475-83.

317. Han, X., et al., *Factors influencing the electrospray intrasource separation and selective ionization of glycerophospholipids.* J Am Soc Mass Spectrom, 2006. **17**(2): p. 264-74.

318. Koivusalo, M., et al., *Quantitative determination of phospholipid compositions by ESI-MS: effects of acyl chain length, unsaturation, and lipid concentration on instrument response.* J Lipid Res, 2001. **42**(4): p. 663-72.

319. Han, X., *Lipidomics for precision medicine and metabolism: A personal view.* Biochim Biophys Acta Mol Cell Biol Lipids, 2017. **1862**(8): p. 804-807.

320. Kohlwein, S.D., *Opinion articles on lipidomics - A critical assessment of the state-of-the-art.* Biochim Biophys Acta Mol Cell Biol Lipids, 2017. **1862**(8): p. 729-730.

Appendix A (Supplementary Data for Chapter 8)

Table A.1 Lipids with Full-Acyl Identifications (FAID) in whole blood from the Danish National Survey of Diet and Physical Activity using SimLipid software.

m/z	Main Class	Lipid Sub-Class	Brutto-Species	Medio-Species	Matched Ion Intensity (Sum)
648.6290	Ceramides	N-acylsphingosines (ceramides)	Cer 42:1	Cer d18:1_24:0	164.39
810.5660	Oxidized glycerophospholipids	Oxidized glycerophosphocholines	PC 38:4	PC 18:0_20:4 OH[S]	72.22
673.4810	Glycerophosphates	Diacylglycerophosphates	PA 34:1	PA 16:0_18:1	312.23
671.4670	Glycerophosphates	Diacylglycerophosphates	PA 34:2	PA 16:0_18:2	218.09
673.4800	Glycerophosphates	Diacylglycerophosphates	PA 35:1	PA 18:1_17:0	286.04
671.4660	Glycerophosphates	Diacylglycerophosphates	PA 35:2	PA 17:0_18:2	168.38
701.5100	Glycerophosphates	Diacylglycerophosphates	PA 36:1	PA 18:0_18:1	303.51
699.4950	Glycerophosphates	Diacylglycerophosphates	PA 36:2	PA 18:1_18:1	215.15
701.5100	Glycerophosphates	Diacylglycerophosphates	PA 37:1	PA 18:0_19:1	250.90
701.5140	Glycerophosphates	Diacylglycerophosphates	PA 37:1	PA 18:1_19:0	288.21
723.4980	Glycerophosphates	Diacylglycerophosphates	PA 38:4	PA 18:0_20:4	239.37
723.4940	Glycerophosphates	Diacylglycerophosphates	PA 39:4	PA 19:0_20:4	179.01
722.4970	Glycerophosphocholines	Diacylglycerophosphocholines	PC 28:0	PC 12:0_16:0	191.18
722.4970	Glycerophosphocholines	Diacylglycerophosphocholines	PC 28:0	PC 14:0_14:0	169.50
750.5270	Glycerophosphocholines	Diacylglycerophosphocholines	PC 29:0	PC 14:0_15:0	94.48
750.5280	Glycerophosphocholines	Diacylglycerophosphocholines	PC 30:0	PC 12:0_18:0	137.92
748.5130	Glycerophosphocholines	Diacylglycerophosphocholines	PC 30:1	PC 14:1_16:0	123.71
718.5380	Glycerophosphocholines	Diacylglycerophosphocholines	PC 31:0	PC 15:0_16:0	218.83
716.5230	Glycerophosphocholines	Diacylglycerophosphocholines	PC 31:1	PC 13:0_18:1	161.38
776.5440	Glycerophosphocholines	Diacylglycerophosphocholines	PC 31:1	PC 15:0_16:1	86.55
776.5450	Glycerophosphocholines	Diacylglycerophosphocholines	PC 31:1	PC 16:0_15:1	102.40
714.5100	Glycerophosphocholines	Diacylglycerophosphocholines	PC 31:2	PC 13:0_18:2	160.46
714.5080	Glycerophosphocholines	Diacylglycerophosphocholines	PC 31:2	PC 15:1_16:1	90.42
712.4910	Glycerophosphocholines	Diacylglycerophosphocholines	PC 31:3	PC 13:0_18:3	130.76
778.5600	Glycerophosphocholines	Diacylglycerophosphocholines	PC 32:0	PC 14:0_18:0	145.83
778.5570	Glycerophosphocholines	Diacylglycerophosphocholines	PC 32:0	PC 16:0_16:0	244.81
776.5450	Glycerophosphocholines	Diacylglycerophosphocholines	PC 32:1	PC 14:0_18:1	184.44
776.5430	Glycerophosphocholines	Diacylglycerophosphocholines	PC 32:1	PC 16:0_16:1	253.29
714.5080	Glycerophosphocholines	Diacylglycerophosphocholines	PC 32:2	PC 14:0_18:2	274.37
774.5280	Glycerophosphocholines	Diacylglycerophosphocholines	PC 32:2	PC 14:1_18:1	131.51
774.5280	Glycerophosphocholines	Diacylglycerophosphocholines	PC 32:2	PC 16:1_16:1	155.65
712.4930	Glycerophosphocholines	Diacylglycerophosphocholines	PC 32:3	PC 14:0_18:3	207.45
786.5270	Glycerophosphocholines	Diacylglycerophosphocholines	PC 32:3	PC 14:1_18:2	129.39
724.4910	Glycerophosphocholines	Diacylglycerophosphocholines	PC 32:4	PC 12:0_20:4	71.55
792.5730	Glycerophosphocholines	Diacylglycerophosphocholines	PC 33:0	PC 15:0_18:0	213.14
792.5750	Glycerophosphocholines	Diacylglycerophosphocholines	PC 33:0	PC 16:0_17:0	217.38
790.5590	Glycerophosphocholines	Diacylglycerophosphocholines	PC 33:1	PC 15:0_18:1	160.25
790.5600	Glycerophosphocholines	Diacylglycerophosphocholines	PC 33:1	PC 16:0_17:1	133.79
790.5600	Glycerophosphocholines	Diacylglycerophosphocholines	PC 33:1	PC 16:1_17:0	105.93
818.5550	Glycerophosphocholines	Diacylglycerophosphocholines	PC 33:2	PC 14:1_19:1	56.06
788.5410	Glycerophosphocholines	Diacylglycerophosphocholines	PC 33:2	PC 15:0_18:2	261.29
742.5380	Glycerophosphocholines	Diacylglycerophosphocholines	PC 33:2	PC 15:1_18:1	150.67
788.5420	Glycerophosphocholines	Diacylglycerophosphocholines	PC 33:2	PC 16:0_17:2	164.12

788.5440	Glycerophosphocholines	Diacylglycerophosphocholines	PC 33:2	PC 16:1_17:1	178.58
740.5230	Glycerophosphocholines	Diacylglycerophosphocholines	PC 33:3	PC 15:0_18:3	108.31
800.5440	Glycerophosphocholines	Diacylglycerophosphocholines	PC 33:3	PC 15:1_18:2	134.31
786.5280	Glycerophosphocholines	Diacylglycerophosphocholines	PC 33:3	PC 16:1_17:2	72.44
738.5070	Glycerophosphocholines	Diacylglycerophosphocholines	PC 33:4	PC 13:0_20:4	170.63
738.5080	Glycerophosphocholines	Diacylglycerophosphocholines	PC 33:4	PC 15:0_18:4	81.66
738.5060	Glycerophosphocholines	Diacylglycerophosphocholines	PC 33:4	PC 15:1_18:3	128.00
736.4900	Glycerophosphocholines	Diacylglycerophosphocholines	PC 33:5	PC 13:0_20:5	160.95
806.5890	Glycerophosphocholines	Diacylglycerophosphocholines	PC 34:0	PC 14:0_20:0	106.42
806.5910	Glycerophosphocholines	Diacylglycerophosphocholines	PC 34:0	PC 16:0_18:0	208.68
744.5560	Glycerophosphocholines	Diacylglycerophosphocholines	PC 34:1	PC 14:0_20:1	168.70
744.5540	Glycerophosphocholines	Diacylglycerophosphocholines	PC 34:1	PC 16:0_18:1	262.82
804.5750	Glycerophosphocholines	Diacylglycerophosphocholines	PC 34:1	PC 18:0_16:1	148.28
742.5380	Glycerophosphocholines	Diacylglycerophosphocholines	PC 34:2	PC 16:0_18:2	253.85
742.5390	Glycerophosphocholines	Diacylglycerophosphocholines	PC 34:2	PC 16:1_18:1	204.42
742.5380	Glycerophosphocholines	Diacylglycerophosphocholines	PC 34:2	PC 18:0_16:2	122.76
800.5440	Glycerophosphocholines	Diacylglycerophosphocholines	PC 34:3	PC 14:0_20:3	157.01
800.5440	Glycerophosphocholines	Diacylglycerophosphocholines	PC 34:3	PC 16:0_18:3	269.90
800.5440	Glycerophosphocholines	Diacylglycerophosphocholines	PC 34:3	PC 16:1_18:2	236.17
798.5280	Glycerophosphocholines	Diacylglycerophosphocholines	PC 34:4	PC 12:0_22:4	104.94
798.5280	Glycerophosphocholines	Diacylglycerophosphocholines	PC 34:4	PC 14:0_20:4	264.37
798.5280	Glycerophosphocholines	Diacylglycerophosphocholines	PC 34:4	PC 14:1_20:3	144.30
798.5280	Glycerophosphocholines	Diacylglycerophosphocholines	PC 34:4	PC 16:0_18:4	152.35
738.5060	Glycerophosphocholines	Diacylglycerophosphocholines	PC 34:4	PC 16:1_18:3	153.99
798.5290	Glycerophosphocholines	Diacylglycerophosphocholines	PC 34:4	PC 16:2_18:2	149.02
796.5150	Glycerophosphocholines	Diacylglycerophosphocholines	PC 34:5	PC 14:0_20:5	227.52
796.5130	Glycerophosphocholines	Diacylglycerophosphocholines	PC 34:5	PC 14:1_20:4	194.92
796.5140	Glycerophosphocholines	Diacylglycerophosphocholines	PC 34:5	PC 16:1_18:4	102.95
820.6070	Glycerophosphocholines	Diacylglycerophosphocholines	PC 35:0	PC 17:0_18:0	106.31
818.5910	Glycerophosphocholines	Diacylglycerophosphocholines	PC 35:1	PC 16:0_19:1	163.09
818.5900	Glycerophosphocholines	Diacylglycerophosphocholines	PC 35:1	PC 16:1_19:0	125.34
818.5920	Glycerophosphocholines	Diacylglycerophosphocholines	PC 35:1	PC 17:0_18:1	212.67
818.5940	Glycerophosphocholines	Diacylglycerophosphocholines	PC 35:1	PC 17:1_18:0	189.52
816.5760	Glycerophosphocholines	Diacylglycerophosphocholines	PC 35:2	PC 13:0_22:2	110.63
816.5740	Glycerophosphocholines	Diacylglycerophosphocholines	PC 35:2	PC 15:0_20:2	143.92
816.5750	Glycerophosphocholines	Diacylglycerophosphocholines	PC 35:2	PC 17:0_18:2	245.56
816.5750	Glycerophosphocholines	Diacylglycerophosphocholines	PC 35:2	PC 17:1_18:1	187.00
816.5740	Glycerophosphocholines	Diacylglycerophosphocholines	PC 35:2	PC 17:2_18:0	167.80
812.5450	Glycerophosphocholines	Diacylglycerophosphocholines	PC 35:4	PC 13:0_22:4	72.13
812.5410	Glycerophosphocholines	Diacylglycerophosphocholines	PC 35:4	PC 15:0_20:4	242.64
812.5440	Glycerophosphocholines	Diacylglycerophosphocholines	PC 35:4	PC 15:1_20:3	118.47
812.5430	Glycerophosphocholines	Diacylglycerophosphocholines	PC 35:4	PC 17:0_18:4	110.03
766.5390	Glycerophosphocholines	Diacylglycerophosphocholines	PC 35:4	PC 18:2_17:2	195.95
824.5440	Glycerophosphocholines	Diacylglycerophosphocholines	PC 35:5	PC 15:0_20:5	126.94
764.5240	Glycerophosphocholines	Diacylglycerophosphocholines	PC 35:5	PC 15:1_20:4	185.37
824.5450	Glycerophosphocholines	Diacylglycerophosphocholines	PC 35:5	PC 17:2_18:3	96.25
762.5070	Glycerophosphocholines	Diacylglycerophosphocholines	PC 35:6	PC 13:0_22:6	168.64
762.5070	Glycerophosphocholines	Diacylglycerophosphocholines	PC 35:6	PC 15:1_20:5	148.79
808.5110	Glycerophosphocholines	Diacylglycerophosphocholines	PC 35:6	PC 17:2_18:4	59.57
834.6230	Glycerophosphocholines	Diacylglycerophosphocholines	PC 36:0	PC 16:0_20:0	188.10

834.6240	Glycerophosphocholines	Diacylglycerophosphocholines	PC 36:0	PC 18:0_18:0	216.35
832.6070	Glycerophosphocholines	Diacylglycerophosphocholines	PC 36:1	PC 16:0_20:1	183.74
832.6070	Glycerophosphocholines	Diacylglycerophosphocholines	PC 36:1	PC 16:1_20:0	126.50
772.5840	Glycerophosphocholines	Diacylglycerophosphocholines	PC 36:1	PC 18:0_18:1	236.62
830.5910	Glycerophosphocholines	Diacylglycerophosphocholines	PC 36:2	PC 16:0_20:2	175.39
830.5920	Glycerophosphocholines	Diacylglycerophosphocholines	PC 36:2	PC 16:1_20:1	112.04
770.5700	Glycerophosphocholines	Diacylglycerophosphocholines	PC 36:2	PC 18:0_18:2	253.20
830.5910	Glycerophosphocholines	Diacylglycerophosphocholines	PC 36:2	PC 18:1_18:1	220.35
828.5740	Glycerophosphocholines	Diacylglycerophosphocholines	PC 36:3	PC 16:0_20:3	246.16
828.5750	Glycerophosphocholines	Diacylglycerophosphocholines	PC 36:3	PC 16:1_20:2	101.18
828.5760	Glycerophosphocholines	Diacylglycerophosphocholines	PC 36:3	PC 18:0_18:3	192.97
828.5760	Glycerophosphocholines	Diacylglycerophosphocholines	PC 36:3	PC 18:1_18:2	281.48
766.5390	Glycerophosphocholines	Diacylglycerophosphocholines	PC 36:4	PC 14:0_22:4	201.41
766.5380	Glycerophosphocholines	Diacylglycerophosphocholines	PC 36:4	PC 16:0_20:4	246.64
826.5600	Glycerophosphocholines	Diacylglycerophosphocholines	PC 36:4	PC 16:1_20:3	163.30
766.5370	Glycerophosphocholines	Diacylglycerophosphocholines	PC 36:4	PC 18:0_18:4	143.48
826.5610	Glycerophosphocholines	Diacylglycerophosphocholines	PC 36:4	PC 18:1_18:3	177.29
826.5610	Glycerophosphocholines	Diacylglycerophosphocholines	PC 36:4	PC 18:2_18:2	230.56
824.5410	Glycerophosphocholines	Diacylglycerophosphocholines	PC 36:5	PC 14:0_22:5	158.61
824.5430	Glycerophosphocholines	Diacylglycerophosphocholines	PC 36:5	PC 14:1_22:4	100.26
764.5240	Glycerophosphocholines	Diacylglycerophosphocholines	PC 36:5	PC 16:0_20:5	258.81
824.5450	Glycerophosphocholines	Diacylglycerophosphocholines	PC 36:5	PC 16:1_20:4	243.66
824.5420	Glycerophosphocholines	Diacylglycerophosphocholines	PC 36:5	PC 18:1_18:4	141.64
824.5450	Glycerophosphocholines	Diacylglycerophosphocholines	PC 36:5	PC 18:2_18:3	295.15
822.5300	Glycerophosphocholines	Diacylglycerophosphocholines	PC 36:6	PC 14:0_22:6	225.51
822.5270	Glycerophosphocholines	Diacylglycerophosphocholines	PC 36:6	PC 14:1_22:5	130.33
762.5070	Glycerophosphocholines	Diacylglycerophosphocholines	PC 36:6	PC 16:1_20:5	197.19
822.5270	Glycerophosphocholines	Diacylglycerophosphocholines	PC 36:6	PC 18:3_18:3	182.63
762.5070	Glycerophosphocholines	Diacylglycerophosphocholines	PC 36:6	PC 18:4_18:2	200.69
834.5280	Glycerophosphocholines	Diacylglycerophosphocholines	PC 36:7	PC 14:1_22:6	101.97
760.4910	Glycerophosphocholines	Diacylglycerophosphocholines	PC 36:7	PC 18:3_18:4	110.74
832.5130	Glycerophosphocholines	Diacylglycerophosphocholines	PC 36:8	PC 18:4_18:4	100.88
844.6060	Glycerophosphocholines	Diacylglycerophosphocholines	PC 37:2	PC 17:1_20:1	132.73
844.6100	Glycerophosphocholines	Diacylglycerophosphocholines	PC 37:2	PC 18:1_19:1	148.95
844.6060	Glycerophosphocholines	Diacylglycerophosphocholines	PC 37:2	PC 18:2_19:0	198.73
840.5750	Glycerophosphocholines	Diacylglycerophosphocholines	PC 37:4	PC 17:0_20:4	193.29
792.5530	Glycerophosphocholines	Diacylglycerophosphocholines	PC 37:5	PC 17:0_20:5	111.74
792.5530	Glycerophosphocholines	Diacylglycerophosphocholines	PC 37:5	PC 17:1_20:4	115.57
836.5460	Glycerophosphocholines	Diacylglycerophosphocholines	PC 37:6	PC 15:0_22:6	215.02
836.5430	Glycerophosphocholines	Diacylglycerophosphocholines	PC 37:6	PC 17:2_20:4	111.26
834.5290	Glycerophosphocholines	Diacylglycerophosphocholines	PC 37:7	PC 15:1_22:6	102.62
788.5230	Glycerophosphocholines	Diacylglycerophosphocholines	PC 37:7	PC 17:2_20:5	99.36
860.6350	Glycerophosphocholines	Diacylglycerophosphocholines	PC 38:1	PC 16:0_22:1	169.17
860.6370	Glycerophosphocholines	Diacylglycerophosphocholines	PC 38:1	PC 18:0_20:1	140.96
858.6210	Glycerophosphocholines	Diacylglycerophosphocholines	PC 38:2	PC 18:0_20:2	195.96
858.6220	Glycerophosphocholines	Diacylglycerophosphocholines	PC 38:2	PC 18:1_20:1	147.93
858.6200	Glycerophosphocholines	Diacylglycerophosphocholines	PC 38:2	PC 20:0_18:2	190.99
856.6040	Glycerophosphocholines	Diacylglycerophosphocholines	PC 38:3	PC 18:0_20:3	253.14
856.6060	Glycerophosphocholines	Diacylglycerophosphocholines	PC 38:3	PC 18:1_20:2	170.55
856.6050	Glycerophosphocholines	Diacylglycerophosphocholines	PC 38:3	PC 18:2_20:1	214.62

854.5920	Glycerophosphocholines	Diacylglycerophosphocholines	PC 38:4	PC 16:0_22:4	207.31
854.5920	Glycerophosphocholines	Diacylglycerophosphocholines	PC 38:4	PC 18:0_20:4	239.28
854.5930	Glycerophosphocholines	Diacylglycerophosphocholines	PC 38:4	PC 18:1_20:3	262.88
854.5900	Glycerophosphocholines	Diacylglycerophosphocholines	PC 38:4	PC 18:2_20:2	190.24
792.5540	Glycerophosphocholines	Diacylglycerophosphocholines	PC 38:5	PC 16:0_22:5	210.01
792.5540	Glycerophosphocholines	Diacylglycerophosphocholines	PC 38:5	PC 16:1_22:4	177.64
852.5770	Glycerophosphocholines	Diacylglycerophosphocholines	PC 38:5	PC 18:0_20:5	220.46
852.5740	Glycerophosphocholines	Diacylglycerophosphocholines	PC 38:5	PC 18:1_20:4	204.23
852.5740	Glycerophosphocholines	Diacylglycerophosphocholines	PC 38:5	PC 18:2_20:3	171.21
852.5760	Glycerophosphocholines	Diacylglycerophosphocholines	PC 38:5	PC 18:3_20:2	158.48
790.5370	Glycerophosphocholines	Diacylglycerophosphocholines	PC 38:6	PC 16:0_22:6	235.86
850.5580	Glycerophosphocholines	Diacylglycerophosphocholines	PC 38:6	PC 16:1_22:5	127.07
850.5590	Glycerophosphocholines	Diacylglycerophosphocholines	PC 38:6	PC 18:1_20:5	224.19
850.5590	Glycerophosphocholines	Diacylglycerophosphocholines	PC 38:6	PC 18:2_20:4	243.13
850.5610	Glycerophosphocholines	Diacylglycerophosphocholines	PC 38:6	PC 18:3_20:3	114.24
848.5440	Glycerophosphocholines	Diacylglycerophosphocholines	PC 38:7	PC 16:1_22:6	217.19
848.5420	Glycerophosphocholines	Diacylglycerophosphocholines	PC 38:7	PC 18:2_20:5	224.60
848.5430	Glycerophosphocholines	Diacylglycerophosphocholines	PC 38:7	PC 18:3_20:4	212.03
788.5230	Glycerophosphocholines	Diacylglycerophosphocholines	PC 38:7	PC 18:4_20:3	162.07
786.5080	Glycerophosphocholines	Diacylglycerophosphocholines	PC 38:8	PC 18:4_20:4	195.09
882.6240	Glycerophosphocholines	Diacylglycerophosphocholines	PC 39:4	PC 17:0_22:4	87.53
882.6210	Glycerophosphocholines	Diacylglycerophosphocholines	PC 39:4	PC 19:0_20:4	53.43
880.6080	Glycerophosphocholines	Diacylglycerophosphocholines	PC 39:5	PC 17:0_22:5	91.05
810.5080	Glycerophosphocholines	Diacylglycerophosphocholines	PC 40:10	PC 20:5_20:5	103.94
884.6410	Glycerophosphocholines	Diacylglycerophosphocholines	PC 40:3	PC 18:1_22:2	106.99
884.6410	Glycerophosphocholines	Diacylglycerophosphocholines	PC 40:3	PC 18:2_22:1	138.16
882.6230	Glycerophosphocholines	Diacylglycerophosphocholines	PC 40:4	PC 18:0_22:4	218.21
882.6230	Glycerophosphocholines	Diacylglycerophosphocholines	PC 40:4	PC 20:2_20:2	125.68
880.6060	Glycerophosphocholines	Diacylglycerophosphocholines	PC 40:5	PC 18:0_22:5	198.41
880.6050	Glycerophosphocholines	Diacylglycerophosphocholines	PC 40:5	PC 18:1_22:4	119.53
880.6060	Glycerophosphocholines	Diacylglycerophosphocholines	PC 40:5	PC 20:1_20:4	150.49
880.6050	Glycerophosphocholines	Diacylglycerophosphocholines	PC 40:5	PC 20:2_20:3	102.83
878.5910	Glycerophosphocholines	Diacylglycerophosphocholines	PC 40:6	PC 18:0_22:6	227.48
878.5930	Glycerophosphocholines	Diacylglycerophosphocholines	PC 40:6	PC 18:1_22:5	128.80
878.5910	Glycerophosphocholines	Diacylglycerophosphocholines	PC 40:6	PC 18:2_22:4	114.77
878.5910	Glycerophosphocholines	Diacylglycerophosphocholines	PC 40:6	PC 20:3_20:3	149.37
876.5770	Glycerophosphocholines	Diacylglycerophosphocholines	PC 40:7	PC 18:1_22:6	199.56
874.5590	Glycerophosphocholines	Diacylglycerophosphocholines	PC 40:8	PC 18:2_22:6	197.12
874.5590	Glycerophosphocholines	Diacylglycerophosphocholines	PC 40:8	PC 20:4_20:4	216.49
916.6990	Glycerophosphocholines	Diacylglycerophosphocholines	PC 42:1	PC 18:1_24:0	156.16
898.5590	Glycerophosphocholines	Diacylglycerophosphocholines	PC 42:10	PC 20:4_22:6	158.33
512.3000	Glycerophosphocholines	Monoacylglycerophosphocholines	PC 14:0	PC 14:0_0:0	221.49
540.3300	Glycerophosphocholines	Monoacylglycerophosphocholines	PC 16:0	PC 16:0_0:0	209.68
538.3150	Glycerophosphocholines	Monoacylglycerophosphocholines	PC 16:1	PC 16:1_0:0	222.28
568.3640	Glycerophosphocholines	Monoacylglycerophosphocholines	PC 18:0	PC 18:0_0:0	209.45
566.3460	Glycerophosphocholines	Monoacylglycerophosphocholines	PC 18:1	PC 18:1_0:0	210.77
564.3320	Glycerophosphocholines	Monoacylglycerophosphocholines	PC 18:2	PC 18:2_0:0	230.44
562.3140	Glycerophosphocholines	Monoacylglycerophosphocholines	PC 18:3	PC 18:3_0:0	235.37
596.3930	Glycerophosphocholines	Monoacylglycerophosphocholines	PC 20:0	PC 20:0_0:0	170.92
594.3760	Glycerophosphocholines	Monoacylglycerophosphocholines	PC 20:1	PC 20:1_0:0	204.50

590.3470	Glycerophosphocholines	Monoacylglycerophosphocholines	PC 20:3	PC 20:3_0:0	212.40
588.3330	Glycerophosphocholines	Monoacylglycerophosphocholines	PC 20:4	PC 20:4_0:0	219.28
586.3150	Glycerophosphocholines	Monoacylglycerophosphocholines	PC 20:5	PC 20:5_0:0	236.92
622.4070	Glycerophosphocholines	Monoacylglycerophosphocholines	PC 22:1	PC 22:1_0:0	132.49
612.3310	Glycerophosphocholines	Monoacylglycerophosphocholines	PC 22:6	PC 22:6_0:0	230.00
690.5060	Glycerophosphoethanolamines	Diacylglycerophosphoethanolamines	PE 33:0	PE 17:0_16:0	186.51
718.5390	Glycerophosphoethanolamines	Diacylglycerophosphoethanolamines	PE 34:0	PE 18:0_16:0	244.27
716.5240	Glycerophosphoethanolamines	Diacylglycerophosphoethanolamines	PE 34:1	PE 16:1_18:0	107.05
714.5050	Glycerophosphoethanolamines	Diacylglycerophosphoethanolamines	PE 34:2	PE 16:0_18:2	266.40
714.5070	Glycerophosphoethanolamines	Diacylglycerophosphoethanolamines	PE 34:2	PE 18:1_16:1	116.85
712.4930	Glycerophosphoethanolamines	Diacylglycerophosphoethanolamines	PE 34:3	PE 14:0_20:3	112.57
712.4910	Glycerophosphoethanolamines	Diacylglycerophosphoethanolamines	PE 34:3	PE 16:0_18:3	254.29
712.4920	Glycerophosphoethanolamines	Diacylglycerophosphoethanolamines	PE 34:3	PE 18:2_16:1	119.93
710.4750	Glycerophosphoethanolamines	Diacylglycerophosphoethanolamines	PE 34:4	PE 20:4_14:0	201.56
718.5380	Glycerophosphoethanolamines	Diacylglycerophosphoethanolamines	PE 35:0	PE 18:0_17:0	185.34
718.5390	Glycerophosphoethanolamines	Diacylglycerophosphoethanolamines	PE 35:0	PE 19:0_16:0	212.80
716.5230	Glycerophosphoethanolamines	Diacylglycerophosphoethanolamines	PE 35:1	PE 16:0_19:1	190.82
716.5230	Glycerophosphoethanolamines	Diacylglycerophosphoethanolamines	PE 35:1	PE 16:1_19:0	109.90
730.5390	Glycerophosphoethanolamines	Diacylglycerophosphoethanolamines	PE 35:1	PE 18:1_17:0	205.67
714.5070	Glycerophosphoethanolamines	Diacylglycerophosphoethanolamines	PE 35:2	PE 17:0_18:2	164.51
714.5070	Glycerophosphoethanolamines	Diacylglycerophosphoethanolamines	PE 35:2	PE 17:1_18:1	79.26
712.4910	Glycerophosphoethanolamines	Diacylglycerophosphoethanolamines	PE 35:3	PE 17:0_18:3	154.47
712.4920	Glycerophosphoethanolamines	Diacylglycerophosphoethanolamines	PE 35:3	PE 17:1_18:2	112.91
772.5170	Glycerophosphoethanolamines	Diacylglycerophosphoethanolamines	PE 35:3	PE 17:2_18:1	135.48
724.4920	Glycerophosphoethanolamines	Diacylglycerophosphoethanolamines	PE 35:4	PE 15:0_20:4	229.15
782.4990	Glycerophosphoethanolamines	Diacylglycerophosphoethanolamines	PE 35:5	PE 17:1_18:4	118.67
746.5700	Glycerophosphoethanolamines	Diacylglycerophosphoethanolamines	PE 36:0	PE 16:0_20:0	141.92
746.5710	Glycerophosphoethanolamines	Diacylglycerophosphoethanolamines	PE 36:0	PE 18:0_18:0	149.25
744.5530	Glycerophosphoethanolamines	Diacylglycerophosphoethanolamines	PE 36:1	PE 16:0_20:1	196.43
744.5570	Glycerophosphoethanolamines	Diacylglycerophosphoethanolamines	PE 36:1	PE 16:1_20:0	104.76
744.5540	Glycerophosphoethanolamines	Diacylglycerophosphoethanolamines	PE 36:1	PE 18:0_18:1	255.62
778.5130	Glycerophosphoethanolamines	Diacylglycerophosphoethanolamines	PE 36:2	PE 14:0_22:2	107.32
742.5380	Glycerophosphoethanolamines	Diacylglycerophosphoethanolamines	PE 36:2	PE 14:1_22:1	101.87
742.5400	Glycerophosphoethanolamines	Diacylglycerophosphoethanolamines	PE 36:2	PE 16:0_20:2	146.02
742.5390	Glycerophosphoethanolamines	Diacylglycerophosphoethanolamines	PE 36:2	PE 18:0_18:2	243.50
742.5390	Glycerophosphoethanolamines	Diacylglycerophosphoethanolamines	PE 36:2	PE 18:1_18:1	214.48
740.5230	Glycerophosphoethanolamines	Diacylglycerophosphoethanolamines	PE 36:3	PE 16:1_20:2	103.99
740.5230	Glycerophosphoethanolamines	Diacylglycerophosphoethanolamines	PE 36:3	PE 18:0_18:3	129.13
740.5230	Glycerophosphoethanolamines	Diacylglycerophosphoethanolamines	PE 36:3	PE 18:1_18:2	302.96
740.5230	Glycerophosphoethanolamines	Diacylglycerophosphoethanolamines	PE 36:3	PE 20:3_16:0	254.45
738.5060	Glycerophosphoethanolamines	Diacylglycerophosphoethanolamines	PE 36:4	PE 16:0_20:4	267.51
738.5080	Glycerophosphoethanolamines	Diacylglycerophosphoethanolamines	PE 36:4	PE 16:1_20:3	106.03
738.5070	Glycerophosphoethanolamines	Diacylglycerophosphoethanolamines	PE 36:4	PE 18:1_18:3	284.44
738.5060	Glycerophosphoethanolamines	Diacylglycerophosphoethanolamines	PE 36:4	PE 18:2_18:2	168.67
738.5090	Glycerophosphoethanolamines	Diacylglycerophosphoethanolamines	PE 36:4	PE 18:4_18:0	101.21
736.4900	Glycerophosphoethanolamines	Diacylglycerophosphoethanolamines	PE 36:5	PE 18:2_18:3	182.06
736.4910	Glycerophosphoethanolamines	Diacylglycerophosphoethanolamines	PE 36:5	PE 20:4_16:1	116.46
736.4910	Glycerophosphoethanolamines	Diacylglycerophosphoethanolamines	PE 36:5	PE 20:5_16:0	279.10
734.4760	Glycerophosphoethanolamines	Diacylglycerophosphoethanolamines	PE 36:6	PE 18:3_18:3	114.21
734.4760	Glycerophosphoethanolamines	Diacylglycerophosphoethanolamines	PE 36:6	PE 22:6_14:0	142.55

746.5700	Glycerophosphoethanolamines	Diacylglycerophosphoethanolamines	PE 37:0	PE 18:0_19:0	74.30
744.5530	Glycerophosphoethanolamines	Diacylglycerophosphoethanolamines	PE 37:1	PE 17:0_20:1	135.14
744.5540	Glycerophosphoethanolamines	Diacylglycerophosphoethanolamines	PE 37:1	PE 18:0_19:1	190.31
744.5550	Glycerophosphoethanolamines	Diacylglycerophosphoethanolamines	PE 37:1	PE 18:1_19:0	155.13
742.5380	Glycerophosphoethanolamines	Diacylglycerophosphoethanolamines	PE 37:2	PE 17:0_20:2	108.31
742.5380	Glycerophosphoethanolamines	Diacylglycerophosphoethanolamines	PE 37:2	PE 18:1_19:1	201.09
742.5370	Glycerophosphoethanolamines	Diacylglycerophosphoethanolamines	PE 37:2	PE 18:2_19:0	150.35
740.5220	Glycerophosphoethanolamines	Diacylglycerophosphoethanolamines	PE 37:3	PE 17:0_20:3	160.04
740.5240	Glycerophosphoethanolamines	Diacylglycerophosphoethanolamines	PE 37:3	PE 18:2_19:1	209.05
740.5240	Glycerophosphoethanolamines	Diacylglycerophosphoethanolamines	PE 37:3	PE 18:3_19:0	103.29
752.5240	Glycerophosphoethanolamines	Diacylglycerophosphoethanolamines	PE 37:4	PE 17:0_20:4	217.09
752.5230	Glycerophosphoethanolamines	Diacylglycerophosphoethanolamines	PE 37:4	PE 17:1_20:3	85.62
738.5070	Glycerophosphoethanolamines	Diacylglycerophosphoethanolamines	PE 37:4	PE 18:3_19:1	196.34
736.4920	Glycerophosphoethanolamines	Diacylglycerophosphoethanolamines	PE 37:5	PE 17:0_20:5	169.53
750.5070	Glycerophosphoethanolamines	Diacylglycerophosphoethanolamines	PE 37:5	PE 17:1_20:4	115.62
736.4920	Glycerophosphoethanolamines	Diacylglycerophosphoethanolamines	PE 37:5	PE 18:4_19:1	83.71
772.5840	Glycerophosphoethanolamines	Diacylglycerophosphoethanolamines	PE 38:1	PE 16:0_22:1	147.49
772.5830	Glycerophosphoethanolamines	Diacylglycerophosphoethanolamines	PE 38:1	PE 18:0_20:1	186.64
772.5850	Glycerophosphoethanolamines	Diacylglycerophosphoethanolamines	PE 38:1	PE 20:0_18:1	106.71
770.5700	Glycerophosphoethanolamines	Diacylglycerophosphoethanolamines	PE 38:2	PE 16:0_22:2	128.19
770.5670	Glycerophosphoethanolamines	Diacylglycerophosphoethanolamines	PE 38:2	PE 18:1_20:1	242.08
770.5690	Glycerophosphoethanolamines	Diacylglycerophosphoethanolamines	PE 38:2	PE 20:0_18:2	107.83
770.5700	Glycerophosphoethanolamines	Diacylglycerophosphoethanolamines	PE 38:2	PE 20:2_18:0	193.14
768.5530	Glycerophosphoethanolamines	Diacylglycerophosphoethanolamines	PE 38:3	PE 18:1_20:2	116.06
768.5520	Glycerophosphoethanolamines	Diacylglycerophosphoethanolamines	PE 38:3	PE 18:2_20:1	81.88
768.5530	Glycerophosphoethanolamines	Diacylglycerophosphoethanolamines	PE 38:3	PE 20:3_18:0	245.92
766.5370	Glycerophosphoethanolamines	Diacylglycerophosphoethanolamines	PE 38:4	PE 16:0_22:4	241.92
766.5380	Glycerophosphoethanolamines	Diacylglycerophosphoethanolamines	PE 38:4	PE 18:0_20:4	279.61
766.5380	Glycerophosphoethanolamines	Diacylglycerophosphoethanolamines	PE 38:4	PE 18:1_20:3	272.93
766.5390	Glycerophosphoethanolamines	Diacylglycerophosphoethanolamines	PE 38:4	PE 18:2_20:2	138.93
764.5220	Glycerophosphoethanolamines	Diacylglycerophosphoethanolamines	PE 38:5	PE 16:1_22:4	100.36
764.5230	Glycerophosphoethanolamines	Diacylglycerophosphoethanolamines	PE 38:5	PE 18:2_20:3	149.20
764.5220	Glycerophosphoethanolamines	Diacylglycerophosphoethanolamines	PE 38:5	PE 18:3_20:2	109.51
764.5230	Glycerophosphoethanolamines	Diacylglycerophosphoethanolamines	PE 38:5	PE 20:4_18:1	257.23
764.5230	Glycerophosphoethanolamines	Diacylglycerophosphoethanolamines	PE 38:5	PE 20:5_18:0	240.89
762.5070	Glycerophosphoethanolamines	Diacylglycerophosphoethanolamines	PE 38:6	PE 16:0_22:6	269.17
762.5080	Glycerophosphoethanolamines	Diacylglycerophosphoethanolamines	PE 38:6	PE 18:3_20:3	117.55
762.5070	Glycerophosphoethanolamines	Diacylglycerophosphoethanolamines	PE 38:6	PE 20:4_18:2	259.68
762.5050	Glycerophosphoethanolamines	Diacylglycerophosphoethanolamines	PE 38:6	PE 20:5_18:1	269.49
760.4920	Glycerophosphoethanolamines	Diacylglycerophosphoethanolamines	PE 38:7	PE 18:2_20:5	217.77
760.4910	Glycerophosphoethanolamines	Diacylglycerophosphoethanolamines	PE 38:7	PE 18:3_20:4	183.03
820.5120	Glycerophosphoethanolamines	Diacylglycerophosphoethanolamines	PE 38:7	PE 22:6_16:1	54.41
772.5850	Glycerophosphoethanolamines	Diacylglycerophosphoethanolamines	PE 39:1	PE 18:1_21:0	108.80
772.5850	Glycerophosphoethanolamines	Diacylglycerophosphoethanolamines	PE 39:1	PE 19:0_20:1	134.93
770.5710	Glycerophosphoethanolamines	Diacylglycerophosphoethanolamines	PE 39:2	PE 17:0_22:2	75.48
770.5710	Glycerophosphoethanolamines	Diacylglycerophosphoethanolamines	PE 39:2	PE 18:2_21:0	87.18
770.5700	Glycerophosphoethanolamines	Diacylglycerophosphoethanolamines	PE 39:2	PE 19:0_20:2	129.59
770.5700	Glycerophosphoethanolamines	Diacylglycerophosphoethanolamines	PE 39:2	PE 19:1_20:1	200.99
768.5540	Glycerophosphoethanolamines	Diacylglycerophosphoethanolamines	PE 39:3	PE 19:0_20:3	149.92
766.5370	Glycerophosphoethanolamines	Diacylglycerophosphoethanolamines	PE 39:4	PE 17:0_22:4	162.78

766.5390	Glycerophosphoethanolamines	Diacylglycerophosphoethanolamines	PE 39:4	PE 19:0_20:4	141.10
766.5400	Glycerophosphoethanolamines	Diacylglycerophosphoethanolamines	PE 39:4	PE 19:1_20:3	135.34
764.5240	Glycerophosphoethanolamines	Diacylglycerophosphoethanolamines	PE 39:5	PE 19:0_20:5	143.28
764.5230	Glycerophosphoethanolamines	Diacylglycerophosphoethanolamines	PE 39:5	PE 19:1_20:4	155.25
762.5090	Glycerophosphoethanolamines	Diacylglycerophosphoethanolamines	PE 39:6	PE 19:1_20:5	186.68
762.5070	Glycerophosphoethanolamines	Diacylglycerophosphoethanolamines	PE 39:6	PE 22:6_17:0	190.00
820.5150	Glycerophosphoethanolamines	Diacylglycerophosphoethanolamines	PE 39:7	PE 17:1_22:6	110.69
796.5860	Glycerophosphoethanolamines	Diacylglycerophosphoethanolamines	PE 40:3	PE 20:0_20:3	145.05
794.5680	Glycerophosphoethanolamines	Diacylglycerophosphoethanolamines	PE 40:4	PE 20:4_20:0	168.72
794.5700	Glycerophosphoethanolamines	Diacylglycerophosphoethanolamines	PE 40:4	PE 22:4_18:0	209.49
792.5540	Glycerophosphoethanolamines	Diacylglycerophosphoethanolamines	PE 40:5	PE 18:1_22:4	250.19
792.5540	Glycerophosphoethanolamines	Diacylglycerophosphoethanolamines	PE 40:5	PE 20:0_20:5	103.02
792.5550	Glycerophosphoethanolamines	Diacylglycerophosphoethanolamines	PE 40:5	PE 20:1_20:4	174.94
790.5390	Glycerophosphoethanolamines	Diacylglycerophosphoethanolamines	PE 40:6	PE 18:0_22:6	227.32
790.5400	Glycerophosphoethanolamines	Diacylglycerophosphoethanolamines	PE 40:6	PE 18:2_22:4	144.66
790.5370	Glycerophosphoethanolamines	Diacylglycerophosphoethanolamines	PE 40:6	PE 20:2_20:4	129.36
790.5360	Glycerophosphoethanolamines	Diacylglycerophosphoethanolamines	PE 40:6	PE 20:3_20:3	113.12
788.5230	Glycerophosphoethanolamines	Diacylglycerophosphoethanolamines	PE 40:7	PE 20:2_20:5	115.63
788.5240	Glycerophosphoethanolamines	Diacylglycerophosphoethanolamines	PE 40:7	PE 20:3_20:4	247.16
788.5230	Glycerophosphoethanolamines	Diacylglycerophosphoethanolamines	PE 40:7	PE 22:6_18:1	271.47
786.5080	Glycerophosphoethanolamines	Diacylglycerophosphoethanolamines	PE 40:8	PE 20:3_20:5	103.74
786.5070	Glycerophosphoethanolamines	Diacylglycerophosphoethanolamines	PE 40:8	PE 20:4_20:4	207.00
786.5070	Glycerophosphoethanolamines	Diacylglycerophosphoethanolamines	PE 40:8	PE 22:6_18:2	226.61
794.5700	Glycerophosphoethanolamines	Diacylglycerophosphoethanolamines	PE 41:4	PE 19:0_22:4	119.22
794.5700	Glycerophosphoethanolamines	Diacylglycerophosphoethanolamines	PE 41:4	PE 20:4_21:0	106.28
792.5540	Glycerophosphoethanolamines	Diacylglycerophosphoethanolamines	PE 41:5	PE 19:1_22:4	158.08
790.5400	Glycerophosphoethanolamines	Diacylglycerophosphoethanolamines	PE 41:6	PE 19:0_22:6	166.43
788.5230	Glycerophosphoethanolamines	Diacylglycerophosphoethanolamines	PE 41:7	PE 19:1_22:6	171.10
810.5070	Glycerophosphoethanolamines	Diacylglycerophosphoethanolamines	PE 42:10	PE 20:4_22:6	253.03
810.5070	Glycerophosphoethanolamines	Diacylglycerophosphoethanolamines	PE 42:10	PE 20:5_22:5	102.88
718.5380	Glycerophosphoethanolamines	Diacylglycerophosphoethanolamines	PE-NMe2 32:0	PE-NMe2 16:0_16:0	213.52
744.5540	Glycerophosphoethanolamines	Diacylglycerophosphoethanolamines	PE-NMe2 34:1	PE-NMe2 16:0_18:1	268.14
526.2950	Glycerophosphoethanolamines	Monoacylglycerophosphoethanolamines	LysoPE 22:5	LysoPE 22:5_0:0	189.89
452.2770	Glycerophosphoethanolamines	Monoacylglycerophosphoethanolamines	PE 16:0	PE 16:0_0:0	145.65
480.3090	Glycerophosphoethanolamines	Monoacylglycerophosphoethanolamines	PE 18:0	PE 18:0_0:0	205.48
476.2780	Glycerophosphoethanolamines	Monoacylglycerophosphoethanolamines	PE 18:2	PE 18:2_0:0	170.38
508.3400	Glycerophosphoethanolamines	Monoacylglycerophosphoethanolamines	PE 20:0	PE 20:0_0:0	58.38
500.2780	Glycerophosphoethanolamines	Monoacylglycerophosphoethanolamines	PE 20:4	PE 20:4_0:0	177.08
498.2630	Glycerophosphoethanolamines	Monoacylglycerophosphoethanolamines	PE 20:5	PE 20:5_0:0	193.97
528.3100	Glycerophosphoethanolamines	Monoacylglycerophosphoethanolamines	PE 22:4	PE 22:4_0:0	65.59
524.2800	Glycerophosphoethanolamines	Monoacylglycerophosphoethanolamines	PE 22:6	PE 22:6_0:0	293.86
781.4890	Glycerophosphoglycerols	Diacylglycerophosphoglycerols	PG 31:1	PG 14:0_17:1	67.60
809.5170	Glycerophosphoglycerols	Diacylglycerophosphoglycerols	PG 33:1	PG 16:0_17:1	80.65
807.5020	Glycerophosphoglycerols	Diacylglycerophosphoglycerols	PG 33:2	PG 16:1_17:1	107.84
807.5020	Glycerophosphoglycerols	Diacylglycerophosphoglycerols	PG 33:2	PG 17:1_16:1	106.87
835.5310	Glycerophosphoglycerols	Diacylglycerophosphoglycerols	PG 35:2	PG 16:1_19:1	101.10
833.5160	Glycerophosphoglycerols	Diacylglycerophosphoglycerols	PG 35:3	PG 17:1_18:2	103.63
833.5180	Glycerophosphoglycerols	Diacylglycerophosphoglycerols	PG 35:3	PG 17:2_18:1	102.10
833.5170	Glycerophosphoglycerols	Diacylglycerophosphoglycerols	PG 35:3	PG 18:1_17:2	114.66
833.5180	Glycerophosphoglycerols	Diacylglycerophosphoglycerols	PG 35:3	PG 18:2_17:1	106.02

861.5490	Glycerophosphoglycerols	Diacylglycerophosphoglycerols	PG 37:3	PG 15:1_22:2	85.06
785.5350	Glycerophosphoglycerols	Diacylglycerophosphoglycerols	PG 37:3	PG 17:0_20:3	116.07
861.5500	Glycerophosphoglycerols	Diacylglycerophosphoglycerols	PG 37:3	PG 18:2_19:1	104.43
859.5330	Glycerophosphoglycerols	Diacylglycerophosphoglycerols	PG 37:4	PG 19:1_18:3	104.17
859.5330	Glycerophosphoglycerols	Diacylglycerophosphoglycerols	PG 37:4	PG 20:3_17:1	101.82
857.5180	Glycerophosphoglycerols	Diacylglycerophosphoglycerols	PG 37:5	PG 15:1_22:4	100.22
857.5210	Glycerophosphoglycerols	Diacylglycerophosphoglycerols	PG 37:5	PG 17:0_20:5	101.17
857.5160	Glycerophosphoglycerols	Diacylglycerophosphoglycerols	PG 37:5	PG 17:1_20:4	105.62
857.5180	Glycerophosphoglycerols	Diacylglycerophosphoglycerols	PG 37:5	PG 20:4_17:1	118.33
857.5180	Glycerophosphoglycerols	Diacylglycerophosphoglycerols	PG 37:5	PG 22:4_15:1	104.44
785.5350	Glycerophosphoglycerols	Diacylglycerophosphoglycerols	PG 38:3	PG 18:0_20:3	105.68
887.5650	Glycerophosphoglycerols	Diacylglycerophosphoglycerols	PG 39:4	PG 20:3_19:1	103.75
885.5470	Glycerophosphoglycerols	Diacylglycerophosphoglycerols	PG 39:5	PG 19:1_20:4	103.44
885.5490	Glycerophosphoglycerols	Diacylglycerophosphoglycerols	PG 39:5	PG 20:4_19:1	103.43
883.5360	Glycerophosphoglycerols	Diacylglycerophosphoglycerols	PG 39:6	PG 20:5_19:1	112.36
881.5160	Glycerophosphoglycerols	Diacylglycerophosphoglycerols	PG 39:7	PG 17:1_22:6	104.72
881.5170	Glycerophosphoglycerols	Diacylglycerophosphoglycerols	PG 39:7	PG 22:6_17:1	111.54
909.5500	Glycerophosphoglycerols	Diacylglycerophosphoglycerols	PG 41:7	PG 19:1_22:6	101.34
909.5520	Glycerophosphoglycerols	Diacylglycerophosphoglycerols	PG 41:7	PG 22:6_19:1	103.18
719.5330	Phosphosphingolipids	Sphingomyelins	SM 32:1	SM d16:1_16:0	103.08
747.5650	Phosphosphingolipids	Sphingomyelins	SM 34:1	SM d16:1_18:0	109.08
687.5430	Phosphosphingolipids	Sphingomyelins	SM 34:1	SM d18:1_16:0	100.39
745.5480	Phosphosphingolipids	Sphingomyelins	SM 34:2	SM d18:1_16:1	105.09
745.5490	Phosphosphingolipids	Sphingomyelins	SM 34:2	SM d18:2_16:0	108.29
775.5950	Phosphosphingolipids	Sphingomyelins	SM 36:1	SM d16:1_20:0	110.42
803.6280	Phosphosphingolipids	Sphingomyelins	SM 38:1	SM d16:1_22:0	100.18
829.6440	Phosphosphingolipids	Sphingomyelins	SM 40:2	SM d18:1_22:1	118.39
829.6440	Phosphosphingolipids	Sphingomyelins	SM 40:2	SM d18:2_22:0	118.19
859.6900	Phosphosphingolipids	Sphingomyelins	SM 42:1	SM d18:0_24:1	122.62
857.6730	Phosphosphingolipids	Sphingomyelins	SM 42:2	SM d18:2_24:0	123.33
887.7230	Phosphosphingolipids	Sphingomyelins	SM 44:1	SM d18:1_26:0	136.71
659.5120	Phosphosphingolipids	Ceramide phosphoethanolamines	PE-Cer 35:1	PE-Cer d15:1_20:0	101.25
781.4890	Glycerophosphoinositols	Diacylglycerophosphoinositols	PI 30:0	PI 16:0_14:0	70.43
781.4890	Glycerophosphoinositols	Diacylglycerophosphoinositols	PI 31:0	PI 14:0_17:0	66.93
809.5180	Glycerophosphoinositols	Diacylglycerophosphoinositols	PI 32:0	PI 16:0_16:0	102.71
807.5030	Glycerophosphoinositols	Diacylglycerophosphoinositols	PI 32:1	PI 16:1_16:0	119.31
807.5010	Glycerophosphoinositols	Diacylglycerophosphoinositols	PI 33:1	PI 16:1_17:0	109.43
833.5160	Glycerophosphoinositols	Diacylglycerophosphoinositols	PI 34:2	PI 18:1_16:1	118.53
833.5180	Glycerophosphoinositols	Diacylglycerophosphoinositols	PI 34:2	PI 18:2_16:0	114.77
833.5190	Glycerophosphoinositols	Diacylglycerophosphoinositols	PI 35:2	PI 16:1_19:1	114.33
833.5160	Glycerophosphoinositols	Diacylglycerophosphoinositols	PI 35:2	PI 17:0_18:2	106.68
833.5200	Glycerophosphoinositols	Diacylglycerophosphoinositols	PI 35:2	PI 17:1_18:1	76.42
861.5490	Glycerophosphoinositols	Diacylglycerophosphoinositols	PI 36:2	PI 18:2_18:0	108.22
859.5340	Glycerophosphoinositols	Diacylglycerophosphoinositols	PI 36:3	PI 18:0_18:3	107.25
859.5340	Glycerophosphoinositols	Diacylglycerophosphoinositols	PI 36:3	PI 18:2_18:1	116.29
859.5330	Glycerophosphoinositols	Diacylglycerophosphoinositols	PI 36:3	PI 20:3_16:0	113.38
857.5180	Glycerophosphoinositols	Diacylglycerophosphoinositols	PI 36:4	PI 16:1_20:3	93.79
857.5170	Glycerophosphoinositols	Diacylglycerophosphoinositols	PI 36:4	PI 18:2_18:2	105.58
857.5170	Glycerophosphoinositols	Diacylglycerophosphoinositols	PI 36:4	PI 20:4_16:0	117.16
861.5480	Glycerophosphoinositols	Diacylglycerophosphoinositols	PI 37:2	PI 18:1_19:1	106.08

861.5480	Glycerophosphoinositols	Diacylglycerophosphoinositols	PI 37:2	PI 18:2_19:0	104.70
859.5340	Glycerophosphoinositols	Diacylglycerophosphoinositols	PI 37:3	PI 18:2_19:1	106.35
859.5340	Glycerophosphoinositols	Diacylglycerophosphoinositols	PI 37:3	PI 18:3_19:0	103.02
857.5180	Glycerophosphoinositols	Diacylglycerophosphoinositols	PI 37:4	PI 15:0_22:4	100.29
857.5180	Glycerophosphoinositols	Diacylglycerophosphoinositols	PI 37:4	PI 17:0_20:4	111.37
887.5650	Glycerophosphoinositols	Diacylglycerophosphoinositols	PI 38:3	PI 20:3_18:0	111.91
885.5480	Glycerophosphoinositols	Diacylglycerophosphoinositols	PI 38:4	PI 18:0_20:4	112.39
885.5500	Glycerophosphoinositols	Diacylglycerophosphoinositols	PI 38:4	PI 18:1_20:3	100.69
883.5330	Glycerophosphoinositols	Diacylglycerophosphoinositols	PI 38:5	PI 18:3_20:2	105.77
883.5330	Glycerophosphoinositols	Diacylglycerophosphoinositols	PI 38:5	PI 20:4_18:1	116.81
883.5340	Glycerophosphoinositols	Diacylglycerophosphoinositols	PI 38:5	PI 20:5_18:0	114.70
881.5190	Glycerophosphoinositols	Diacylglycerophosphoinositols	PI 38:6	PI 16:0_22:6	117.99
881.5180	Glycerophosphoinositols	Diacylglycerophosphoinositols	PI 38:6	PI 18:4_20:2	107.85
887.5660	Glycerophosphoinositols	Diacylglycerophosphoinositols	PI 39:3	PI 19:0_20:3	104.67
885.5480	Glycerophosphoinositols	Diacylglycerophosphoinositols	PI 39:4	PI 19:0_20:4	105.55
883.5340	Glycerophosphoinositols	Diacylglycerophosphoinositols	PI 39:5	PI 19:0_20:5	102.37
883.5330	Glycerophosphoinositols	Diacylglycerophosphoinositols	PI 39:5	PI 19:1_20:4	107.88
881.5190	Glycerophosphoinositols	Diacylglycerophosphoinositols	PI 39:6	PI 22:6_17:0	112.48
909.5480	Glycerophosphoinositols	Diacylglycerophosphoinositols	PI 40:6	PI 18:0_22:6	116.34
909.5500	Glycerophosphoinositols	Diacylglycerophosphoinositols	PI 40:6	PI 20:1_20:5	100.12
909.5500	Glycerophosphoinositols	Diacylglycerophosphoinositols	PI 40:6	PI 20:2_20:4	100.74
909.5510	Glycerophosphoinositols	Diacylglycerophosphoinositols	PI 40:6	PI 20:3_20:3	101.39
909.5510	Glycerophosphoinositols	Diacylglycerophosphoinositols	PI 41:6	PI 19:0_22:6	103.68
599.3200	Glycerophosphoinositols	Monoacylglycerophosphoinositols	PI 18:0	PI 18:0_0:0	134.63
619.2870	Glycerophosphoinositols	Monoacylglycerophosphoinositols	PI 20:4	PI 20:4_0:0	170.82
762.5300	Glycerophosphoserines	Diacylglycerophosphoserines	PS 34:0	PS 16:0_18:0	118.85
810.5080	Glycerophosphoserines	Diacylglycerophosphoserines	PS 35:1	PS 14:1_21:0	76.69
810.5090	Glycerophosphoserines	Diacylglycerophosphoserines	PS 35:1	PS 17:1_18:0	113.38
810.5050	Glycerophosphoserines	Diacylglycerophosphoserines	PS 35:1	PS 20:0_15:1	103.83
772.5160	Glycerophosphoserines	Diacylglycerophosphoserines	PS 35:2	PS 17:1_18:1	148.24
772.5140	Glycerophosphoserines	Diacylglycerophosphoserines	PS 35:2	PS 18:2_17:0	103.44
834.5510	Glycerophosphoserines	Diacylglycerophosphoserines	PS 36:1	PS 14:0_22:1	117.30
788.5430	Glycerophosphoserines	Diacylglycerophosphoserines	PS 36:1	PS 18:0_18:1	267.97
788.5430	Glycerophosphoserines	Diacylglycerophosphoserines	PS 36:1	PS 18:1_18:0	274.64
788.5430	Glycerophosphoserines	Diacylglycerophosphoserines	PS 36:1	PS 20:1_16:0	206.38
786.5290	Glycerophosphoserines	Diacylglycerophosphoserines	PS 36:2	PS 16:0_20:2	175.61
786.5290	Glycerophosphoserines	Diacylglycerophosphoserines	PS 36:2	PS 18:0_18:2	277.86
786.5290	Glycerophosphoserines	Diacylglycerophosphoserines	PS 36:2	PS 18:1_18:1	205.73
786.5290	Glycerophosphoserines	Diacylglycerophosphoserines	PS 36:2	PS 18:2_18:0	280.09
772.5130	Glycerophosphoserines	Diacylglycerophosphoserines	PS 36:2	PS 20:2_16:0	97.72
784.5130	Glycerophosphoserines	Diacylglycerophosphoserines	PS 36:3	PS 18:0_18:3	111.70
784.5120	Glycerophosphoserines	Diacylglycerophosphoserines	PS 36:3	PS 18:1_18:2	168.80
784.5130	Glycerophosphoserines	Diacylglycerophosphoserines	PS 36:3	PS 18:2_18:1	232.09
784.5120	Glycerophosphoserines	Diacylglycerophosphoserines	PS 36:3	PS 18:3_18:0	60.09
782.4970	Glycerophosphoserines	Diacylglycerophosphoserines	PS 36:4	PS 16:0_20:4	355.04
782.4970	Glycerophosphoserines	Diacylglycerophosphoserines	PS 36:4	PS 18:2_18:2	234.11
782.4980	Glycerophosphoserines	Diacylglycerophosphoserines	PS 36:4	PS 18:4_18:0	101.75
782.4970	Glycerophosphoserines	Diacylglycerophosphoserines	PS 36:4	PS 20:3_16:1	176.45
782.4970	Glycerophosphoserines	Diacylglycerophosphoserines	PS 36:4	PS 20:4_16:0	339.55
780.4800	Glycerophosphoserines	Diacylglycerophosphoserines	PS 36:5	PS 16:0_20:5	197.02

780.4800	Glycerophosphoserines	Diacylglycerophosphoserines	PS 36:5	PS 20:5_16:0	235.46
788.5430	Glycerophosphoserines	Diacylglycerophosphoserines	PS 37:1	PS 18:0_19:1	237.35
788.5420	Glycerophosphoserines	Diacylglycerophosphoserines	PS 37:1	PS 18:1_19:0	228.60
788.5440	Glycerophosphoserines	Diacylglycerophosphoserines	PS 37:1	PS 19:0_18:1	229.89
788.5440	Glycerophosphoserines	Diacylglycerophosphoserines	PS 37:1	PS 19:1_18:0	256.64
786.5270	Glycerophosphoserines	Diacylglycerophosphoserines	PS 37:2	PS 18:1_19:1	210.19
786.5280	Glycerophosphoserines	Diacylglycerophosphoserines	PS 37:2	PS 18:2_19:0	229.49
786.5290	Glycerophosphoserines	Diacylglycerophosphoserines	PS 37:2	PS 19:0_18:2	218.06
786.5270	Glycerophosphoserines	Diacylglycerophosphoserines	PS 37:2	PS 19:1_18:1	159.27
786.5280	Glycerophosphoserines	Diacylglycerophosphoserines	PS 37:2	PS 20:2_17:0	165.86
798.5280	Glycerophosphoserines	Diacylglycerophosphoserines	PS 37:3	PS 17:0_20:3	126.83
798.5270	Glycerophosphoserines	Diacylglycerophosphoserines	PS 37:3	PS 18:2_19:1	139.43
798.5270	Glycerophosphoserines	Diacylglycerophosphoserines	PS 37:3	PS 18:3_19:0	102.99
784.5130	Glycerophosphoserines	Diacylglycerophosphoserines	PS 37:3	PS 19:1_18:2	151.66
798.5280	Glycerophosphoserines	Diacylglycerophosphoserines	PS 37:3	PS 20:3_17:0	104.37
782.4970	Glycerophosphoserines	Diacylglycerophosphoserines	PS 37:4	PS 17:0_20:4	235.30
782.4980	Glycerophosphoserines	Diacylglycerophosphoserines	PS 37:4	PS 17:1_20:3	209.65
796.5130	Glycerophosphoserines	Diacylglycerophosphoserines	PS 37:4	PS 18:3_19:1	117.11
796.5140	Glycerophosphoserines	Diacylglycerophosphoserines	PS 37:4	PS 20:4_17:0	147.38
780.4800	Glycerophosphoserines	Diacylglycerophosphoserines	PS 37:5	PS 17:0_20:5	160.19
812.5440	Glycerophosphoserines	Diacylglycerophosphoserines	PS 38:3	PS 18:0_20:3	267.58
812.5440	Glycerophosphoserines	Diacylglycerophosphoserines	PS 38:3	PS 18:1_20:2	190.97
812.5440	Glycerophosphoserines	Diacylglycerophosphoserines	PS 38:3	PS 18:2_20:1	211.45
798.5280	Glycerophosphoserines	Diacylglycerophosphoserines	PS 38:3	PS 20:0_18:3	100.29
798.5280	Glycerophosphoserines	Diacylglycerophosphoserines	PS 38:3	PS 20:1_18:2	103.10
812.5450	Glycerophosphoserines	Diacylglycerophosphoserines	PS 38:3	PS 20:2_18:1	163.55
812.5440	Glycerophosphoserines	Diacylglycerophosphoserines	PS 38:3	PS 20:3_18:0	278.74
796.5150	Glycerophosphoserines	Diacylglycerophosphoserines	PS 38:4	PS 16:0_22:4	63.98
810.5310	Glycerophosphoserines	Diacylglycerophosphoserines	PS 38:4	PS 18:0_20:4	286.26
810.5290	Glycerophosphoserines	Diacylglycerophosphoserines	PS 38:4	PS 18:1_20:3	199.87
810.5280	Glycerophosphoserines	Diacylglycerophosphoserines	PS 38:4	PS 18:2_20:2	168.78
810.5270	Glycerophosphoserines	Diacylglycerophosphoserines	PS 38:4	PS 18:3_20:1	162.96
810.5290	Glycerophosphoserines	Diacylglycerophosphoserines	PS 38:4	PS 20:0_18:4	124.31
810.5300	Glycerophosphoserines	Diacylglycerophosphoserines	PS 38:4	PS 20:2_18:2	160.87
810.5290	Glycerophosphoserines	Diacylglycerophosphoserines	PS 38:4	PS 20:3_18:1	197.12
810.5310	Glycerophosphoserines	Diacylglycerophosphoserines	PS 38:4	PS 20:4_18:0	298.50
810.5290	Glycerophosphoserines	Diacylglycerophosphoserines	PS 38:4	PS 22:4_16:0	167.05
808.5120	Glycerophosphoserines	Diacylglycerophosphoserines	PS 38:5	PS 18:0_20:5	313.46
808.5130	Glycerophosphoserines	Diacylglycerophosphoserines	PS 38:5	PS 18:1_20:4	308.93
808.5120	Glycerophosphoserines	Diacylglycerophosphoserines	PS 38:5	PS 18:2_20:3	183.93
808.5120	Glycerophosphoserines	Diacylglycerophosphoserines	PS 38:5	PS 20:1_18:4	102.11
808.5120	Glycerophosphoserines	Diacylglycerophosphoserines	PS 38:5	PS 20:3_18:2	188.42
808.5130	Glycerophosphoserines	Diacylglycerophosphoserines	PS 38:5	PS 20:4_18:1	314.72
808.5120	Glycerophosphoserines	Diacylglycerophosphoserines	PS 38:5	PS 20:5_18:0	311.43
806.4960	Glycerophosphoserines	Diacylglycerophosphoserines	PS 38:6	PS 16:0_22:6	311.47
806.4960	Glycerophosphoserines	Diacylglycerophosphoserines	PS 38:6	PS 18:1_20:5	201.17
806.4980	Glycerophosphoserines	Diacylglycerophosphoserines	PS 38:6	PS 18:2_20:4	280.36
806.4980	Glycerophosphoserines	Diacylglycerophosphoserines	PS 38:6	PS 18:3_20:3	104.51
806.4980	Glycerophosphoserines	Diacylglycerophosphoserines	PS 38:6	PS 20:2_18:4	108.58
806.4950	Glycerophosphoserines	Diacylglycerophosphoserines	PS 38:6	PS 20:4_18:2	277.65

806.4960	Glycerophosphoserines	Diacylglycerophosphoserines	PS 38:6	PS 20:5_18:1	220.78
806.4980	Glycerophosphoserines	Diacylglycerophosphoserines	PS 38:6	PS 22:6_16:0	329.97
812.5440	Glycerophosphoserines	Diacylglycerophosphoserines	PS 39:3	PS 19:0_20:3	227.65
812.5440	Glycerophosphoserines	Diacylglycerophosphoserines	PS 39:3	PS 19:1_20:2	199.46
812.5440	Glycerophosphoserines	Diacylglycerophosphoserines	PS 39:3	PS 20:2_19:1	55.60
812.5430	Glycerophosphoserines	Diacylglycerophosphoserines	PS 39:3	PS 20:3_19:0	204.34
826.5600	Glycerophosphoserines	Diacylglycerophosphoserines	PS 39:3	PS 21:0_18:3	57.50
812.5440	Glycerophosphoserines	Diacylglycerophosphoserines	PS 39:3	PS 22:1_17:2	170.28
810.5280	Glycerophosphoserines	Diacylglycerophosphoserines	PS 39:4	PS 19:0_20:4	224.29
810.5270	Glycerophosphoserines	Diacylglycerophosphoserines	PS 39:4	PS 19:1_20:3	192.94
810.5290	Glycerophosphoserines	Diacylglycerophosphoserines	PS 39:4	PS 20:3_19:1	85.43
810.5290	Glycerophosphoserines	Diacylglycerophosphoserines	PS 39:4	PS 20:4_19:0	204.89
810.5280	Glycerophosphoserines	Diacylglycerophosphoserines	PS 39:4	PS 22:2_17:2	182.24
822.5280	Glycerophosphoserines	Diacylglycerophosphoserines	PS 39:5	PS 17:1_22:4	102.63
808.5120	Glycerophosphoserines	Diacylglycerophosphoserines	PS 39:5	PS 19:0_20:5	230.30
808.5120	Glycerophosphoserines	Diacylglycerophosphoserines	PS 39:5	PS 19:1_20:4	232.88
808.5130	Glycerophosphoserines	Diacylglycerophosphoserines	PS 39:5	PS 20:4_19:1	207.27
808.5120	Glycerophosphoserines	Diacylglycerophosphoserines	PS 39:5	PS 20:5_19:0	197.43
806.4990	Glycerophosphoserines	Diacylglycerophosphoserines	PS 39:6	PS 17:0_22:6	226.71
806.4970	Glycerophosphoserines	Diacylglycerophosphoserines	PS 39:6	PS 17:2_22:4	208.05
820.5140	Glycerophosphoserines	Diacylglycerophosphoserines	PS 39:6	PS 19:1_20:5	111.23
806.4970	Glycerophosphoserines	Diacylglycerophosphoserines	PS 39:6	PS 22:6_17:0	230.20
838.5600	Glycerophosphoserines	Diacylglycerophosphoserines	PS 40:4	PS 18:0_22:4	253.66
838.5600	Glycerophosphoserines	Diacylglycerophosphoserines	PS 40:4	PS 22:4_18:0	259.58
836.5430	Glycerophosphoserines	Diacylglycerophosphoserines	PS 40:5	PS 18:1_22:4	193.52
836.5440	Glycerophosphoserines	Diacylglycerophosphoserines	PS 40:5	PS 20:0_20:5	182.50
836.5440	Glycerophosphoserines	Diacylglycerophosphoserines	PS 40:5	PS 20:1_20:4	210.88
836.5460	Glycerophosphoserines	Diacylglycerophosphoserines	PS 40:5	PS 20:2_20:3	104.40
836.5450	Glycerophosphoserines	Diacylglycerophosphoserines	PS 40:5	PS 20:3_20:2	173.03
836.5440	Glycerophosphoserines	Diacylglycerophosphoserines	PS 40:5	PS 20:4_20:1	200.19
836.5430	Glycerophosphoserines	Diacylglycerophosphoserines	PS 40:5	PS 20:5_20:0	172.52
836.5430	Glycerophosphoserines	Diacylglycerophosphoserines	PS 40:5	PS 22:4_18:1	178.43
834.5290	Glycerophosphoserines	Diacylglycerophosphoserines	PS 40:6	PS 18:0_22:6	307.85
834.5290	Glycerophosphoserines	Diacylglycerophosphoserines	PS 40:6	PS 18:2_22:4	148.14
834.5290	Glycerophosphoserines	Diacylglycerophosphoserines	PS 40:6	PS 20:1_20:5	140.85
834.5300	Glycerophosphoserines	Diacylglycerophosphoserines	PS 40:6	PS 20:2_20:4	159.55
834.5290	Glycerophosphoserines	Diacylglycerophosphoserines	PS 40:6	PS 20:3_20:3	166.71
834.5280	Glycerophosphoserines	Diacylglycerophosphoserines	PS 40:6	PS 20:5_20:1	183.78
834.5280	Glycerophosphoserines	Diacylglycerophosphoserines	PS 40:6	PS 22:4_18:2	143.39
834.5290	Glycerophosphoserines	Diacylglycerophosphoserines	PS 40:6	PS 22:6_18:0	325.73
832.5130	Glycerophosphoserines	Diacylglycerophosphoserines	PS 40:7	PS 18:1_22:6	285.58
832.5130	Glycerophosphoserines	Diacylglycerophosphoserines	PS 40:7	PS 20:2_20:5	167.55
832.5130	Glycerophosphoserines	Diacylglycerophosphoserines	PS 40:7	PS 20:3_20:4	226.30
832.5120	Glycerophosphoserines	Diacylglycerophosphoserines	PS 40:7	PS 20:4_20:3	222.93
832.5130	Glycerophosphoserines	Diacylglycerophosphoserines	PS 40:7	PS 22:6_18:1	282.76
830.4960	Glycerophosphoserines	Diacylglycerophosphoserines	PS 40:8	PS 18:2_22:6	269.87
830.4970	Glycerophosphoserines	Diacylglycerophosphoserines	PS 40:8	PS 20:3_20:5	205.92
830.4970	Glycerophosphoserines	Diacylglycerophosphoserines	PS 40:8	PS 20:4_20:4	359.57
830.4980	Glycerophosphoserines	Diacylglycerophosphoserines	PS 40:8	PS 20:5_20:3	194.51
830.4980	Glycerophosphoserines	Diacylglycerophosphoserines	PS 40:8	PS 22:4_18:4	150.54

830.4960	Glycerophosphoserines	Diacylglycerophosphoserines	PS 40:8	PS 22:6_18:2	258.53
838.5590	Glycerophosphoserines	Diacylglycerophosphoserines	PS 41:4	PS 19:0_22:4	215.99
838.5590	Glycerophosphoserines	Diacylglycerophosphoserines	PS 41:4	PS 22:4_19:0	171.03
836.5450	Glycerophosphoserines	Diacylglycerophosphoserines	PS 41:5	PS 19:1_22:4	181.15
836.5440	Glycerophosphoserines	Diacylglycerophosphoserines	PS 41:5	PS 20:5_21:0	200.31
836.5450	Glycerophosphoserines	Diacylglycerophosphoserines	PS 41:5	PS 22:4_19:1	176.12
834.5290	Glycerophosphoserines	Diacylglycerophosphoserines	PS 41:6	PS 19:0_22:6	226.37
834.5290	Glycerophosphoserines	Diacylglycerophosphoserines	PS 41:6	PS 22:6_19:0	179.98
832.5140	Glycerophosphoserines	Diacylglycerophosphoserines	PS 41:7	PS 19:1_22:6	271.29
832.5110	Glycerophosphoserines	Diacylglycerophosphoserines	PS 41:7	PS 22:6_19:1	213.27
854.4960	Glycerophosphoserines	Diacylglycerophosphoserines	PS 42:10	PS 20:4_22:6	341.57
854.4960	Glycerophosphoserines	Diacylglycerophosphoserines	PS 42:10	PS 22:6_20:4	326.47
524.3000	Glycerophosphoserines	Monoacylglycerophosphoserines	PS 18:0	PS 18:0_0:0	191.53
544.2670	Glycerophosphoserines	Monoacylglycerophosphoserines	PS 20:4	PS 20:4_0:0	205.92
255.2330	Fatty Acyls	Fatty Acids & Conjugates	FFA 16:0	FFA 16:0	3.93
283.2643	Fatty Acyls	Fatty Acids & Conjugates	FFA 18:0	FFA 18:0	3.67
281.2486	Fatty Acyls	Fatty Acids & Conjugates	FFA 18:1	FFA 18:1	4.27
279.2330	Fatty Acyls	Fatty Acids & Conjugates	FFA 18:2	FFA 18:2	0.75
277.2173	Fatty Acyls	Fatty Acids & Conjugates	FFA 18:3	FFA 18:3	0.03
303.2330	Fatty Acyls	Fatty Acids & Conjugates	FFA 20:4	FFA 20:4	0.03
301.2173	Fatty Acyls	Fatty Acids & Conjugates	FFA 20:5	FFA 20:5	0.02
327.2330	Fatty Acyls	Fatty Acids & Conjugates	FFA 22:6	FFA 22:6	0.01
670.6496	Sterols	Steryl Esters	CE 16:0	CE 18:0	27.32
666.6183	Sterols	Steryl Esters	CE 18:0	CE 18:2	73.65
664.6027	Sterols	Steryl Esters	CE 18:2	CE 18:3	0.81
690.6183	Sterols	Steryl Esters	CE 20:4	CE 20:4	10.62
688.6027	Sterols	Steryl Esters	CE 20:5	CE 20:5	0.80
714.6183	Sterols	Steryl Esters	CE 22:6	CE 22:6	0.59
803.6970	Triradylglycerols	Triacylglycerols	TAG 45:3	TAG 13:0_15:1_17:2	139.27
803.6990	Triradylglycerols	Triacylglycerols	TAG 45:3	TAG 14:1_14:1_17:1	81.00
803.6990	Triradylglycerols	Triacylglycerols	TAG 45:3	TAG 14:1_15:1_16:1	256.41
803.6990	Triradylglycerols	Triacylglycerols	TAG 45:3	TAG 15:1_15:1_15:1	58.00
794.8790	Triradylglycerols	Triacylglycerols	TAG 47:1	TAG 15:0_17:1_15:0	4506.95
829.7980	Triradylglycerols	Triacylglycerols	TAG 47:4	TAG 13:0_14:0_20:4	564.77
851.8810	Triradylglycerols	Triacylglycerols	TAG 48:0	TAG 16:0_16:0_16:0	14808.38
803.7010	Triradylglycerols	Triacylglycerols	TAG 48:1	TAG 14:0_14:0_20:1	84.00
803.6990	Triradylglycerols	Triacylglycerols	TAG 48:1	TAG 14:1_17:0_17:0	116.19
803.7010	Triradylglycerols	Triacylglycerols	TAG 48:1	TAG 16:0_16:0_16:1	72.00
865.8420	Triradylglycerols	Triacylglycerols	TAG 49:0	TAG 16:0_16:0_17:0	486.51
879.9880	Triradylglycerols	Triacylglycerols	TAG 50:0	TAG 14:0_17:0_19:0	5824.36
879.9190	Triradylglycerols	Triacylglycerols	TAG 50:0	TAG 14:0_18:0_18:0	16221.80
879.9890	Triradylglycerols	Triacylglycerols	TAG 50:0	TAG 16:0_16:0_18:0	12835.63
877.9730	Triradylglycerols	Triacylglycerols	TAG 50:1	TAG 14:0_16:1_20:0	5370.49
877.9720	Triradylglycerols	Triacylglycerols	TAG 50:1	TAG 16:0_16:1_18:0	25346.72
877.9730	Triradylglycerols	Triacylglycerols	TAG 50:1	TAG 16:1_17:0_17:0	28121.04
829.9630	Triradylglycerols	Triacylglycerols	TAG 50:2	TAG 14:0_16:0_20:2	178645.25
829.9640	Triradylglycerols	Triacylglycerols	TAG 50:2	TAG 14:0_18:1_18:1	1038.50
829.9630	Triradylglycerols	Triacylglycerols	TAG 50:2	TAG 15:0_15:0_20:2	96535.21
829.9630	Triradylglycerols	Triacylglycerols	TAG 50:2	TAG 16:0_16:0_18:2	53.21
829.9620	Triradylglycerols	Triacylglycerols	TAG 50:2	TAG 16:0_16:1_18:1	1217.35

875.8870	Triradylglycerols	Triacylglycerols	TAG 50:2	TAG 16:0_17:1_17:1	3760.14
863.8620	Triradylglycerols	Triacylglycerols	TAG 50:8	TAG 14:1_14:1_22:6	1540.35
894.0130	Triradylglycerols	Triacylglycerols	TAG 51:0	TAG 16:0_17:0_18:0	1023.18
891.8660	Triradylglycerols	Triacylglycerols	TAG 51:1	TAG 17:0_17:0_17:1	361.16
850.9560	Triradylglycerols	Triacylglycerols	TAG 51:1	TAG 17:0_17:1_17:0	73689.79
889.8480	Triradylglycerols	Triacylglycerols	TAG 51:2	TAG 15:0_17:1_19:1	688.56
889.8480	Triradylglycerols	Triacylglycerols	TAG 51:2	TAG 16:1_16:1_19:0	570.70
839.8200	Triradylglycerols	Triacylglycerols	TAG 51:4	TAG 15:1_17:2_19:1	359.48
839.8200	Triradylglycerols	Triacylglycerols	TAG 51:4	TAG 17:0_17:2_17:2	349.40
839.8190	Triradylglycerols	Triacylglycerols	TAG 51:4	TAG 17:1_17:1_17:2	57.35
908.0300	Triradylglycerols	Triacylglycerols	TAG 52:0	TAG 13:0_17:0_22:0	1637.90
908.0360	Triradylglycerols	Triacylglycerols	TAG 52:0	TAG 16:0_18:0_18:0	3882.06
906.0120	Triradylglycerols	Triacylglycerols	TAG 52:1	TAG 16:0_16:1_20:0	14065.07
905.8280	Triradylglycerols	Triacylglycerols	TAG 52:1	TAG 16:0_18:0_18:1	4904.37
906.0110	Triradylglycerols	Triacylglycerols	TAG 52:1	TAG 16:1_18:0_18:0	6706.23
903.9970	Triradylglycerols	Triacylglycerols	TAG 52:2	TAG 16:0_18:0_18:2	7792.06
901.9100	Triradylglycerols	Triacylglycerols	TAG 52:3	TAG 16:0_18:1_18:2	4467.09
901.9100	Triradylglycerols	Triacylglycerols	TAG 52:3	TAG 17:1_17:2_18:0	4496.45
899.9650	Triradylglycerols	Triacylglycerols	TAG 52:4	TAG 16:1_18:1_18:2	6761.58
897.9550	Triradylglycerols	Triacylglycerols	TAG 52:5	TAG 14:0_16:1_22:4	2561.28
851.8790	Triradylglycerols	Triacylglycerols	TAG 52:5	TAG 16:0_16:1_20:4	267.74
851.8790	Triradylglycerols	Triacylglycerols	TAG 52:5	TAG 16:0_18:1_18:4	13501.87
851.8790	Triradylglycerols	Triacylglycerols	TAG 52:5	TAG 16:1_18:1_18:3	415.34
891.8640	Triradylglycerols	Triacylglycerols	TAG 52:8	TAG 14:1_18:4_20:3	8155.46
889.8490	Triradylglycerols	Triacylglycerols	TAG 52:9	TAG 14:1_18:4_20:4	2806.90
917.8890	Triradylglycerols	Triacylglycerols	TAG 53:2	TAG 15:1_19:0_19:1	1831.05
917.8880	Triradylglycerols	Triacylglycerols	TAG 53:2	TAG 17:1_17:1_19:0	975.33
915.8700	Triradylglycerols	Triacylglycerols	TAG 53:3	TAG 17:0_17:2_19:1	185.20
915.8710	Triradylglycerols	Triacylglycerols	TAG 53:3	TAG 17:1_17:1_19:1	1504.44
915.8710	Triradylglycerols	Triacylglycerols	TAG 53:3	TAG 17:1_17:2_19:0	6915.88
865.8420	Triradylglycerols	Triacylglycerols	TAG 53:5	TAG 17:2_17:2_19:1	624.28
932.0420	Triradylglycerols	Triacylglycerols	TAG 54:2	TAG 16:0_18:1_20:1	3434.26
932.0430	Triradylglycerols	Triacylglycerols	TAG 54:2	TAG 16:1_18:0_20:1	14691.40
885.9660	Triradylglycerols	Triacylglycerols	TAG 54:2	TAG 18:0_18:1_18:1	3216.90
929.9830	Triradylglycerols	Triacylglycerols	TAG 54:3	TAG 14:1_18:1_22:1	2313.94
883.9500	Triradylglycerols	Triacylglycerols	TAG 54:3	TAG 16:0_18:1_20:2	10847.42
883.9520	Triradylglycerols	Triacylglycerols	TAG 54:3	TAG 16:0_18:2_20:1	20877.06
883.9510	Triradylglycerols	Triacylglycerols	TAG 54:3	TAG 18:0_18:0_18:3	349.97
883.9500	Triradylglycerols	Triacylglycerols	TAG 54:3	TAG 18:0_18:1_18:2	11902.15
927.9660	Triradylglycerols	Triacylglycerols	TAG 54:4	TAG 14:1_18:1_22:2	2784.81
882.0060	Triradylglycerols	Triacylglycerols	TAG 54:4	TAG 16:0_16:0_22:4	685.09
882.0050	Triradylglycerols	Triacylglycerols	TAG 54:4	TAG 16:0_18:0_20:4	4001.49
882.0130	Triradylglycerols	Triacylglycerols	TAG 54:4	TAG 16:0_18:1_20:3	179.93
927.9320	Triradylglycerols	Triacylglycerols	TAG 54:4	TAG 16:0_18:2_20:2	10813.14
927.9680	Triradylglycerols	Triacylglycerols	TAG 54:4	TAG 16:1_18:1_20:2	2691.05
881.9350	Triradylglycerols	Triacylglycerols	TAG 54:4	TAG 18:0_18:0_18:4	27966.03
927.9680	Triradylglycerols	Triacylglycerols	TAG 54:4	TAG 18:0_18:2_18:2	3984.79
925.9930	Triradylglycerols	Triacylglycerols	TAG 54:5	TAG 16:0_16:1_22:4	7909.25
879.9190	Triradylglycerols	Triacylglycerols	TAG 54:5	TAG 16:0_18:0_20:5	25178.23
879.9880	Triradylglycerols	Triacylglycerols	TAG 54:5	TAG 16:0_18:1_20:4	9693.33

879.9890	Triradylglycerols	Triacylglycerols	TAG 54:5	TAG 16:0_18:2_20:3	913.51
879.9890	Triradylglycerols	Triacylglycerols	TAG 54:5	TAG 16:0_18:3_20:2	8070.61
879.9890	Triradylglycerols	Triacylglycerols	TAG 54:5	TAG 16:0_18:4_20:1	15346.41
879.9190	Triradylglycerols	Triacylglycerols	TAG 54:5	TAG 16:1_18:0_20:4	18214.19
879.9200	Triradylglycerols	Triacylglycerols	TAG 54:5	TAG 16:1_18:1_20:3	20539.07
925.9940	Triradylglycerols	Triacylglycerols	TAG 54:5	TAG 16:1_18:2_20:2	6137.23
925.9150	Triradylglycerols	Triacylglycerols	TAG 54:5	TAG 17:1_17:1_20:3	5979.67
879.9890	Triradylglycerols	Triacylglycerols	TAG 54:5	TAG 18:0_18:1_18:4	17578.16
879.7430	Triradylglycerols	Triacylglycerols	TAG 54:5	TAG 18:0_18:2_18:3	238.38
879.9890	Triradylglycerols	Triacylglycerols	TAG 54:5	TAG 18:1_18:1_18:3	7113.67
877.9730	Triradylglycerols	Triacylglycerols	TAG 54:6	TAG 16:0_18:1_20:5	24098.29
877.9730	Triradylglycerols	Triacylglycerols	TAG 54:6	TAG 16:0_18:2_20:4	6806.74
877.9740	Triradylglycerols	Triacylglycerols	TAG 54:6	TAG 16:0_18:3_20:3	5522.61
877.9720	Triradylglycerols	Triacylglycerols	TAG 54:6	TAG 18:0_18:2_18:4	17085.33
877.9030	Triradylglycerols	Triacylglycerols	TAG 54:6	TAG 18:1_18:1_18:4	29682.70
877.7960	Triradylglycerols	Triacylglycerols	TAG 54:6	TAG 18:1_18:2_18:3	4405.41
875.8850	Triradylglycerols	Triacylglycerols	TAG 54:7	TAG 14:1_20:1_20:5	6023.35
875.9570	Triradylglycerols	Triacylglycerols	TAG 54:7	TAG 16:0_18:2_20:5	11878.13
875.9560	Triradylglycerols	Triacylglycerols	TAG 54:7	TAG 16:0_18:3_20:4	4909.17
875.8880	Triradylglycerols	Triacylglycerols	TAG 54:7	TAG 16:0_18:4_20:3	4278.12
875.8870	Triradylglycerols	Triacylglycerols	TAG 54:7	TAG 16:1_18:1_20:5	5718.66
875.8870	Triradylglycerols	Triacylglycerols	TAG 54:7	TAG 16:1_18:2_20:4	8460.51
875.8860	Triradylglycerols	Triacylglycerols	TAG 54:7	TAG 18:1_18:2_18:4	18487.84
875.8860	Triradylglycerols	Triacylglycerols	TAG 54:7	TAG 18:1_18:3_18:3	21474.83
875.8890	Triradylglycerols	Triacylglycerols	TAG 54:7	TAG 18:2_18:2_18:3	6164.54
873.8710	Triradylglycerols	Triacylglycerols	TAG 54:8	TAG 18:2_18:2_18:4	5386.37
901.9820	Triradylglycerols	Triacylglycerols	TAG 55:1	TAG 15:0_19:1_21:0	3393.77
897.9660	Triradylglycerols	Triacylglycerols	TAG 55:3	TAG 17:1_19:1_19:1	1986.27
897.9540	Triradylglycerols	Triacylglycerols	TAG 55:3	TAG 18:1_18:1_19:1	3815.50
897.9530	Triradylglycerols	Triacylglycerols	TAG 55:3	TAG 18:1_18:2_19:0	5172.88
895.9540	Triradylglycerols	Triacylglycerols	TAG 55:4	TAG 17:0_18:0_20:4	7337.21
895.9540	Triradylglycerols	Triacylglycerols	TAG 55:4	TAG 18:0_18:3_19:1	206.04
895.9540	Triradylglycerols	Triacylglycerols	TAG 55:4	TAG 18:2_18:2_19:0	153.68
911.9900	Triradylglycerols	Triacylglycerols	TAG 56:3	TAG 16:0_20:0_20:3	141.29
911.9890	Triradylglycerols	Triacylglycerols	TAG 56:3	TAG 18:0_18:0_20:3	17526.57
911.9900	Triradylglycerols	Triacylglycerols	TAG 56:3	TAG 18:0_18:1_20:2	7281.84
911.9900	Triradylglycerols	Triacylglycerols	TAG 56:3	TAG 18:0_18:2_20:1	3411.76
911.9900	Triradylglycerols	Triacylglycerols	TAG 56:3	TAG 18:0_18:3_20:0	10800.97
909.9740	Triradylglycerols	Triacylglycerols	TAG 56:4	TAG 18:0_18:0_20:4	29657.88
909.9720	Triradylglycerols	Triacylglycerols	TAG 56:4	TAG 18:0_18:1_20:3	12778.69
910.0510	Triradylglycerols	Triacylglycerols	TAG 56:4	TAG 18:4_19:0_19:0	601.76
908.0340	Triradylglycerols	Triacylglycerols	TAG 56:5	TAG 16:0_18:1_22:4	6118.22
908.0350	Triradylglycerols	Triacylglycerols	TAG 56:5	TAG 16:0_20:1_20:4	1273.70
908.0360	Triradylglycerols	Triacylglycerols	TAG 56:5	TAG 18:0_18:0_20:5	2922.34
908.0320	Triradylglycerols	Triacylglycerols	TAG 56:5	TAG 18:0_18:1_20:4	1329.35
908.0310	Triradylglycerols	Triacylglycerols	TAG 56:5	TAG 18:0_18:2_20:3	926.22
905.9410	Triradylglycerols	Triacylglycerols	TAG 56:6	TAG 18:0_18:1_20:5	23281.07
906.0110	Triradylglycerols	Triacylglycerols	TAG 56:6	TAG 18:0_18:2_20:4	7897.04
906.0130	Triradylglycerols	Triacylglycerols	TAG 56:6	TAG 18:1_18:1_20:4	4117.68
903.9960	Triradylglycerols	Triacylglycerols	TAG 56:7	TAG 16:0_20:3_20:4	5473.41

901.9090	Triradylglycerols	Triacylglycerols	TAG 56:8	TAG 18:1_18:3_20:4	6206.75
901.9100	Triradylglycerols	Triacylglycerols	TAG 56:8	TAG 18:2_18:2_20:4	5048.87
899.8910	Triradylglycerols	Triacylglycerols	TAG 56:9	TAG 14:0_20:3_22:6	1921.96
899.8900	Triradylglycerols	Triacylglycerols	TAG 56:9	TAG 18:2_18:2_20:5	191.04
927.9680	Triradylglycerols	Triacylglycerols	TAG 57:2	TAG 19:0_19:1_19:1	646.69
925.9510	Triradylglycerols	Triacylglycerols	TAG 57:3	TAG 19:1_19:1_19:1	805.73
915.8710	Triradylglycerols	Triacylglycerols	TAG 57:8	TAG 17:0_18:2_22:6	1823.90
931.0400	Triradylglycerols	Triacylglycerols	TAG 58:10	TAG 20:4_18:2_20:4	219.57
931.9640	Triradylglycerols	Triacylglycerols	TAG 58:7	TAG 16:0_20:2_22:5	3487.92
931.9640	Triradylglycerols	Triacylglycerols	TAG 58:7	TAG 18:0_18:1_22:6	22840.06
931.9630	Triradylglycerols	Triacylglycerols	TAG 58:7	TAG 18:0_20:3_20:4	10322.04
931.9640	Triradylglycerols	Triacylglycerols	TAG 58:7	TAG 18:1_20:1_20:5	17552.39
931.9650	Triradylglycerols	Triacylglycerols	TAG 58:7	TAG 18:1_20:2_20:4	24869.52
931.9640	Triradylglycerols	Triacylglycerols	TAG 58:7	TAG 18:1_20:3_20:3	28459.92
927.9320	Triradylglycerols	Triacylglycerols	TAG 58:9	TAG 16:0_20:5_22:4	31438.99
927.9320	Triradylglycerols	Triacylglycerols	TAG 58:9	TAG 18:1_18:4_22:4	183.22
927.9310	Triradylglycerols	Triacylglycerols	TAG 58:9	TAG 18:1_20:3_20:5	13952.62